
Strathclyde Institute of Pharmacy and Biomedical Sciences

# Corona Discharge-Mediated Immobilisation of Bacteriophages onto Polymeric Surfaces for the Production of Anti-Bacterial Surfaces

A thesis presented for the degree of
Doctor of Philosophy
in the Faculty of Science of the
University of Strathclyde

**Daniel Rosner**
201865828

# Declaration of Author's Right

This thesis is the result of the author's original research. It has been composed by the author and has not been previously submitted for examination which has led to the award of a degree.



Signed: DR

Date: 20/02/2024

# Acknowledgements

I would like to express my deepest gratitude to my supervisor, Dr Yvonne Perrie, for her unwavering support, guidance, and encouragement throughout the entire research process. Her expertise and insightful feedback have been invaluable in shaping and refining this thesis.

I would also like to thank Dr Luis Bimbo, who supervised me for the first two years of the programme. Even after parting ways, he remained in touch, giving advice and encouraging me throughout.

This work would not have been possible without the support of my employer, NexaBiome limited, who sponsored my period of study. I would like to give a heartfelt thanks to all of my amazing colleagues. Special mentions go to my line manager, Chris Bindon, who gave me the time I needed to write up the thesis, Dr Jason Clark, for his expert insights on all aspects of bacteriophage biology, and Dr Gordon Smith, for the occasional joke.

A special thanks also goes out to Dr Emma Bell, who has had the pleasure of listening to my constant ramblings on an almost daily basis for the last five years and who has always been there to provide me with scientific advice and moral support during the most trying times. She never once complained!

I am immensely thankful to my family for their constant love, understanding, and encouragement. Their unwavering support has been my source of strength and motivation throughout this academic journey.

Finally, a heartfelt appreciation goes to all my friends who have been by my side, providing not only emotional support but also offering valuable insights and perspectives. Their encouragement and humour have made the challenging moments more manageable and the successes more joyous.

# Covid-19 Impact Statement

The COVID-19 pandemic has left an indelible mark on the trajectory of this thesis, influencing its course and execution. The pervasive global disruptions, characterized by lockdowns, restricted access to research facilities, and supply chain interruptions, prompted a thorough reassessment of research plans and methodologies. Remote work and virtual collaboration became imperative as traditional modes of scientific inquiry faced unprecedented challenges.

In navigating these obstacles, the pandemic's impact underscored the urgency and relevance of the research topic in the broader context of global health. The collective response of various disciplines to the pandemic, spanning from public health measures to vaccine development, has provided valuable perspectives and inspiration for the ongoing work. Furthermore, the dynamic nature of the pandemic has offered unique opportunities to explore facets of the research process that demand adaptability and resilience.

This impact statement encapsulates not only the challenges faced but also highlights the adaptability and resilience of the research community, demonstrating its capacity to contribute meaningfully to understanding and addressing global challenges in the wake of the COVID-19 pandemic.

# Abstract

The prevalence of antibiotic-resistant bacteria is a global issue with far-reaching implications across various sectors. As alternative strategies to solve problems associated with these microbes are investigated, attention is increasingly turned towards bacteriophages, which can target specific strains of interest and self-amplify because of their virus-like lifecycle. Bacteriophages were originally used to treat bacterial pathogen-borne illnesses. Their scope of application has broadened considerably, and they are now actively being researched for their use across a range of industries. In many cases, phages are incorporated in some form of solid or semisolid-based bioactive product. Several approaches for this have been researched in depth. The work summarised in this thesis focuses on bacteriophage immobilisation, which can be defined as the irreversible fixation of viable phages onto solid surfaces. Here, it is achieved through a novel application of corona discharge as a mediator for linker-free, permanent phage binding onto polymeric surfaces. Following the development and verification of a method for quantifying immobilised phages, the work summarised focuses on demonstrating the efficacy of corona discharge for phage immobilisation onto polymeric surfaces. Additionally, there is an emphasis on improving the post-immobilisation survival and distribution of bacteriophages on the surface in producing solid, dry final products. The thesis concludes with a trial conducted to assess the efficacy of food packaging containing immobilised phages in increasing the shelf-life of cut salad. For most phages considered, corona discharge increased irreversible binding 10-fold, whilst lecithin, sucrose and lutensol emerged as useful substances in the context of drying stability, shelf-life, and surface distribution, respectively. Bacteriophage-incorporated packaging significantly increased the shelf-life of cut salad by almost one full day. It is concluded that corona discharge can be utilised in conjunction with formulated phage to produce antimicrobial products with demonstratable real-world applications.

# Table of Contents

# List of Figures

# List of Tables

# List of Equations

# Abbreviations

| | |
|---|---|
| % | percent |
| (-C=C-) | alkene functionality |
| (-C=O) | carbonyl functionality |
| (-COO-) | carboxyane functionality |
| (-COOC-) | ether functionality |
| ($-NH_2$) | amine functionality |
| (-OH) | hydroxyl functionality |
| °C | degrees temperature |
| µL | microlitre |
| µm | micrometre |
| µM | micromolar |
| AA | ascorbic acid |
| AFM | atomic force microscopy |
| ATCC | American type culture collection |
| BOPP | biaxially oriented polypropylene |
| BSA | bovine serum albumin |
| CFU | cell forming units |
| $cm^{-1}$ | wavenumbers |
| CP | cellophane |
| DNA | deoxyribonucleic acid |
| DPPH | 2,2-diphenyl-1-picrylhydrazyl |
| EDTA | Ethylenediaminetetraacetic acid |
| g | gramme |
| IR | infrared |
| J/min | joules per minute |
| $J/mm^2$ | joules per mm squared |
| $kJ/m^2$ | kilojoules per metre squared |
| m | metre |
| M | molarity |
| m/min | metre per minute |
| mL | millilitre |
| mm | millimetre |
| mm/min | millimetre per minute |

| | |
|---|---|
| mN/m | dyne |
| MOI | multiplicity of infection |
| N6 | nylon 6 |
| nm | nanometre |
| OD | optical density |
| OD(600) | optical density at 600 nanometres |
| PBS | phosphate buffered saline |
| PE-CVD | Plasma-enhanced chemical vapour deposition |
| PEEK | polyether ether ketone |
| PEG | polyethylene glycol |
| PES | polyether sulfone |
| PFU | plaque forming units |
| PHA | polyhydroxyalkanoate |
| PIII | plasma ion immersion implantation |
| PP | polypropylene |
| PVC | polyvinyl chloride |
| QCM | crystal quartz microbalance |
| qPCR | quantitative polymerase chain reaction |
| RBP | receptor binding protein |
| RNA | ribonucleic acid |
| rpm | revolutions per minute |
| SDS | sodium dodecyl sulfate |
| SEM | scanning electron microscopy |
| SIMS | secondary ion mass spectrometry |
| SPR | surface plasmon resonance |
| ss-NMR | solid state nuclear magnetic resonance |
| TEM | transmission electron microscopy |
| VAPGH | virion-associated peptidoglycan hydrolase |
| vol/vol | volume on volume |
| W | watts |
| wt/vol | weight on volume |
| XPS | x-ray photoelctron spectroscopy |

# Chapter 1: Introduction and Literature Review

*Parts of the following chapter were published in the underlying journal review article:*

**Title:** Formulations for Bacteriophage Therapy and the Potential Uses of Immobilization

**Year:** 2021

**Co-author:** Dr Jason Clark

**Journal:** Pharmaceuticals (Basel)

**Volume (Issue):** 14 (4)

**Page:** 359

**doi:** 10.3390/ph14040359

## 1.1 INTRODUCTION

It is estimated that antibiotic-resistant bacterial strains account for approximately 33,000 annual deaths in Europe, emphasising the urgent need to devise novel strategies to tackle this global challenge (Cassini *et al*., 2019). The ability of bacteria to acquire drug resistance through random mutation as well as conjugation-mediated genetic transfer has made bacterial infection and contamination a major concern with far reaching implications. *Pseudomonas aureus* strains have been shown to become resistant to colistin through cross-species plasmid transfer of the MCR-1 gene from resistant strains of *Escherichia coli* (Willmann *et al*., 2017). Other examples of antibiotic-resistant superbugs include methicillin-resistant *Staphylococcus aureus* (MRSA), vancomycin-resistant *Enterococcus* (VRE) and multi-drug-resistant *Mycobacterium tuberculosis* (MDR-TB) (Azam & Tanji, 2019). In the medical sector, the spread of drug resistance has resulted in the emergence of 'superbugs', responsible for an increase in deaths from illnesses previously treatable with conventional antibiotics (Zaman *et al*., 2017). Furthermore, bacterial contamination presents considerable challenges for agricultural systems, with pathogens causing large scale losses of product. In plant farming, Xylella infections threaten the long-term survival of olive trees in Italy and vines in California, potentially decimating their respective olive oil and wine production industries (Cariddi *et al*., 2014). In aquaculture, marine pathogens such as Vibrio bacteria have been observed to infect entire farmed fish and shrimp stocks, drastically reducing production (Vandenberghe *et al*., 2003). As with the medical sector, antibiotics are becoming less reliable due to the increasing occurrence of resistant strains.

The search for alternative strategies to solve these problems has rekindled interest in bacteriophages. These bacterial viruses can target specific strains, leaving other cells unharmed. Additionally, their ability to propagate to high concentrations reduces the need for continuous application. A considerable proportion of bacteriophage-related research now focuses on their application in producing antibacterial materials. Whether controlling for pathogens at a specific site of infection/contamination or developing smart biosensors capable of recognising and quantifying bacterial strains of interest, the demand exists for materials that are both simple to produce and efficient in their mode of operation.

Antibacterial materials can be produced through the straightforward combination of a bioactive component with the material constituents, before structuring the mixture into its intended form, such as a film or powder. Alternatively, the material can be coated with the active component to render it antibacterial. The latter proves to be the more challenging of the two approaches as it requires some type of permanent fixation or 'immobilisation' of the biological agent onto the material's surface. It is, however, advantageous as it allows for the targeting of bacteria at specific points across an interface. The immobilisation of biological agents is a growing field, and research publications concerning effective means to achieve this have increased steadily over the last 20 years. Multiple approaches to immobilisation now exist, including physical, chemical and electrical-based techniques. Of the electrical-based techniques, plasma to mediate immobilisation offers an interesting strategy that potentially allows for a simple way to bind biological agents such as bacteriophages to surfaces without chemical linkers. This is particularly appealing from a commercial point of view with respect to scaled-up production of antimicrobial surfaces.

## 1.2 BIOLOGY AND APPLICATION OF BACTERIOPHAGES

With an estimated population of more than 1031, bacteriophages (or phages) represent the most abundant life form on the planet (Clokie *et al.*, 2011). They are defined as viruses which infect prokaryotes, consisting of genetic material encapsulated in a protein coat or capsid, and function in much the same way as their virion counterparts. Phages were discovered separately by Frederick Twort in 1915 and Felix d'Herelle in 1917 (Duckworth, 1976). Since then, the continuous study of these organisms has resulted in discoveries which have contributed to important developments in modern biology. These include Hershey & Chase's (1952) ground-breaking phage-based experiment confirming that genetic material comprises nucleic acid-based compounds, the discovery of the restriction-modification system leading to the start of gene editing technology, as well as the exploitation of filamentous bacteriophages for phage display, first reported by George Smith in 1985 (Bertani & Weigle, 1953; Smith, 1985). Furthermore, their antibacterial properties made them an interesting topic of study from a biomedical perspective. Despite encouraging initial results, the advent of antibiotics as

a means of combating bacterial infections coupled with the Council on Pharmacy and Chemistry of the American Medical Association concluding that more research was needed to prove the effectiveness of phages resulted in them being side-lined by medical scientists in the West during the mid-20th century (Salmond & Fineran, 2015). Research continued in the former Soviet Union, where phage therapy was established as a central strategy to combat bacterial infections. The Eliava Institute in Georgia remains one of the world's major centres for phage therapy (Parfitt, 2005).

Aside from medical applications, interest in phages has grown considerably across the biotechnology sector, using them in the development of bacterial sensors, food safety and genetic engineering (Harada *et al*., 2018).

### 1.2.1 Morphology and Classification

Bacteriophages are some of the simplest life forms in existence. They do not possess any metabolic systems, are incapable of locomotion and rely entirely on their hosts for reproduction. Bacteriophage hosts are members of the prokaryotes, which include eubacteria, archaea, cyanobacteria and mycoplasmas (Ackermann, 2003). Most bacteriophages measure between 25 – 200 nm in length (Ackermann, 2007).

The primary functions of phages are host cell recognition and binding, insertion of genetic material and lysis or escape from the host cell for subsequent infection. Their structure, whilst primitive, allows them to fulfil these functions. All phages consist of a head comprising genetic material, which can be DNA or RNA that is either single or double-stranded within a protective coat. In most cases, this forms a polyhedrally-shaped virus-like capsid, formed from self-assembled capsomere units made of major coat proteins. Phage heads vary considerably in terms of shape and composition. Members of the Caudoviricetes class have heads that are typically icosahedral in shape. Filamentous phages such as M13 and fd, from the Inoviridae family, possess capsids comprising α-helical major coat protein subunits arranged in an overlapping helical array to form long filament-shaped heads (Marvin *et al*., 2014). The asymmetrical pleomorphic phage L2 lacks a capsid, retaining its genetic contents with a

protein-lipid membrane. Many phages also possess tails of varying sizes. The presence or lack of a tail, virion shape and nucleic acid type were the features most commonly considered in the classification of bacteriophages (Ackermann, 2003).

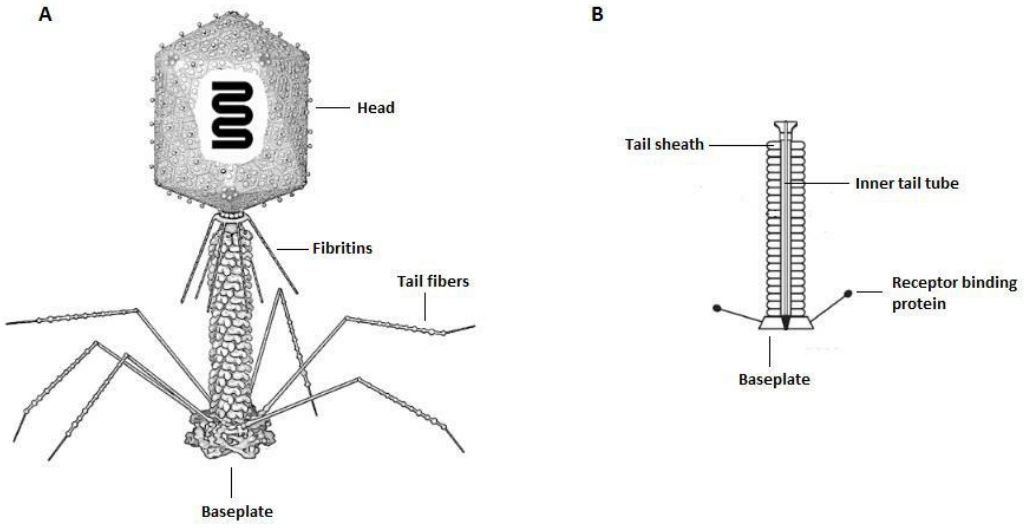


**Figure 1.1:** Diagrams showing the general structure of a tailed bacteriophage (A) as well as a closer look at the tail structure (B). Genetic material is protected by the head, which comprises many capsomere units. The baseplate connects tail fibres with the rest of the tail. Tail fibres are important in the recognition and adsorption of phages to their host cells. Genetic material passes through the inner tail tube following adsorption to enter the host cell, completing the insertion process. Image adapted from Rossmann *et al*. (2005).

Ackermann (2007) carried out an extensive taxonomic study into more than 5000 bacteriophages species. It was concluded that most known bacteriophages (96 %) are comprise a tail (Turner *et al*., 2023). Most of the research into the biology and applications of bacteriophages concerns tailed phages. Despite this, non-tailed phages have been found to be numerous in the marine environment, with up to 92 % of the phages in the upper oceans across the world lacking a tail (Brum *et al*., 2013). Phage tails play a key role in bacteriophage attachment to their hosts and DNA insertion. They are typically made up of several components, such as a central tube encapsulated by a sheath, the end of which is connected to a baseplate out of which tail fibres protrude. Receptor binding proteins (RBP's) are present at the ends of these tail fibres (Ackermann, 2007). For tailed phages, the tail is either contractile or rigid. Tail length can range between 65-570 x 7-10 nm and 20 x 8 nm (Ackermann, 2007).

**Table 1.1:** An example of the now abolished nucleic acid and morphological-based classification system of bacteriophage (ds – double-stranded, ss – single-stranded, L – linear, C – circular, S – superhelical). Families highlighted in red have been abolished.

| Shape | Nucleic acid | Family | Defining features | Example |
|---|---|---|---|---|
| Tailed | dsDNA; L | *Myoviridae* | contractile tail | T4 |
| | dsDNA; L | *Siphoviridae* | long, non-contractile tail | λ |
| | dsDNA; L | *Podoviridae* | short, non-contractile tail | T7 |
| Polyhedral | ssDNA; C | *Microviridae* | conspicuous capsomers | ϕX174 |
| | dsDNA; C, S | *Corticoviridae* | complex capsid, lipids | PM2 |
| | dsDNA; L | *Tectiviridae* | inner lipid vesicle, pseudo tail | PRD1 |
| | ssRNA; L | *Leviviridae* | poliovirus-like | MS2 |
| | dsRNA; S | *Cystoviridae* | envelope, lipids | ϕ6 |
| Filamentous | ssDNA; C | *Inoviridae* | long filaments | fd |
| | | | short rods | MVL1 |
| | dsDNA; L | *Lipothrixviridae* | envelope, lipids | TTV1 |
| | dsDNA; L | *Rudiviridae* | TMV-like | SIRV-1 |
| Pleomorphic | dsDNA; C, S | *Plasmaviridae* | envelope, lipids, no capsid | L2 |
| | dsDNA; C, S | *Fuselloviridae* | lemon-shaped | SSV1 |
| | dsDNA; L, S | *Salterprovirus* | lemon-shaped | His1 |
| | dsDNA; C, S | *Guttaviridae* | droplet-shaped | SNDV |

Initially, phage classification was based purely on observed host ranges. With the advent of electron microscopy, bacteriophage morphologies together with nucleic acid content were also considered, leading to the first classification system. These two features remain major criteria for sorting phages into family ranks. Since the development of efficient and cheap genome sequencing technologies, the number of sequenced phage genomes stored on databases has grown exponentially, leading to genome-based classification schemes such as the Phage Proteomic Tree, phage network clusters and whole genome nucleotide-based grouping. Recently, the Caudovirales class together with the *Myoviridae*, *Siphoviridae* and *Podoviridae* families, were abolished by BAVS with all tailed phages now forming part of the Caudoviricetes class (Turner *et al*., 2023). This is part of a series of moves towards classifying bacteriophages according to evolutionary history.

## 1.2.2 Bacteriophage Functionality

### 1.2.2.1 Host Recognition and Adsorption

Bacteriophages reproduce by inserting their genetic material into their hosts. Once inside, the host cell's transcription, translation and replication proteins interact with phage DNA or RNA to produce new

virion particles. To begin the infection cycle, a phage must first recognise and bind to a suitable host. This is termed 'adsorption'. Many phages demonstrate a two-step adsorption process in which reversible binding is followed by irreversible binding (Bertozzi Silva *et al*., 2016; Yap & Rossmann, 2014). This has most likely arisen as a means of improving the chances of successful adsorption. A phage will first bind reversibly to a host. In the event that its tail fibres do not all successfully bind to surface proteins, it can detach itself from the cell, and adsorption can be attempted again.

RBPs bind to exposed antigens present within the outermost layer of the target cell. In tailed phages, recognition sites are found on the ends of tail fibres. In bacteriophages K3, Ox2 and M1, for example, the protein responsible for adsorption is gp 38, which binds to OmpA, an important structural protein present in the outer membrane of their *E. coli* hosts, initiating the adsorption process (Montag *et al*., 1987). It is believed that adsorption by bacteriophages with contractile tails is mediated by the baseplate. Leiman & Shneider (2012) proposed two mechanisms to explain this. Both rely on the assumption that when in free solution, tail fibres have no fixed orientation. This changes when the phage is adsorbed to a host cell, with the tail fibres all facing the cell surface and pointing away from the virus head, resulting in the baseplate changing to a lower energy conformation. This state facilitates the insertion of genetic material into the host, which will be discussed later in Section 1.2.2. To proceed from the free state to the adsorbed state, it is suggested that one or two tail fibres initially bind to the cell surface. Here, the phage is anchored to the surface but is susceptible to solvent movements and other effects, such as Brownian motion. This gives allows the remaining fibres a chance to bind to their recognition sites so that the phage can assume the adsorbed, irreversible state conformation. It is at this stage of the process, when only attached by a couple of fibres, that attachment is reversible, allowing the bacteriophage to release itself from the host cell should permanent adsorption not be achieved. Studies on the T4 mode of infection support this mechanism (Aksyuk *et al*., 2009; Leiman *et al*., 2004).

A similar mechanism has been suggested for T7 bacteriophage, although in this case, it is believed that adoption of the irreversible state is dependent on two separate signals from the tail fibres and the tail itself, reaching the base plate to initiate a change in conformation (Molineux, 2001). The other mechanism postulated by Leiman & Shneider (2012) derives from the observation that adsorption often

occurs or increases in the presence of divalent cations such as calcium (Kukkaro & Bamford, 2009). The ions bind to cell surface receptors, whose increased surface concentration promotes a baseplate conformational change leading to the tail fibres extending towards the cell surface, which they bind to, resulting in the adsorbed state. Owing to the high level of bacteriophage diversity, various adsorption processes have arisen, such that no single mechanism can apply to every phage.

Bacteriophages have been found to adsorb to almost all parts of the bacterial cell. This includes the walls of both Gram positive and Gram-negative bacteria, bacterial capsules and slime layers as well appendages such as pili and flagella (Guerrero-Ferreira *et al*., 2011; Pickard *et al*., 2010; Shin *et al*., 2012). RBPs play a key role in the host ranges observed in bacteriophages, and alteration of these proteins can result in loss of infectivity against a given host strain (Shin *et al*., 2012). This suggests that changes in RBP's and their corresponding bacterial proteins drive the evolution of phages and their hosts as they adapt to one another. The high specificity of RBPs in relation to their corresponding receptors agrees with the widely reported observation that bacteriophages generally have small host ranges. Despite this, several multiple host species have been reported, including some phages capable of infecting hosts across genera (Bielke *et al*., 2007). Carrying out phage enrichment in the presence of several bacterial strains can isolate phages with larger host ranges (Yu *et al*., 2016).

#### 1.2.2.2 Insertion of Genetic Material

The insertion of phage genetic material into a host cell only takes place once a bacteriophage is irreversibly bound to the cell wall. Following this, a controlled sequence of events involving specific protein interactions takes place, giving rise to insertion. In tailed phages, the tail acts to penetrate the cell envelope and provide safe passage of the DNA or RNA into the host (Kostyuchenko *et al*., 2005; Leiman *et al*., 2004; Molineux, 2001). The proposed mechanisms explaining this process differ between phages. Once the bacteriophage assumes the adsorbed conformation, this initiates the opening of the base of the phage capsid, through which genetic material passes, crossing the tail through the cell envelope and entering the cytoplasm. In phage T7, several proteins have been identified in this process, including

gp7.3, gp14, gp15, gp16 and gp13 (Molineux, 2001). It has been suggested that gp7.3 and gp13 function as 'clogging' proteins, keeping the genetic material sealed until the adsorbed conformation is assumed, resulting in their degradation. Following this, gp14, gp15 and gp16, which are present with the capsid, form complex with each other to form a tube-like structure which penetrates the cell envelop, exposing the cytoplasm. T7 DNA can subsequently travel through the tube into the target cell. In the case of phages with contractile tails, contractile sheaths help drive the tail through the cell envelope (Yap & Rossmann, 2014). In T4 phage, irreversible binding results in subsequent contraction (up to 37 %) of the sheath, which is composed of many repeating gp18 units (Kostyuchenko *et al*., 2003). Degradation enzymes in addition to physical force allow the tail tip to penetrate the cell, into which T4 DNA can now travel. It is believed that contractile tails allow for more efficient infection of host cells. Filamentous phages such as M13, fd and f1 are known to infect *E. coli* host cells by first adsorbing to their F-pilus proteins in the outer membrane through the RBP g3p (Karlsson *et al*., 2003; Lubkowski *et al*., 1999). Since they lack a tail, filamentous phages instead 'pull' on F-pilus proteins and nearby TolA proteins by binding to them using various domains of the g3p protein. This action causes the phage head to insert itself into the inner membrane, following which a protective cap comes off, allowing DNA to enter. With their unrigid, phospholipid-comprised capsids, pleiomorphic phages deliver their genetic material in a unique way compared to their counterparts; by merging with bacterial cell membranes, depositing their contents into the cytoplasm (Ackermann, 2003).

#### 1.2.2.3 Enzymes involved in the Degradation of the Cell Envelope

Whether attempting to infect a host or escape once newly formed within it, bacteriophages need to overcome the obstacle posed by the cell envelope. This refers to the outer layers surrounding the bacterial cell membrane which function to protect the organism from its external environment. In Gram-negative bacteria, an outer membrane surrounds composed primarily of lipopolysaccharides surrounds a rigid peptidoglycan cell wall which, in turn, encapsulates the inner phospholipid bilayer (Silhavy *et al*., 2010). Gram-positive bacteria lack an outer membrane and compensate for this by having a much thicker peptidoglycan layer (Silhavy *et al*., 2010). Phages rely on lytic enzymes to degrade the cell

envelope both from without and within. In some cases, the same enzyme is used for both processes, as has been observed with bacteriophage ϕ6 and the peptidoglycan-degrading enzyme P5 (Mindich & Lehman, 1979).

The first line of defence bacteriophages need to break though is the glycocalyx. This is the outermost layer observed in bacteria and is mainly composed of exopolysaccharide (EPS) fibres (Silhavy *et al*., 2010). It varies in terms of thickness and functions to enhance bacterial mobility and promote biofilm development. Many bacteriophages have EPS-degrading enzymes, including hydrolases and lyases (Roach & Donovan, 2015). The glycocalyx can function to protect the bacterial cell from an immune response by 'shielding' its recognition proteins. It has been suggested that bacteriophage EPS-degrading enzymes can aid the immune system in fighting off bacterial infection by degrading this layer, leaving the cell open to be recognised.

Peptidoglycan (or murein) cell walls consist of alternating strands of N-acetyl-glucosamine (NAG) and N-acetyl-muramic acid (NAM) (Moak & Molineux, 2004). Peptide cross-links join these strands together. Gram-positive bacteria contain much thicker, rigid murein cell walls, which are heavily crosslinked, in contrast to Gram-negative bacteria, which are often just a monolayer in thickness (Silhavy *et al*., 2010). Bacteriophage-encoded muralytic enzymes, known as peptidoglycan hydrolases, are involved in degrading bacterial cell walls (Moak & Molineux, 2004). During infection, virion-associated peptidoglycan hydrolases (VAPGH's), which can be attached to phage components such as the tail or head as well as being present within the capsid alongside the genetic information, begin digesting peptidoglycan following exposure. Peptidoglycan hydrolases consist of a cell binding domain, which binds to carbohydrate components of the cell envelope, whilst a catalytic domain cleaves various bonds. The five major classes of peptidoglycan hydrolases involved in envelope degradation are endo-β-N-acetylglucosaminidase, N-acetylmuramidase, endopeptidase, N-acetylmuramoyl-L- alanine amidase and γ-D-glutaminyl-L-lysine endopeptidase (Rodríguez-Rubio, Martínez, Donovan, *et al*., 2013). In phage T7, one of the domains of protein gp16, which originates from the capsid, possesses VAPGH properties, allowing for cell wall degradation as a channel through the cell envelope is established (Moak & Molineux, 2004). Similarly, the phage head of P22 contains gp4 protein, which

functions in the same way (Olia *et al*., 2006). The VAPGH gp36 of phage ϕKMV forms part of the phage tail (Lavigne *et al*., 2004). An unfolded form of this enzyme is ejected during the infection process. In phage PM2, VAPGH proteins are found in a spherical-based lipid core within the capsid (Kivelä *et al*., 2002).

Lysis from within is enabled through peptidoglycan hydrolases known as endolysins (Rodríguez-Rubio *et al*., 2016). These are coded for by the bacteriophage genome and produced along with other virion components following successful infection. They have a similar structure and function to VAPGH's, and primarily degrade peptidoglycan. Endolysin function is mediated by holin proteins (Wang *et al*., 2000). These act as a molecular clock, responding to triggers to form holes within the bacterial membrane, through which endolysins can pass and begin degrading the cell envelope (Roach & Donovan, 2015; Wang *et al*., 2000). Holins initially occur in a deactivated form, becoming activated as the progeny phage finish their assembly process. The exact triggers that lead to activation remain unclear, however, one likely factor is the energy state of the cell membrane, as has been demonstrated by exposing infected cells to poisons such as cyanide which can trigger the initiation of lysis (Wang *et al*., 2000). By controlling endolytic function, holins play a role in timing lysis such that early lysis, in which phage virions have not yet finished the assembly process, is avoided.

#### 1.2.2.4 Lifecycle

Following successful insertion of genetic material into the host, one of two cycles occurs. In phages which adopt a lytic cycle, the host's metabolic machinery is targeted to replicate the viral genome and produce phage capsids. Virion particles are then assembled. The presence of holins and endolysins, which are coded for by bacteriophage genes, encourage lysis and the subsequent release of phage particles which go on to infect more cells. Phages behaving like this are termed 'lytic' and are associated with relatively quick destruction of their hosts. Temperate phages, on the other hand, enter a lysogenic cycle, typified by the integration of their genetic material into the bacterial genome (Jamal *et al*., 2019). This is carried out by phage integrase enzymes, which cut bacterial DNA or RNA at specific points, allowing for the insertion to occur (Snoeck *et al*., 2019). Bacterial DNA/RNA is cut at the attB site,

allowing for the phage genome, after being cut at attP, to be inserted between the cut ends of attB. Integrases are also able to reverse the process, often in the presence cofactors, to excise the phage genome and induce the lytic cycle.

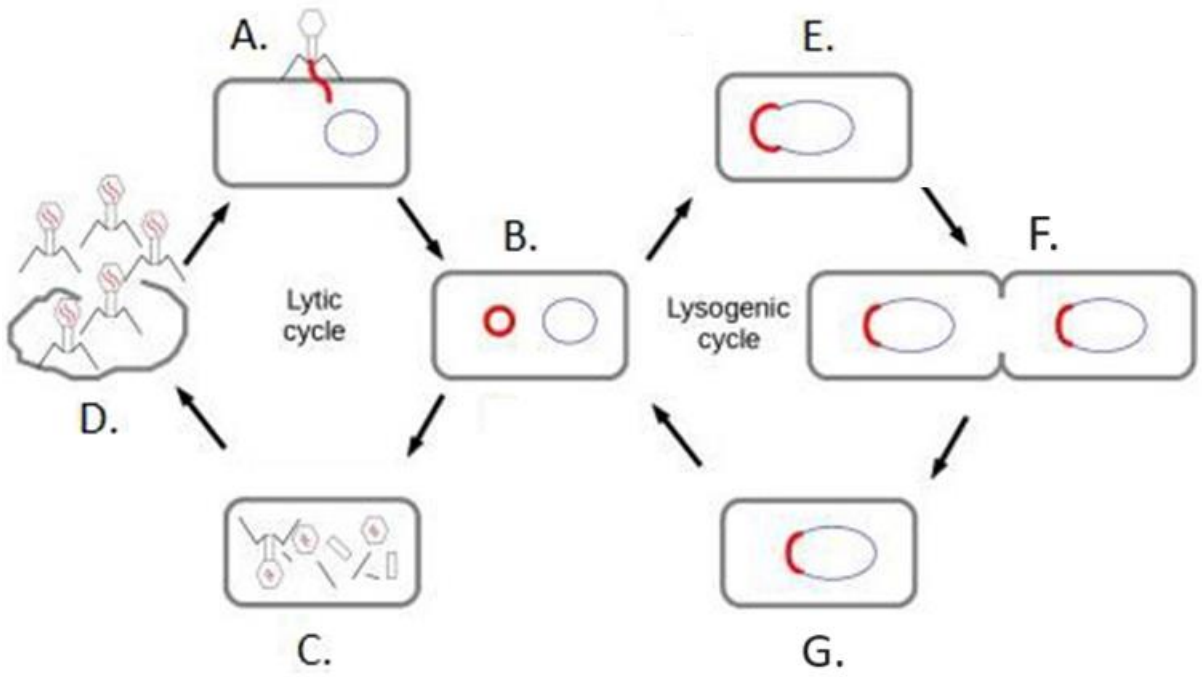


**Figure 1.2:** Lytic and lysogenic phage lifecycles. In the lytic cycle, phage genomic material injected into the host cell (A) gives rise to virion unit construction and assembly using cellular machinery (C). This ultimately results in lysis, with progeny phage being released from the host cell. In the lysogenic cycle, integration of host and phage genetic material takes place after insertion (E). In this state, the phage, now known as a prophage, lies dormant, replicating along with the host as it reproduces (F & G). When triggered, its genetic material is released into the cytoplasm (B) to enter the lytic cycle. Image adapted from Sinha et al. (2018).

When integrated with the bacterial genome, the phage genetic material is known as a 'prophage' which is replicated and passed down through generations as the host reproduces. Specific triggers encourage prophage excision to initiate the production of progeny phages, eventually resulting in lysis from the cell. Lysogeny has been associated with increased bacterial virulence and resistance against other phages and in some cases, has been found to facilitate the acquisition of antibiotic resistance from neighbouring cells (Haaber *et al*., 2016). Regulation between the lytic and lysogenic cycles in temperate phages remains unclear. An increased understanding of the triggers that induce lysis is important to future developments in phage therapy, particularly in cases where lytic phages remain elusive. In this regard, the application of mitomycin c has been reported to induce lysis activity in prophages,

suggesting that lytic activity may be triggered as part of a defence mechanism (Oliveira *et al*., 2017). Filamentous phages are unique in the way they exit the host following propagation. Instead of using lytic proteins to break out of the cell, they are secreted through the cell membrane without lysing the bacteria (Ploss & Kuhn, 2010). This allows for considerably greater production of phage, with filamentous infections of *E. coli* cultures found to produce up to $10^{13}$ virions per mL (Ploss & Kuhn, 2010).

### 1.2.3 Applications and Formulations of Bacteriophage

Most of the research on bacteriophage applications has focused on developing phage therapy as an alternative treatment option to antibiotics. Phages have, however, been applied across other areas too, owing to their unique molecular structures and functions such as specific bacterial recognition, which has been exploited for the development of bacterial biosensors (Gao *et al*., 2016). Furthermore, some popular molecular biology techniques relating to gene and protein studies, are based on exploiting certain bacteriophage proteins as well as virion structure. In addition to therapeutic treatment, their antimicrobial properties have also found use in food preservation (Martínez *et al*., 2019).

An important concept of using bacteriophages to kill pathogenic strains relates to the use of bacteriophage cocktails, that is, the targeting of bacteria with several bacteriophages simultaneously. In cases where a strain develops resistance to one of the phages, it can still be killed by one of the other ones in the cocktail. Experiments have shown cocktails to be considerably more effective than single phage preparations (Chan *et al*., 2013). Further to this is the concept of phage cycling, which involves swapping phages periodically. This has also been shown to reduce the risk of bacterial resistance developing.

Although still relatively new, bacteriophage-based products are starting to be commercialised. These are typically geared towards decontaminating food products and pathogenic detection, and several products are currently available. The development of products for medical purposes has seen slower progress than in other areas. The reasons for this are two-fold: the fact that phages are essentially viruses can make them difficult to market as a treatment option due to negative connotations associated with

viruses in the wider public, and pharmaceutical companies are reluctant to risk investing heavily in a product that consumers may be hesitant to use. In addition to this, even though bacteriophage treatment centres actively using phage-based therapies for patients, such as the Eliava Institute of Bacteriophages, Microbiology and Virology in Georgia and Poland's Hirszfeld Institute of Immunology and Experimental Therapy, there currently exists no formal regulatory framework governing the use of bacteriophages in medical products (Furfaro *et al*., 2018; Hitchcock *et al*., 2023).

**Table 1.2:** Some of the bacteriophage-based products that are commercially available on the market.

| Product | Company | Function/Application |
|---|---|---|
| **SalmoFresh™** | Intralytix | Liquid formulation containing phage cocktail targeting pathogenic *Salmonella* strains for direct application onto high-risk foods such as meat and poultry. |
| **AgriPhage™** | Omnilytics | Liquid formulation containing variable phage cocktails targeting bacteria that cause various plant diseases including tomato spot and apple fire blight. |
| **BioTector** | CheilJedang Corp. | Liquid animal feed additive containing phage cocktail targeting *Salmonella, Clostridium* and *Escherichia coli* strains to increase farming yields. Added to animal feed during manufacturing process. |
| **PGS, PGL, PGE** | Micreos | Liquid formulations of phage cocktails with broad coverage across *Salmonella* (PGS), *Listeria* (PGL) and *E. coli* (PGE) strains. Added to food surfaces post-production or other contaminated surfaces. |
| **PreforPro** | Evogen | Probiotic containing bacteriophage containing a bacteriophage cocktail targeting a broad range of gut bacteria. Administered orally in pill form. |

A challenge relating to incorporating bacteriophages into products relates to their structural and functional stabilisation. Due to their proteinaceous nature, retention of their function is dependent on the preservation of their three-dimensional arrangement. Phages exist freely in aqueous environments; therefore, it follows that if taken out of solution and exposed to harsher conditions as part of a product, phage stability could decrease, resulting in low efficacy. There is growing interest in the immobilisation of phages onto surfaces to stabilise them. Furthermore, some bacteriophage applications are more suited to immobilisation. In phage-based bacterial biosensing, for example, successful detection of the target strain depends on the trapping of bacterial cells onto sensor surfaces, which is only possible if the phages

are bound rigidly to them. Certain medical applications of phages, such as the production of antimicrobial wound dressings, would also be more effective if the phage in question is immobilised to the dressing surface so as to maintain antibacterial activity at the site of infection.

#### 1.2.3.1 Phage-based Biosensing

The high host specificity observed in most phages allows for the discrimination of target strains for biosensing applications. Lysis results in bacterial contents being released into the surrounding area. By using some of these substances, such as ATP, adenylate kinase, galactosidase and glucosidase as markers, the presence of the strain of interest can be confirmed following the application of phage Moghtader *et al*. (2018) managed to confirm the presence *E. coli* K12 cells on gold nanorods by exposing them to T4 phage. The release of biomolecules from host cells following lysis resulted in new bands observed in a Raman spectrum, confirming the presence of the host. VAPGH's and lysins can also be used to directly to initiate cell lysis before detection of the marker (Schuch *et al*., 2002). Alternatively, labelled phages can be used. To this end, *E. coli* phage PP01 was labelled with GFP (Awais *et al*., 2006). The intensity of fluorescence increases following infection of the host due to phage propagation, such that the presence of the bacterial target could be confirmed.

A drawback of tracking internal components of bacterial cells or using labelled phages in the way described is that in phages with exceptionally long latent periods, the time taken to obtain a result can increase. This is not ideal in cases where rapid detection is needed. Furthermore, if the cells are not actively growing, phages will also grow slowly if at all, increasing the risk of a false negative. An alternative, more elaborate means of biosensing using phages is to develop a biosensor. This consists of a recognition element, which is a surface onto which phages have been immobilised, a transducer and a signal processing, amplification and display component. Subsequent trapping of the target bacteria through phage adsorption results in various changes to the surface that can be measured. Guntupalli *et al*., (2008) used MRSA phage as a probe by immobilising monolayers of phage onto glass. Following exposure to the host culture, optical light microscopy was used to measure coverage on the surface, which was directly proportional to the starting concentration of the culture used. Another MRSA

biosensor was prepared by (Tawil *et al*., 2013) through phage immobilisation on a gold surface with surface plasmon resonance spectroscopy used to track increases in plasmon signals following exposure to the bacteria. Other techniques that can be used to track captured bacteria include capacitor impedance and quartz crystal microbalance sensing (Al-Hindi *et al*., 2022; S. Huang *et al*., 2009; Smietana *et al*., 2005).

#### 1.2.3.2 Phage Therapy

Numerous *in vitro* studies demonstrating the effectiveness of bacteriophages in killing antibiotic-resistant bacteria have been reported (Harada *et al*., 2018; Monk *et al*., 2010). In one example, phages CP8 and CP30 were applied to glass-based biofilms of *Campylobacter jejuni*, a major causative agent of gastroenteritis (Siringan *et al*., 2011). More recently, studies involving a 3-phage cocktail demonstrated the efficacy of phages in halting biofilm growth of antibiotic-resistant *Klebsiella pneumoniae* (Zurabov *et al*., 2023). Aside from direct phage treatment, other studies have investigated the use of their encoded VAPGH's and endolysins (Rodríguez-Rubio *et al*., 2016; Rodríguez-Rubio, Martínez, Rodríguez, *et al*., 2013). Interesting *in vivo* results have been reported since phages were discovered, with Hadley's (1928) review summarising early findings. More recently, studies into phage-based products have also yielded promising results. Pyophage, a commercially available phage preparation, was applied through the nasal cavity of a child suffering from cystic fibrosis who had developed a superbug double infection of *Staphylococcus aureus* and *Pseudomonas aeruginosa* (Kutateladze & Adamia, 2008). Treatment was administered three times a day, with symptoms dramatically improving after twenty days and, ultimately, a full recovery. Following *in vivo* experiments, clinical trials represent the next hurdle before the large-scale production and distribution of phage-incorporated medical products can begin. Despite the issues of regulation touched upon earlier, several regulated trials testing such products have been carried out, with more planned for the future (Furfaro *et al*., 2018). Success in clinical trials has not always been as forthcoming, with several high-profile trials failing to demonstrate the efficacy of phage preparations in curing diseases of interest (Rosner & Clark, 2021). Whilst this may be in part due to reasons surrounding poor phage selection and a lack of understanding of the underlying disease, there

is growing consensus that future success in clinical trials will depend on effective delivery of phage therapeutics to the area of infection.

#### 1.2.3.3 Food and Agricultural Safety

Many studies demonstrating the effectiveness of bacteriophages treatments across food and agricultural sectors have been reported (Monk *et al*., 2010). In *Pseudomonas plecoglossicida* infections of Ayu fish, feeding bacteriophage-treated feed pellets has been found to be effective, providing a practical approach for the treatment of large numbers of animals (Park & Nakai, 2003). Phages have been successfully applied against *Erwinia amylovora* infections in apple blossom plants, with the US-based company, Omnilytics, subsequently releasing their 'AgriPhage' product containing a bacteriophage cocktail to treat the pathogen (Svircev *et al*., 2018). Agricultural products incorporating bacteriophages are increasingly being developed and made commercially available as bacteriophages continue to be studied and applied as solutions to bacterial contamination in this sector.

#### 1.2.3.4 Bacteriophage Formulations

As with other protein-based macromolecules, bacteriophages are prone to the effects of protein mis-folding and aggregation as well as denaturation resulting in subsequent loss of functionality when exposed to adverse conditions (Vagenende *et al*., 2009). Previous studies have reported on the sensitivity of phages to organic solvents, pH, temperature, and salinity (Jończyk *et al*., 2011; Litt & Jaroni, 2017; Moghimian *et al*., 2016; Olofsson *et al*., 2001; Silva *et al*., 2014; Taj *et al*., 2014). Several protocols for the long-term storage of free phage have been established by researchers. In general, phages which commonly exist at ambient temperatures can be stored at 4 ˚C for extended periods of time with only limited drops in titer observed in most cases (Ackermann *et al*., 2004; Łobocka *et al*., 2018). It should be noted that survivability is highly variable across bacteriophages, with cases of titers depleting over relatively short amounts of time, even when stored at 4 ˚C (Ackermann *et al*., 2004). Additional preservation is often observed by freezing at -80 ˚C (Jończyk *et al*., 2011). In cases where quick degradation is observed, stability outcomes can be improved using additives such as gelatine, magnesium ions and glycerol (Tovkach *et al*., 2012).

The preparation of bacteriophage formulations for therapeutic delivery presents additional challenges compared to the storage of free phage lysates in the lab. Unlike the latter, which are stored long term in favourable conditions, phage formulations may ultimately be subjected to extreme conditions which will vary depending on their application. In the case of gastrointestinal infections, for example, a therapeutic phage cocktail needs to survive and function in a highly acidic environment, which could prove too adverse for non-formulated phages. Phages existing in dried, non-liquid formulations are generally more stable in the longer term but are still affected by thermal and other stresses, which can produce a drop in titer. Additionally, the actual process by which a given formulation is produced can result in bacteriophage degradation, as exemplified by the processes of freeze-drying and spray-drying (Dini & de Urraza, 2013; Leung *et al*., 2017). All of these factors are considerations in developing stable phage formulations, with the development typically focusing on assessing phage delivery to target bacteria, establishing the extent of the stability a given formulation provides in a range of conditions and improving phage survival during the formulation production process.

Common methods used to produce phage formulations typically rely on some form of encapsulation. This is a broad term that is used to describe various techniques, including emulsification, freeze-drying, spray-drying, liposome encapsulation and electrospinning, in which bacteriophages are coated/surrounded by certain stabilising agents, providing protection against the external environment. Once encapsulated, phages need to be released from the material to target bacterial cells.

As discussed previously, the motivation behind investigating alternative formulations for bacteriophages as opposed to pure lysates revolves around the flexibility this can provide clinicians to deliver phages more effectively at the site of infection and improve patient outcomes. In a localised skin infection, for example, several delivery options are made possible. Emulsion encapsulation would allow for the production of a topical cream to be applied directly at the site of infection (Bean *et al*., 2014; Brown *et al*., 2017). Freeze-drying and spray-drying techniques can be used to produce phage-coated powders, which can then also be incorporated into a cream for direct application, pill-form for oral application as well as incorporation into an inhaler system (Chang *et al*., 2018; Malik *et al*., 2017). Immobilisation could be utilised to produce phage-coated patches for direct application onto the skin (bacteriophage immobilisation is discussed in more detail later). Additionally, there is also the option of applying the

original liquid lysates as either oral drops or as part of a parenteral treatment. Formulations can facilitate viral preservation for longer periods of time in harsher conditions, which facilitates their therapeutic application. A good formulation will also allow for the production of the product at large scale in the knowledge that it can be stored easily with minimal periodical drop in phage titre.

## 1.3 BACTERIOPHAGE IMMOBILISATION APPROACHES FOR PREPARING BIOACTIVE SURFACES

A bioactive surface can be defined as any surface onto which a biological entity has been permanently or temporarily fixed or immobilised, retaining its functionality to provide the surface with its biological properties. A diverse array of biomolecules, including nucleic acids and amino acids, as well as larger proteins, are immobilised onto various surfaces to render them bioactive. There has been considerable interest in enzyme immobilisation; the high diversity of functions observed in this group of proteins makes for many potential applications (Küchler *et al*., 2015; Mohamad *et al*., 2015; Sassolas *et al*., 2012). With their highly strain specific antimicrobial properties, bacteriophages and their encoded proteins are also receiving increased attention as targets for immobilisation, which is particularly useful with respect to the production of antimicrobial surfaces and biosensor devices.

Most of the phage products currently produced are liquid-based. Several potential benefits are acquired through the immobilisation of phages onto surfaces. The stability of bacteriophages when free in aqueous conditions is highly variable; however, effective immobilisation can serve to provide increased longevity over the long term and protect against sudden changes in the surrounding environment (Brown *et al*., 2018; Duyvejonck *et al*., 2021; Leung *et al*., 2018; Ly-Chatain, 2014). Additionally, it facilitates the strategic placement of phages at solid-liquid or solid-gas interfaces, allowing for more applications. In some cases, immobilisation stops phages from aggregating, a stabilising behaviour which arises with changes in aqueous ionic density but which also reduces distribution and, because of this, effectiveness post immobilisation (Pinto *et al*., 2010; Serwer *et al*., 2007).

Early research into adsorption of macromolecules at interphases began in the early 20$^{th}$ century. At the time, adsorption of enzymes and smaller proteins was considered, with researchers studying the effects

of physiochemistry on the extent to which binding took place and how this affected protein function (McClaren, 1954). The field has since diversified, with several approaches emerging for both temporary and permanent immobilisation (Hiep Nguyen & Kim, 2017). Approaches for temporary immobilisation include physical adsorption, electrostatic or charge-based immobilisation and protein-ligand immobilisation, whilst more permanent options include entrapment and covalent linkage. Despite bacteriophage immobilisation being a relatively recent area of research, it has grown substantially over the last 20 years and continues to do so, taking advantage of the groundwork already laid out through research on enzymes.

**Table 1.3:** Studies involving bacteriophage immobilisation using various approaches.

| Type of Immobilisation | Phage | Surface | Advantages/Disadvantages | Reference |
|---|---|---|---|---|
| **Physical Adsorption** | Cocktail | Modified cellulose membranes | Quick and relatively inexpensive approach to bind phages to substrate/process is not directed, increased potential for weak binding. | (Anany *et al*., 2011) |
| **Protein-Ligand** | T4 | Magnetic beads<br>Microcrystalline cellulose beads | Strong binding with controlled orientation, allowing for high binding efficiency for viable phage/complicated process, expensive to scale-up | (Tolba *et al*., 2010) |
| **Electrostatic** | T7 | Cellulose microfibres | Oriented binding of phages to surface, string binding/process expensive to scale-up. | (Vonasek *et al*., 2017) |
| **Covalent linkage** | T4 | Magnetic-fluorescent beads | Strong binding to surface/process more complicated and expensive than physical adsorption. | (Janczuk *et al*., 2017) |
| **Entrapment** | AG10<br>CG4 | Food wrapping paper | Simple process, entrapped phages are stabilised/phages not permanently bound to surface. | (Leung *et al*., 2017) |

In many ways, the challenges faced during enzyme immobilisation are also encountered when immobilising bacteriophages. They need to be fixed permanently such that external physical and chemical effects will not result in the immobilised species being dislodged. In addition to this, they must

be kept in a stable state to ensure that biological function is retained over the long term (Hosseinidoust *et al*., 2014). Bacteriophages, much like enzymes, operate by binding onto protein sites to adsorb onto their hosts. RBPs are usually located in specific regions of the virion. Therefore, spatial orientation post immobilisation also needs to be considered. In the case of tailed phages, 'tail-up' orientation is very much favoured so as not to hinder DNA insertion, with evidence suggesting that controlling orientation can drastically increase the concentration of infective immobilised phage (Ashiani *et al*., 2016; Tolba *et al*., 2010). This does not apply to phages such as PRD1 and PR772, in which RBSs are uniformly distributed on the capsids (Hosseinidoust *et al*., 2011, 2014). The distribution of the phages themselves is also of concern when it comes to immobilisation. Consistent density across the surface is desirable from a research perspective as it allows for more repeatability. Furthermore, phage clustering and non-uniform immobilisation have been observed to hinder bacteriophage function (Naidoo *et al*., 2012). Other considerations include the purity of the phage lysate used for immobilisation. Once grown up, phages are typically removed from a bacterial culture by removing host cells and debris by centrifugation or filtering through 0.22 μm porous membranes (Bonilla *et al*., 2016). Lysates typically contain endolysins as well as small, intracellular proteins, which can reduce immobilisation efficiency by competing with bacteriophages for binding sites. Therefore, it is advisable that purification be carried out prior to immobilisation. Techniques that have been used include dialysis, column chromatography and PEG precipitation (Bonilla *et al*., 2016).

### 1.3.1 Physical Adsorption

Physical adsorption, or physisorption, refers to the adhesion of particles onto a surface brought about by intermolecular interaction such as dispersion forces and dipole-dipole moments, as well as steric and hydrophobic interactions (Cerofolini *et al*., 1998). Dispersion forces, although weak, occur in all molecular species. This makes physical adsorption a ubiquitous occurrence, and consequently, a quick and relatively simple way to immobilise a species onto a substrate without chemically altering the surface. Physiochemical properties of the surrounding environment can have a significant effect on the binding efficiency of physical adsorption. These include physical strain, acidity, temperature and ionic

strength, all of which can act to promote or inhibit immobilisation (Hosseinidoust *et al*., 2014). With regard to temperature, for example, Singh *et al*. (2009) found the density of immobilised phage to decrease by 8 phages/$\mu^2$ after lowering the temperature to ambient from 40 °C.

Unaided physical adsorption refers to the direct application of the adsorbent to an unmodified surface. Some of the succeeding approaches discussed here are also based on the interactions which give rise to physical adsorption, but in these cases, other steps, such as surface pre-activation, have also been carried out to increase effectiveness. The simplicity of unaided physical adsorption means that the sometimes complex preparation steps observed in other processes are avoided. This immobilisation approach typically involves the exposure of the surface in question to a high concentration solution of the absorbate. Bennett *et al*. (1997) carried out some of the preliminary research into phage immobilisation when working to develop a technique for the separation of pathogenic *Salmonella* strains from foodstuffs. Physisorption of the lytic phage Sapphire was achieved by exposing unmodified polystyrene strips to high concentration phage solutions and incubating them overnight. *E. coli* biosensors have been produced in a similar way following the immersion of long-period fibres in bacteriophage T4 lysate (Smietana *et al*., 2005). Unaided physical adsorption is often used as a control when testing out alternative immobilisation strategies (Naidoo *et al*., 2012; Singh *et al*., 2009; Vonasek *et al*., 2017).

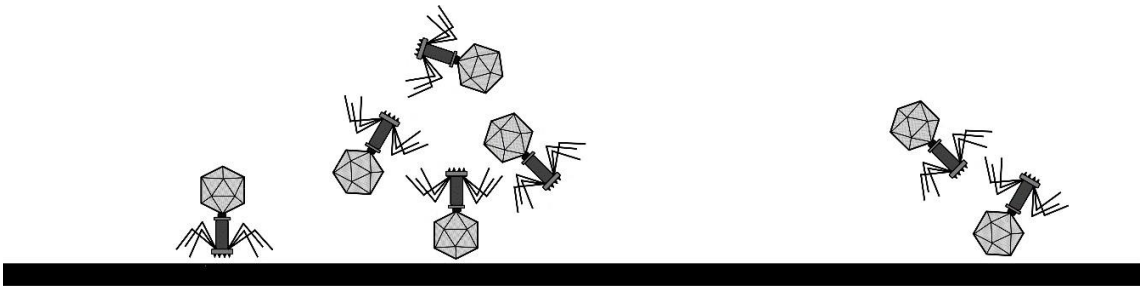

**Figure 1.3:** Physical adsorption of bacteriophages on a surface. Immobilisation is undirected, resulting in inconsistent coating.

One of the drawbacks of this approach is the fact that the process is chemically undirected. The reliance on weaker, random interactions occurring between the phage and surface leaves limited opportunity to direct the process and spatially arrange the attached phage. In most cases, physical adsorption leads to

undesirable disorganised attachment, with adsorbed particles bound in all orientations and with non-uniform spacing. In their comparison of physical adsorption and covalent bond-based immobilisation of cellulase enzyme onto polystyrene, (Hirsh *et al*., 2010) found enzyme unfolding and aggregation to be a common observation in the former. The Langmuir-Blodgett technique has been used as a means of depositing bacteriophages as a monolayer on various substrates (Guntupalli *et al*., 2008, 2011, 2013). This increases uniform spacing between particles, which facilitates the accurate quantification of bound phage and could also increase efficiency in targeting a given host. Using a lytic bacteriophage of *Staphylococcus aureus*, Guntupalli *et al*. (2013) used the Langmuir-Blodgett procedure to develop a simple bacterial sensor capable of detecting the strains in question at a comparable rate to covalently bound phage. The organisation of phages into single layers could also be advantageous with regard to scale-up as a means of reducing phage wastage, therefore decreasing production costs.

Aided physical adsorption refers to techniques that promote the interactions giving rise to physical binding. Dipole-dipole and hydrophobic interactions, as well as electrostatic forces, represent the strongest types of physical binding that occur between a surface and absorbate (Cerofolini *et al*., 1998; Van Voorthuizen *et al*., 2001). Unlike weaker dispersion forces, the occurrence and strength of these three interactions can have a considerable effect on adsorption efficiency. Changing the surface to favour these interactions can therefore help the extent to which bacteriophages adsorb to a surface.

As protein-based entities, bacteriophages consist of both polar and non-polar components. By altering surface layer chemistry to include more polar or non-polar groups, binding efficiency can be improved. The hydrophobic properties of bacteriophages, as with all viruses, depends on the biochemical structure of the capsid. In the case of hydrophobicity, the occurrence of both polar and non-polar amino acid residues makes it difficult to predict. This is illustrated by the opposing results concerning the hydrophobicity of MS2 bacteriophage reported in two separate studies despite both using the same hydrophobicity assay (Farkas *et al*., 2015; Pinto *et al*., 2010; Rosenberg, 2006). Nevertheless, hydrophobic-based adsorption of MS2 has been reported on numerous occasions (Aronino *et al*., 2009; Bales *et al*., 1993; Han *et al*., 2006; Van Voorthuizen *et al*., 2001). Farkas *et al*. (2015) reported on the adsorption of MS2 bacteriophage onto organosilane-coated sand particles. Whilst the phage did not

adsorb strongly to unmodified particles, adsorption increased dramatically following exposure to their hydrophobic counterparts, with the Absorption Index changing from 0.06 to 0.91, as reported by the authors. Limited work has been carried out on other bacteriophages. A reason for this could be fears that hydrophobic interactions can disrupt protein function by encouraging unfolding or alternative folding arrangements, as has been reported for the hydrophobic-mediated immobilisation of enzymes (Wu *et al*., 2011). Most of the cited studies were, in fact, carried out with intention of developing techniques for the removal of viral contaminants. Phage stability was therefore not prioritised.

Just as hydrophobic bonds have high affinity for each other, the same can be said of regions of high polarity. In covalent bonds between atoms of different electronegativities, the electron cloud is distributed unevenly, with either atom assuming a partial positive or negative charge. Opposite partial charges from different covalent bonds are attracted to each other, bringing about dipole-dipole interactions. This activity can be encouraged to aid in phage immobilisation. Polar amino acid side-chains within the capsid are targeted through the alteration of the surface with other polar groups. Singh *et al*. (2009) improved the immobilisation efficiency of T4 on gold surfaces by applying layers of sugars and amino acid coatings, resulting in up to a 7-fold increase in bacteriophage adsorption. Similar loading increases have been observed on gold surfaces with *S. aureus* bacteriophages (Tawil *et al*., 2013). Adsorption has also been enhanced through the addition of phage to printing ink formulations. With polar molecules in the ink resulting in phage retention on the surface following printing (Mangin *et al*., 2008).

Just as hydrophobic bonds have high affinity for each other, the same can be said of regions of high polarity. In covalent bonds between atoms of different electronegativities, the electron cloud is distributed unevenly, with either atom assuming a partial positive or negative charge. Opposite partial charges from different covalent bonds are attracted to each other, bringing about dipole-dipole interactions. This activity can be encouraged to aid in phage immobilisation. Polar amino acid side-chains within the capsid are targeted through the alteration of the surface with other polar groups. (Singh *et al*., 2009) improved the immobilisation efficiency of T4 on gold surfaces by applying layers of sugars and amino acid coatings, resulting in up to a 7-fold increase in bacteriophage adsorption. Similar loading

increases have been observed on gold surfaces with *S. aureus* bacteriophages (Tawil *et al*., 2013). Adsorption has also been enhanced through the addition of phage to printing ink formulations. With polar molecules in the ink resulting in phage retention on the surface following printing (Mangin *et al*., 2008).

### 1.3.2 Charge-based Immobilisation

In charge-directed immobilisation, electrostatic attraction between permanent opposing charges on the surface and adsorbent is used to bring about immobilisation. These are considerably stronger than interactions occurring through the interactions discussed thus far. Bacteriophages are often found to consist of charged regions; phage heads usually possess a net negative charge with the opposite being true for their tails (Anany *et al*., 2011; Van Voorthuizen *et al*., 2001). They have been shown to bind tail-down or tail-up, depending on the net charge present on the surface (Cademartiri *et al*., 2010). It follows that the application of positive charges to surfaces is a favoured strategy in order to bind phages in the desired orientation.

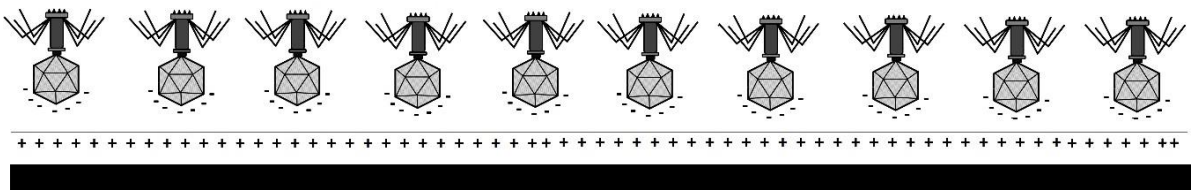

**Figure 1.4:** Charge-directed immobilisation. The negatively charge phage capsids electrostatically bind to cationic layers, resulting in a preferable 'tail-up' orientation of bound phage.

Anany *et al*. (2011) carried out charge-based immobilisation of phage cocktails targeting *E. coli* and *Listeria* host strains. Phage cocktails of different concentrations were applied to cellulose disks pre-treated with 0.5 % wt/vol polyvinylamine polymer. It was concluded that the net positive charge on treated surfaces led to increased immobilisation.

Similar results were also reported by Cademartiri *et al*. (2010), and Vonasek *et al*. (2017). Owing most likely to the relative strength of electrostatic interactions, comparison studies show this to result in more

phage binding compared to other reversible approaches (Vonasek *et al*., 2017). On the other hand, it has been shown to perform less efficiently than covalent-based immobilisation (Bone *et al*., 2018). The technique can be applied in conjunction with other immobilisation approaches as a means of guaranteeing the desired bacteriophage orientation with enhanced attachment strength (Zhou *et al*., 2017). A recent study found that the application of alternating current across a gold surface functionalised with polar molecules resulted in a dense, ordered layer of phages in tail-up conformation (Richter *et al*., 2017).

As with physical adsorption, electrostatic binding is also influenced by physiochemical properties of the medium, such as ionic strength and pH, which can directly affect protein charge through the isoelectric effect, as shown by (Peng *et al*., 2011), who increased the pH level in the surrounding medium beyond the isoelectric point of tobacco mosaic virus. The negative charge on the phage heads was increased, leading to increased tail-up orientation on gold surfaces.

### 1.3.3 Protein-Ligand Immobilisation

The natural tendencies of proteins to adsorb to certain ligands can be exploited to for the purpose of bacteriophage immobilisation. The surface and absorbate are coupled with a binding protein and its corresponding ligand, respectively, with the interaction and subsequent immobilisation occurring once they encounter one another.

Streptavidin is a protein that occurs in the bacterium *Streptomyces avidinii* (Tytgat *et al*., 2015). It has a very strong affinity for biotin, a vitamin involved in several metabolic processes, and binds to it through one of the strongest non-covalent interactions known (Houk *et al*., 2003). Protein-ligand interactions like this have been used for bacteriophage immobilisation (Ashiani *et al*., 2016; Cademartiri *et al*., 2010; Gervais *et al*., 2007; Horikawa *et al*., 2011; Ong *et al*., 1989; Tolba *et al*., 2010). Ligands such as biotin are normally crosslinked to bacteriophages through ester activation with N-hydroxysuccinimide (NHS) and other carboimmides. NHS-biotin reacts with primary amines found in side-chains of amino acids such as lysine, as well as terminal amino groups of polypeptides, resulting in the permanent attachment of biotin. This covalent process is known as biotinylation and there are

numerous examples of it being carried out with enzymes (Sassolas *et al*., 2012; Tran *et al*., 2015).

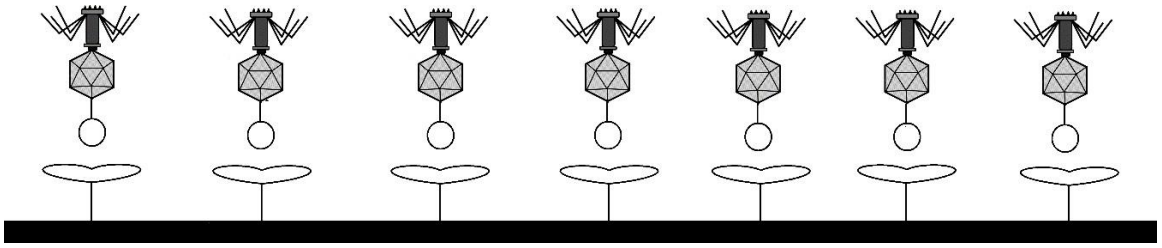

**Figure 1.5:** Scheme showing protein-ligand immobilisation. The incorporation of a binding protein with the phage head facilitates immobilisation with ligand-coated surfaces.

Alternatively, the gene coding for the ligand or binding protein of interest can be integrated with the bacteriophage genome. Tolba *et al*. (2010) fused the genes *bccp* and *cbm*, which code for biotin carboxyl carrier protein and cellulose binding domain, respectively, with the *soc* gene of T4 phage. The protein coded for by *soc*, small outer capsid protein, forms part of the phage capsid, resulting in the expression of biotin carboxyl carrier protein or cellulose binding protein on the T4 head, which permitted subsequent affinity immobilisation onto respective streptavidin and cellulose-comprising surfaces. Coupling a phage with a binding agent this way allows for the strategic positioning of the latter. This is especially relevant to tailed phage immobilisation, in which having the viruses fixed in the 'tail-up' orientation is desired. The major downside to this approach is the complexity of the procedure, which would require time to plan out and execute effectively before moving on to immobilisation. In addition to this, altering a phage's genome can potentially result in undesired changes to its activity, such as a decreased burst size and an extended latency period (Tolba *et al*., 2010). Bacteriophage attachment using protein-ligand interactions has been shown to be effective, with Gervais *et al*. (2007) reporting a 15-fold increase in phage binding compared to unaided physisorption. Despite this, one comparison with electrostatic-based attachment found the latter to be more effective (Vonasek *et al*., 2017).

### 1.3.4 Entrapment and Layer-by-Layer Assembly

Entrapment involves the biological species being contained within an insoluble, microporous layer such as hydrogel, which is then applied onto the surface. Despite it being a non-covalent technique, it is

considered irreversible since the absorbate is essentially trapped within the layer, providing increased protection against harsh conditions. Entrapment has been carried out to a limited extent with regard to bacteriophage immobilisation. Leung *et al*. (2017) encapsulated three phages targeting *Listeria*, *Salmonella* and *E. coli* strains in a pullalan-trehalose formulation for use as a coating. In this state, phage infectivity was preserved for up to 3 months. The main concern with entrapment with respect to immobilisation is that by trapping the viruses within an insoluble layer, contact and subsequent adsorption with target bacterial cells is unlikely unless the phages happen to be situated at or close to the surface of the entrapping layer. Nevertheless, an antibacterial wound dressing material, PhageBioDerm, consisting of an entrapped phage cocktail, has been developed and is commercially available (Guang-Han *et al*., 2016).

Layer-by-layer assembly refers to the layering of weak polyelectrolytic substances. Layers possessing opposite charges are stacked on top of one another, with bacteriophages applied in between each layer. Success with this approach has been reported with bacteriophage M13, in which the authors report on the formation of a consistent monolayer at the top surface due to the phages migrating through the layers (Yoo *et al*., 2006). It was found that coating substances with a higher tendency to permit the movement of particles through the layers were more suited to monolayer formation.

### 1.3.5 Covalent and Cross-linker (Covalent)

All of the approaches discussed so far have not involved the alteration of substances through the formation of new chemical bonds. Covalent immobilisation represents the most permanent and irreversible form of attachment. It is often cited as the most effective immobilisation approach for both bacteriophages and enzymes, with one study reporting a 37-fold increase in phage binding efficiency with covalent attachment compared to unaided physical adsorption (Hirsh *et al*., 2010; Singh *et al*., 2009).

Bacteriophages react covalently through amino acid residues protruding from their viral capsids. These include carboxylic groups from glutamine and aspartic acid, amines from lysine, sulfide groups from cysteine and phenols from tyrosine (Lee & Wang, 2006). In some cases, phages have been observed to

bond on mere exposure to certain substrates. M13 phage, for example, readily binds to sulfur particles covalently through carboxylic acid functional groups on glutamine and aspartic acid residues (Chen *et al*., 2013). It should be noted that spontaneous reactions with substrates are a rare occurrence; in most cases, phages need to be encouraged to form bioconjugates, which are subsequently immobilised onto the surface. This is similar to the biotinylation technique described in section 2.2.3, except in this case, the phage is cross-linked directly to the surface as opposed to an affinity- binding protein. As with protein-ligand immobilisation, carboiimide-based cross-linking is often favoured as a means of bioconjugation in covalent-based immobilisation (Bone *et al*., 2018; Hosseinidoust *et al*., 2011; Janczuk *et al*., 2017). Janczuk *et al*. (2017) used EDC to activate carboxylic groups on magnetic fluorescent beads. Subsequent phage attachment via lysine residues resulted in the formation of amide linkages to EDC. Non-carbodiimide-based cross-linkers that have been applied to bacteriophage immobilisation include glutaraldehyde and maleic anhydride (Pearson *et al*., 2013; Singh *et al*., 2009).

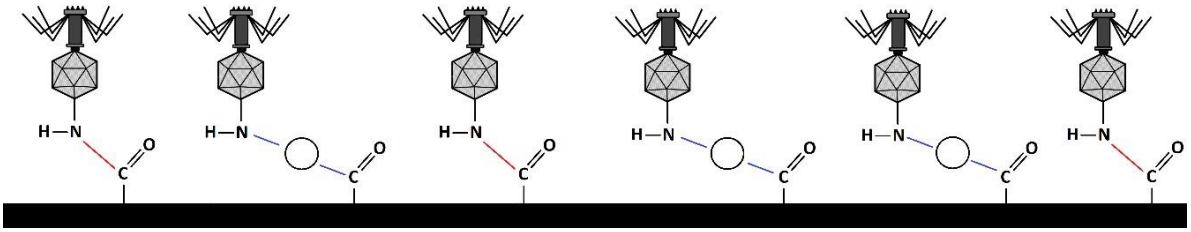


**Figure 1.6:** Covalent immobilisation of phages occurs through direct reaction of amino acid residues protruding from the phage capsid with functional groups on the surface (red bonds), or indirect linker-based attachment (blue bonds).

The direct covalent binding of bacteriophages to surface in the absence of cross-linkers has also been reported (Nogueira *et al*., 2017). Here, the authors attached vB_Pae_Kakheti25, which is lytic to *Pseudomonas aeruginosa*, onto polycaprolactone fibres. Fibres were subjected to acidic conditions prior to bacteriophage attachment, and effective killing of the host was observed even after 25 rinses, demonstrating the robustness of the attachment. Simpler processes such as the one described are appealing as a means of producing bioactive surfaces on a large scale. One of the more recent approaches for covalent attachment of biological substances centres around the plasma treatment of surfaces to mediate immobilisation (discussed in Section 1.4).

The main drawbacks to covalent attachment arise from the potential disruptions to phage activity after

bond formation. If bonding occurs with a residue in close proximity to the phage adsorption site, this can get in the way of subsequent adsorption to the bacterial host. Adsorption can also be disrupted by the rigidity of the bond, which reduces movement of the phage, on which it is believed to be reliant (see Section 1.2.1). On the other hand, evidence does suggest that covalent linkage acts to stabilise bacteriophages over the long term. In addition to this, physiochemical effects are much less likely to interfere with the process. When it comes to direct comparison studies between covalent and non-covalent methods, most of them have concluded that the former is considerably more efficient in terms of binding efficiency and bacteriophage stability.

## 1.4 PLASMA-MEDIATED IMMOBILISATION OF BIOLOGICAL ENTITIES

The ionisation of gaseous particles through electron bombardment results in the formation of plasma (Bitterncourt, 2004). Gas in this state typically consists of a mixture of ionised particles, free electrons and radicals. Plasmas can be generated by electrically charging electrodes beyond a threshold level, after which they to discharge. Due to the large amount of high energy particles within plasma, it can react with and cause chemical changes on surfaces it is applied to (Thissen, 2015). Corona discharge is a low power electrical discharge occurring close to or at atmospheric pressure (Veldhuizen & Rutgers, 2001). It forms when small diameter electrodes, such as needles and wires, are coupled with high voltages. A resultant plasma region between the electrodes arises, together with a characteristic hissing noise.

The application of plasma results in chemical changes occurring on treated surfaces (Collaud *et al*., 1994). These can be exploited to permanently coat surfaces with substances of interest. In general, plasma has been found to allow for substances to be deposited consistently, resulting in the production of a layer of uniform thickness and limited damage to the adsorbate (Favia & D'Agostino, 1998).

As the applications for plasma treatment continue to broaden, research into plasma-mediated immobilisation of biomolecules has emerged as an area of great interest (Bilek & McKenzie, 2010). The biological entities most commonly considered for plasma-mediated immobilisation include oligonucleotides, polypeptides and enzymes (Frenzel *et al*., 2017; Hirsh *et al*., 2010; Tran *et al*., 2016;

Yeo *et al*., 2017). Examples of it being used for bacteriophages remain few and far between. However, one study has shown it to be effective in attaching T4 phage to polyhydroxyalkanoate surfaces (Wang *et al*., 2016). Compared to chemical-based immobilisation, plasma offers a simpler, quicker approach which, in some cases, has been found to be equally or more effective in terms of binding efficiency. The use of plasma as a means of carrying out linker-free immobilisation is of particular interest to researchers. Of the various plasma techniques available, there remains limited research into the corona discharge-mediated immobilisation of biomolecules and microorganisms.

### 1.4.1 Chemical Characteristics of Plasma

Plasma refers to gas in which a large proportion of atoms and molecules exist in an excited state. When a plasma is generated, electron impact collisions lead to the formation of radicals and positively and negatively charged ions (Bitterncourt, 2004; Zhang *et al*., 2019). Radicals contain unpaired valence electrons, making them highly unstable species that, in most cases react spontaneously when they encounter other particles. This, coupled with continuous ionization processes, makes for a dynamic system in which a large variety of reactions occur simultaneously. Radicals and other reactive species together with electrons bring about surface modification when they come into contact with a material. In air plasma, common active species derive from free oxygen and nitrogen gas. These include ozone ($O_3$), nitrous oxide ($N_2O$), nitrogen oxide (NO), nitrogen dioxide ($NO_2$), nitrous and nitric acid ($HNO_2$ and $HNO_3$) and dinitrogen pentoxide ($N_2O_5$). These species can break down into positive, negative and neutrally charged particles, as demonstrated below:

**Table 1.4:** Common products that form following the collision of electrons and other gaseous species in plasma. Collisions can result in the removal of an electron from a species, producing a positive charge. They can also result in the splitting up of molecules into base atoms.

| Reaction | Products |
|---|---|
| $\mathbf{e + N_2}$ | $N_2^+ + e + e$ |
| | $N + N + e$ |
| $\mathbf{e + N}$ | $N + e$ |
| | $N_2^+ + e + e$ |

| | |
|---|---|
| $\mathbf{e + O_2}$ | $O + O + e$ |
| | $O_2^+ + e + e$ |
| $\mathbf{e + O_3}$ | $O + O_2 + e$ |
| $\mathbf{e + O}$ | $O^+ + e + e$ |
| $\mathbf{e + H_2}$ | $H + H + e$ |
| | $H_2^+ + e + e$ |
| $\mathbf{e + H_2O}$ | $H_2O^+ + e + e$ |
| | $OH^+ + H + e + e$ |
| | $O^+ + H_2 + e + e$ |
| | $H_2^+ + O + e + e$ |
| | $OH + H + e$ |

Of particular significance to negative corona discharge is the generation of ozone gas (O3) which, as is observed in low power plasmas, is one of the major by-products when carried out in unaltered air (Chen & Davidson, 2003; Pavlovich *et al*., 2014). Other important chemical species include hydrogen peroxidase and hydroxyl species, which both contribute to functional group formation on surfaces. The former arises from the ionisation of water molecules, meaning its concentration within the plasma is linked to the humidity in the surrounding air (Liu *et al*., 2016).

The chemical processes occurring within the plasma are numerous and complex. A comprehensive study discussing the reactions occurring within air plasma and their kinetics was carried out by (Maulois *et al*., 2016). Reactions and the occurrence of certain species are heavily influenced by the constituents of the surrounding gas, as well as variables in the generation of plasma. In their comparative study on plasmas generated in various gases, (Takamatsu *et al*., 2014) found that carbon dioxide generated the most singlet oxygen, argon produced the most hydroxyl (OH) radicals, whilst a nitrogen-oxygen gas mixture produced the most nitrous oxide (NO) of the gases tested. The high variability in results can make plasma studies difficult to replicate. Furthermore, when it comes to industrial applications, most plasma processes are carried out in atmospheric air (Pignata *et al*., 2017). This is simpler and more cost effective, but differences in air composition across geographical regions as well as variations brought about by weather changes make consistent treatment results challenging from a quality control perspective (Zhang *et al*., 2019).

1.4.2 Effect of Plasma Treatment on Polymer Surface Chemistry

Materials can be treated by corona discharge by placing them in the inter-electrode space as plasma is generated. For most studies on surface changes as well as industrial processes, a sheet of the material in question is passed under the corona source electrode using an automated flat-bed, which also functions as the collecting electrode, in a wire-to-plane configuration. The corona-generated plasma, which contains a mixture of electrons, ions and radicalised gas particles, bombards the material's surface. Reactive species encountering the surface react with it, resulting in the generation of new polar functional groups following treatment. The identity of these functional groups depends on the contents of the plasma, which can vary depending on the components of the gas from which the corona discharge is generated.

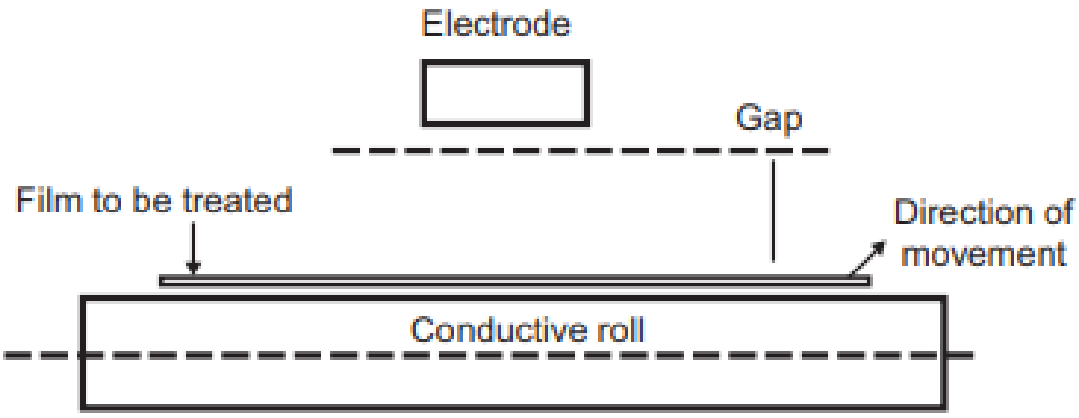


**Figure 1.7:** Wire-to-plane schematic for corona discharge treatment of polymer sheets.

In the case of unaltered air, it is predominantly oxygen reactive species that interact with the surface. O'Hare *et al*. (2002) reported on the incorporation of several oxygen-containing functional groups on corona discharge-treated polypropylene surface, namely hydroxyls (-OH), carbonyls (-C=O]), peroxy's (-C-OO), esters (-C-O-C-O), carboxylanes (-COO-) and carbonate (OC(O)O). These results agree with those of other studies on various polymeric surfaces. However, species' proportional representation on the surface varies (Comyn *et al*., 1996; Hillborg & Gedde, 1998; Iwata *et al*., 1988; Kalapat *et al*., 2013). When it comes to the identification of functional groups, the spectroscopic techniques most favoured are X-ray photoelectron spectroscopy (XPS), secondary ion mass spectrometry (SIMS) and Fourier

Transform Infrared spectroscopy (FTIR) (Morent *et al*., 2008). Using either of the latter two in conjunction with XPS represents an effective way of getting a full picture of the chemical situation on the surface and just below it (XPS penetrates the top layer, yielding information from depths between 5 – 10 nm). This is relevant due to the tendency for layers in soft polymers to reorganise themselves, with new functional groups migrating below the surface (Hillborg & Gedde, 1998) In some silicone-based polymers, this can happen within minutes of treatment (Natyanun & Pussadee, 2018).

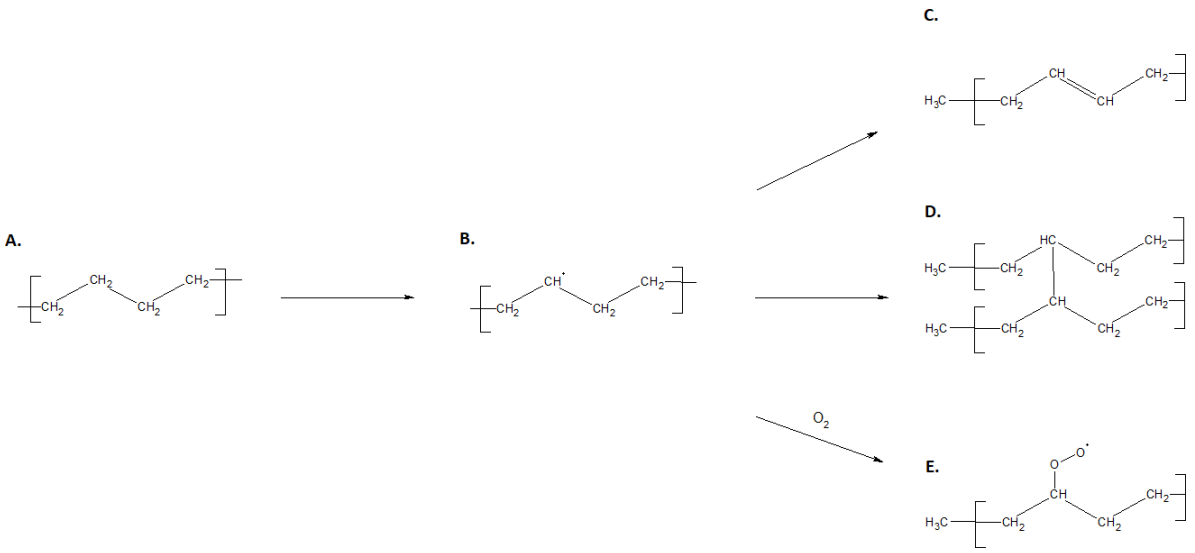


**Figure 1.8:** Mechanism for some common plasma-mediated reactions on polymers. These include hydrogen abstraction (A to B) for the formation of free radicals on the surface. These free radicals can induce further hydrogen abstractions on adjacent carbon atoms (B-C), resulting in unsaturation on the surface, abstraction on other molecules resulting in crosslinking (B-D) and Image adapted from Kuzuya *et al*. (1993). Species present in the air can be attacked by the surface radical resulting in their incorporation onto the surface (B-E).

Radical formation in organic polymers typically involves hydrogen abstraction from surface carbon atoms. Once these are generated, several types of reaction path may ensue. The polymer can form new bonds in the absence of external species provided by the corona. The radicalised carbon species can attack adjacent atoms, resulting in another hydrogen abstraction. This leads to the formation of a double bond. A loss of saturation is, in fact, often observed in saturated polymers following plasma treatment. Alternatively, hydrogen abstraction can take place across polymer chains, which produces crosslinks. The free radical can also react with gaseous molecules in the air, initiating the formation of functional groups. Reactive species from the plasma can also interact with the polymer, which results in new

functional groups being formed. These different pathways can be exploited in order to influence the final product. For example, by altering the air such that it contains a volatile organic compound, this can be made to radicalise and deposit on the polymer's surface to produce a graft polymer.

The introduction of polar functional groups results in a surface of increased wettability and surface energy (Lehocký *et al*., 2003). Recording these changes has become standard in corona discharge and other plasma-based studies. This is usually done by taking water contact angle measurements, which typically reduce as the surfaces become more polar. After treating polyethylene with dielectric barrier discharge treatment for 5 seconds, (De Geyter *et al*., 2007) recorded a contact angle reduction of 48.2 °. This corresponded to a surface energy increase of 24.9 $mJ/m^2$. The extent to which surface energy increases is related to the amount of energy used for a given pass (see equation 1). When treating polypropylene using corona treatment, Kalapat *et al*. (2013) observed that the extent to which surface energy increased was proportional to the discharge energy applied.

Equation 1.1 $$Corona\ Discharge\ Energy\ (J/mm^2) = \frac{Power\ delivered\ (J/min)}{Linear\ Speed\ (mm\backslash min) \times electrode\ width\ (mm)}$$

Covalent bonds are permanent, and therefore surface energy changes following treatment would be expected to remain unaltered. However, molecules situated below heavier oxidised layers can diffuse to the surface, covering the modified surface. This, together with molecular rotation, in which functional groups rotate to face inwards, results in the recovery of hydrophobicity following treatment. After an initial increase in surface energy following corona treatment, polypropylene surface energy was found to decrease slightly after 90 days (Kalapat *et al*., 2013). The highest recorded energy drop was reported to be 7.8 $kJ/m^2$. Such decreases in surface energy can be much more dramatic in soft polymers such as polydimethylsiloxane, in which hydrophobic recovery has been observed to initiate immediately after treatment (Hillborg & Gedde, 1998). Crosslinking reduces electron rotation, disrupting hydrophobic recovery. As with surface energy, the extent to which crosslinking occurs depends on the amount of energy being used to drive the plasma. More high-energy plasma techniques such as plasma-immersion

ion implantation (PIII) have been shown to promote crosslinking more than others (Bilek & McKenzie, 2010).

As already discussed, the initial formation of surface radicals is what encourages functional group formation. These can be analysed using electron spin resonance spectroscopy (ESR), as was demonstrated by Kuzuya *et al*. (1993) in their post plasma treatment analysis of polyethylene. Here, ESR analysis was used to identify mid-chain alkyl as well as allylic radicals arising on the surface. Similarly, plasma generated polypeptides were analysed using ESR following treatment with argon plasma (Kuzuya *et al*, 1993). Radicals resulting from hydrogen abstraction from glycine (-CO-C˙H-NH-), L-alanine (-CO-C˙H-$CH_2$-NH-) and L-serine (-CO-C˙H-$CH_2$-OH-NH-) residues were identified. Wakelin *et al*. (2015) analysed surfaces of medical grade polyether ether ketone (PEEK) following PIII treatment. They observed an initial increase in surface radical density which was proportional to treatment time. As functional oxygen and nitrogen groups started forming following exposure to air, radical density was found to decrease. A permanent presence of radicals was observed to remain on the PEEK surfaces, with both functional group and radical densities appearing to stabilise after approximately 1000 minutes of ageing time. A simpler method of assessing radical activity on surfaces involves the use of stable free radical molecules such as 2,2-diphenyl-1-picrylhydrazyl (DPPH), which reacts with free radicals resulting in the pairing of its lone electron and a colour change at about 320 nm (Hristea *et al*., 2006; Kedare & Singh, 2011). DPPH was used to assess radical content of PIII- treated polypropylene prior to oligonucleotide immobilisation (Tran *et al*., 2016). Increased stabilisation of radicals can be achieved by increasing surface exposure time to plasma treatment as well as storing treated surfaces in vacuum conditions (Bilek & McKenzie, 2010). Retention of free radicals on surfaces of corona discharge-treated materials remains understudied.

### 1.4.3 Plasma-mediated Attachment of Biomolecules

The two major forms of plasma treatment relevant to the attachment of biomolecules are direct plasma treatment and plasma-enhanced chemical vapour deposition (PE-CVD) (Favia & D'Agostino, 1998). In the former, cold plasmas using reactive or inert gases such as oxygen, nitrogen, water vapour argon

and helium are generated and used to treat a surface. As discussed in the previous section, the result is a thin layer of grafted polar functional groups. PE-CVD involves feeding volatile, often organic or silica-based, compounds into the plasma chamber for deposition onto the surface. The coating layer that forms from this process is relatively thick (up to $10^3$ nm) and comprises monomer (this term refers to the chemical being used) fragments which have reacted with and formed part of the surface. Both these processes change the surface dramatically and, depending on the route followed, can allow for immobilisation of biomolecules of interest.

As a technique, corona discharge has been applied for various purposes such as the neutralisation of static charges, manufacture of ozone, sanitation of pool water and industrial printing of plastic packages. Despite this, it has thus far been neglected as a means of immobilising biological entities when compared to other forms of plasma treatment. The few studies that have been carried out have focused on its ability to aid in physical adsorption through polar group formation (Comyn *et al*., 1996). (Lee & Lee, 2008) observed that polyethylene treated with corona discharge in air retained adsorbed albumin on its surface more effectively than its untreated counterparts following rinsing with tetronic 1504. In the same study, the authors reported on the new hydrophilic properties of the sheets as conducive to more efficient spreading of bacterial cell on the surface, facilitating analysis of their growth process.

Covalent attachment has been successfully carried out using other forms of plasma treatment (Bilek & McKenzie, 2010; Kondyurin *et al*., 2018; Pearson *et al*., 2013; Tran *et al*., 2016). As with chemical-based approaches discussed in Chapter 3, this can be achieved through linkers. In their covalent immobilisation of phages T1 and ϕ11, Pearson *et al*. (2013) first grafted maleic anhydride onto polyethylene and polytetrafluoroethylene surface using microwave plasma. This acted as a linker through amide bonding with amine residues on the phages. (Wang *et al*., 2016) used reactive ion etching on polyhydroxyalkanoate surfaces for EDC/sulfo-NHS linker-based immobilisation of T4 phage. The linker was attached to the surface either through a reaction with plasma generated carboxylate groups on the surface or through graft polymerisation of acrylic acid with the subsequent addition of the linker. T4 bacteriophage was then covalently bound to the surface. The authors of this study compared immobilisation efficiency of plasma-treatment with and without linkers. An interesting observation was

the higher efficiencies for immobilisation performed in the absence of linkers. Considering the drawbacks of using linkers to attach biological entities, this has considerable implications for plasma-based techniques in biological immobilisation.

Linker-free immobilisation can occur through direct reaction of the adsorbate with free radicals on the surface, resulting in covalent bond formation (Hirsh *et al*., 2010). Alternatively, the vaporised absorbate monomers can be exposed to plasma treatment before their graft polymerisation onto the surface, as demonstrated by Pegalajar-Jurado *et al*. (2014) with 1,8-cineole onto silicone and glass slides. Whilst the latter has been shown to work with simpler organic molecules, direct treatment of complex proteins, enzymes and bacteriophages could result in a loss of function or neutralisation. Of the plasma-techniques available, PIII is heavily favoured for linker free covalent immobilisation (Bilek & McKenzie, 2010). This is most likely because it promotes crosslinking, which acts to reduce hydrophobic recovery, reducing the loss of modified layers and retaining free radicals more effectively (Hirsh *et al*., 2010). The way this is typically carried out is through direct exposure of PIII-treated surfaces to the adsorbate, with the simplicity of the process making it especially appealing. Tropoelastin immobilised onto polyethersulfone (PES) this way was found to be strongly adsorbed whilst retaining its biofunctionality (Yeo *et al*., 2017).

## 1.5 ANALYSIS OF IMMOBILISED BACTERIOPHAGE

The evaluation of surfaces containing immobilised phage is an important aspect of the analysis that is carried out following the production of these bioactive materials. Analysis can either be quantitative, in which bacteriophage surface concentration is determined, or it can concern more qualitative features such as orientation and bond characteristics of covalent attachment. These respective analyses yield important information, allowing for the evaluation of the immobilisation technique used and comparison with other approaches.

### 1.5.1 Quantification

A diverse array of approaches have been used for quantifying immobilised bacteriophage. Activity assays are amongst the most common tests carried out (Cademartiri *et al*., 2010). These involve considering inevitable consequences of phage-host interactions, such as the cytotoxic effect, and developing an assay for quantification. To this end, (Mangin *et al*., 2008) evaluated the amount of gravure-printed T4 phage on paper squares by observing zones of clearing following incubation on the bacterial lawn. From this simple analysis, the authors concluded that gravure cell volume did not make a difference in the amount of phage immobilised; however, notable clearing was only recorded for immobilisation carried out using lysates of at least $10^7$ PFU/mL, suggesting that this was the minimum starting concentration for effective killing of the *E. coli* host. The same group carried out similar tests for a subsequent study testing the effectiveness of a cationic pre-coat layer (Jabrane *et al*., 2009). Alternatively, the effect of phage-immobilised material on decreasing bacterial growth can be tested in solution (Nogueira *et al*., 2017). This allows for more effective enumeration compared to measuring clearing on plates, as the decrease in viable bacteria can be tracked. For immobilisation onto smaller surfaces such as silica pellets, simple dilution of the activated material in a suitable buffer followed by plaque assays can suffice, although thorough rinsing to remove any unbound phage should be carried out prior to this (Cademartiri *et al*., 2010). For larger surfaces, such as sheets and fibres, the amount of phage rinsed off can be compared between controls and immobilisation treatment. Any differences would indicate the amount of permanently bound phage using the given immobilisation approach. This was carried out by (Vonasek *et al*., 2017) to quantify phage immobilised onto electrospun cellulose nanofibers. Another assay-based method could involve considering phage-host binding. This interaction results in the trapping of bacterial cells on the surface. Therefore, counting the number of bacterial cells removed from a culture following exposure to a phage-immobilised surface can indicate the amount of phages immobilised on the material surface. Activity assays are indirect and, as such, are prone to more errors than more direct alternatives. On the other hand, since they rely on successful binding or infection of the bacterial host, they allow for the quantification of viable phages only.

Approaches which cannot differentiate between viable and non-viable phage include molecular

techniques such as quantitative PCR (qPCR) (Kłopot *et al*., 2017). When selecting a bacteriophage gene to track using this procedure, those coding for structural coat or tail proteins are generally favoured over those coding for enzymes (Tolba *et al*., 2010). A drawback of qPCR as a means of quantifying immobilised phage is the difficulty in achieving consistency in results and the relatively cumbersome nature of sample preparation. Furthermore, whilst it can be applied to bacteriophages with well-characterised genomes such as T4 or M13, working with a less studied phage would require the sequencing of the genome and gene analysis to select a suitable reference gene.

Various types of microscopy, including scanning electron microscopy (SEM), transmission electron microscopy TEM and atomic force microscopy (AFM), have been used to quantify immobilised phage (Horikawa *et al*., 2011). Singh *et al*. (2009) used SEM to visualise the bound phages and estimate phage density on each surface. In a similar study, Naidoo *et al*. (2012) report on using SEM to quantify phages T4, P22 and NCTC12673 on functionalised gold and their bacterial hosts following exposure to the newly produced bioactive surfaces. The staining of bacteriophages with fluorescent dyes allows for their visualisation and quantification using fluorescence microscopy (Singh *et al*., 2009; Zhou *et al*., 2017). Wang *et al*. (2016) used this approach to quantify SYBR green-stained T4 phage on polyhydroxyalkanoate (PHA) surfaces. Using analytical software packages to quantify phages based on fluorescence intensity could potentially remove bias, which is an unavoidable consequence of direct counting methods such as these. This has been demonstrated by Bone *et al*. (2018).

Spectroscopic analysis is often used to confirm the presence of phage on surfaces following immobilisation through the identification of spectral bands emerging due to functional groups such as carbonyls (-C=O) and amines ($-NH_2$) groups, which are ubiquitous in proteins. Although normally used as a qualitative tool, it can potentially also be applied for quantification purposes. Hirsh *et al*. (2010) used FTIR to compare normalised amide peak intensities as a means of quantifying immobilised cellulase enzyme on polystyrene surfaces. The authors confirmed the effectiveness of covalently bound enzymes in remaining attached following successive SDS rinses. This was not the case for their physically adsorbed counterparts, which were successfully removed from the polystyrene surface. It should be noted that as of yet, there has not been any reporting of vibration spectroscopic techniques

such as FTIR and Raman spectroscopy for accurate quantifying of immobilised phage. X-ray photoelectron spectroscopy, on the other hand, could potentially be applied for this purpose by considering unique oxygen peaks arising due to trapped water inside the protein coats of bound phages. This has been used by Wang *et al*. (2016) to compare quantities of T4 phage immobilised onto polyhydroxyalkanoate surfaces through various methods. Mass-sensitive techniques relying on quartz crystal microbalances (QCM) have been used to track bacterial capture in biosensors (Dixon, 2008; Guntupalli *et al*., 2013; Olsson *et al*., 2016). The technique may also find use in the real-time enumeration of phages as they are immobilised onto a surface. Surface plasmon resonance have been used for this purpose (Tawil *et al*., 2013). The ability to be used in real-time tracking of phage immobilisation could uncover new information concerning the kinetics of phage attachment.

### 1.5.2 Qualitative Analysis

Microscopic analysis represents the only direct way to confirm the orientation of immobilised phage. Electron microscopy is the technique most used in this regard (Bone *et al*., 2018; Cademartiri *et al*., 2010; Tolba *et al*., 2010). Bone *et al*., (2018) made use of TEM to analyse T4 bacteriophage bound to silica particles. The resultant image showed phage heads bound to the substrate, suggesting that amide coupling between the phage head and the activated silica surface had occurred, as desired by the authors. Similarly, SEM has also been used to elucidate information concerning the orientation of bound phage. (Singh *et al*., 2009)immobilised modified T4 onto streptavidin-coated gold surfaces by inserting a ligand-protein in the phage head. SEM imaging was used to visualise the bound phage and confirm the 'tail-up' orientation.

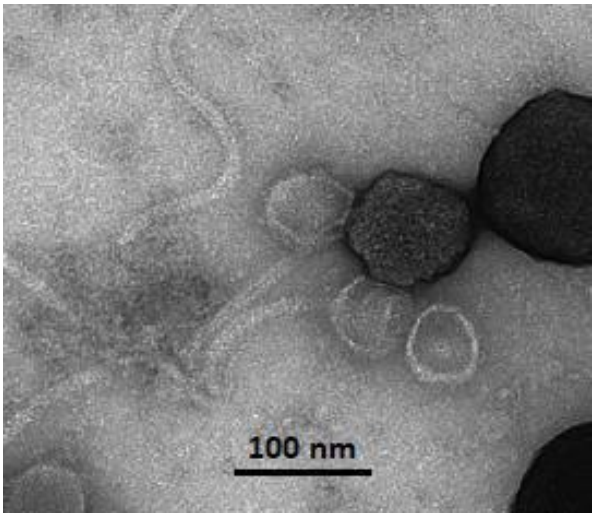


**Figure 1.9:** TEM image showing phage AG11 immobilised in tail-up orientation on APTES-functionalised silica particles. Image obtained from Cademartiri *et al.* (2010).

Fluorescent microscopy has been utilised to ascertain quantitative information indirectly, as demonstrated by Wang *et al*. (2016) when they tracked SYBR green-stained *E coli* 11303 host cells on polyhydroxyalkanoate (PHA) surfaces containing immobilised T4 phage. Having already determined the surface density of phages, also through SYBR green staining, the authors could then compare this with the amount of trapped host cells observed. Bacterial capture was less than what was expected, given the amount of phage on the surface, leading to the conclusion that some of the phages were unable to bind to the bacteria due to their orientation not being conducive to host binding.

Aside from bacteriophage orientation, other qualitative-related experiments include the characterisation of new bonds formed in covalent-based immobilisation. Circumstantial evidence of covalent binding can be obtained through rinsing experiments with protein rinsing agents such as SDS (Bilek & McKenzie, 2010; Kratz *et al*., 2015). Substances such as these disrupt binding interactions between proteins that are physically adsorbed to surfaces. Covalent bonds remain unaffected, with surfaces retaining more phage activity than their physically adsorbed counterparts. Many phage immobilisation studies include rinsing data as proof of covalent immobilisation taking place (Cademartiri *et al*., 2010; Farkas *et al*., 2015; Vonasek *et al*., 2017). Whilst this is useful circumstantial evidence, it cannot be used to characterise the bonding interaction taking place. For this, spectroscopic techniques have proven to be a useful asset. As already discussed, many covalent-based approaches result in the formation of a

amide linkage between the bacteriophage and the underlying substrate. FTIR has been used by Pearson *et al*. (2013) to obtain proof of these linkages by showing the Amide I and II bands obtained following the immobilisation phages T1 and ϕ11 onto activated polyethylene and polytetrafluoroethylene. Similarly, Nogueira *et al*. (2017) reported on the immobilisation of vB_Pae_Kakheti25 phage on polycaprolactone nanofibers, showing amide-generated FTIR bands. An issue with FTIR is the difficulty that can be encountered in differentiating bands occurring due to newly formed linkages from those due to amide bonds within the phage protein coat. For this reason, XPS is generally preferred as using this technique, every chemical state of a given elemental on and just under the material's surface is considered. This means that subtle differences in the energy state of amide bond-forming atoms, which correspond to their location in the phage or on the surface, can also be considered. After exposing M13 bacteriophage to sulfur particles, Chen *et al*. (2013) used XPS in conjunction with FTIR to conclude that binding between the phage and substrate occurred through the establishment of covalent bonds between O-C=O groups from glutamate or aspartate amino acids and sulfur, resulting in S-O and C-S covalent bonds. Furthermore, after the immobilisation of *S. aureus* phage onto polyethylene glycol-functionalised gold nanoparticles, XPS analysis confirmed the covalent attachment of the phages through amide linkage between phage amine groups and carboxyl groups present on PEG (Tawil *et al*., 2013). XPS has been used on numerous occasions in the assessment of bound biological substances and its use in conjunction with vibrational spectroscopy is well documented (Chen *et al*., 2013; Dutta *et al*., 2016; Tran *et al*., 2016; Wang *et al*., 2016). Other spectroscopic techniques which have been applied to the analysis of bonding interactions include solid-state nuclear magnetic (ss-NMR) resonance and time of flight secondary ion mass spectrometry (TOF-SIMS), although these are yet to have been used in the case of immobilised phage (Coad *et al*., 2013; Fauré *et al*., 2014; Martin *et al*., 2018).

### 1.6 PROJECT AIM AND OBJECTIVES

As a field of study, the production of antimicrobial materials through bacteriophage incorporation has received considerably more attention in recent years. Despite this, several unmet challenges remain. In terms of quantification, limited work has been carried out to develops simple, *in vitro* methods for

enumerating viable phages in the immobilised state. In most cases, activity has been demonstrated qualitatively by showing reductions in bacterial growth or quantitatively through complicated microscopy-based methods or overly simplistic application of the plaque assay to solid substrate. Both of these approaches cannot be relied on for accurate quantification of viable, immobilised phages, which is be required to study and optimise the immobilisation process.

As plasma-based approaches to immobilise biological entities become increasingly favoured, there is a need to investigate more broadly the relationship between surface activation and immobilisation. This is likely to be vary considerably depending on the substrate, particle being immobilised as well as the plasma process considered. The work detailed in this thesis focuses specifically on the relationship between corona discharge-mediated activation of plastic surfaces and subsequent binding of bacteriophages, making it the first study of this kind. Furthermore, whilst the development of bacteriophage formulations is not a new field of investigation, the effects of formulation components on bacteriophage shelf-life, drying durability and distribution in the context of corona-discharge mediated immobilisation remains understudied.

Aside from a handful of clinical trials, mainly using unformulated bacteriophage cocktails, the application of bacteriophages in real-world applications remains an understudied area. This is especially relevant to immobilised bacteriophages, for which the majority of work carried out has typically involved small-scale *in vitro* studies. There is a need for demonstrable outcomes using immobilised phage-based products in an up-scaled context to illustrate their applicability to wider industrial processes.

The aim of this project was to assess corona discharge (a form of plasma discharge treatment) as an immobilisation technique for bacteriophages on polymeric surfaces. The major objectives that were carried out to achieve these are listed below:

1. Establishing reliable methods for the quantification of bacteriophages in the immobilised state.

Work was carried out to develop assaying techniques for the enumeration of viable bacteriophages associated with substrates. The aim was to develop protocols that were relatively quick and simple to perform, so they could form a major aspect of all other experiments performed for this project.

2. Demonstrating the ability of corona discharge to immobilise bacteriophages.

This involved determining the effect of corona discharge treatment on various polymeric film surfaces. Following this, experiments were carried out to prove that such treatment encourages the irreversible binding of bacteriophages onto considered substrates. The ability of immobilised bacteriophages to retain their infectivity was also considered.

3. Improving the stability and distribution of bacteriophage post-immobilisation

Experiments focused on using formulations to improve the post-immobilisation survival of bacteriophages specifically after drying, as well as over extended periods of storage. The ability of selected formulations to promote phage distribution over film surfaces was also considered.

4. Demonstrating the efficacy of immobilised bacteriophage in a real-world application

The work in this chapter involved the scaled-up immobilisation of bacteriophages onto food packaging films. Experiments to demonstrate the effectiveness of a free-phage cocktail in slowing salad leaf spoilage was carried out by a trial involving salad bags incorporating the immobilised phage cocktail.

# Chapter 2: Development and Verification of *In vitro* Enumeration Protocols for Immobilised Bacteriophages

## 2.1 INTRODUCTION

Quantifying bacteriophages in liquid lysates is a straightforward process. The plaque assay technique is the most favoured procedure used to this day, owing to its simplicity as well as accuracy, and has been established as a standardised method of bacteriophage quantification (Baer & Kehn-Hall, 2014). More elaborate methods for quantifying free phage include the use of nanoparticle tracking analysis (Sausset *et al*., 2023). The incorporation of bacteriophages onto/into solid substrata is a relatively new field of study and, as such, limited research has been carried out into establishing reliable methods for enumerating bacteriophages in the immobilised state. Quick and accurate quantification is key to the study and optimisation of the immobilisation process and is therefore prioritised for this opening chapter, the central aim of which is to develop a verifiable assay for viable, immobilised phages.

Some advanced techniques have been reported on with respect to determining phage surface concentration. These include microscopic techniques such as SEM, TEM, AFM and fluorescence microscopy (Gervais *et al*., 2007; Horikawa *et al*., 2011; Hosseinidoust *et al*., 2011; Naidoo *et al*., 2012; Singh *et al*., 2009; Zhou *et al*., 2017). Limited use of advanced spectroscopic techniques including XPS and QCM has also been reported (Evoy *et al*., 2010; C. Wang *et al*., 2016). Whilst microscopic and spectroscopic techniques offer interesting alternatives for the quantification of immobilised phage, they are not necessarily straightforward to perform, and the equipment required is considerably expensive and not always readily available. This justifies the need for simple, *in vitro* techniques than can be carried out in a laboratory without advanced equipment.

The nature of the substrate onto which phages are bound to can present certain obstacles to successful enumeration. Where smaller particulate surfaces such as powders are concerned, plaque assays can potentially be used as a means of quantification by suspending a known quantity of the substrate in liquid and diluting from there. This was demonstrated by Cademartiri *et al*. (2010), who quantified phages bound to modified silica particles in this manner. The extent to which this can be extended to other powder-based substrates is unclear. Vonasek *et al.* (2017) quantified T4 phage bound to cellulose fibres by sonicating in phage buffer and quantifying phages in the resulting liquid through plaque assays. A concern with this approach is the effect of sonication on bacteriophage viability, which could result

in an underestimation of phage concentration, as well as incomplete dissociation of the fibres such that effective dilution during the plaque assay is hindered. This is especially relevant in the case of polymer films, due to their considerably larger size. Indirect counting methods such as comparisons between amounts of phage rinsed off for immobilised and control groups can be used to approximate phage concentration within a material, as demonstrated by Vonasek *et al*. (2017). Much like free phage, immobilised phage concentration can also be estimated using qPCR (Cademartiri *et al*., 2010; Kłopot *et al*., 2017; Tolba *et al*., 2010). Microscopic imaging represents the most direct means of determining the concentration of immobilised phage on the surface (Naidoo *et al*., 2012; Tawil *et al*., 2013; Tolba *et al*., 2010). In the case of SEM, TEM and AFM-based techniques, sample preparation time as well as equipment costs render the quantification through imaging unsuitable in cases where large numbers of samples require processing. In addition to challenges with consistency, a major draw-back of the techniques discussed so far is the inability to distinguish between viable and non-viable bacteriophages.

To assay for viable bacteriophages on a surface, their activity needs to be tracked over time. This can then be compared with standards of known quantities to estimate the number of active phages present on or in the material. There are several ways this can be carried out. Nogueira *et al*., (2017) immobilised phage PCL-vB_Pae-Kakheti25 onto wound dressing fibres and tracked cytotoxic activity agiainst the phage's corresponding *Pseudomonas aeruginosa* host to determine whether phage surface concentration remained stable following successive rinses. As demonstrated by Bennett *et al*. (1997), biosorbents consisting of immobilised phage can be used to remove strains of interest from a solution through phage-host binding. In the authors' case, this was carried out to remove *Salmonella* from food materials as opposed to quantifying the phages present, however, this approach could theoretically be utilised to quantify phages present on/in a material based on the number of host cells removed from a solution of known concentration. More elaborate means of tracking immobilised phage activity involve the use of surface plasmon resonance, cyclic voltammetry, electrochemical impedance spectroscopy and crystal quartz microbalances (Farooq *et al*., 2018; Guntupalli *et al*., 2013; Tawil *et al*., 2013; Wang *et al*., 2022). In these cases, the trapping of host cells onto surfaces containing viable, immobilised phages results in changes to the refractive index, electrical properties and mass of the surface in

question. These changes can be detected and standardised against phage immobilisation standards using the respective techniques.

For this section of work, 2 activity-based assays are described and attempted. The underlying principle behind these assays is that of 'equivalence bacteriophage loading'. This term refers to the establishment of free phage activity standards to which the sample being tested can be compared to. The result of the assay refers not to the actual number of phages immobilised on a piece of material, but rather, the free phage concentration that it is equivalent to in terms of activity. The first assay is based on bacteriophage growth. At the end of the latency period, a lytic event occurs, resulting in the phage progeny bursting out of their host cells. This corresponds to a rise in bacteriophage concentration which can be detected through plaque assays. Assuming a consistent starting host cell concentration, the increase in bacteriophage concentration following the first burst is dependent on the initial number of viable phages. By determining the post lysis concentration for a range of starting phage concentration standards, the equivalent loading concentration for the material containing immobilised phage can then be determined by comparing post lysis concentration with those of the standards. The other assay attempted is based on the same principles, with cell death being considered instead of bacteriophage growth. This is tracked by measuring changes in turbidity of an incubating culture in terms of optical density as cells propagate or die.

The bacteriophages T4, T5, ST3 and PLS27 were considered for the assays being attempted. T4 and T5 formerly belonged to the now defunct *Myoviridae* and *Siphoviridae* phage families, respectively (Yap & Rossmann, 2014; Zivanovic *et al*., 2014). They infect strains of *Escherichia coli* and represent two of the more well studied bacteriophages, featuring frequently in academic publications. ST3 infects the *Salmonella enterica* serovar typhimurium 50498. This phage is a NexaBiome lab isolate, with this work representing the first time it has been studied in any detail. PLS27 is a type-phage originally isolated by Jarrell & Kropinski (1981). It belonged to the *Podoviridae* before the family was abolished and infects *Pseudomonas aeruginosa* AK44. Demonstrating the applicability of an assay to multiple phages is key to the establishment of a standardised protocol for immobilised phage quantification. It is anticipated that an assay which is shown to be accurate and efficient will be applied as the primary quantitative tool

for future experiments forming part of this collection of works.

## 2.2 MATERIALS AND METHODS

### 2.2.1 Materials and Instruments

Nutrient agar and broth (Sigma Aldrich, UK); Brain Heart Infusion agar and broth (Sigma Aldrich, UK); Tryptic Soy agar and broth (Sigma Aldrich, UK); bacteriological agar (Sigma Aldrich, UK); 250 mL conical flasks (Fisherbrand, UK); chloroform (Fisher, UK), phosphate buffered saline (Gibco, UK); bacteriophages T4, T5, ST3 and PLS27; *Escherichia coli* 11303; *Salmonella enterica serovar typhimurium* 50498; *Pseudomonas aeruginosa* AK44; 0.22 µm syringe filter units (Thermofisher, UK); Stericup quick-release 0.22 µm filter unit (Millipore, UK); MaxQ 6000 orbital incubator (Thermo Scientific, UK); Whirlimixer vortex spinner (Nickel-Electro ltd, UK); Heraeus megafuge 16 centrifuge (ThermoScientific, UK); Snakeskin dialysis membrane (ThermoScientific, UK); 1 grade filter paper, sterile loops (Fisher, UK); 50 mL Falcon tubes (Fisher, UK); 20 uL, 200 uL and 1000 uL Rainin pipettes (Mettler Toledo, UK); 0.22 µm Stericup filtration units (Merck Millipore, UK); Ultrospec 10 Cell Density Meter (Biochrom, UK).

### 2.2.2 Bacteriophage Propagation and Purification

To prepare host working cultures, single cell overnight cultures were prepared from cryobead and glycerol stocks. After being allowed to thaw, a single cryobead was removed and streaked over agar within a Petri dish, as described by Ogodo *et al*. (2022). In the case of glycerol stocks, whilst still frozen, a small amount of the stock was scraped off using a sterile loop before streaking on agar plates using the same technique. After overnight incubation at 37 °C, a single colony from the resulting plate streak was removed and transferred to a 50 mL Falcon tube containing 10 mL of sterile broth. This was left to incubate overnight at 37 °C and an rpm of 100 to 220 in an orbital shaker to obtain a working overnight culture. Nutrient media were used for *E. coli* propagation while *S. enterica* was grown using brain heart media. Tryptic soy media were used for *P. aeruginosa*. Plate streak outs were stored at 4 °C and used for preparation of fresh cultures for up to 1 week before and re-streaking.

The bacteriophages considered for this study were propagated using plate overlays. 100 µL of high concentration (> 1 x $10^8$ PFU/mL) bacteriophage solution was placed at the centre of an agar plate using a pipette. Following this, 2.5 mL of a 1:10 host cell to soft agar solution was placed onto the agar plate and spread evenly by gently rotating the plate before leaving to dry. At least 10 plates were produced in this manner for a given bacteriophage. As with the bacterial host cells, nutrient media were used to propagate T4 and T5 phages with brain heart media being used for ST3. Tryptic soy media was used for PLS27. After being left to incubate at 37 °C overnight, the plates were checked to confirm that no bacterial growth had occurred across the top layer (indicating successful phage growth). 8 mL of phosphate buffered saline (PBS) were then placed over each top layer, with the Petri dishes being and left to stand at 4 °C overnight to allow for sufficient transfer of phage from the top layer into the buffer solution. The PBS was then collected from the plates, passed through a 0.22 µm filter and collected. After quantification through a plaque assay, the phage lysate was purified using a dialysis membrane (Baer & Kehn-Hall, 2014). Once secured inside the membrane, the lysate was placed into a large beaker containing PBS at a 100:1 volume ratio and left to stand at 4 °C for 1 - 2 days. The PBS solution was replaced three times during the dialysis process. On removal, purified lysates were filtered through a 0.22 µm membrane using a Stericup filtration unit and stored at 4 °C until further use.

### 2.2.3 Characterisation of Bacteriophage Growth

Single step growth curves were carried out to determine the point at which lysis occurs following exposure of a host strain to a given bacteriophage. To achieve this, phages needed to be exposed to log phase host cells, such that following absorption and injection of the phage genetic material, viral synthesis, assembly, and lysis would ensue unhindered. To prepare log phase bacterial cultures, 100 uL of overnight culture were placed in 50 mL Falcon tubes containing 10 mL of broth. The tubes were placed slanting in an orbital incubator at 37 °C and an rpm of 150. Host cell cultures were left to grow until demonstrating an absorbance of 0.4 at 600 nm before being exposed to phage.

Prior to carrying out the phage growth curves, the concentration of the log phase *E. coli*, *S. enterica* and *P. aeruginosa* strains at an OD 600 of 0.4 was determined using the method detailed by Miles *et al*.

(1938). To initiate the growth curve experiment, 100 uL of log phase host cells were added to 50 mL Falcon tubes containing 10 mL phage in sterile broth at a multiplicity of infection (MOI) of 0.01. The phage solutions were quantified using a plaque assay prior to addition of the bacteria (this was assumed to be the bacteriophage initial concentration ([T = 0])). Care was taken to ensure the broth was preheated to the relevant growth temperature (37 °C in all cases) before introducing the host cells. Following addition of the bacteria, the phage-host mixture was homogenised by gently inverting the universal tube once. A timer was started, and the tube was placed at a slant in the orbital incubator at 200 rpm and 37 °C. 500 µL aliquots of the phage-host mixture were sampled using sterile 2 mL syringes at 5-minute intervals over an hour. Each aliquot was immediately filtered through a 0.22 µm syringe filter into an Eppendorf tube and stored at 4 °C. After all the aliquots corresponding to each time point were collected, plaque assays performed on them. The resultant phage concentration values were recorded and graphs plotting phage concentration against time were constructed (see Figure 2.3). These were then used to determine the time taken for each of the phages considered to complete a lytic cycle at the given conditions. This was identified by selecting a time point 5 minutes after the initial bacteriophage spike in phage concentration (from henceforth this time point will be referred to as T(l)).

### 2.2.4 Equivalence Loading Based on Bacteriophage Growth

50 mL Falcon tubes containing 10 mL of broth and bacteriophage at a range of concentrations ($x10^0$, $x10^2$, $x10^4$ and $x10^6$ PFU/mL) were prepared and preheated to 37 °C. 100 µL of a log phase culture (OD 600 = 0.4) of the corresponding host were added to each tube. Following gentle mixing by a single inversion, the tubes were placed, slanting, inside the orbital incubator set to 200 rpm and 37 °C. The tubes were left to incubate until the T(l) point of phage in question. In the case of T4 and ST3, this was reached after 25 minutes of incubation while for T5, this was observed on the 35-minute mark (see Figure 2.3). On reaching the T(l) point, aliquots were removed from each of the tubes and filtered through 0.22 µm membranes. Phages were then quantified using plaque assays. After the data was collected, the T(l) concentration was plotted against the initial phage concentration (Figure 2.4).

2.2.5 Equivalence Loading Based on Cytotoxicity

50 mL Falcon tubes containing phage in broth were prepared in the same way as detailed in the previous section. 100 µL of log phase host culture (OD 600 = 0.4) were added to the tubes. The tubes were left to incubate over a 2-hour period, with OD readings taken every half an hour. After the data was collected, graphs plotting absorbance at 600 nm against time were constructed for the three phages at the x $10^0$, x $10^2$, x $10^4$ and x $10^6$ PFU/mL concentrations.

2.2.6 Assay Verification

Following the analysis of the initial equivalence loading results, it was decided that the assay based on bacteriophage growth would be taken forward (see Sections 2.3.2). For each phage, the equivalence loading protocol described in Section 2.2.4 was carried out across a range of initial bacteriophage concentrations spanning 8 logs ($10^0$ PFU/mL to $10^8$ PFU/mL). A sample size of 35 was considered for bacteriophages T4 and T5 whilst 21 samples were used for ST3 and PLS27. Initial concentrations were determined using plaque assays. Graphs plotting assayed initial concentrations determined using the equivalence loading assay against actual initial concentrations (as determined by the plaque assays) were constructed. A Wilcoxon matched pairs signed rank test was carried out on the assayed and actual data sets for each phage to determine whether they differed significantly from each other.

## 2.3 RESULTS AND DISCUSSION

2.3.1 Characterisation of Bacteriophage Growth

All strains considered demonstrated standard aerobic bacterial growth, entering the log phase within a couple of hours of incubation and growing steadily over the 7-hour period (Figure 2.1). A concentration of roughly $10^8$ colony forming units (CFU) per mL was recorded for each strain once an OD 600 of 0.4 was reached (see Table 2,1). *E. coli* 11303 took approximately 3.5 hours to reach the desired absorbance, with *S. enterica* 50498 taking about 30 minutes to 1 hour less. *P. aeruginosa* AK44 was the slowest growing of the three, reaching an absorbance of 0.4 after 4 hours. These times were cut by about an hour and a half each when broth was preheated, and rpm increased to 200 (all subsequent experiments

were carried using these altered conditions to conserve time). The OD 600 absorbance reading of 0.4 was chosen to ensure that the host cells in question would be firmly in the log phase. This sufficed for the strains considered, however, for slower growing bacteria, such as *Helicobacter pylori* and certain strains of *Bartonella*, the latter of which can take weeks to reach growth saturation, a lower absorbance reading would need to be selected to make assaying more manageable (Lagier *et al*., 2015). This would also apply to anaerobic bacteria, which are generally slower growing than their aerobic counterparts (Eberly *et al*., 2022).

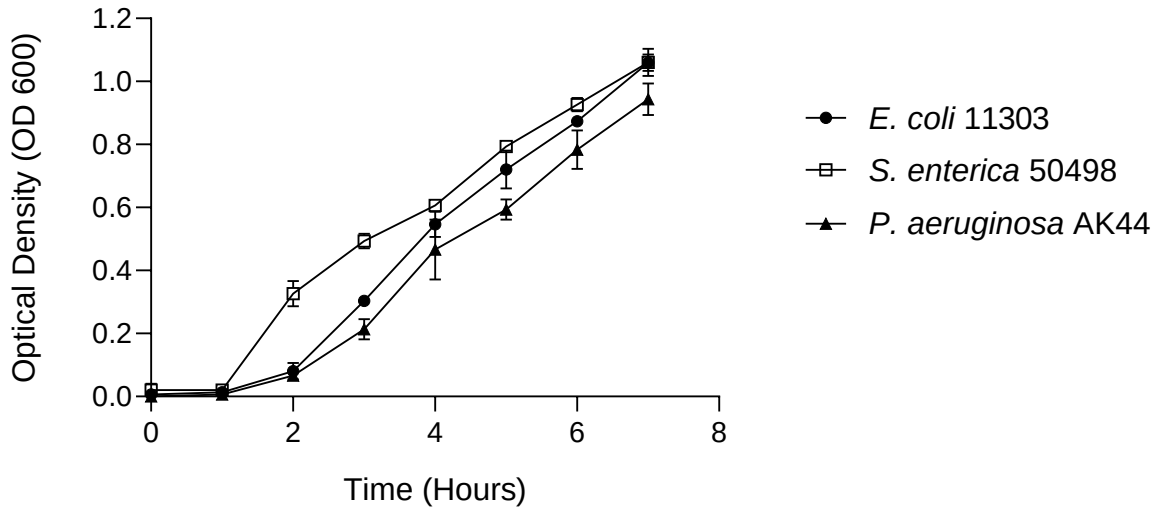


**Figure 2.1:** Graph showing growth of host strains *E. coli* 11303, *S. enterica* ser typhimurium 50498 and *P. aeruginosa* AK44 in terms of optical density at 600 nm over time. Optical density measurements were taken every hour for each strain over 7 hours. All cultures were incubated at 37 °C at an rpm of 150 (n = 3).

**Table 2.1:** Concentrations of bacterial host strains at an optical density (OD 600) of 0.4.

| Bacterial Host | Optical Density (OD 600) | Concentration (CFU/mL) |
|---|---|---|
| *E. coli* 11303 | 0.4 | 3.87E+08 ± 9.81E+07 |
| *S. enterica* 50498 | 0.4 | 4.07E+08 ± 1.37E+08 |
| *P. aeruginosa* AK44 | 0.4 | 4.63E+08 ± 1.82E+08 |

All four bacteriophages yielded clear, observable lytic plaques during plaque assay enumeration (Figure 2.2). These typically presented as circular clearings on the bacterial lawn which could be counted in order to determine bacteriophage concentration as per the standard plaque assay protocol followed (Baer & Kehn-Hall, 2014).

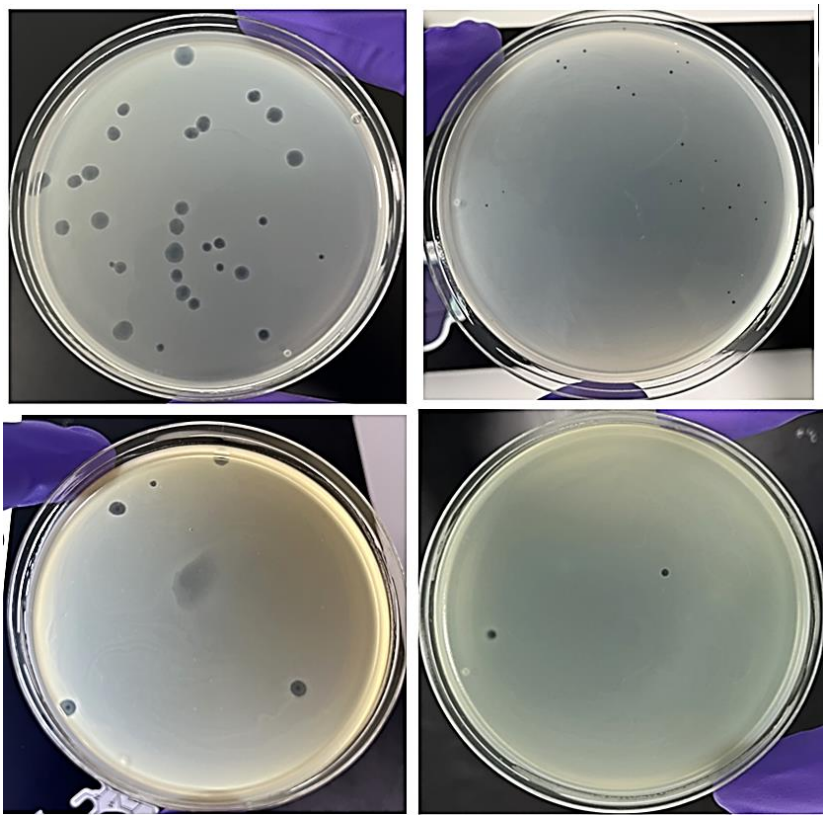

**Figure 2.2:** Images of plaques of bacteriophages T4 (top-left), T5 (top-right), ST3 (bottom-left) and PLS27. Photos were taken after carrying out plaque assays of the respective bacteriophages over bacterial lawns of *E. coli* 11303 (T4 and T5), *S. enterica* 50498 (ST3) and P. aeruginosa AK44 (PLS27).

In terms of growth curves, phages T4 and ST3 demonstrated growth from $10^4$ to about $10^8$-$10^9$ PFU/mL within 1 hour (Figure 2.3). T5 grew at a slightly slower rate, reaching just under $10^8$ PFU/mL after the same amount of time. PLS27 was the slowest growing of the phages considered, with the first rise in concentration recorded after 40 minutes. The objective of these growth curves was to determine the point at which the first lytic event occurs for the given phages at the specified conditions. In the case of T5, this is clearly visible after the 25-minute mark, corresponding to a 2-log increase in concentration. A second burst appears to take place on the 50-minute mark, confirming a latency period of 25 minutes. This has been reported in the literature as being between 38 to 44 minutes long (De Paepe & Taddei, 2006; Raya *et al*., 2011). The difference could be due to the conditions set up for this experiment. It is possible that using host cells further along their growth curve may encourage faster or slower binding with the phages. Furthermore, different host strains of *E. coli* were used during this study and the one

carried out by Raya *et al*. ( 2011). Whilst *E. coli* 11303 is a B-type *E. coli* strain, *E. coli* O157:H7 (O-type) was favoured in the quoted study. The choice of bacterial strain has a profound impact on phage-host kinetics and is a likely contributor towards this difference.

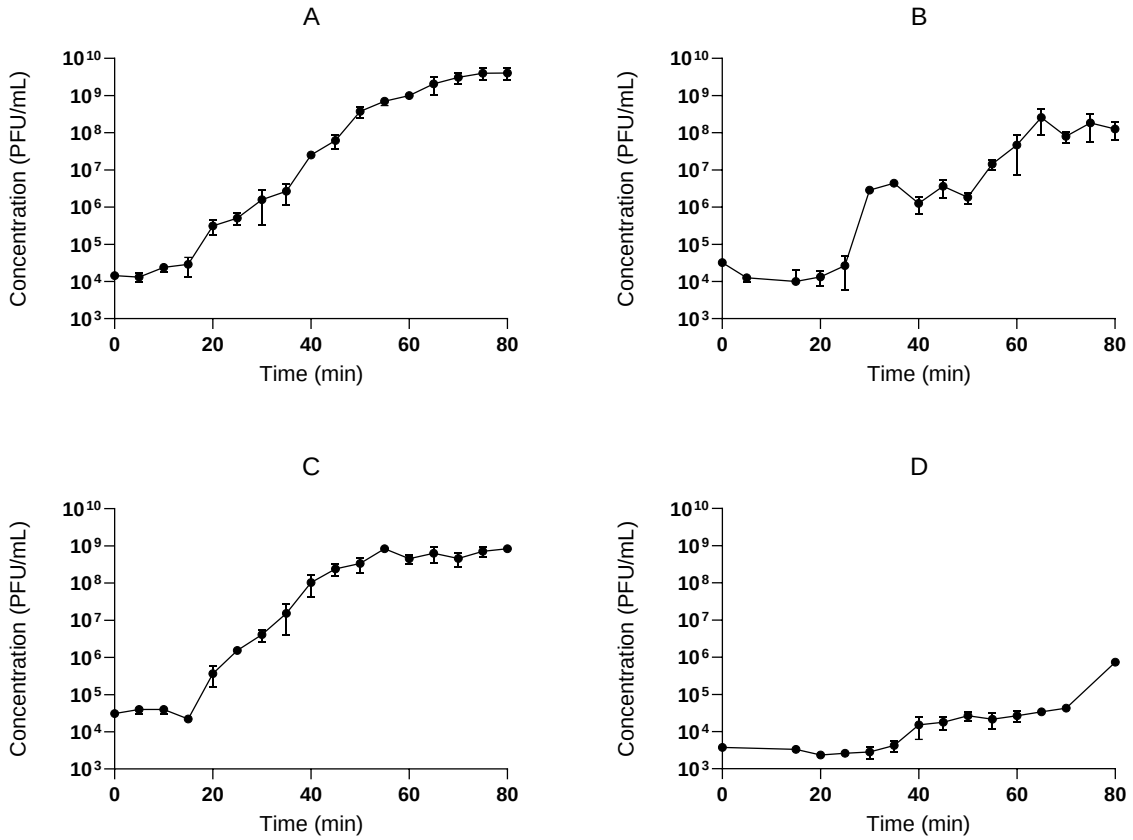


**Figure 2.3:** Growth curves of bacteriophages T4 (A), T5 (B), ST3 (C) and PLS27 (D). Phages were exposed to corresponding host cells in the mid-log phage (OD 600 of 0.4) at T = 0 minutes before bacteriophage enumeration was carried out using plaque assays every 5 to 10 minutes (n = 3).

The bursts are less defined for T4 and ST3, potentially due to their faster latency periods. For both phages, lysis occurred within about 20 minutes, with an approximate 1.5 log increase. Phage T4 has been reported previously to have a latency period of 23 minutes, corresponding to the results presented here (De Paepe & Taddei, 2006). This whilst this represents the first data gathered on bacteriophage ST3. De Paepe & Taddei (2006) refer to the employment of a bacteriophage binding step whereby phages were incubated with mid-log phase host cells on ice for 10 minutes before resuspending the culture in pre-heated broth to initiate bacterial (and bacteriophage) growth. The inclusion of this step was to encourage phages to enter the latency period, and subsequent lysis, in unison and it is likely that a more defined burst could

have been achieved for T4 and ST3 through this approach. Whilst this is the case for free bacteriophages, the primary objective of this work was to develop an assay for phages immobilised to substrates which would make the resuspension step particularly problematic to carry out. Whilst lysis was observed at the expected time-point for T4, the lack of a stabilisation period following the first burst in the case of both T4 and ST3 could be a potential source of error for the assay, emphasising the need for verification of the protocol (discussed in Section 2.3.3). PLS27 took the longest amount of time to begin lysing out of the cells following exposure, with an approximate 1-log increase in concentration being recorded after 40 minutes had passed. A second burst was observed 40 minutes later. The concentration rise corresponds to what is reported by the Felix d'Herelle Centre, where a burst size of 10 is specified for the phage (Felix d'Herelle Reference Centre for Bacterial Viruses, 2006). A shorter latency period of 32 minutes is also reported. This difference can be explained by the fact that in the original experiment detailing the growth kinetics of PLS27, a different strain of *P. aeruginosa* (AK1012) was used instead of the AK44 strain referred to here (Jarrell & Kropinski, 1981).
All four phages discussed here exhibited a lytic burst within an hour of incubation with their corresponding host cells. Phages exhibiting slower growth rates would not necessarily be a suitable candidate for a quantitative assay of this nature due to the impracticality of longer waiting times. In such cases, bacteriophage growth could be improved by altering incubation conditions. The addition of calcium or magnesium, for example, has been shown to increase the adsorption rate of bacteriophage some bacteriophages, which would potentially decrease the time for lysis to occur (Kukkaro & Bamford, 2009).

### 2.3.2 Bacteriophage Equivalence Loading Standard Curves

#### 2.3.2.1 Bacteriophage Growth Assay

To establish equivalence loading standard curves, the T(l) time point needed to be defined from each bacteriophage growth curve shown in Figure 2.3. Depending on the bacteriophage being considered, T(l) was set 5 to 10 minutes after the first lytic event was observed. For T4 and ST3, this was 25 minutes, whilst T5 and PLS27 were assigned T(l) values of 35 and 50 minutes, respectively.

Directly proportionality between concentrations at T(0) ([T(0)]) and T(l) ([T(l)]) was demonstrated for

the 4 bacteriophages being considered. Examples of standard curves for each bacteriophage are provided in Figure 2.4. For the majority of cases, plots of log10 [T(l)] against log10 [T(0)] yielded $r^2$ values exceeding 0.9, suggesting strong correlations and making the graphs adequate for assaying purposes.

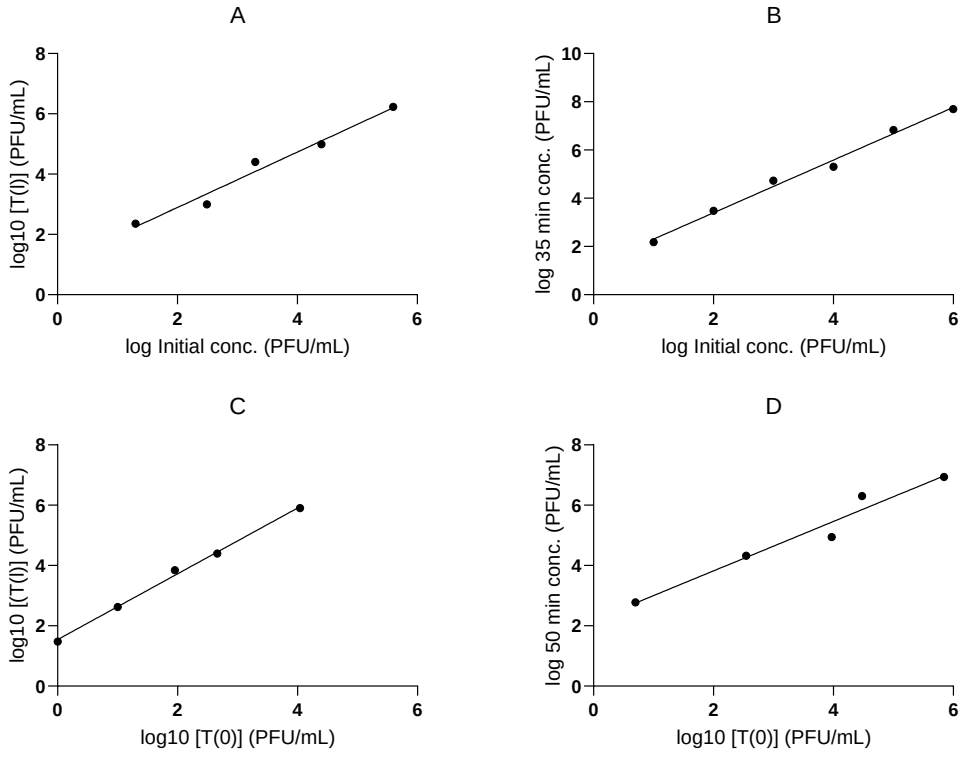


**Figure 2.4:** Equivalence loading standard curves showing plots of log10 of concentration at T(l) ([T(l)]) vs log10 of concentration at T(0) ([T(0)]) for bacteriophages T4 (A), T5 (B), ST3 (C) and PLS27 (D). In this example, all 4 logged graphs yielded r2 values exceeding 0.9. The respective line equations for the T4, T5, ST3 and PLS27 graphs are Y = 0.9194*X + 1.054, Y = 1.093*X + 1.211, Y = 1.091*X + 1.542 and Y = 0.8197*X + 2.182.

To use the equivalence loading standard curves to quantify an unknown starting concentration of viable phages ([T(0)]), the line equations obtained from the linear regression of the logged graphs needed to be used to define the bacteriophage starting concentration in terms of [T(l)]. The working for this is shown below using the linear graph equation, y = mx + c:

Let y = log[T(l)] and x = log[T(0)];

Equation 2.1 $$log10[T(l)] = m \times log10[T(0)] + c$$

Equation 2.2 $$log10[T(0)] = \left(\frac{log10[T(l)]}{m}\right) - c$$

Equation 2.3 $$[T(0)] = 10^{\left(\frac{log10[T(l)]}{m}\right)} - c$$

With [T(0)] now defined in terms of [T(l)], the values for gradient and y-intercept for a given phage's log graph could be substituted into Equation 2.3 to determine [T(0)] from a [T(l)] value. Using the line equations provided in Figure 2.4, and substituting the values for m and c, the following equations for T4 (2.4), T5 (2.5), ST3 (2.6) and PLS27 (2.7) are derived:

Equation 2.4 $$[T(0)] = 10^{\left(\frac{log10[T(l)]}{0.9194}\right)} - 1.054$$

Equation 2.5 $$[T(0)] = 10^{\left(\frac{log10[T(l)]}{1.093}\right)} - 1.211$$

Equation 2.6 $$[T(0)] = 10^{\left(\frac{log10[T(l)]}{1.091}\right)} - 1.542$$

Equation 2.7 $$[T(0)] = 10^{\left(\frac{log10[T(l)]}{0.8197}\right)} - 2.182$$

It is important to note that [T(0)] represents the starting concentration corresponding to an equivalent concentration of free bacteriophages. In practice, this would be used to work backwards to quantify the number of phages per unit area or mass of the material that is being tested. As stated in the methodology, incubation was carried out in 10 mL of broth for this assay. Therefore, the total number of phages in the liquid at T(0) can be quantified by multiplying [T(0)] by 10. The resulting value can then be divided by the mass or area of the material being tested to obtain a value for phage concentration (PFU per unit

mass or area).

### 2.3.2.2 Cytotoxicity Assay

In terms of the equivalence assay based on cytotoxicity, clear differences were observed between the different phage concentrations in terms of absorbance over time (Figure 2.5). Higher phage concentration resulted in a quicker decline in absorbance. In the case of the highest concentrations for T4 and ST3, the decline was almost immediate, with absorbance almost reduced to 0 by the first time point. For both phages, there is a clear separation between the other three concentration standards by the hour mark. However, at no time point was there a clear difference across the entire standard range.

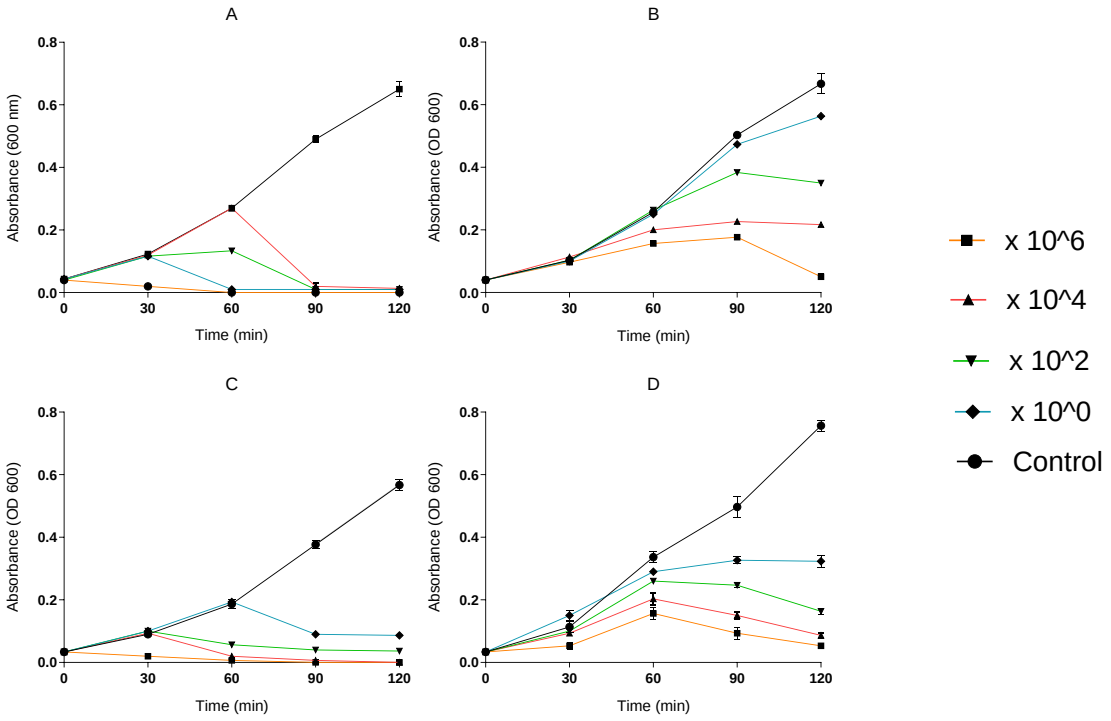


**Figure 2.5:** Graphs plotting optical density (absorbance at 600 nm) against time following exposure of bacteriophages T4 (A), T5 (B), ST3 (C) and PLS27 (D) to their corresponding host cells. Phages were exposed to host cells in the mid-log phage (OD 600 of 0.4) at T = 0 minutes before optical density measurements were taken every half an hour for 120 minutes (n = 3).

The decline was slower for both T5 and PLS27, with the $10^6$ PFU/mL standard only beginning to decline at the 1.5 and 1-hour marks of the respective phages. As shown through the growth curves, this slower response is most likely due to the more extended latency period of both phages compared to T4 and ST3.

For both phages, there were points of clear separation across the concentration standard range (90 and 120 minutes for T5 and 60, 90 and 120 minutes for PLS27). These time-points would be best suited for assaying as they could determine bacteriophage concentration over a broader range. To demonstrate this, the 90-minute time point from the absorbance graph of PLS27 (Figure 2.5D) was used to construct a graph of optical density against starting bacteriophage concentration, expressed as log 10 [T(0)] (Figure 2.6).

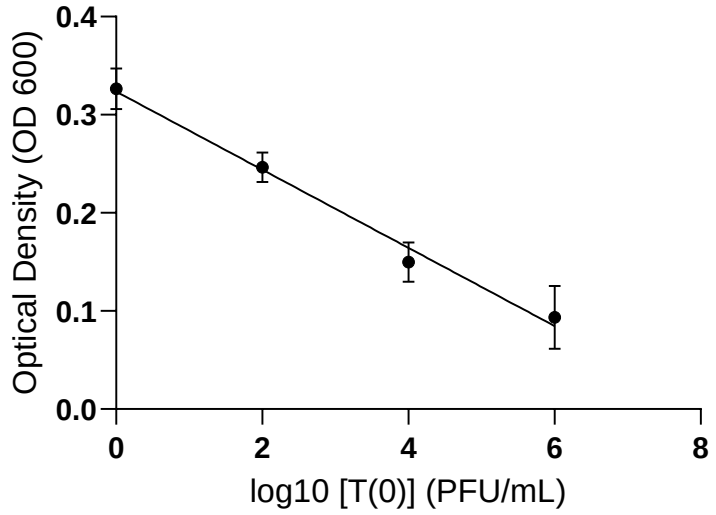


**Figure 2.6:** Graph plotting optical density (absorbance at 600 nm) of *P. aeruginosa* AK44 against the log10 of [T(0)] of bacteriophage PLS27 after 90 minutes of incubation (see Figure 2.5D). Linear regression analysis of the line yielded an R2 value of 0.9492. The equation for the above line is Y = -0.03983*X + 0.3237.

Following a regression analysis of the resulting line, an equation for calculating starting bacteriophage concentration for the example given in Figure 2.6 can be derived using the y = mx +c linear equation as shown below:

Let y = OD (600) and x = log[T(0)];

Equation 2. 8

$$[T(0)] = 10^{\left(\frac{OD(600)}{-0.03983}\right)} - 0.3237$$

There are several issues which could influence the effectiveness of an absorbance-based assay for quantifying bacteriophages. Whilst the example above yielded a strong regression line which could be used to enumerate PLS27 across a 6-log range, in cases where the bacteriophages are too fast acting, determining an optimal time point to take measurements is more challenging. This was the case for T4 and ST3 (Figures 2.5A and 2.5C), in which optical densities dropped rapidly for phages at the higher concentrations such that none of the time points selected would be useable for quantification across a broad range of concentrations. An automated plate reader could be used as a means of continuously measuring optical density to overcome this problem. However, since this assay would ultimately be aimed for use on material containing immobilised bacteriophages, it is likely that the presence of such material in a well plate would affect absorption readings. Additionally, for the two phages (T5 and PLS27), where a good degree of separation between concentration standards was observed, this took a minimum of 1 hour. This would make the absorbance-based assay more cumbersome of the two procedures being considered, increasing waiting times, especially when considering that this assay would form the basis of most quantification work for immobilised phages moving forward. In the case of the bacteriophage growth-based assay, samples were immediately filtered through a 0.22 µm once T(l) was reached. Once filtered, the phages in the filtered samples could be enumerated in the knowledge that their concentrations would not change significantly over time since the cells had already been removed. This was not the case for the absorption assay. Whilst taking readings of multiple samples, there was considerable time pressure to carry this out as quickly as possible due to the presence of viable phages and cells together in the sample tubes. This increases the risk of inaccurate results. Finally, optical density is not a direct measure of cell concentration but of light scatter caused by particles in a solution (Mira *et al*., 2022). This means that in some cases, cell debris as well as phage-immobilised material may interfere with the density readings, further influencing the results. Additionally, in their studies on *E. coli* and *Listeria innocua,* Lewis *et al*. (2014) found that optical density was not directly proportional to cell viability. For these reasons, it was decided that the bacteriophage growth-based equivalence phage loading assay would be taken forward as the primary means of quantification for immobilised phages in future work. Verification of this assay is described in the following section. Despite the optical density-based assay not being used as the primary quantification tool for

immobilised phage, the results presented in this section broadly agree with those of similar experiments conducted elsewhere. In their studies on *Pectobacterium caratovorum*, Kim *et al*. (2022) reported reduced optical densities in cultures inoculated with bacteriophages POP12, POP15 and POP17 after 1 hour of incubation when compared to the control group. In a similar experiment, Liu *et al*. (2022) showed the efficacy of four bacteriophages targeting *Staphylococcus aureus* ATCC25925 through reductions in optical density which were observed after 1 hour, 90 minutes or 120 minutes depending on the bacteriophage being considered. This could justify the use of optical density-based experiments as a confirmatory test of efficacy for bacteriophage-based products as opposed to a quantification tool.

### 2.3.3 Verification of Equivalence Phage Loading Assay

To verify the equivalence phage loading assay, it was required to demonstrate that there was no significant difference between the assayed concentration values and actual concentration values, which were determined using a plaque assay. Assayed and actual values were directly proportional to each other, yielding regression lines of $R^2$ values exceeding 0.9 for all four phages (Figure 2.7).

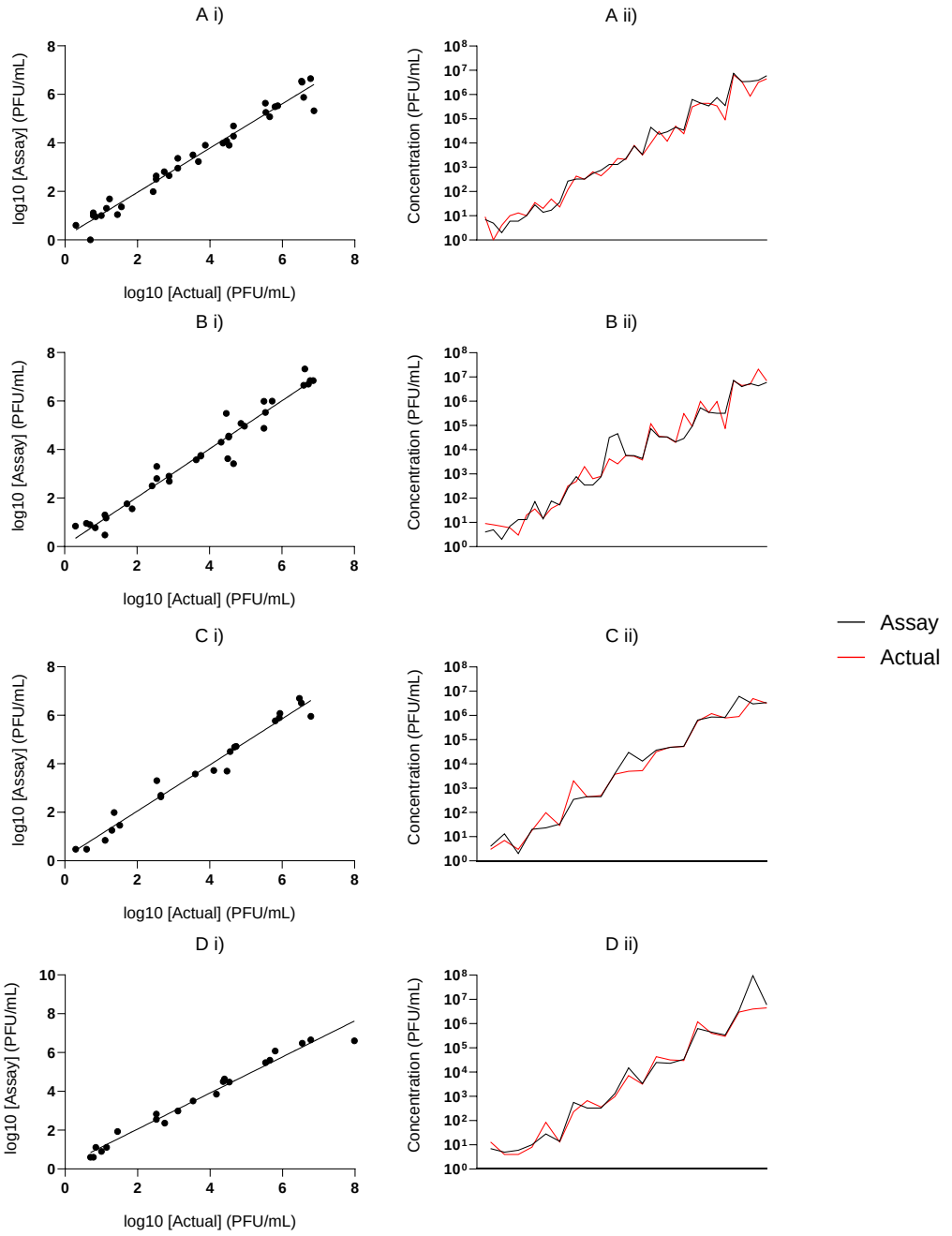


**Figure 2.7:** Regression lines (i) plotting log10 of assayed concentrations against log10 of actual concentrations for T4 (A), T5 (B), ST3 (C) and PLS27 (D). The line equations for T4, T5, ST3 and PLS27 are Y = 0.9119*X + 0.1391, Y = 0.9944*X + 0.04462, Y = 0.9516*X + 0.1439 and Y = 0.9305*X + 0.1930, respectively. The respective $R^2$ values of the line equations are 0.9693, 0.9562, 0.9716 and 0.9740. A visual comparison showing the joined scatter plots for assayed and actual concentrations has also been included (ii).

The results presented in Figure 2.7 do not show that the assayed values and their actual counterparts are the same, but that there is a strong, predictable relationship between them. This means that in the case that a significant difference was found between them, the regression lines could be used to correct the

assayed concentrations accordingly. All data sets considered had data which was not normally distributed, as determined by D'Agostino & Pearson, Anderson-Darling, Shapiro-Wilk and Kolmogorov-Smirnov tests of normality (Table 2.2).

**Table 2.2:** Tests of normality (D'Agostino & Pearson, Anderson-Darling, Shapiro-Wilk and Kolmogorov-Smirnov) results for actual and assayed concentrations values of bacteriophages T4, T5, ST3 and PLS27. Analysis was carried out using GraphPad Prism 9.

| Test of Normality | | Bacteriophage | | | | | | | |
|---|---|---|---|---|---|---|---|---|---|
| | | T4 | | T5 | | ST3 | | PLS27 | |
| | | Actual | Assay | Actual | Assay | Actual | Assay | Actual | Assay |
| Shapiro-Wilk test | P value | >0.0001 | >0.0001 | >0.0001 | >0.0001 | >0.0001 | >0.0001 | >0.0001 | >0.0001 |
| | Passed normality test (alpha=0.05) ? | No | No | No | No | No | No | No | No |

A non-parametric Wilcoxon two-tailed matched pairs test was used to compare assayed and actual concentration values of T4, T5, ST3 and PLS27 (Table 2.3). In each case, no significant difference was found between assayed and actual values.

**Table 2.3:** Results from the Wilcoxon matched pairs test comparing assayed vs actual concentration values for bacteriophages T4, T5, ST3 and PLS27. Analysis was carried out using GraphPad Prism 9.

| Wilcoxon matched pairs signed rank test | Assayed vs Actual Bacteriophage Concentration Values | | | |
|---|---|---|---|---|
| | T4 | T5 | ST3 | PLS27 |
| Number of pairs | 35 | 35 | 21 | 21 |
| P value | 0.0624 | 0.8620 | 0.1818 | 0.1877 |
| Significantly different (P<0.05)? | No | No | No | No |

The results from this test confirmed that the equivalence phage loading assay was equivalent to a plaque assay in terms of determining bacteriophage concentrations. It can, therefore, be taken forward as an enumeration protocol. It is important to note that when using this procedure to enumerate immobilised bacteriophages, an assumption that must be made is that all viable phages bound to the material behave similarly to their free counterparts in solution. It is possible that some bound phages would be physically hindered from adsorbing to available host cells in time for the first burst on account of them being bound

to another surface. This would result in a slight underestimation of the total bound viable phages. At the time of writing, the assay discussed here represents the first of its kind whereby bacteriophage growth is used to estimate bacteriophage concentration. Most of the studies involving the assessment of viable immobilised phages that have been carried out to date have been more qualitative in their application. Nogueira *et al*. (2017) used optical density measurements to demonstrate the efficacy of immobilised phages on wound dressings in a similar way to the experiment described in Section 2.2.5, however, this was not developed into a verified assay for quantification. Other quantification approaches have relied on the tendency of the substrate in question to disintegrate or disperse in solution, allowing for subsequent enumeration through plaque assays. Plaque assays have also been used to quantify phages incorporate into dried powders, on the assumption that a homogenous powder suspension can be maintained in the diluting solution. Cademartiri *et al*. (2010) quantified T4 phages immobilised to silica beads by dissolving these in PBS and carrying out plaque assays. Such an approach would not be suitable for phages immobilised onto film surfaces. The use of more advanced techniques such as fluorescence microscopy and surface plasmon resonance has also been employed for quantification purposes (Tawil *et al*., 2013; C. Wang *et al*., 2016). Despite the potential advantages of these approaches with regard to accuracy, the arduous nature of sample preparation and limited scale of operation justifies the necessity for more simple approaches such as the assay described here.

## 2.4 CONCLUSIONS AND FURTHER WORK

The results of this section of work show that bacteriophages can be assayed by tracking their growth rate as well as the rate at which they kill host cells. Of the two assays tested, equivalence loading based on bacteriophage growth appears more suited to obtaining accurate readings can be more widely applied across phage species. It also allows for more efficient processing of samples.

The bacteriophage growth-based assay was not significantly different from plaque assays when it came to enumerating free phage solutions. With the assumption that bound bacteriophages behave the same way as their free counterparts, this assay can be used to estimate the free-phage equivalence of phages immobilised onto solid substrates.

The assays described allows for determining equivalence up to a concentration of $10^6$ PFU/mL and could be applied to film as well as powder-based materials in the future. The enumeration protocols described here will be applied in other experiments forming part of this collection of works accordingly.

# Chapter 3: Evaluation and Optimisation of Corona Discharge-Mediated Immobilisation of Bacteriophages onto Polymeric Films

## 3.1 INTRODUCTION

As bacteriophage immobilisation continues to grow as a field of study, so has the emergence of techniques used to mediate phage binding to the surface in question. Most of the immobilisation processes for bioactive substances currently favoured involve some form of chemical mediation. However, plasma-based techniques are increasing in popularity (Bilek & McKenzie, 2010; Kondyurin *et al*., 2018; L. Martin *et al*., 2016). This is in part due to their relative simplicity, allowing for an easier and less costly process, which is especially relevant for upscaled production. The use of corona discharge treatment for immobilisation purposes is understudied; however, like other plasma-based techniques, it does offer an interesting alternative to more traditional strategies for immobilisation. The aim of this section of work is to assess corona discharge treatment as a technique for bacteriophage immobilisation on polymeric surfaces.

For plasma-based techniques, activation is typically achieved through direct exposure to plasma. The most used plasma-based technique for immobilising biomolecules is plasma immersion ion implantation (PIII). This has been applied to bind species such as proteins and nucleotides onto various substrates (Hirsh *et al*., 2010; Tran *et al*., 2016; Yeo *et al*., 2017). PIII is believed to facilitate the formation of covalent linkages with the surface as it generates stable surface radicals, which readily form bonds when exposed to the species being immobilised (Bilek & McKenzie, 2010). Numerous studies have also reported on non-specific binding interactions between plasma-treated surfaces and proteins (Lee & Lee, 2008; Kiaei *et al*., 1993; Recek *et al*., 2013). Such interactions arise due to chemical changes occurring on the surface after the radicals react with other chemical species to form more stable functional groups. When using air-based corona discharge, oxygen- containing functionalities typically arise. These include hydroxyls (-OH), carbonyls (-C=O) and ethers (-COOC-). Several studies on hydrophobic polymers have shown the incorporation of these groups on the surface following exposure to corona discharge (Iwata *et al*., 1988; Sutherland *et al*., 1994). Changing the source gas generating the corona discharge results in different functionalities arising.

Nitrogen and ammonia-based corona discharge treatment, for example, encourages formation of nitrogen-containing functionalities (Courval *et al*., 1976). Whilst it is anticipated that corona discharge will encourage functional group-driven immobilisation through non-specific binding, it is unclear whether it would also facilitate stable surface radical formation to encourage covalent attachment of bacteriophages. For a detailed explanation of corona discharge generation, see Appendix A.

The aim of this chapter was to use corona discharge to irreversibly bind, or immobilise, bacteriophages to polymeric surfaces. This encompassed two major objectives: the determination of chemical and physical changes occurring on corona discharge-treated surfaces, as well as the quantification of bacteriophages immobilised to surfaces following a rinsing challenge. Corona discharge was generated using the EST system developed by Tantec (DE). This is a bespoke unit consisting of a moving belt over a flat-bed electrode which passes under a rotating source electrode in a wire-plane configuration. The polymers polyethylene, polypropylene, polyvinyl chloride, cellophane and nylon 6 were considered, providing a selection of common surfaces routinely used for wide array of industrial applications. Effects of corona discharge on these surfaces was assessed in terms of surface energy and presence of surface radicals, both of which would be expected to increase following corona discharge treatment. In the case of polyethylene, polypropylene and nylon 6, changes to were also assessed in terms of FTIR.

In addition to evaluating the effect of corona discharge on these surfaces, subsequent immobilisation of bacteriophages is also described. As with the previous chapter, phages T4, T5, ST3 and PLS27 were focused on. Using the bacteriophage equivalence loading assay developed in the previous chapter, experiments were carried out to determine whether corona discharge treatment increased phage binding efficiency on Polyethylene and Nylon 6 surfaces. The specific phage and surface onto which it is being immobilised are also likely to play a role in the success of the procedure.

The use of corona discharge for immobilising bacteriophages is a novel application that is not very well understood. The wide array of experiments carried out here were chosen to begin building an understanding around the key aspects of the process. It is anticipated that the results obtained will be key to future optimisation work.

## 3.2 MATERIALS AND METHODS

### 3.2.1 Materials and Instruments

Medium density polyethylene film; polypropylene film; polyvinyl chloride film; cellophane film; ≥ 95% 2,2-diphenyl-1-picrylhydrazyl powder (Alfa Aesar, UK); (Fisher Scientific, UK); bovine serum albumin; Tween 20; disk puncher (Vaessen Creative, NL), DYNE pen test kit (DYNE Testing, UK); EST corona discharge system (Tantec, DE); IRSPIRIT FTIR spectrometer (Shimadzu, JP); 12-well plates (Corning, USA); 0.22 µm syringe filter unit (Thermofisher, UK); Stericup quick-release 0.22 µm filter unit (Millipore, UK); Whirlimixer vortex spinner (Nickel-Electro ltd, UK); Heraeus megafuge 16 centrifuge (Thermo Scientific, UK); Snakeskin dialysis membrane (Thermo Scientific, UK); tube roller;1 grade filter paper (Whatman, UK); FLUOstar Omega plate reader (BMG, UK); distilled water; 10 µL, 100 µL and 1000 µL pipettes (Eppendorf, UK); plastic Petri dishes (Fisher Brand, UK); 50 mL Falcon tubes (Thermo Scientific, UK); 20 mL universal tubes (Thermo Scientific, UK); ES-80 orbital incubator (Grant Bio, UK); 1.5 mL microcentrifuge tubes (Thermo Scientific, UK); model 45 colorimeter (Fisher Scientific, UK); sterile forceps (Mediware, DE).

### 3.2.2 Corona discharge treatment of surfaces

The source electrode height on the EST was set to 3 mm. The EST generator was switched on and the power electrode power was set to 200 W. The rotating belt was switched on to confirm that it was moving correctly, and the corona discharge was activated to ensure that no arching occurred. Cut discs were placed onto the belt and passed between the interelectrode space for treatment. The extent to which surfaces were treated was altered by increasing or decreasing the speed at which they passed through the discharge (see Equation 3.1).

Equation 3.1

$$Corona\ Discharge\ Energy\ (kJ/m^2) = \frac{Power\ delivered\ (kJ/min)}{Linear\ Speed\ (m/min) \times electrode\ width\ (m)}$$

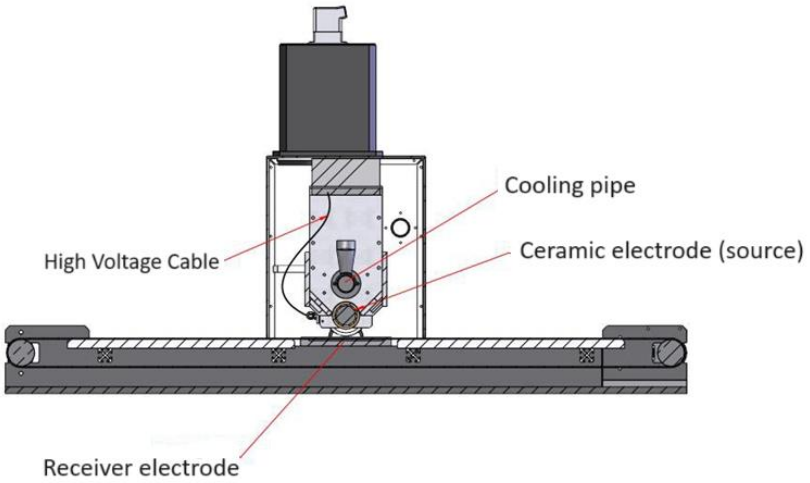


**Figure 3.1:** Schematic of the EST system used to treat polymers. The EST system consists of a belt-driven flatbed which passes through the corona chamber. Corona discharge passing from the ceramic source electrode to the receiving electrode (counter electrode) is intercepted by any material present on the belt, resulting in the material's activation.

### 3.2.3 Assessment of Polymer Surface Energy

DYNE pens were used to assess surface energy by following the procedure specified in the manufacturer's instructions (DyneTesting, n.d.). Polyethylene, cellophane, polyvinyl chloride, polypropylene, and nylon 6 sheets were tested following 5.2, 13.3, 40 and 400 kJ/m$^2$ of corona discharge treatment from the EST corona discharge generator. Untreated sheets were also assessed to establish a surface energy baseline for each surface. Tests were carried out immediately after treatment as well as 1 hour, 3 hours, 1 day, 1 week, and 2 weeks later. Assessment of treated polyethylene and nylon 6 was also carried out using a K100 Force Tensiometer. This was carried out just after corona discharge treatment. 1.6 cm diameter polyethylene disk cut outs and 1.5 cm x 1.5 cm nylon 6 squares were assessed at dipping/receding speeds of 10 mm/min and a final depth 10 mm. Water was used as a reference liquid.

### 3.2.4 FTIR of Corona Discharge-Treated Surfaces

FTIR analysis of polyethylene and nylon 6 sheets was carried out using an IR SPIRIT FTIR spectrometer. Small sections of polymer sheet were treated with 5.2, 40 and 400 kJ/m$^2$ of corona discharge and immediately stored in sealed Petri dishes. Samples were analysed the following day.

3.2.5 Assessing Radical Concentration on Activated Surfaces

Radical activity on corona-treated polyethylene and nylon 6 surfaces was assessed by assaying against the radical scavenger, diphenyl-1-picrylhydrazyl (DPPH). A curve showing concentration vs absorbance at 520 nm was constructed for the compound. This was done by measuring the optical density at 520 across a range of concentrations falling between $1 \times 10^{-5}$ and $1 \times 10^{-4}$ M. Concentration standards were prepared by dissolving quantities of DPPH in methanol in 50 mL Falcon tubes wrapped in aluminium foil to slow the light-mediated decomposition of the DPPH To measure optical density, 1 mL aliquots of each standard were added to 1 mL cuvettes and analysed using a model 45 colorimeter, with methanol being used as a blank. A radical scavenging reaction standard curve was then constructed using ascorbic acid. To do this, the wells of a 12-well plate were filled with 3 mL of $1 \times 10^{4}$ M DPPH. A working stock of ascorbic acid was prepared by dissolving 0.75 g of the chemical in 10 mL of deionised water. This equated to a concentration of $4.26 \times 10^{-3}$ M. The working stock was diluted by a ratio of 9:10 12 times. Each dilution, including the undiluted working stock, was then added to the wells containing DPPH (see Table 3.1). The plate lid was replaced, and the whole plate was covered with aluminium foil and stored in a dark cupboard for 30 minutes. Following this, optical densities of samples at 520 nm were measured using the model 45 colorimeter.

**Table 3.1:** Table showing different quantities of ascorbic acid (AA) added to $1 \times 10^{-4}$ M DPPH. Data from the resultant optical density measurements at 520 nm was used to construct a standard curve for reactivity between DPPH and ascorbic acid.

| DPPH Conc. (M) | DPPH Volume (mL) | AA Conc. (M) | AA Volume (mL) | Final AA Conc. (M) |
|---|---|---|---|---|
| $1 \times 10^{-4}$ | 2.97 | $4.36 \times 10^{-3}$ | 0.03 | $4.36 \times 10^{-5}$ |
| $1 \times 10^{-4}$ | 2.97 | $3.92 \times 10^{-3}$ | 0.03 | $3.92 \times 10^{-5}$ |
| $1 \times 10^{-4}$ | 2.97 | $3.53 \times 10^{-3}$ | 0.03 | $3.53 \times 10^{-5}$ |
| $1 \times 10^{-4}$ | 2.97 | $3.18 \times 10^{-3}$ | 0.03 | $3.18 \times 10^{-5}$ |
| $1 \times 10^{-4}$ | 2.97 | $2.86 \times 10^{-3}$ | 0.03 | $2.86 \times 10^{-5}$ |
| $1 \times 10^{-4}$ | 2.97 | $2.57 \times 10^{-3}$ | 0.03 | $2.57 \times 10^{-5}$ |

| | | | | |
|---|---|---|---|---|
| $1 \times 10^{-4}$ | 2.97 | $2.32 \times 10^{-3}$ | 0.03 | $2.32 \times 10^{-5}$ |
| $1 \times 10^{-4}$ | 2.97 | $2.09 \times 10^{-3}$ | 0.03 | $2.09 \times 10^{-5}$ |
| $1 \times 10^{-4}$ | 2.97 | $1.88 \times 10^{-3}$ | 0.03 | $1.88 \times 10^{-5}$ |
| $1 \times 10^{-4}$ | 2.97 | $1.69 \times 10^{-3}$ | 0.03 | $1.69 \times 10^{-5}$ |
| $1 \times 10^{-4}$ | 2.97 | $1.52 \times 10^{-3}$ | 0.03 | $1.52 \times 10^{-5}$ |
| $1 \times 10^{-4}$ | 2.97 | $1.37 \times 10^{-3}$ | 0.03 | $1.37 \times 10^{-5}$ |
| $1 \times 10^{-4}$ | 2.97 | $1.23 \times 10^{-3}$ | 0.03 | $1.23 \times 10^{-5}$ |

1.6 cm diameter polyethylene disks and 1.5 cm x 1.5 cm nylon 6,6 squares were prepared using a disk puncher and scalpel, respectively. Polyethylene and nylon 6 samples were treated with 5.2, 13.3, 40 and 400 kJ/m$^2$ of corona discharge treatment as explained in Section 3.2.2. Immediately following treatment, disks were placed into a well of a 12-well plate containing 3 mL of DPPH at a concentration of $1 \times 10^{-4}$ mol/L. Plates were wrapped in foil and stored in darkness for half an hour before optical density at 520 nm was measured as already described. Controls comprising DPPH on its own and DPPH with untreated substrates were also considered. Radical scavenging activity was assessed by comparing any drops in optical density observed with the ascorbic acid standard curve.

### 3.2.6 Development of a Rinsing Protocol for Immobilised Phage

Bovine serum albumin (BSA) and Tween 20 were considered as rinsing buffers for immobilised phages. 0.5 % (vol/vol) solutions of both substances were prepared in PBS. 1 mL aliquots of each were placed in 1.5 mL Eppendorf tubes. 100 uL of bacteriophages T4, T5, ST3 and PLS27 were added separately to each rinsing buffer to a final concentration of $10^6$ PFU/mL. Bacteriophages comprising each sample were enumerated immediately as well as 2, 6 and 24 hours later. This was carried out through plaque assays as detailed by Baer & Kehn-Hall, (2014). Tween 20 was taken forward as a rinsing buffer based on these results (see Figure 3.8).

To assess rinsing, phages were first immobilised onto corona-treated film. 1.6 cm diameter polyethylene disks were treated with 40 kJ/m$^2$ of corona discharge, as explained in Section 3.2.2. Following this, each

treated substrate was placed in 50 mL falcon tubes containing 10 mL of bacteriophage at a concentration of $10^8$ PFU/mL. All four bacteriophages were considered. Falcon tubes were left on a tube roller spinning at 10 rpm for 10 minutes. Following this, each disk was removed using sterile forceps and placed in Falcon tubes containing 10 mL of 0.5 % vol/vol Tween 20 in PBS. The tube was inverted gently three times before the disk was removed again and placed into a fresh Falcon tube containing the rinsing buffer. This process was carried out a total of 8 times. Bacteriophages concentration in each rinsing tube was determined using plaque assays.

### 3.2.7 Rinsing of Bacteriophages Immobilised onto Polyethylene and Nylon 6

1.6 cm diameter polyethylene disks and 1.5 cm x 1.5 cm nylon 6 squares were prepared using a disk puncher and scalpel, respectively. Substrate samples were treated with corona discharge at intensities of 5.2, 40 and 400 kJ/m$^2$ treatment settings. Untreated controls were also considered.

Immobilisation was carried out using the K100 force tensiometer. Treated substrates were secured to the instrument using the probe clip, which held them directly over a glass vessel containing the bacteriophage solution at an approximate concentration of $10^6$ PFU/mL. The instrument was used to dip the substrates into the phage solution at a dipping speed of 10 mm/min. Once a depth of 10 mm was reached, the substrate was held for 1 minute before receding from the liquid at a speed of 10 mm/min.

Following removal from the force tensiometer, substrates were immediately rinsed as explained in Section 3.2.6. A total of 5 rinses were carried out. Following rinsing, phages remaining bound on the substrate were quantified using the bacteriophage loading equivalence loading assay described in Section 2.2.4.

### 3.2.8 Assessing the Cytotoxicity of an Immobilised Phage Cocktail

To prepare a phage cocktail, bacteriophages T4, ST3 and PLS27, at approximate individual concentrations of $10^8$ PFU/mL, were combined in a 1:1:1 volumetric ratio. 1.6 x 1.6 Polyethylene disks were considered for this section of work. The disks were activated as explained in Section

3.2.2 at a treatment intensity of 5.2 kJ/m$^2$. To immobilise the phage cocktail, corona discharge-treated disks were placed in 50 mL Falcon tubes containing 10 mL of the cocktail. Tubes were sealed and left to rotate on a tube roller at 10 rpm for 1 hour. Following this, they were rinsed 5 times in the Tween 20 rinsing buffer as described in Section 3.2.6. Rinsed disks were stored in PBS at 4 °C until further use.

The immobilised cocktail was exposed to growing cultures of *E. coli* 11303, *S. enterica* and *P. aeruginosa* AK44 to assess cytotoxicity. Starter cultures of each strain were prepared by adding 100 uL of overnight culture to 10 mL of nutrient broth, brain heart infusion broth and tryptic soy broth, respectively. Starter cultures were incubated at 37 °C at an rpm of 200. Once an OD (600) of 4 was reached, 100 uL of culture was added to 50 mL Falcon tubes containing broth preheated to 37 °C and a single rinsed disk onto which the cocktail was immobilised. Optical density readings were measured every half an hour using a model 45 colorimeter set to 600 nm. Control disks prepared by soaking corona discharge-treated disks in PBS were also considered.

## 3.3 RESULTS AND DISCUSSION

### 3.3.1 Effect of corona discharge treatment on polymer film surface energy

Using DYNE pens, the respective surface energies of untreated polyethylene, polypropylene, polyvinyl chloride and cellophane were found to lie within a 30 - 33 mN/m range (see Table 3.2). Nylon 6 had the highest resting surface energy at 36 mN/m. Cellophane was found to have the lowest surface energy at 30 mN/m. This was an unexpected result, with the oxygen-based functional groups prevalent with cellophane expected to give rise to higher surface energies than the more hydrophobic, non-polar structures of polypropylene and polyethylene (Polymer Properties Database, 2015). The same is true of PVC, which contains chlorine groups, giving rise to higher polarity on the surface. For both polymers, surface energy readings are typically closer to 40 mN/m due to the presence of these polar components (Polymer Properties Database, 2015). At the time of writing, it was not clear why this result was observed however, the disparity could be due to a surface contamination or an additional surface coating by the manufacturer. The surface energy values recorded for PE and PP fell between the 28 – 35 mM/m range

typically reported in the literature (Lindner *et al*., 2018).

**Table 3.2:** Mean surface energies of polyethylene (PE), cellophane (CP), nylon 6 (N6), polypropylene (PP) and polyvinyl chloride (PVC) as determined by Dyne pens (see Section 3.2.3).

| Material | Mean Surface Energy (mN/m) |
|---|---|
| PE | 31.2 |
| CP | 30 |
| N6 | 36 |
| PP | 32.8 |
| PVC | 31.6 |

As anticipated, all 5 polymers recorded increased surface energy measurements following corona discharge treatment (see Figure 3.2). Increases in surface energy appear to be proportional to the intensity of the discharge applied. The lowest treatment setting applied (5.2 kJ/m$^2$) resulted in a mean increase of about 2 to 4 mN/m in all 5 polymers. This increased linearly with 13.3 kJ/m$^2$ as well as 40 kJ/m$^2$. Differences were observed in the way surface energy changed at a much higher treatment intensity (40 kJ/m$^2$), where for polyethylene, polypropylene, and nylon 6 it increased beyond the range of the DYNE pens (> 60 mN/m) whilst for polyvinyl chloride and cellophane, it remained below 60 mN/m, suggesting that a level of saturation had been reached for the latter pair.

These results correspond to findings of Comyn *et al*. (1996), who found that air-based corona discharge treatment of poly(etheretherketone) resulted in increased surface polarity, with surface energy readings for treated surfaces rising to almost double those of their untreated counterparts. XPS analysis revealed an increase in oxygen atoms incorporated on the surface, with the authors attributing this to the formation of carboxylane (-COO-) groups. Park and Jin (2001) reported similar such surface energy increases in low density PE following corona treatment on account of carboxylane and carbonyl (-C=O) functionalities arising on the surface. Novák *et al*. (2006) recorded a surface energy of 55 mN/m for corona discharge-treated PE, which is comparable to that observed following the treatment intensity of 40 kJ/m$^2$ used in this study. The effective oxidation of the polymers treated with corona discharge explains the increased surface energy readings observed in this study.

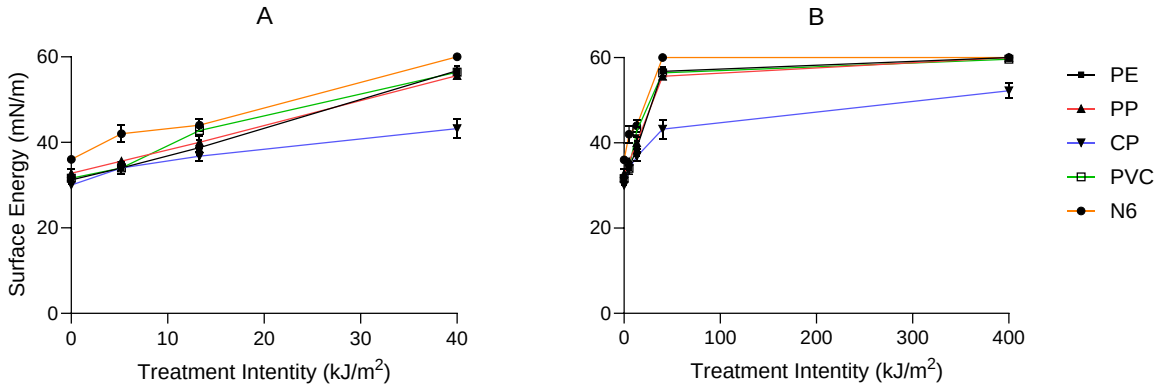


**Figure 3.2:** Surface energy readings for polyethylene (PE), polypropylene (PP), polyvinyl chloride (PVC), cellophane (CP) and Nylon 6 (N6) following varying treatment intensities of corona discharge (n = 5). Two graphs have been provided to show the surface energy increase up to 40 kJ/m$^3$ of corona discharge treatment (A) and 400 kJ/m$^3$.

Of the polymers considered, polyethylene, polypropylene, polyvinyl chloride and nylon 6 appeared to retain most of their increased surface energies for an extended period of time (Figure 3.3). Following 40 kJ/m$^2$ of corona discharge treatment, the surface energies of all four surfaces decreased by around 2-3 mN/m over a week. Polyethylene and polypropylene appeared to remain stable after day 7, with only minor decreases occurring over the second week. Polyvinyl chloride decreased at a slightly faster rate compared to the other two polymers. Nylon exhibited a slow but steady decline during the test period, with its surface energy decreasing by about 5 mN/m. In the case of cellophane, there was an immediate drop in surface energy, resulting in it almost returning to its resting surface energy after just 1 day. By day 3, it had dropped to its baseline of 30 mN/m, which it remained at for the duration of the testing period.

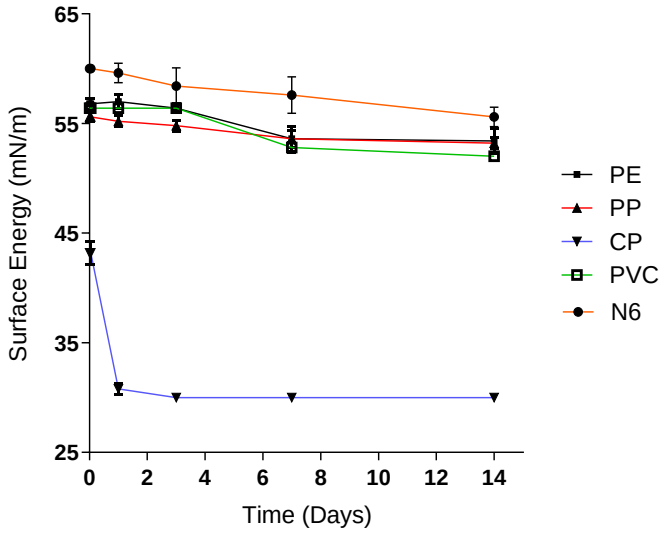


**Figure 3.3:** Tracking of surface energy of polyethylene (PE), polypropylene (PP), polyvinyl chloride (PVC), cellophane (CP) and Nylon 6 (N6) following 400 kJ/m$^2$ of treatment (n = 5).

These decreases can be attributed to hydrophobic recovery of the polymers, in which functional groups are lost from the surface through bond rotation or diffusion of polymer units away from the surface (Mozetič, 2023). All plasma and corona discharge-treated polymers exhibit varying degrees of hydrophobic recovery (Mozetič, 2023). The quick rate of recovery observed for CP has been observed in other polymers such as polystyrene (Lau *et al*., 2022). For the study in question, the authors reported a sudden drop in surface energy over a 72-hour period before stabilization for plasma-treated polystyrene films. Most studies on the hydrophobic recovery of plasma-treated polymers has been carried out on PE (Mozetič, 2023). Novák *et al*. (2006) reported on a steady decline in surface energy for corona discharge-treated PE, before stabilisation at 40 Nm/m after 1 month of storage at ambient conditions. In their studies on polyolefins, Encinas *et al*. (2010) found no evidence of hydrophobic recovery during the first 20 days of incubation. The authors used plasma treatment to increase the surface energy of low-density PE. Gradual hydrophobic recovery did occur gradually after a prolonged storage period of 270 days. The samples considered for this experiment were only analysed for a two-week period. Based on results reported elsewhere, it is anticipated that the respective surface energies of PE, PP, PVC and N6 would continue to decrease gradually before stabilising at a level higher than the baseline.

The extent to which hydrophobic recovery occurs in different polymers could have implications for bacteriophage immobilisation. A rate of hydrophobic recovery that is too fast and extensive may significantly reduce the number of phage binding sites across the surface, reducing immobilisation efficiency. Phages would typically be exposed to a corona discharge-treated surface immediately after treatment, which could mitigate this, however, it remains unclear whether hydrophobic recovery could negatively affect viably bound phages. The dispersion of the top surface layers could result in the re-positioning of bound phages such they would be physically impeded from adsorbing to bacterial cells. There is scope for further study into the effect of hydrophobic recovery on both phage binding efficiency as well as phage that has already been bound. If it is the case that faster rates of hydrophobic recovery come at a detriment to the phage immobilisation process, this would justify development of a polymer screening test which could be used to determine whether a given polymer would be a good or poor candidate for phage immobilisation based on its rate of hydrophobic recovery following corona discharge-mediated activation.

### 3.3.2 FTIR of corona-treated polyethylene, polypropylene and nylon 6

Changes in surface energy can be explained by the formation and incorporation of polar groups mediated by corona discharge. The presence of electronegative centres on an otherwise hydrophobic surface increases the extent to which non-specific binding processes occur, increasing wettability as demonstrated with the DYNE pen tests. FTIR spectra generated for polyethylene and polypropylene are shown in Figure 3.4. Chemical changes on the surfaces appeared to be very similar for both polymers, an expected result given their similar chemical structure.

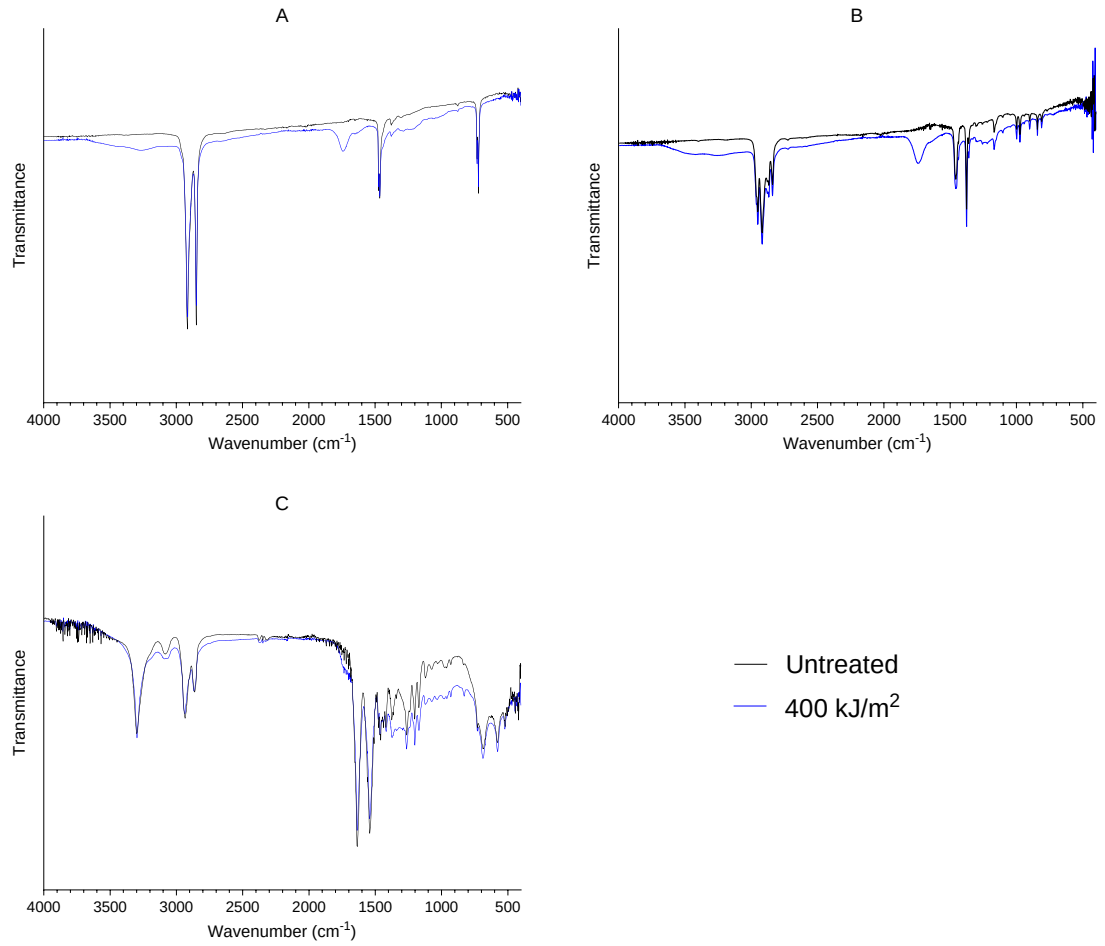


**Figure 3.4:** FTIR spectra for PE (A), PP (B) and N6 (C) before and after corona discharge treatment. 400 kJ/m$^2$ of corona discharge were applied to each treated surface.

With increasing treatment intensity, a new and distinct band emerged at 1700 cm$^{-1}$ for both polyethylene and polypropylene. This corresponds to carbonyl (C=O) stretches from carbonyl groups, most likely forming part of carboxylic acid (-COOH) functional groups. This corresponds to results reported by Wakelin *et al.* (2015) in which a IR peaks attributed to carbonyl groups were observed in polyether ketone surfaces following treatment with PIII. For both polymers, a very small shoulder to the right of this band, at about 1600 cm$^{-1}$ is also observed. This can be assigned to alkene (-C=C-) stretching, indicating that corona discharge treatment leads to the desaturation of parts of the polymer backbone. Another smaller broad band emerged between 1300 – 1100 cm$^{-1}$, which could correspond to ether (-COOC-) functional groups. These can arise through crosslinking mediated by peroxide radicals. The final band of note is a broad band at 3600 – 3200 cm$^{-1}$. This suggests the presence of alcoholic hydroxyl (-

OH) groups, with this region of the spectra corresponding to H-bonding interactions occurring between these groups. The emergence of this broad band corresponds to results obtained by Wang *et al.* (2022) following corona discharge treatment of high-density PE. These results are comparable with other studies involving air-generated corona discharge treatment; however, the intensities of the new bands are relatively slight compared to other more high-energy techniques such as PIII (Comyn *et al*., 1996; Iwata *et al.*, 1988; Lu *et al.*, 2010).

Surface changes due to corona discharge treatment were more subtle in the case of N6. The spectrum for the untreated samples was reflective of those generated in previous studies (Spyridakis *et al*., 2022). The band at 3300 $cm^{-1}$ can be attributed to N-H stretching with the smaller band at 3088 $cm^{-1}$ arising due to the overtone of the amide II band. C-H stretching vibrations give rise to bands at 2938 $cm^{-1}$ and 2865 $cm^{-1}$, with an -OH shoulder similar to those in treated polyethylene and polypropylene also present. The strong bands at 1640 $cm^{-1}$ and 1540 $cm^{-1}$ are due to C=O stretching of the amide I and amide II bands respectively. Bands at 1461 $cm^{-1}$ and 1261 $cm^{-1}$ correspond to $CH_2$ scissoring and C-H bending respectively. Finally, a C-N-C scissor vibration results in the band at 689 $cm^{-1}$. The fact that Nylon 6 already has polar groups makes changes brought about by corona discharge harder to visualise with FTIR. Despite this, there was a notable increase in noise occurring between 1400 $cm^{-1}$ and 900 $cm^{-1}$. This is indicative of increased bond diversity on the surface, suggesting the incorporation of oxygen functionalities.

Whether through non-specific binding interactions or covalent bonding, the chemical changes occurring on corona discharge-activated surfaces are expected to play a key role in subsequent bacteriophage attachment. For the former, the increased polar functionality would encourage dipole-dipole interactions with polar amino acid residues on the bacteriophage coat to facilitate adsorption as has been previously reported when exposing functionalised surfaces to phages (Hosseinidoust *et al*., 2014). Amino acid residues key to covalent attachment of bacteriophages include lysine, cystine, aspartic/glutamic acid and tyrosine (Lee & Wang, 2006). It is anticipated that these would interact with the newly incorporated oxygen-based groups on the functionalised substrate to produce amide linkages, irreversibly binding the phage to the surface.

### 3.3.3 Generation of free radicals on polyethylene, polypropylene and nylon surfaces following treatment

Free radicals generated on corona-treated surfaces were assayed by recording the colour change of DPPH solutions as they reacted with them. The characteristic purple colour of the compound changed to a reddish-brown colour, signifying partial degradation (Figure 3.5). In cases where total degradation occurred, such as when adding high concentrations of ascorbic acid standards, complete decolourisation was observed, with a pale-yellow solution remaining.

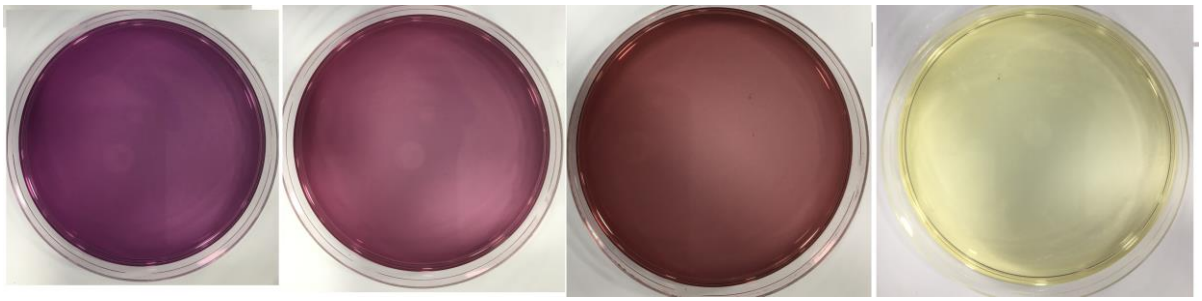

**Figure 3.5:** Colour change of DPPH as it degraded. From left to right, undegraded DPPH, followed by increasing levels of degradation until full decolourisation was observed, with a pale-yellow solution remaining.

A directly proportional relationship was observed between DPPH concentration and absorbance. The concentrations considered ranged from 0.1 – 0.01 mM of DPPH (Figure 3.6). Inverse proportionality was observed for ascorbic acid, whereby increasing the concentration of ascorbic acid added to wells containing DPPH resulted in increased reactivity and thus, lower absorbance at 520 nm.

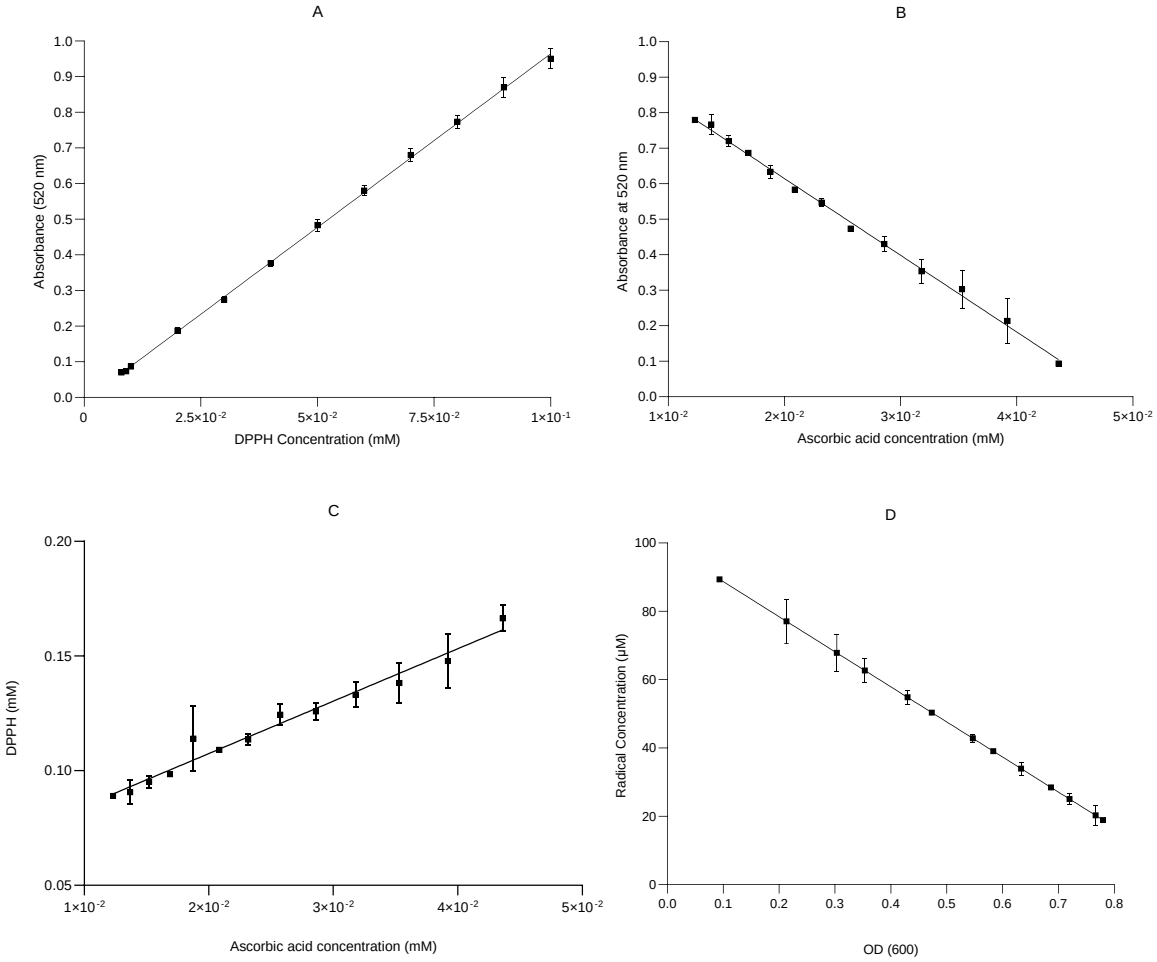


**Figure 3.6:** Graphs showing absorbance at 520 nm against DPPH concentration (n = 3) (A), absorbance at 520 nm against ascorbic acid concentration (n = 3) (B), DPPH concentration against ascorbic acid concentration (n = 3) (C) and radical concentration against OD (600) (n = 3) (D). Respective line equations for graphs A to D are Y = 9.744*X - 0.01014, Y = -21.61*X + 1.047, Y = 2.285*X + 0.06171 and Y = -102.6*X + 98.96, with respective $R^2$ values of 0.99, 0.96, 0.92 and 0.97.

Ascorbic acid reacted with DPPH at a stoichiometric ratio of 1:2.4 (Figure 6C). This is similar to the ratio of 1.9 reported by Angeli *et al*. (2021). The authors of this study exposed 125 uM solutions of DPPH to varying concentrations of ascorbic acid (10, 20, 50, 100, 200, 400 and 800 µM). Optical density readings at 515 nm were taken after 3 minutes of incubation, with degradation of DPPH calculated as a function of the drop in absorbance at 515 nm. The slightly higher ratio observed here could be due to the considerably longer incubation time of 30 minutes, which may have encouraged further degradation of the DPPH radicals. Conversely, Tran *et al*. (2016) exposed PIII-treated polypropylene surfaces to DPPH for 90 minutes before taking optical density readings, with a clear

difference emerging between treated and untreated samples. These differences highlight a need for defining the optimal time point for optical density readings in future DPPH-based radical scavenging assays. Another possibility for the higher ratio reported here could be that the DPPH may have become less stable following the addition of liquid into the well. Regardless of this discrepancy, a strong linear relationship was established between reactive concentrations of DPPH and ascorbic acid, allowing for the generation of a graph predicting 'radical concentration' as a function of optical density (Figure 6D).

Radical concentration for both polyethylene and nylon 6 increased following corona discharge treatment (Figure 3.7). In all cases, apart from the lowest corona discharge intensity, nylon 6 had a higher mean radical surface concentration than polyethylene, although the values are within the standard error of each other.

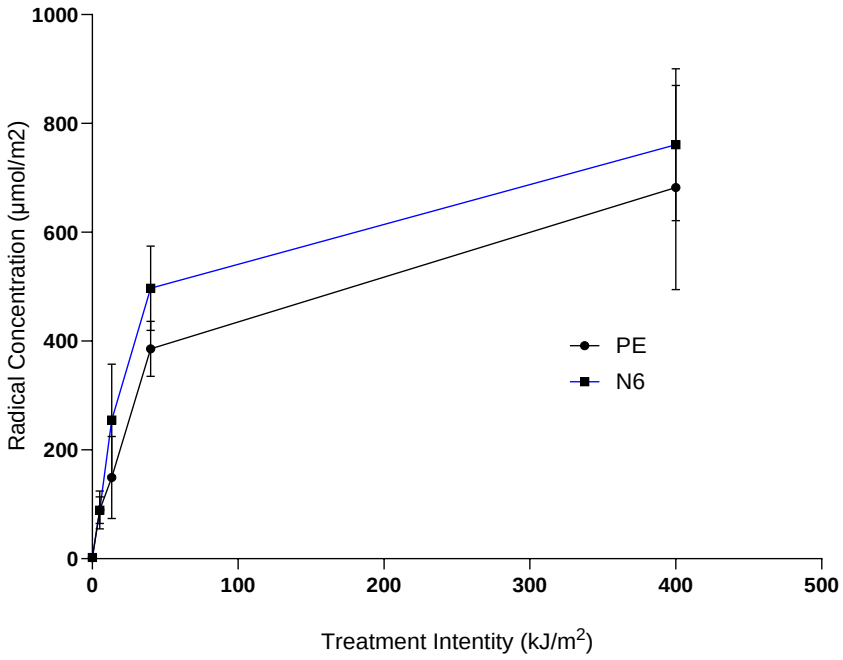


**Figure 3.7:** Estimated surface radical concentration for PE and N6 surfaces at various intensities of corona discharge treatment (n = 8).

Both polymers behaved similarly to one another with respect to radical generation. A directly proportional relationship between treatment intensity and surface radical concentration was observed until a treatment intensity of 40 kJ/m$^2$. The increase in concentration between 40 and 400 kJ/m$^2$ is considerably less steep. This could indicate that a saturation point may be approaching the polymer

surfaces considered here. Radicals generated through corona and plasma are highly reactive species which are generally unstable (Ershov *et al*., 2014). Despite this, some radicals generated on the surface can persist for longer periods on account of becoming embedded within the polymer layers (Bilek & McKenzie, 2010). This could explain why some radical activity was detected during this test. This result shows that in addition to increased polarity, radical-mediated covalent binding may also occur when a corona discharge-treated surface comes into contact with bacteriophages.

3.3.4 Rinsing assay development

The addition of 0.05 % Tween 20 did not affect the viability of free bacteriophages over a twenty-four-hour period, with phage concentration keeping in line with the PBS control over the test period (Figure 3.8). This was not an unexpected result; Tween 20 has been widely used as a rinsing agent for proteins and does not typically cause denaturation (Santos Gomes *et al*., 2022; Zhao *et al*., 2022). In the case of BSA, a pronounced drop was observed, whereby half of the phages were deactivated by the two-hour mark. This continued over the entire test period, with final concentrations dropping below $10^5$ PFU/mL.

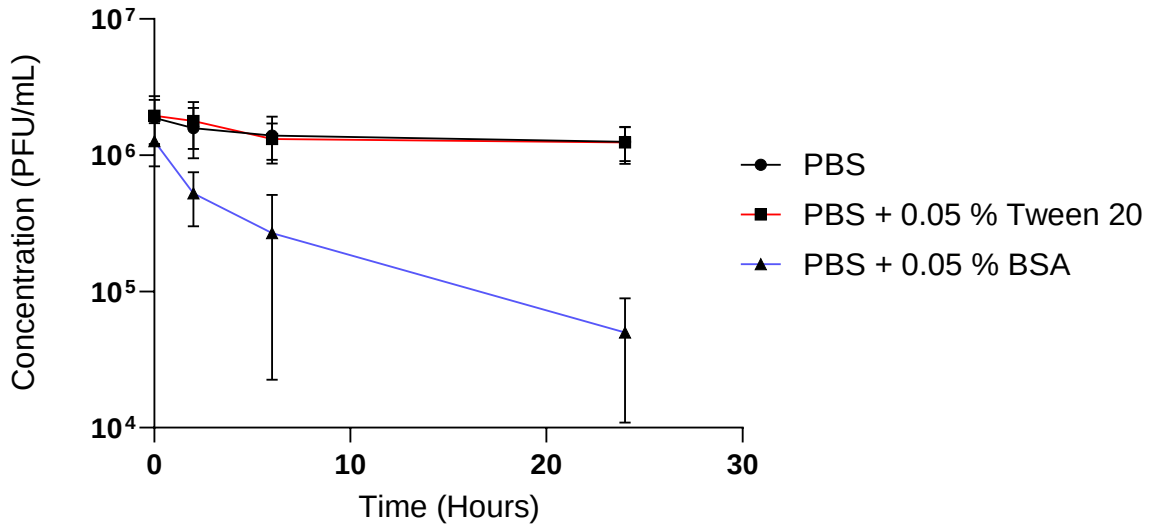


**Figure 3.8:** Survival of bacteriophages over a 24-hour period in PBS (control), and PBS supplemented with 0.05 % tween 20 and 0.05 % BSA. Data of bacteriophages T4, T5, ST3 and PLS27 was pooled to make graph simpler (n = 12).

The larger error bars within observed for the BSA curve suggests a degree of variation across the phages considered in terms of degradation rates. This degradation may have been due to BSA particles biding

to bacteriophage recognition sites. This contradicts findings elsewhere in which *Salmonella* and *Bacillus* phages maintained their ability to adsorb to their corresponding host cells whilst being exposed to BSA (Huang *et al*., 2009). In this study, the authors immobilised mixtures of bacteriophages and BSA onto magnetoelastic resonator surfaces to develop biosensors. BSA was used to block bacteria from binding to the sensor surface through non-specific interactions, allowing for the deduction that any cell detected on the surface would have been caught by the immobilised phages. Despite this, tween 20 was taken forward as a rinsing buffer owing to the apparent degradation observed with BSA.

All four bacteriophages considered behaved similarly during the rinsing tests. A mean rinse-off concentration of $10^5 – 10^6$ PFU/mL was recorded for all phages following the first rinse (Figure 3.9).

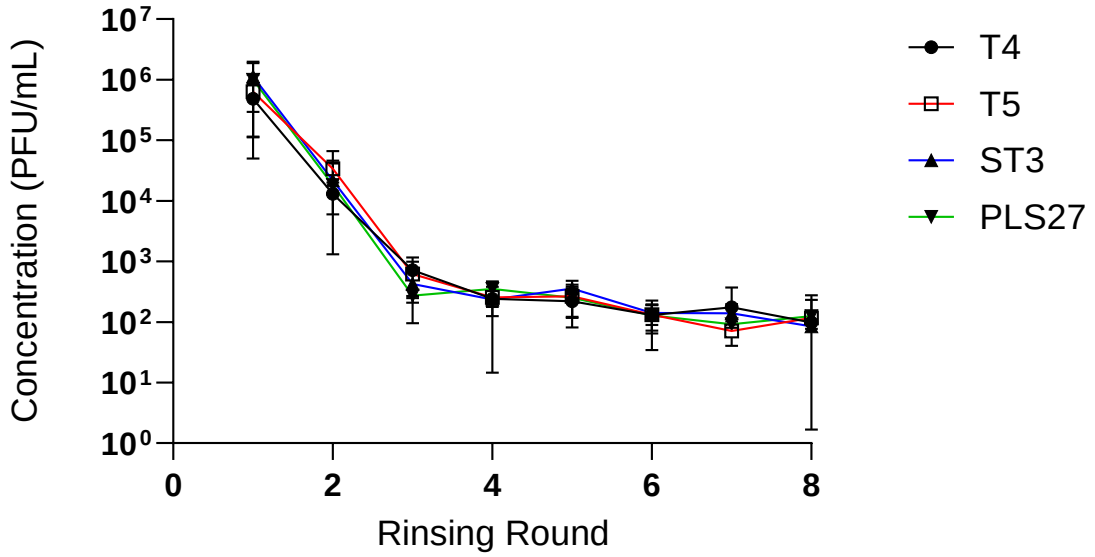


**Figure 3.9:** Concentration of bacteriophage T4, T5, ST3 and PLS27 found in 10 mL rinsing buffer following successive rinses (n = 3).

This decreased sharply over the next three rinses (approximately 1 – 1.5 logs per rinse) before appearing to stabilise by the fourth rinse. Between $10^2$ - $10^3$ PFU/mL of phage were recorded in each rinse-off after this point. The phages being rinsed off are most likely unbound or weakly adsorbed, requiring minimal disruption to be removed from the surface and into the wash buffer. A proportion of them may not have been in any contact with the surface but suspended in droplets carried along with the

polyethylene disks between rinses. The reason for carrying out the rinsing assay was to determine the point at which all weakly bound phages were removed following successive rinses, leaving only their 'immobilised' counterparts. Naidoo *et al*. (2012) employed a similar rinsing step to remove unbound T4 and P22 phage particles from the gold nanoparticle substrate surface. The authors chemically immobilised the phages by exposing them to gold surfaces functionalized with dithiobis(succinimidyl propionate). To remove non-covalently attached phages, surfaces were rinsed with PBS followed by 10% solution of ethanolamine in PBS, although the number of rinses carried out to achieve this was not specified. Whilst the rinsing protocol described here did not extend beyond 8 rounds, the relatively low and stable rinse-off concentrations observed following the third rinse suggests that most bound phages were removed during the preliminary rinses. Based on this, a five-rinse protocol was taken forward for immobilised phage experiments in this chapter. This included the first three rinses, in which most of the phages were removed, together with an extra two rinses following stabilisation.

### 3.3.5 Bacteriophage Immobilisation on Polyethylene and Nylon 6

Results for bacteriophage binding on PE and N6 are presented in terms of post rinse surface concentration and percentage binding (Figure 3.10). Percentage binding efficiencies for each sample type were calculated by considering the starting bacteriophage concentration, volume of liquid loaded onto each surface, and the final concentration following the rinses. The way percentage efficiency varied across sample types was similar to the post-rinse surface concentration results. This confirms that differences observed between corona discharge intensities were not due to varying volumes of liquid loading onto the surfaces due to increased wettability. Binding efficiencies ranged between $10^{-1}$ % to $10^{-6}$ %. The aim of this experiment was not to achieve the highest possible binding efficiency but to ascertain differences in binding efficiencies across corona discharge treatment intensities considered. As such, the relatively low efficiency can be explained by the automated dipping method using the force tensiometer in which polymer surfaces were exposed to small volumes of phage lysate for a short time (approximately 3 minutes) before rinsing. It is anticipated that higher rates of binding efficiency would be achieved by submerging the substrate in phage lysate for longer periods of time.

The extent to which bacteriophages were bound 'irreversibly' to polymer surfaces varied across corona discharge intensities for bacteriophages T4, T5 and ST3 on both polyethylene and nylon 6 surfaces. In the case of all three phages, untreated surfaces retained the lowest concentration of viable bacteriophages following 5 rounds of rinsing. The best-performing treatment intensities for the three phages in terms of phage retention were 5.2 and 40 kJ/m$^2$. In all cases, these two treatment settings resulted in at least a log increase in phage surface concentration after rinsing. For T5 and ST3, 5.2 kJ/m$^2$ of treatment resulted in slightly better phage retention, whilst for T4, 40 kJ/m$^2$ was the more effective of the two intensities. It should be noted that these are mean values, with both intensity settings being within error of each other, as can be observed in Figures 3.10. These results are not unexpected. The surface analyses presented earlier in this chapter suggest that increasing corona treatment intensity results in the incorporation of polar functionalities on the polymer surface in question, as well as a higher number of free radicals. Assuming that the presence of both promotes stronger phage-substrate binding through non-specific interactions and covalent bonding, this could explain the higher number of bacteriophages being retained after the rinsing rounds were carried out. Interestingly, retention of T4, T5 and ST3 decreased at the highest corona discharge treatment setting of 400 kJ/m$^2$ for both polymer surfaces considered. This suggests that it is possible to 'overtreat' a surface, rendering it less able to retain bound phages. Corona discharge treatment involves the bombardment of a surface with high-energy chemical species (Chang *et al*., 1991). Through post-treatment SEM analysis, Yang *et al*., (2022) showed that increasing corona discharge treatment intensity was associated with cracks appearing on the silicone rubber surfaces being considered. Similar results have also been reported for epoxy resin (Yang *et al*., 2024). Such disruptions are likely to be caused by a combination of the increased crosslinking occurring on the surface during treatment together with the heat generated during treatment (Yang *et al*., 2022). Physically disrupted surfaces may be more prone to incurring losses of immobilised phage during rinsing. This may be due to entire surface layers being washed off. Another possibility is the increased embedding of phages in the surface due to the prevalence of cracks and pores, such that their tail fibres are impeded from adsorbing onto bacterial cells. It is anticipated that defining the precise point at which corona discharge ceases to be conducive to increased phage binding would need to be applied to any candidate substrate prior to phage immobilisation in an upscaled setting.

Another unexpected result is the apparent lack of effect on the retention of PLS27 bacteriophage following corona discharge treatment, with no notable difference between untreated and treated surfaces. This strongly indicates that specific characteristics of this bacteriophage act to promote strong adsorption on the surfaces considered, regardless of how activated they are. Viral particles have been shown to bind onto surfaces through both polar and hydrophobic interactions on account of respective polar and hydrophobic residues present with coat capsid proteins (Hosseinidoust *et al*., 2014). A high frequency of both of these residue types within the coating structure of bacteriophage PLS27 would explain its ability to bind strongly with both hydrophobic and polar surfaces, superseding the effects of surface functionalisation through corona discharge treatment. Further studies into the protein structure of the PLS27 capsid are required to confirm this.

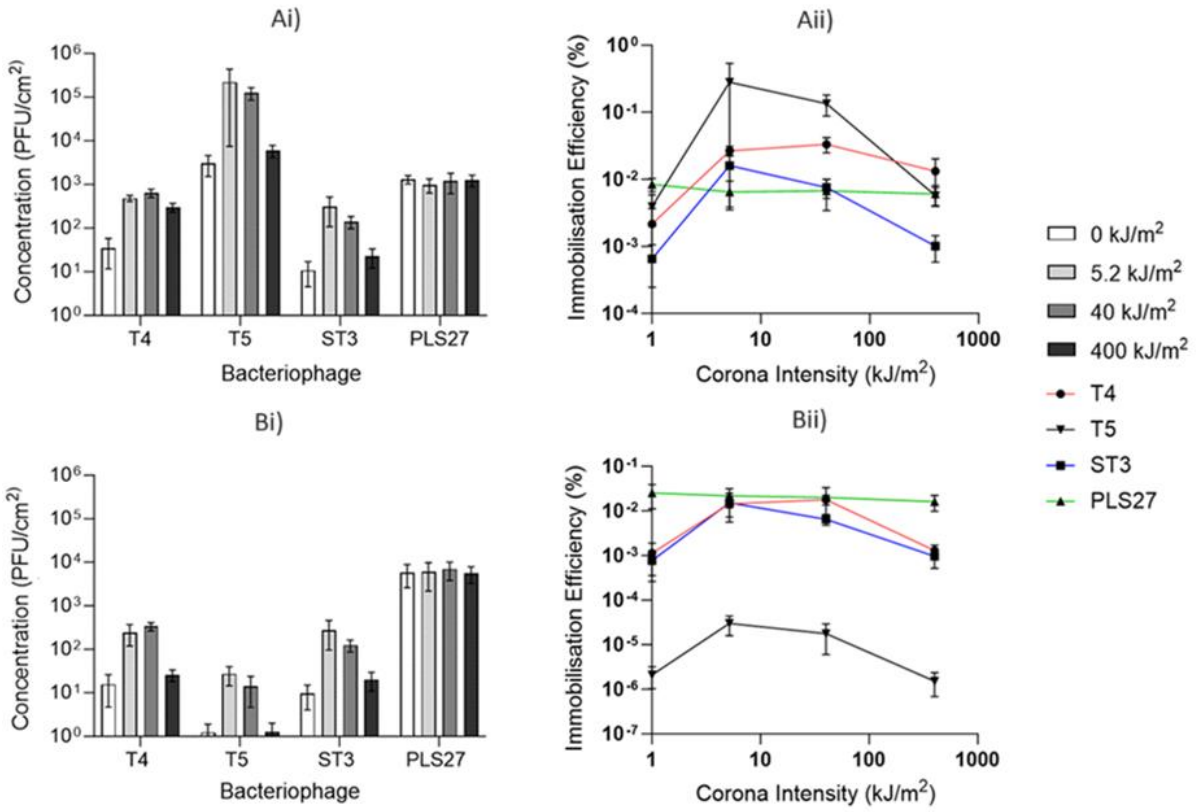


**Figure 3.10:** Histograms showing mean post-rinse concentrations (i) for bacteriophages T4, T5, ST3 and PLS27 on PE (A) and N6 (B) surfaces. Data for 5.2 kJ/m², 40 kJ/m², 400 kJ/m² of corona discharge treatment as well as a no treatment control is shown. Graphs (right) showing the mean immobilisation efficiency (ii) of each sample type are also included (n = 8).

Aside from the differences between bacteriophage types and corona discharge treatment intensity, the

polymer surfaces themselves also appeared to influence binding in the case of T5 (Figure 3.10). Percentage efficiency rose by approximately 3 logs for all treatment intensities when immobilising to polyethylene compared to nylon 6. As was the case with PLS27, this does suggest that biochemical characteristics on the T5 capsids give rise to increased binding on the polyethylene surface compared to nylon through hydrophobic interactions. It is also clear that corona discharge acts to increase T5 binding further on both surfaces, provided the surface is not over-treated, as was the case for 400 $kJm^2$ of treatment. Physical interactions may also be at play here. Bernardy & Malley (2023) showed that recovery of MS-2 viral particles decreased significantly with increased surface porosity during rinsing experiments, with viruses getting 'stuck' within the micro-crevices on the surfaces. A lack of pores on the nylon 6 surfaces compared to polyethylene could act to reduce post-rinse retention of the T5 phage. SEM or TEM imagining could be applied in future studies to confirm this. For the rest of the bacteriophages, binding efficiency remained fairly consistent between the two surfaces at each treatment intensity, suggesting that chemical and physical differences between polyethylene and nylon 6 did not have as pronounced an effect on their binding mechanisms.

These results show that corona discharge treatment can mediate irreversible binding of bacteriophages onto polymeric surfaces. Despite this, there are many factors that affect the efficiency of the process, including choice of bacteriophage, substrate, and corona discharge intensity. Further work could focus on carrying out an expanded study on a large range of surfaces to determine their tendency to promote immobilisation of specific bacteriophages. An expanded range of treatment intensities would also be important in order to confirm the hypothesis of surface overtreatment as well as establish optimised treatment intensities for specific bacteriophage-substrate pairings. The mechanism for corona discharge-mediated bacteriophage immobilisation remains unclear. Many studies have found that phages bind to polar groups on the surfaces, so it is likely that non-specific binding interactions are taking place to facilitate immobilisation (Hosseinidoust *et al*., 2014). These results cannot elucidate the extent to which free radical-mediated covalent linkage occurs. Wang *et al*. (2016) showed that plasma-activate polyhydroxyalkanoate surfaces formed covalent linkages with T4 phages applied to the substrate using XPS analysis. Furthermore, several studies have demonstrated the usefulness of plasma-based treatments in activating and covalently binding proteins onto surfaces through the formation of

surface radicals (Bilek & McKenzie, 2010; L. J. Martin *et al*., 2018; Yeo *et al*., 2017). Martin *et al*. (2018) used plasma polymerization to produce a radical-functionalised surface on titanium substrates. The authors postulated that the high surface radical concentration post-treatment allowed for the covalent binding of a synthetic linear polymer. Similarly, Yeo *et al*. (2017) used PIII to covalently bind tropoelastin onto polyethersulphone surfaces. It is likely that phage-surface binding observed in this section of work results from both surface radical activity and non-specific dipole-dipole interactions by incorporating polar functionalities on the surfaces after corona discharge treatment. Further experiments are required to determine which of these mechanisms is more effective.

### 3.3.6 Cytotoxic effect of an immobilised bacteriophage cocktail

Polyethylene disks onto which an immobilised cocktail of bacteriophages T4, ST3 and PLS27 were immobilised were effective in halting the growth of respective host cultures of *E. coli* 11303, *S. enterica* 50498 and *P. aeruginosa* AK44 in *in vitro* conditions (Figure 3.11). In the case of T4 and ST3, growth appeared to slow after about an hour, with the optical density of host cultures deteriorating steadily after this point. In the case of PLS27, a slowdown in growth was observed slightly later (about 1.5 hours), after which the optical density of *P. aeruginosa* steadily declined. As shown in the previous chapter (Section 2.3.1), PLS27 has a longer burst time than T4 and ST3, therefore this delay was expected. Optical densities of all strains exposed to the immobilised cocktail were reduced to 0 within the four-hour testing period. The PBS control did not differ significantly from the host controls. Plasma-treated surfaces can adversely affect microbial growth, justifying the need for a corona discharge + PBS control (Ma *et al*., 2022). The fact that this was not the case here allows for the assumption that the cytotoxic effect observed in all cases was due to the immobilised cocktail.

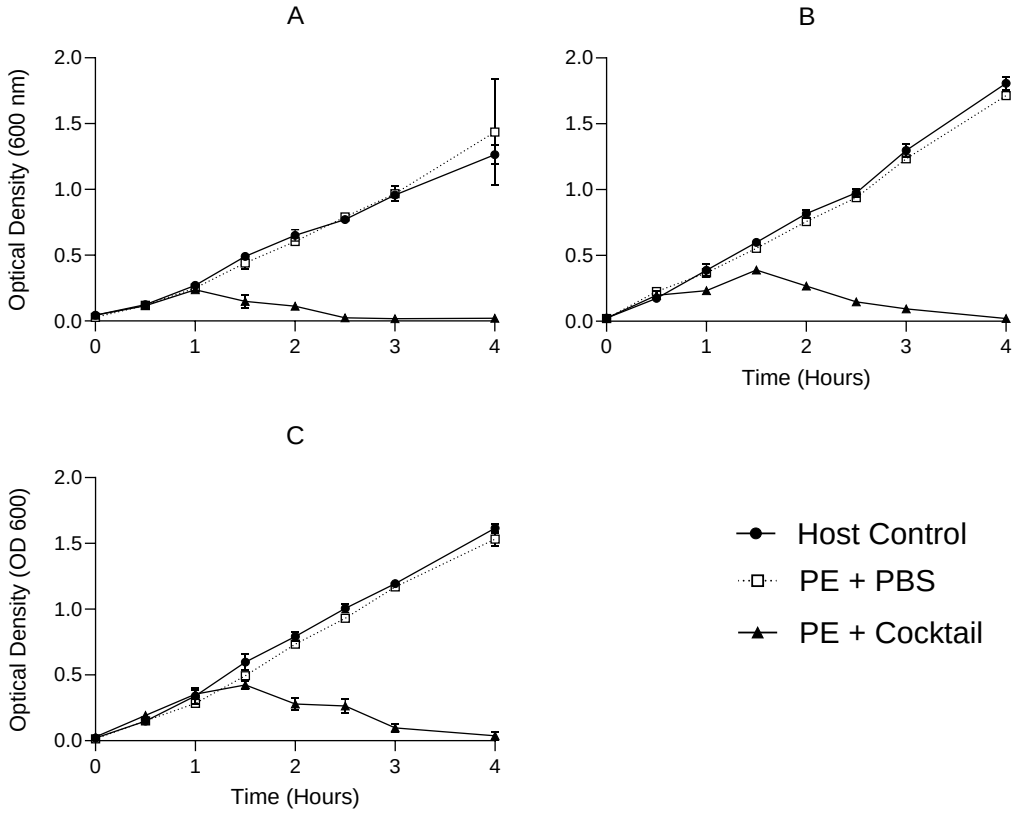


**Figure 3.11:** Graphs showing the growth of *E.coli* 11303 (A), *S. enterica* 50498 (B) and *P. aeruginosa* AK44 (C) expressed in terms of OD(600) against time. Included within each graph are curves for host growth challenged with PE disks containing an immobilised cocktail comprising bacteriophage T4, ST3 and PLS27, corona-treated PE control disks which exposed to PBS, as well as a host only control (n = 3).

The results presented here correspond to the findings of Nogueira *et al*. (2017), who showed that growing cultures of *P. aeruginosa* exposed to wound dressings containing immobilised vB_Pae-Kakheti25 phage exhibited a noticeable drop in rate of optical density increase compared to the control group after half an hour of incubation. Optical density readings flatlined after this point before beginning to decline after about 180 minutes. No quantification work was carried out on the immobilised cocktail in the work presented here; however, the relative ease at which growth was disrupted suggests that sufficient numbers of each phage were present on the polyethylene disks in order to bring about a cytotoxic effect. Disk samples were subjected to 5 rinses in the Tween 20 rinsing solution described earlier (Section 3.2.7); therefore, it is assumed that the activity of the remaining, strongly immobilised phages is bringing about the cytotoxic effect. To carry out immobilisation, disks were submerged in the cocktail and agitated over a one-hour period. This represents a considerably greater exposure to phage

lysate than what was done for the previous immobilisation experiment (Section 3.2.7), and it is anticipated that binding efficiency would be higher because of this.

## 3.4 CONCLUSIONS AND FURTHER WORK

Corona discharge has been shown to have a comparable effect on polymer films as other plasma-based techniques. The results of the DPPH assay showed that corona discharge treatment is associated with the generation of surface radicals, whilst FTIR results confirmed the incorporation of oxygen-based functional groups on treated polymer films. Degradation of free surface radicals on interaction with air molecules is likely to play a major role in the incorporation of these groups. Modified surfaces have higher surface energies on account of the polarities of the introduced functionalities. Surface energy was found to increase linearly with corona discharge treatment up to an intensity of 40 $kJ/m^2$. Results for CP and PVC suggest that a treatment saturation point exists for polymers beyond which surface energy will not increase further. Activated polymers appear to have varying rates of hydrophobic recovery, with cellophane returning to its baseline within 1 day. Rates of hydrophobic recovery are likely a consequence of the chemical and physical characteristics of the surface in question. It is anticipated that slower rates of recovery will be associated with improved immobilisation outcomes with respect to bacteriophages. This could form the basis of a new area of investigation, the results of which could be applied as part of a screening process for selecting the polymers most suitable for bacteriophage immobilisation.

The post-rinse phage concentration results generated for PE and N6 surfaces show that corona discharge treatment improves phage immobilisation efficiency by increasing the proportion of strong or irreversible binding occurring on the surface. For all phages apart from PLS27, post-rinse surface concentration improved at least 10-fold apart from at the highest treatment intensity of 40 $kJ/m^2$, suggesting that overtreatment of surfaces can result in phage losses following challenges such as rinsing. Determination of the treatment intensity at which phage immobilisation efficiency begins to decrease for given polymer types would make for a key area of investigation moving forward. Future work should also focus on carrying out phage immobilisation in a vacuum to promote radical-mediated binding to increase the proportion of

permanently immobilised phages. Corona discharge had no effect on the immobilisation efficiency of PLS27, suggesting that physical and biochemical characteristics of the phage particles also play a role when it comes to corona-mediated immobilisation. The choice of substrate can also influence the efficiency of the process. The results for T5 showed that there is a considerable improvement for PE over N6 surfaces, suggesting that physical differences between polymers give rise to different outcomes for certain bacteriophages. Therefore, an important future area of interest is the assessment of the immobilisation potential of specific phages on a variety of key polymers of interest. This would allow for the targeted pairing of phages with preferred substrates, which would be commercially relevant in a scaled-up process.

Finally, corona discharge-mediated immobilisation is shown to allow for the incorporation of bacteriophage cocktails onto polymeric surfaces. The results presented here suggest that even after extensive rinsing, enough irreversibly bound phages are retained on the surface and able to disrupt the growth of all corresponding host strains. This gives confidence to future experiments where the immobilisation of phage cocktails is considered. Furthermore, the ability to immobilise bacteriophages onto surfaces using a relatively simple and quick method has been demonstrated. This could have implications for incorporation into manufacturing processes.

# Chapter 4: Improving Stability and Surface Distribution of Immobilised Phage for Scaled-Up Production

## 4.1 INTRODUCTION

Most of the research that has been carried out on bacteriophage immobilisation has primarily been concerned with attempting novel approaches to achieve it and developing protocols from them. Early-stage research like this typically involves setting up small scale experiments that are easier to repeat and optimise and less wasteful. A major aspect of product development is transitioning from small scale research-level experiments to larger scale production. In such a context, preserving bacteriophage stability post-immobilization and ensuring comprehensive phage distribution across the intended surface are critical. This chapter's primary focus is on optimising post immobilization stability and distribution of bacteriophages on polymer sheets within a scaled-up framework.

Bacteriophage stability is a major concern when it comes to products containing immobilised phages. Many phages in solution can be stored at 4 °C in phosphate-buffered saline or freezing conditions below – 20 °C in glycerol or dimethyl sulfoxide for extended periods, retaining their titers over the long term (Fortier & Moineau, 2009; Golec *et al*., 2011; Marton *et al*., 2021). Despite this, there is variation between phages when it comes to stability in free form (Duyvejonck *et al*., 2021). Whilst bacteriophages can be stored as dry formulations through freeze drying and spray drying techniques, when in an immobilised state on a surface, as is the case for the work presented here, they are susceptible to desiccation and temperature-related stresses, resulting in substantial loss of activity (Malik *et al*., 2017b). Various additives can be used to increase phage stability following drying. Furthermore, the drying process presents several challenges to bacteriophage viability. Being composed mainly of proteins, the structural integrity of bacteriophages is reliant on H-bonds, dipole-dipole interactions and sulfide bridges between the amino acids comprising their coat proteins as well as H-bonds between these proteins and surrounding water molecules. Loss of these water molecules from the system results in additional H-bonds being established within and between proteins (Zhang *et al*., 2020). This results in protein denaturation as well as aggregation, which both contribute to a loss in bacteriophage viability.

The use of sugars such as trehalose, sucrose, lactose and pullalan is well documented in the stabilization of dried bacteriophages (Chang *et al*., 2017; Choi *et al*., 2023; Kamali *et al*., 2022; Zheng, 2023). Proteins such as leucine have also been studied extensively (Chang *et al*., 2017). Most of the research

involving the use of additives to increase phage stability has been carried out in the context of freeze and spray drying, whereby the substance in question acts as an excipient to stabilize the phages; however, some studies have been carried out specifically on immobilised phage. For example, Leung *et al*., (2018) used pullalan-trehalose formulations to preserve bacteriophages immobilised onto food packaging. For the work detailed here, five candidate stabilizer substances are considered, including leucine, sucrose, trehalose, lutensol and lecithin. The last two are surfactants, which have been used in the context of PEG protein and bacteriophage stability, respectively, through the formation of emulsions (Balcão *et al*., 2014; Martínez-Negro *et al*., 2022). Two aspects of immobilised phage stability are considered in this work; stability during the drying process and post-drying shelf-life.

The previous chapter described an immobilisation protocol in which small, activated polymer disc cut outs were gently dipped into the phage lysate in question before being removed. Such a set up would be difficult to achieve on a mass scale due to the stop-start nature of the procedure. The films would, in practice, be considerably larger than the discs and in massive quantities, which would render this a highly inefficient process. A more feasible solution would be for the corona discharge and phage to be applied onto the film as it moves through the discharge field, allowing for the design of a continuous process which would be relatively simple to apply industrially. Plastic films are manufactured through several processes, including extrusion stretching, thinning and blowing processes (Mckean, 2017). All these processes require the film to be in a constant state of motion as it passes from one stage of a given process to the other (Mckean, 2017). This is mediated by roller systems that move the film along (Mckean, 2017). Films are often modified after they are produced. This includes printing coloured inks onto the surface and other substances, such as antimist layers, in the case of food packaging (Sason *et al*., 2019; Szentgyörgyvölgyi, 2016). As with the initial production process, this involves passing the film through a roller system, during which substances of interest can be applied onto the polymer surface. To increase surface wettability of polymers, corona discharge is typically used to treat the surfaces before applying the desired substance (Izdebska, 2016). This supports the case for industrialized immobilisation of phages onto polymer films since in many cases, a corona discharge generator already features in the manufacturing setup.

A key aspect of post-production modification of polymers is the application of substances using gravures (Q. Huang & Zhu, 2018; Ramirez & Tumolva, 2018; Szentgyörgyvölgyi, 2016). The cells within gravures allow for consistent coating of uniform thickness along the surface and their cylindrical shape allows for continuous application as the films moves through the roller system. Should gravure application allow for successful binding of bacteriophages, then this would represent a viable approach to achieve scaled up immobilisation. Limited research has been carried out on gravures with respect to bacteriophage immobilisation onto plastic film; however, T4 phage been applied via gravure onto paper surfaces as part of a 'bio-ink' solution (Jabrane *et al*., 2011; Mangin *et al*., 2008). The authors in both these studies report the apparent resistance the phage to the shear forces arising through the gravures.

For this section of work, bacteriophage immobilisation was carried out on corona discharge-treated polymer sheets using a simple automated gravure system. Unlike paper sheets, which absorb liquid applied onto them, aqueous solutions placed onto plastic sheets remain on the surface until they dry off. This can potentially make immobilisation difficult to achieve, depending on the extent to which reticulation occurs. In cases of high reticulation, phages will not distribute evenly over the surface, resulting in 'gaps' in bioactivity. This would not be desirable from a commercial product point of view, especially where consistency and quality control are key to successful manufacturing. As shown in Chapter 3, corona discharge treatment results in increased surface energy, and, therefore wettability, and chemicals such as isopropanol and surfactants are often used in industry to facilitate wetting of the surface by the liquid applied (Szentgyörgyvölgyi, 2016). These could also apply to bacteriophage immobilisation provided their presence does not affect phage viability. Part of this work will involve analysing immobilised surfaces to assess phage distribution. Whilst performing the page loading assay described in Chapter 1 on sheet cut outs will provide useful insight, work will be carried out to establish a more encompassing assay which will allow for assessment of larger areas of film. Successful demonstration of bacteriophage immobilisation on scaled-up quantities of polymer sheets could have significant implications for bioactive surfaces as a field of study as well as an industrial process.

## 4.2 MATERIALS AND METHODS

### 4.2.1 Materials and Instruments

Nutrient agar and broth (Sigma Aldrich, UK); tryptic soy agar and broth (Sigma Aldrich, UK); brain heart infusion agar and broth (Sigma Aldrich, UK), phosphate buffered saline (Gibco, UK); distilled water, sucrose (Sigma Aldrich, UK), lecithin (Sigma Aldrich, UK), Lutensol T089 (BASF, GE), isopropanol (Sigma Aldrich, UK), beeswax (Rhoose Point Remedies, UK);T4 bacteriophage; *Escherichia coli* 11303, T5 bacteriophage; ST3 bacteriophage, *Salmonella enterica* 50498, PLS27 bacteriophage, *Pseudomonas aeruginosa* AK44, 0.5 mm polyethylene sheets (The Plastic Shop, UK), 0.5 mm nylon 6 film (The Plastic Shop, UK); 24-well plates, 0.22 µm syringe filter units, Tantec EST corona treater, sterile scalpels (Mediware, DE); 1000 uL, 200 uL and 20 uL pipette fillers (Rainin, UK); MB25 moisture analyser (OHAUS, USA); incubator; laminar flow hood, Mx-T6-S tube roller (DLAB Scientific Instrument Inc, USA); 50 mL falcon tubes; 1.5 mL microcentrifuge tubes, K Control Coater (RK Instruments, UK); PRO 50 mm Spring Clamp (RS Components, UK); EVA A4 foam sheets (Creativ Company, UK), 250 mL conical flasks (Fisherbrand, UK); 0.22 µm syringe filter unit (Thermofisher, UK); Stericup quick-release 0.22 µm filter unit (Millipore, UK); Whirlimixer vortex spinner (Nickel-Electro ltd, UK); Heraeus megafuge 16 centrifuge (Thermo Scientific, UK); Snakeskin dialysis membrane (Thermo Scientific, UK); 1 grade filter paper (Whatman, USA); Ultrospec 10 Cell Density Meter (Biochrom, UK).

### 4.2.2 Bacteriophage Propagation and Purification

Purified lysates of bacteriophages T4, T4, ST3 and PLS27 were produced as detailed in Chapter 2 (see section 2.1.2).

### 4.2.3 Drying Protocol Development

To develop a drying protocol, two methods were considered and assessed in their ability to reduce the percentage moisture of wet surfaces. 3 cm by 3 cm cutouts of N6 were used as substrate surfaces. They were prepared on a chopping board using sterile single use scalpels. Surfaces were wetted by first

treating them with corona discharge at a power of 200 W, and electrode height of 4 mm and a belt speed of 7.75 m/min. Following this, 300 uL of either PBS or T4 bacteriophage lysate were applied onto the Nylon 6 squares. Drying was carried out by incubating the wet squares overnight at 30 °C, as well as by subjecting them to laminar flow overnight in a biological safety cabinet at room temperature. A list of all samples considered is shown below:

**Table 4.1:** List of samples considered for development of the drying protocol.

| Sample | Substrate | Phage/PBS Added | Corona Treatment | Drying Method | Moisture Analysis |
|---|---|---|---|---|---|
| 1 | Nylon 6 Square | 300 uL T4 (1 x $10^8$ PFUmL) | 200W, 7.75 m/min, 4 mm height | Incubator 30 ˚C (Overnight) | After drying |
| 2 | Nylon 6 Square | 300 uL T4 (1 x $10^8$ PFUmL) | 200W, 7.75 m/min, 4 mm height | Laminar Flow Hood (Overnight) | After drying |
| 3 | Nylon 6 Square | 300 uL PBS | 200W, 7.75 m/min, 4 mm height | Incubator 30 ˚C (Overnight) | After drying |
| 4 | Nylon 6 Square | 300 uL PBS | 200W, 7.75 m/min, 4 mm height | Laminar Flow Hood (Overnight) | After drying |
| 5 | Nylon 6 Square | 300 uL T4 (1 x $10^8$ PFUmL) | 200W, 7.75 m/min, 4 mm height | N/A | Moisture tested once sample prepared |
| 6 | Nylon 6 Square | PBS | 200W, 7.75 m/min, 4 mm height | N/A | Moisture tested once sample prepared |
| 7 | Nylon 6 Square | N/A | 200W, 7.75 m/min, 4 mm height | N/A | Immediately |

Effectiveness of the protocols was assessed by comparing the percentage moisture of samples which had undergone drying with the baseline set by assessing dry nylon 6 squares.

### 4.2.4 Assessing Free Phage Survival in Formulations

Leucine, lecithin, lutensol, sucrose and trehalose were considered for bacteriophage formulations. For each substance, 2 % wt/vol and 10 % solutions were produced by adding 1 g and 5 g to 50 mL of PBS in 50 mL Falcon tubes. In the case of leucine, only a 2 % solution was prepared due to the sparingly soluble nature of the protein. Following preparation, solutions were mixed on an Mx-T6-S tube roller

for 1 hour at the minimum speed setting. 900 uL of each solution were added to microcentrifuge tubes, followed by 100 uL of bacteriophages T4, T5, ST3 and PLS27 at concentrations ranging from $10^6 – 10^7$ PFU/mL. Control samples were also prepared using 900 uL of distilled water and PBS. In total, 44 samples were prepared (see Table 4.2).

**Table 4.2:** List of bacteriophage formulations considered. Each of the 4 phages were added to distilled water, PBS, 2 % leucine, as well as 2 & and 10 % solutions of sucrose, trehalose, lutensol and lecithin.

| Sample | Formulation | Bacteriophage |
|---|---|---|
| 1 | Distilled water | T4 |
| 2 | Distilled water | T5 |
| 3 | Distilled water | ST3 |
| 4 | Distilled water | PLS27 |
| 5 | PBS | T4 |
| 6 | PBS | T5 |
| 7 | PBS | ST3 |
| 8 | PBS | PLS27 |
| 9 | 2 % leucine | T4 |
| 10 | 2 % leucine | T5 |
| 11 | 2 % leucine | ST3 |
| 12 | 2 % leucine | PLS27 |
| 13 | 2 % sucrose | T4 |
| 14 | 2 % sucrose | T5 |
| 15 | 2 % sucrose | ST3 |
| 16 | 2 % sucrose | PLS27 |
| 17 | 10 % sucrose | T4 |
| 18 | 10 % sucrose | T5 |
| 19 | 10 % sucrose | ST3 |
| 20 | 10 % sucrose | PLS27 |
| 21 | 2 % trehalose | T4 |
| 22 | 2 % trehalose | T5 |
| 23 | 2 % trehalose | ST3 |
| 24 | 2 % trehalose | PLS27 |
| 25 | 10 % trehalose | T4 |
| 26 | 10 % trehalose | T5 |
| 27 | 10 % trehalose | ST3 |
| 28 | 10 % trehalose | PLS27 |
| 29 | 2 % lutensol | T4 |
| 30 | 2 % lutensol | T5 |
| 31 | 2 % lutensol | ST3 |
| 32 | 2 % lutensol | PLS27 |
| 33 | 10 % lutensol | T4 |
| 34 | 10 % lutensol | T5 |
| 35 | 10 % lutensol | ST3 |
| 36 | 10 % lutensol | PLS27 |
| 37 | 2 % lecithin | T4 |
| 38 | 2 % lecithin | T5 |
| 39 | 2 % lecithin | ST3 |
| 40 | 2 % lecithin | PLS27 |

| | | |
|---|---|---|
| 41 | 10 % lecithin | T4 |
| 42 | 10 % lecithin | T5 |
| 43 | 10 % lecithin | ST3 |
| 44 | 10 % lecithin | PLS27 |

Once prepared, the solutions were homogenised by spinning the tubes for 3 seconds on a Whirlimixer vortex spinner. Solutions were then stored at room temperature. Bacteriophages in each formulation were quantified on days 1, 3 and 12. This was carried out using the plaque assay technique (Baer & Kehn-Hall, 2014).

### 4.2.5 Assessing Drying and Shelf-Life of Bacteriophage Formulations Immobilised onto Nylon Squares

The formulations considered in Section 4.2.4 were prepared, with a target starting bacteriophage concentration of $10^6$ PFU/mL. 2 cm by 2 cm nylon 6 squares were cut using a sterile scalpel on a chopping board. Squares were treated with corona discharge using the EST system at a power setting of 200 W, a belt speed of 7.75 m/min and an electrode height of 4 mm. Following treatment, 100 uL of each formulation were pipetted onto a treated nylon 6 square. Squares were placed on a flat tray and dried overnight in an incubator set to 30 °C. Enumeration of bacteriophages was carried out the following day. To do this, the equivalence bacteriophage loading assay developed in Chapter 2 was utilised (see Section 2.2.4).

A post-drying shelf-life experiment was also conducted. For this, the following formulations were considered: 2 % wt/vol sucrose, 2 % wt/vol lecithin and a 2 % wt/vol sucrose/2 % wt/vol lecithin combined formulation. PBS was used as a solvent for each formulation. Free-phage concentration in each formulation was set to approximately $10^6$ PFU/mL. Immobilisation and drying on nylon 6 squares were carried out as detailed in the paragraph above. Following this, squares were placed in sealed Petri dishes and stored at 30 °C in an incubator. The equivalence bacteriophage loading assay described in Chapter 2 (see Section 2.2.4) was carried out on the following days after storage: 1, 7, 14, 28, 56, 112 and 224.

4.2.6 Assessing distribution of bacteriophage formulations immobilised onto polyethylene sheets

The following formulations were considered: PBS (no formulation), 15 % isopropanol (IPA), 2 % sucrose, 2 % lutensol and a 2 % sucrose/2 % lutensol/2 % lecithin mixed formulation. Solutions were prepared in 50 uL falcon tubes. PBS was used as a solvent for all formulations. The four bacteriophages being considered were added to the formulations at a final free phage concentration of $10^8$ PFU/mL. 20 cm by 30 cm sheets of polyethylene were cut on a chopping board using a sterile scalpel.

Sheets were treated with corona discharge using the EST system at a power setting of 200 W, a belt speed of 7.75 m/min and an electrode height of 4 mm. After treatment, sheets were immediately secured on the flat bed of a K Control Coater. The brown colour-coded gravure, corresponding to an 80-micron surface layer thickness, was installed on the device. 5 mL of bacteriophage formulation was applied to the top of the polyethylene sheet. A single, downward coating was carried out at a speed of 1 m/min across the sheet. After coating, the sheet was removed and left to air dry at room temperature overnight.

To enumerate bacteriophages across the sheets, an adapted protocol for the bacteriophage equivalence loading assay described in Chapter 2 (see Section 2.2.4) was carried out. 12 cm by 8 cm rectangles were cut out of the phage-immobilised sheets using a sterile scalpel. The wells of a 24-well plate were filled with 2 mL of nutrient, tryptic soy or brain heart infusion broth, depending on the bacteriophage being enumerated. Each well was inoculated with 20 uL overnight culture of the corresponding host cells. The lid was replaced on the well plate, and the cells were left to incubate at 37 °C until an OD (600) of 0.4 was reached. The well plate was removed from the incubator, and the lid was removed. A small amount of beeswax was applied across the circular well tips of each well using a cotton bud. The 12 cm by 8 cm sheet cut out was then placed (phage side down) onto the well plate such that each well was covered by part of the polyethylene sheet. A 10 cm by 6 cm by 1 cm cut-out of foam was placed on top of the well plate, covering the polyethylene sheet. The well plate lid was then secured on the top of the plate using four PRO 50 mm Spring Clamp on each corner of the plate. The well plate was then inverted and left to incubate until the first lytic burst occurred. After this, the liquid in each well was filtered through a 0.22 µm filter. Bacteriophages were enumerated using the plaque assay technique (Baer & Kehn-Hall, 2014). As for the protocol developed in Chapter 2, the initial bacteriophage concentration was determined using a loading

curve constructed using free-phage standards, which were prepared in 24-well plates as opposed to Falcon tubes.

## 4.3 RESULTS AND DISCUSSION

### 4.3.1 Comparison of laminar flow and incubation-based drying

Nylon 6 had a baseline percentage moisture of 0.85 % (Table 4.3). This was reduced further to 0.54 % and 0.79 % following respective incubation and laminar flow-mediated drying techniques. These values were within error of each other, suggesting no significant difference between the drying techniques. It would be expected that most substrates would contain trace amounts of water, introduced either during their production processes or through water droplets settling on the surface during periods of high atmospheric humidity. When it came to drying wetted samples, there was no notable difference between incubation and laminar flow, with both methods resulting in post-drying percentage moisture ranging from 0.32 % to 0.41 % above the baseline.

**Table 4.3:** Results of moisture analysis of samples before and after air, laminar flow and incubator-mediated drying.

| Sample | Drying Method | Mean Initial Percentage Moisture (%) | Mean Post-Drying Percentage Moisture (%) |
|---|---|---|---|
| Nylon 6 | Incubation at 30 °C | 0.85 ± 0.09 | 0.54 ± 0.10 |
| Nylon 6 | Laminar Flow | 0.85 ± 0.09 | 0.79 ± 0.07 |
| Nylon 6 + PBS | Incubation at 30 °C | 29.50 ± 0.50 | 1.21 ± 0.60 |
| Nylon 6 + PBS | Laminar Flow | 29.50 ± 0.50 | 1.17 ± 0.52 |
| Nylon 6 + PBS | Air-Dried | 29.50 ± 0.50 | 6.47 ± 0.80 |
| Nylon 6 + T4 | Incubation at 30 °C | 32.56 ± 0.50 | 1.24 ± 0.61 |
| Nylon 6 + T4 | Laminar Flow | 32.56 ± 0.50 | 1.18 ± 0.44 |
| Nylon 6 + T4 | Air-Dried | 32.56 ± 0.50 | 8.60 ± 0.76 |

Both techniques were more effective than the air-dried controls (Table 4.3 and Figure 4.1), which dried samples to mean percentage moistures of 6.47 and 8.60 for PBS and T4 coated surfaces, respectively. This demonstrated the importance of not relying on the natural drying process for later experiments in

this chapter. The primary reason for drying samples was to stress the bacteriophages sufficiently to determine the formulations that were best at protecting them. In the case of air-dried samples, the higher resulting percentage moisture values may have promoted the survival of unformulated phages, making it considerably more challenging to elucidate any differences between formulations.

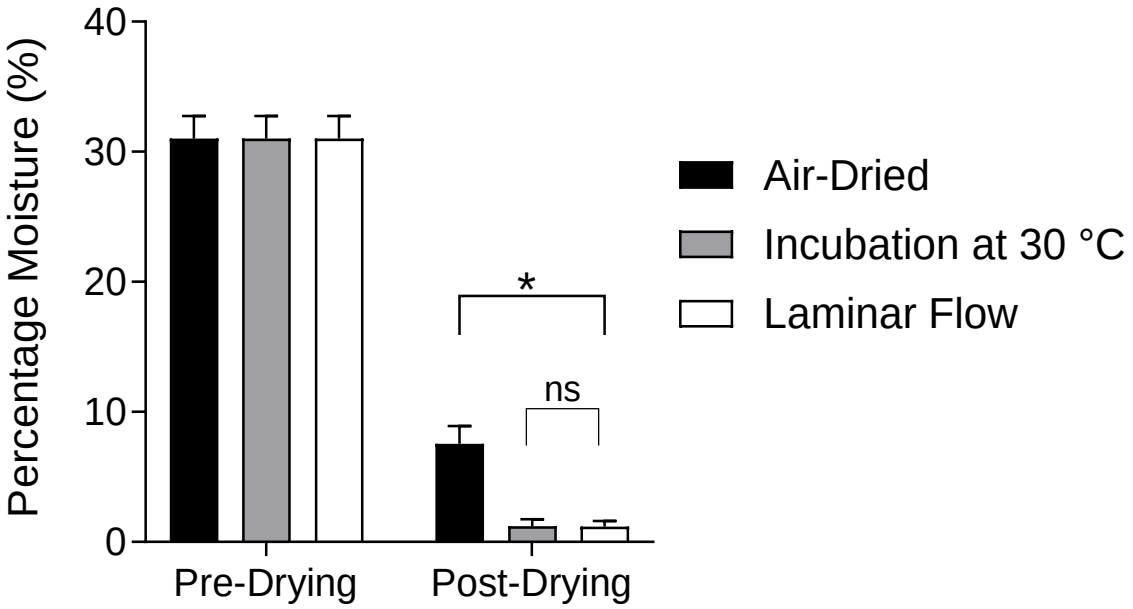


**Figure 4.1:** Histogram showing mean percentage moisture values for pooled phage and PBS solutions deposited on Nylon 6 squares before and after drying (n = 6).

The presence of purified phage lysate on the nylon 6 surface did not influence the extent to which drying occurred, suggesting that any potential anti-desiccation effects brought about by the added components of a bacteriophage lysate were negligible (Table 4.3 and Figure 4.1). Despite there being no difference in efficiency between the drying methods, it was decided that the incubation protocol would be taken forward as a standard drying protocol due to the anticipation that subjecting bacteriophage formulations to an elevated temperature for twenty-four hours would stress the samples to a greater extent in terms of phage stability. It should be noted that in a scaled-up setting, a faster, more efficient drying protocol would be required to maintain high productivity.

4.3.2 Effect of formulations of stability of free and immobilised phage

Following sample preparation, phage activity either remained relatively unchanged (within the same log of concentration) or demonstrated a sharp drop over the first twenty-four hours of incubation. After this period elapsed, phage activity stabilised or continued to decline at a more gradual rate. In some cases, phage activity continued decreasing sharply over the entire test period.

Drops in phage activity were expected to occur for most formulations due to the temperature the experiment was conducted at. Many bacteriophages, including the four considered here, demonstrate optimal stability at 4 °C (Fortier & Moineau, 2009). The fact that they were held at ambient temperature was a significant stressor, evidenced by the pronounced deterioration observed in the case of the distilled water and PBS controls (Figure 4.2). Whilst some bacteriophages have been shown to remain stable in pure water, many typically lose activity on account of phage particles rupturing due to osmotic effects (Jończyk-Matysiak *et al*., 2019). This explains why the pure water controls exhibited the highest rate of deterioration for all phages considered.

With the exception of bacteriophage PLS27, drops in activity were observed for 2 % sucrose solution. These ranged between 2 logs (T5) and 3 logs (T4 and ST3) over the 12-day testing period. At an increased sucrose concentration of 10 %, the rate of decline reduced considerably for T4 and ST3, with respective log drops of 1 and 0. The rate of decline for T5 remained unchanged. It should be noted that despite these declines, all phages exposed to 10 % sucrose had improved shelf-life compared to the PBS controls. Similarly, in the case of trehalose formulations, all phage formulations were at least 1 log higher in concentration than the PBS controls with the exception of phage ST3. Sugars are effective at stabilising proteins in solution by acting as osmolytes to reduce aggregation and denaturation (Back *et al*., 1979; Ohtake *et al*., 2011).

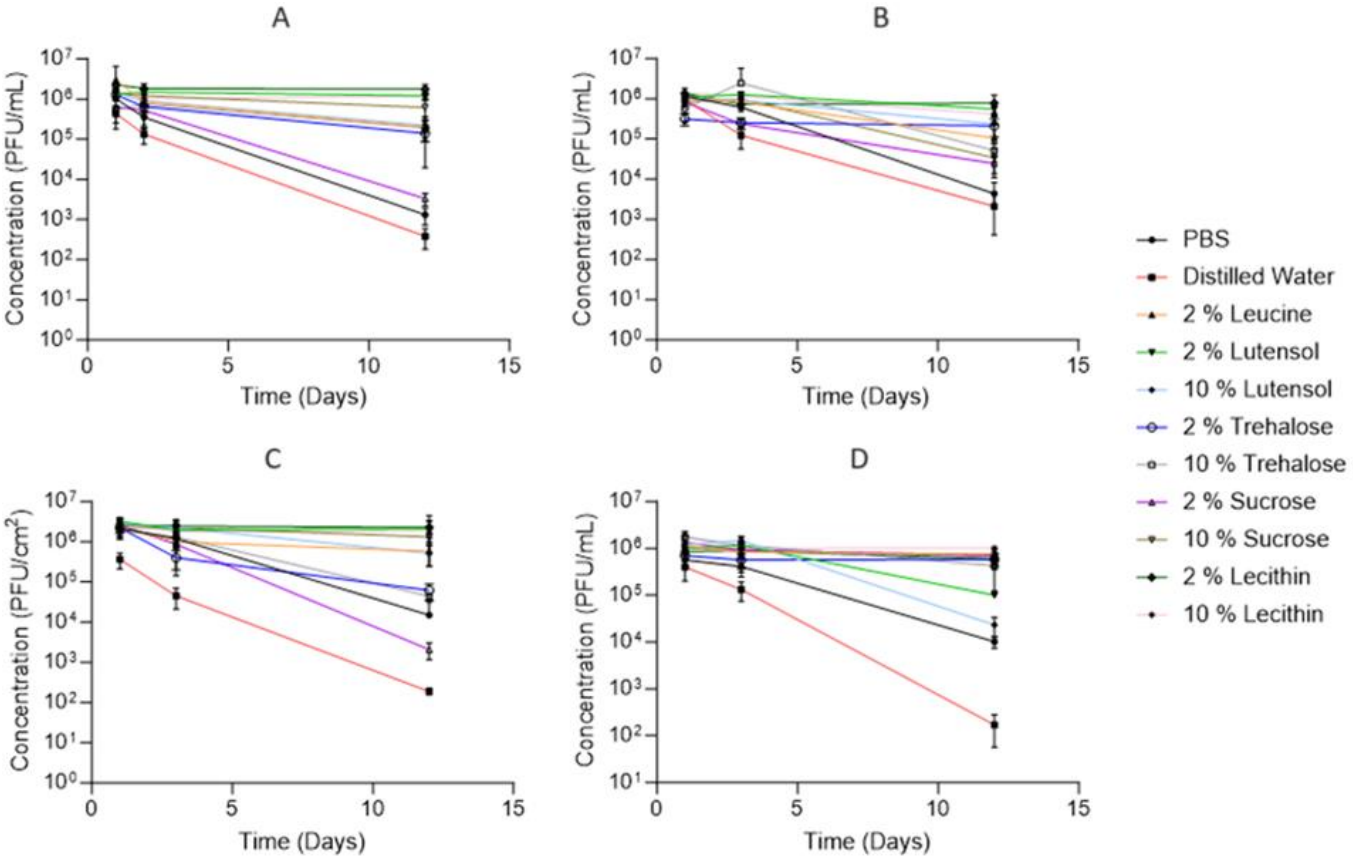


**Figure 4.2:** Survival of bacteriophages T4 (A), T5 (B), ST3 (C) and PLS27 (D) over a 12-day period. All formulations were stored at room temperature, with phages being quantified on days 1, 3 and 12 using plaque assays (n = 3).

Although extensive studies on phage survival in lutensols have not been carried out, Fister *et al*. (2016) found phage P100 activity to be stable for at least 24 hours following exposure to up to 5 % Lutensol AO7. The results for T4, ST3 and T5 suggest that lutensol may act as be a stabiliser for free phage at non-refrigerated temperatures, with minimal decline observed over the test period. PLS27 was unique amongst the phages considered in that it did deteriorate when suspended in lutensol. Furthermore, its activity remained stable in the presence of trehalose whilst for the other three phages, activity declined by about 1 log over the test period. A similar observation was made for formulations containing 2 % leucine. These results suggest that there are distinct differences between the biochemical structures of phages T4, T5 and ST3 compared to PLS27. It is possible that these are the same differences that gave rise to the unique immobilisation patterns observed for PLS27 in the previous chapter (see Section 3.3.5).

The lecithin formulations proved to be universally stable for all phages considered. As already discussed, surfactants can have stabilising effects on bacteriophage particles through emulsification. The use of lecithin as a bacteriophage stabiliser has been reported previously by Balcão *et al*. (2014), who used it alongside other substances to encapsulate phages of *Salmonella enterica* in water-in-oil-in-water emulsions. The authors report the phages retaining activity up to a temperature of 39 °C. The results here suggest that the emulsions formed by lecithin could offer stabilisation to a wide range of bacteriophage species.

As already discussed, these results suggest that declines in bacteriophage activity observed across the formulations tested are due to the temperature stress experienced over the test period. All of the formulations were produced by dissolving the components in question in PBS. Nearly all of the phage-formulation combinations performed better than the PBS controls, either by stabilising over the initial days of the test period or by deteriorating at a slower rate by the last test day. This indicates that they did not adversely affect phage viability over the long term. The only exception to this was the ST3/2 % sucrose combination, whereby phage concentration was 1 log lower than the PBS control by the end of the test period. This was an unexpected result despite the formulation also performing poorly for T4 and T5 (without their final concentrations dropping below the PBS control). The fact that at a higher concentration, there was a notable improvement in performance in these three phages suggests that sucrose acts as a stabiliser at a sufficient concentration. It would be worth carrying out a repeat experiment to confirm that 2 % sucrose is antagonistic to ST3 survival at ambient temperature, and the result seen here is not an outlier.

The long-term stability of free phage formulations, whilst not entirely relevant to this section work, whereby phages were immobilised and dried, could have serious implications for the scaled-up manufacture of phage-immobilised surfaces. At production volumes, there is a need to maintain refrigerated conditions either onsite or during transit. The addition of a stabiliser to free phage preparations could potentially eliminate the need for a cold chain, significantly cutting costs from the process. This work was conducted to confirm the short-term stability of the phages in the various formulations, as immobilisation and subsequent drying was planned to occur within twenty-four hours

of their preparation. Despite some differences in phage survival over the first few days of testing, none of the formulations (including the water and PBS controls) exhibited total degradation immediately. As such, they were all taken forward for drying stability testing.

### 4.3.3 Effect of formulations on drying stability

An important factor to consider when it comes to the coating of surfaces with various formulations is the extent to which the surface changes physically. Significant changes may be unacceptable from an aesthetic point of view depending on the final application of the surface but could also functionally hinder the active component. A preferable result would be one in which there is no discernible difference between coated and uncoated surfaces. All of the formulations considered gave rise to observable differences of varying degrees following drying (Figure 4.3).

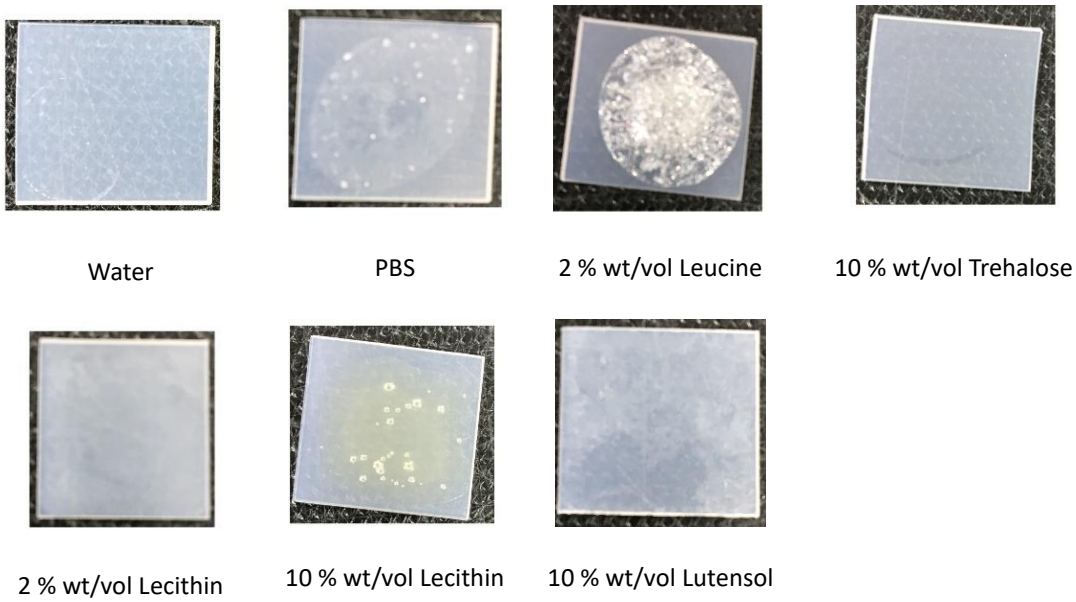


**Figure 4.3:** Images of 3 cm x 3 cm nylon squares with immobilised phage formulations. Photos taken after overnight incubation at 30 °C after the phages were immobilised.

The most dramatic of these were surfaces coated with 2 % leucine, in which a white region of considerable rugosity resulted where the droplet was applied. Droplets tended to form a shallow dome-

like structure, which could be seen 'sticking out' of the surface when observed from the side. This result was likely due to the tendency of leucine to supersaturate during the evaporation of water, resulting in the crystalline dome structure observed (Feng *et al*., 2011). No structures formed for any of the other formulations, although noticeable staining did occur in some cases. For 10 % lecithin, surfaces took on the characteristic yellow colour associated with lecithin formulations over the application area. This yellow colour was almost completely eliminated when 2 % lecithin was used, but considerable blushing could still be observed on the surface. Similar blushing was observed for both lutensol formulations. In the case of PBS alone, salt crystals forming as a result of water evaporation were observed over the area of application. The most visibly unchanged surfaces were those that were coated in both strengths of the sugars considered, trehalose and sucrose. No visible blushing occurred for these formulations, but a faint outline where the original formulation droplet was applied was visible in some cases. Many sugars are known to form thin glass layers when immobilised onto surfaces through a process known as vitrification, and while not evident in the images taken, it is possible that small sugar glass layers did form in the case of trehalose and sucrose formulations (Mensink *et al*., 2017).

Overnight incubation at 30 °C was sufficient as a stressor to completely degrade all four bacteriophages considered when deposited onto the surface suspended in pure water or PBS (Figure 4.4). This is consistent with previous studies in which unformulated phages completely degraded during drying ( Leung *et al*., 2018). 10 % lecithin provided the highest degree of protection against drying, with all phage preparations remaining within a log of the starting quantity. The same was true of 2 % lecithin, albeit at a slightly lower rate of survival. As already mentioned, the tendency of lecithin to encapsulate proteins is a likely reason for the high rates of survival observed for both concentrations (Řepka *et al*., 2023). Furthermore, the fact that it comprises a diverse mixture of lipids, including phospholipids, triglycerides, fatty acids sterols, does increase its ability to form stable oil/water emulsions and thus, increasing the applicability of the substance to broader range of bacteriophages in the context of stabilisation (Tabaniag *et al.*, 2023).

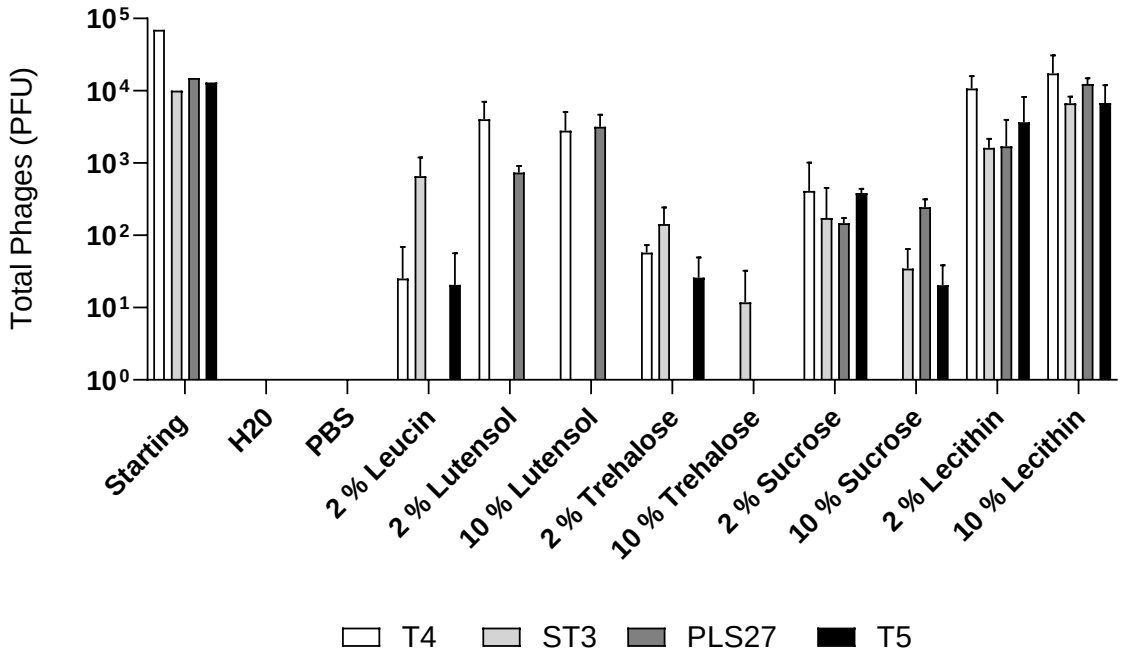


**Figure 4.4:** Mean total number of phages T4, ST3, PLS27 and T5 immobilised onto nylon 6 and overnight drying at 30 °C. The starting phage numbers have also been provided (n = 3).

The only other formulation that provided uniform protection to all the phages considered was 2 % sucrose, an unexpected result given its poor performance regarding the long-term stability of free T4, T5 and ST3. There was reduced survival for T4, ST3 and T5 phages dried in 10 % sucrose, complete degradation for T4 and an approximate 1 log reduction for ST3 and T5, while PLS27 survival improved slightly. This result once again demonstrates a distinction between PLS27 and the other phages discussed previously. The other sugar formulation considered, trehalose, was not as effective as sucrose when it came to post-drying stability. Only 3 of the four phages survived drying when in 2 % trehalose (PLS27 degraded completely) compared to the full complement in the latter, and of the phages that did survive, T4 and T5 post-drying concentrations were approximately 1 log lower than their 2 % sucrose counterparts. ST3 was the only phage to survive drying in 10 % trehalose. The use of trehalose and sucrose for the stabilisation of dried phages has been reported previously, with both compounds being used as excipients for phages undergoing spray and freeze drying (Malik *et al*., 2017b). The most likely mechanism for sugar-mediated stabilisation is through vitrification, which is the formation of thin glass layers on the film surface (Zheng, 2023). Phages entrapped within these glass layers are protected

against drying stresses due to the structural stability provided by the vitrified sugar. Aside from showing that some sugars may perform better than others when it comes to stabilising phages during drying, these results also demonstrate differences between bacteriophage species in terms of the extent to which they can be stabilised using sugar-based formulations. Such differences could arise from tertiary and quaternary structural differences between phage coat proteins as well as bacteriophage size and shape (Zhang *et al*., 2020). This underlines the need for further assessment of the thermostabilities of individual phages.

Further differences were observed between PLS27 and the rest of the phages considered with respect to leucine formulations, whereby PLS27 was the only phage which did not survive the drying process. As already discussed previously, this suggests significant differences between PLS27 and the other phages considered regarding the way its coat proteins interact with external molecules to bring about increased stability. Leucine is the most popular protein-based excipient for the freeze and spray-drying of bacteriophages; however, this is mainly due to its ability to disperse effectively in aerosolised applications (Y. Zhang *et al*., 2020). Despite this, its tendency to form crystalline structures may have contributed to survival of T4, T5 and ST3 during the drying procedure carried out here. This would correspond to a separate study whereby protein microcrystals of glutamine and glycine were found to stabilise bacteriophage undergoing air drying (Alvarez-Gonzalez *et al*., 2012).

Lutensol at both 2 % and 10 % strength was an effective stabiliser of bacteriophages T4 and PLS27 phage. For both phages, it was second only to lecithin in terms of post drying concentration, with PLS27 in 10 % lutensol actually performing slightly better than 2 % lecithin. Neither ST3 or T5 survived drying when suspended in lutensol at both concentrations. As a non-ionic surfactant with polar regions, it is likely that T4 and PLS27 were protected through the formation of emulsions in a similar fashion to lecithin. This result demonstrates the way in which formulations can act to stabilise phages against different stresses. Whilst lutensol was ineffective at stabilising the activity of PLS27 stored at ambient non-refrigerated conditions, it demonstrated a protective effect when exposing the immobilised phage to drying at elevated temperatures. It is unclear why no protective effect was observed for the other two phages considered. One possibility could be that any protected effect afforded by lutensol to ST3 and

T5 is significantly reduced at the drying temperature used. This could be tested in a future experiment by subjecting immobilised phage to lower drying temperatures and comparing lutensol survival to a PBS control.

Several conclusions can be drawn from this drying experiment. Firstly, lecithin was found to be an effective stabiliser for all bacteriophages considered, followed by sucrose at the lower 2 % wt/vol strength. All the other formulations exhibited selective protection to some of the 4 phages considered, but not all. These differences further reinforce the hypothesis that there is considerable variation between bacteriophage species in the way they can be stabilised during post-immobilisation drying and that this should be considered when optimising a scaled-up immobilisation of bacteriophages. For the purpose of this chapter work, lecithin and sucrose were taken forward for shelf-life testing experiments due to their relative success at protecting all phage species during the drying process. Of the sucrose formulations, this was 2 % sucrose, the only concentration exhibiting universal stabilisation. In the case of lecithin, 2 % was also selected on account of it, resulting in a more unchanged surface than its higher strength counterpart. It is important to note that the drying procedure utilised may have been harsher than one that immobilised phages could face in a scaled-up operation.

### 4.3.4 Effect of sucrose and lecithin-based formulations on the shelf-life of immobilised phage

Regarding shelf-life testing, lecithin-based formulations performed better during the initial preparation of the samples, where they were dried immediately following immobilisation using the protocol described previously (Figure 4.5). At day 0 (pre-drying), the assumed starting bacteriophage count was about $10^6$ plaque-forming units per nylon 6 square following immobilisation. Following drying (day 0 to day 1), phages in lecithin formulations dropped slightly, but remained within a log of the initial quantity. When it came to sucrose formulations, whilst all phages survived, a drop exceeding 2 logs was observed from day 0 to day 1. These results align with the findings reported in the previous section in whereby all phages in 2 % wt/vol sucrose subjected to overnight drying at 30 °C survived, albeit with an accompanying drop of approximately 2-logs for each phage (see Section 4.3.3).

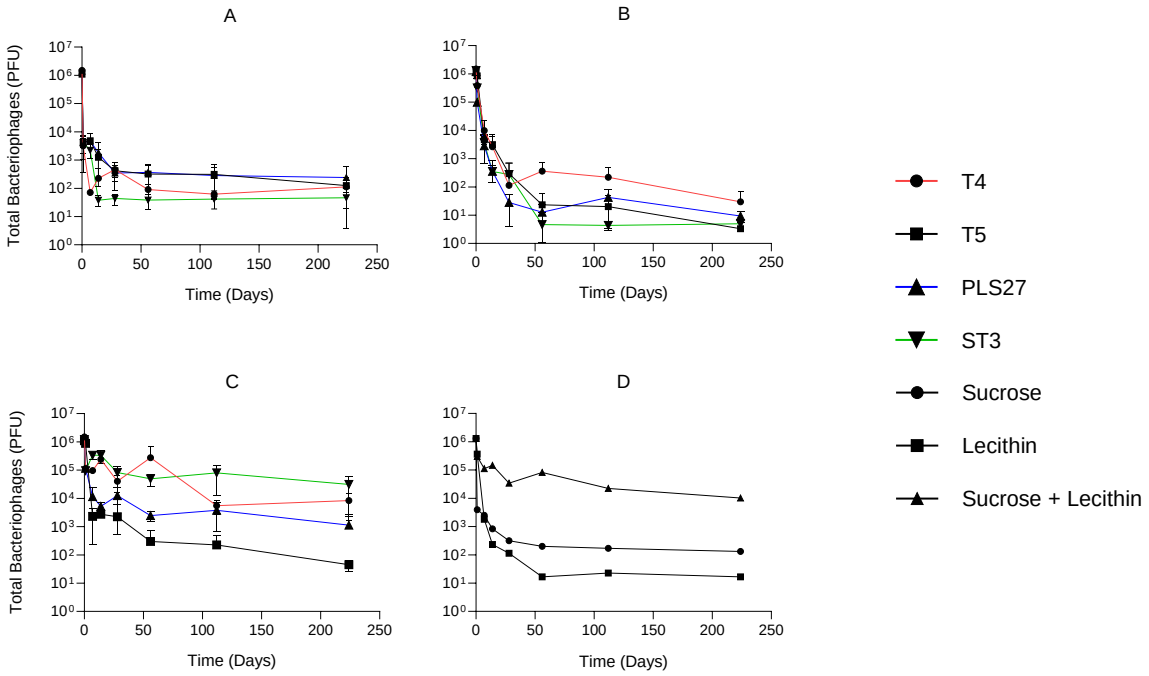


**Figure 4.5:** Results of the shelf-life experiment for 2 % wt/vol sucrose (A), 2 % wt/vol lecithin (B) and 2 % wt/vol lecithin/sucrose (C) formulations for bacteriophages T4, T5, PLS27 and ST3. Testing was carried out on day 0, 1, 7, 14, 28, 56, 112 and 224, with phages quantified using the phage loading protocol developed in Chapter 2. A graph showing the pooled shelf-life data for the phages is also presented for comparison of 2 % wt/vol sucrose, 2 % wt/vol lecithin and 2 % wt/vol sucrose/lecithin formulations (D) (n = 3).

Whilst lecithin exhibited improved survival over the drying period (day 0 to day 1) compared to sucrose, mean bacteriophage concentrations dropped sharply once incubation of the dried samples commenced, with all phages reducing in number to below 1000 PFU per sample after 1 month. For all phages, the sharp drop subsided by the 56-day mark before the decline continued at a slower rate until the end of the test period. An exception to this was ST3, which had already dropped to below 10 phages per sample by day 56 and appeared to remain at this level. By the last time point, all phages had either dropped to below 10 phages per sample or were declining steadily to this point. Conversely, for sucrose, after the initial sharp drop during the drying process, immobilised phages appeared to stabilise at quantities of 10 – 1000 phages per sample. From the 28-day time point until the end of the test period, mean bacteriophage quantities for all phage-sucrose formulations remained broadly unchanged, with only T5 exhibiting a gradual decline between days 112 and 224. These results suggest that whilst sucrose is not

as effective as lecithin in protecting immobilised phages during drying, it does provide increased shelf-life over the long term. Zheng (2023) reported on the use of 10% wt/vol sucrose for the long-term storage of freeze-dried phage, showing a shelf-time of over 1000 days when stored at 4 °C. Additionally, Manbua *et al*. (2022) found both trehalose and sucrose-based formulations to be effective at maintaining the viability of dried phage for up to 45 days at 25 °C. This hypothesis is further supported by the results of the combined lecithin/sucrose formulations. For all phages with the exception of T5, all phages immobilised as part of the combined formulation survived maintained an activity exceeding 1000 PFU per sample over the entire test period. When pooling the data of all the phages together, a clear difference is observed showing a 2 to 3 log improvement for the combined formulation over the individual sucrose and lecithin formulations for both drying as well as long term viability. This suggests that lecithin and sucrose have different modes of action with respect to the stability of immobilised phages, with the former providing protection against drying and the latter contributing to increased shelf-life. The results also show that for phages T4, ST3 and PLS27, the combination of these substances results in the phages accruing the protective benefits of both. This corresponds to the findings of other studies concerning the preparation of combined formulations. Leung *et al*. (2017) utilised an excipient matrix comprising trehalose, mannitol and leucine to prepare an inhalable, spray-dried powder containing the *Pseudomonas aeruginosa* phage PEV2. The final product was stable due to the presence of trehalose, bulked with mannitol and easily aerosolised on account of leucine. In the case of T5, even though sucrose did marginally improve long-term shelf-life compared with lecithin, the combined formulation was not sufficient to retain activity above 1000 PFU per sample by the end of the period, indicating that the phage in question may be particularly susceptible to degradation in the long-term. It also suggests that sucrose may not be the optimal shelf-life stabiliser for T5. This corresponds to the mixed success reported for sucrose with respect to dried phage stability (Y. Zhang *et al*., 2020).

The result presented here reinforces the idea that stresses experienced by immobilised phages on account of drying and long-term exposure to elevated temperatures are fundamentally different. During drying, the loss of water molecules in significant mechanical stresses, challenging the phage structural integrity, whilst, during post-drying incubation, the primary stress is caused by elevated temperatures

whereby excessive heat energy disrupts bond structures of key viral components, resulting in a loss of activity (Y. Zhang *et al*., 2020). Structural changes within the dried formulation, such as recrystallisation in the case of sugar-based formulations, as well as changes in water content due to relative humidity conditions, are also associated with a reduction in post-drying bacteriophage viability (Mensink *et al*., 2017; Yazdi *et al*., 2023). To meet these challenges, optimised formulations comprising substances suited to protecting bacteriophages against these stresses needs to be considered.

### 4.3.5 Effect of formulations on the distribution and binding efficiency of immobilised phage

Bacteriophage distribution was assessed by constructing heat maps from the 24-well plate phage loading data, where each grid represented a well (Figure 4.6). A non-corona discharge control, whereby phages were applied onto untreated polyethylene sheets, was included to demonstrate the effect of corona discharge on bacteriophage distribution. As discussed in the previous chapter (see Section 3.3), corona discharge increases the surface energy of treated surfaces through the incorporation of polar chemical species. This increases wettability, allowing solutions to disperse more easily over the surface. In the case of the non-corona control, substantial levels of reticulation were observed when the PE sheets were left to air dry. This resulted in large regions on the surface where no phage activity was observed (see Figure 4.6). Aside from demonstrating the importance of corona discharge for bacteriophage distribution, this result also suggests that the unformulated phages considered are also susceptible to degradation during a much gentler drying process (for this experiment, samples were allowed to air dry at ambient conditions). Leung *et al*. (2018) reported complete degradation of unformulated LISTEX P100 phages following a similar 24-hour air drying procedure, supporting this finding. This would also suggest that corona discharge itself may in some way stabilise phages against drying pressures. One explanation for this could be the inability of immobilised phages to aggregate after the removal of water molecules, resulting in a higher number of viable phages.

Of the three formulations considered, 15 % IPA performed the worst in terms of both distribution and mean surface concentration (Figure 4.7 and Table 4.4). The only phage where an even distribution appeared to occur was T4, albeit at a low mean concentration of about 16 phages per $cm^2$. IPA is not

recognised as a stabiliser against drying stresses, with the substance being selected due to it being an established promoter for surface wettability (Tåg *et al*., 2012). In a previous study, IPA was found to reduce the viability of MS2 phage on plastic and stainless-steel surfaces, reinforcing this idea (Chen *et al*., 2022). Despite this, the authors did not report complete or near-complete degradation of the phage considered. Furthermore, in another study, 3 bacteriophage species were found to be reasonably stable in solutions of IPA at 50 % (vol/vol) strength and lower (Cao *et al*., 2023). The poorer performance of the IPA formulation observed here is likely due to a combination of extended exposure to air drying and partial degradation due to IPA. These results suggest that IPA may be unsuitable as an additive to bacteriophage formulations or that improved phage survival may be obtained by lowering the IPA concentration. This should be confirmed before any future experiments involving the chemical.

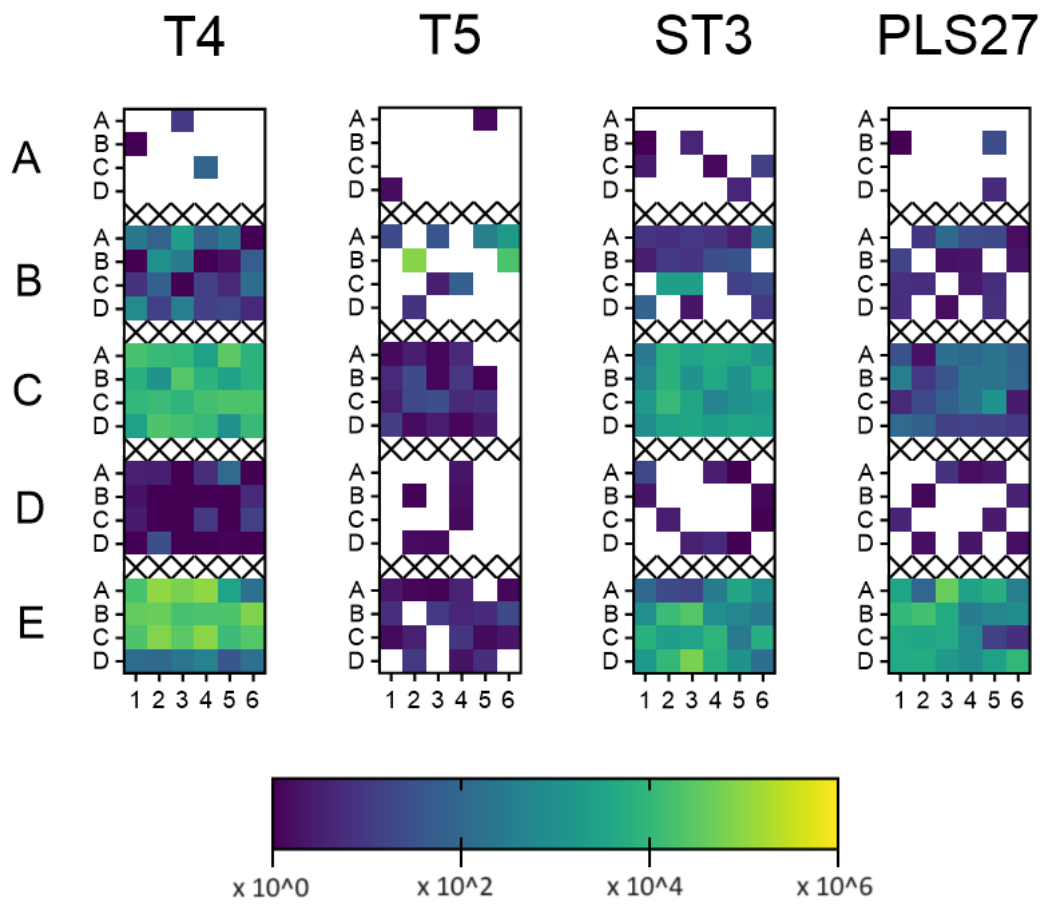


**Figure 4.6:** Heat maps showing mean phage surface concentrations of phages T4, T5, ST3 and PLS27 following gravure-application on PE sheets. Phage formulations containing 2 % vol/vol sucrose (C), 15 % IPA (D) and 2 % lutensol (E) were considered as well as unformulated controls deposited onto corona discharge-treated (B) and untreated polyethylene surfaces (A). A colour key provides phage surface concentration (PFU/cm$^2$) values. Each square represents the mean of 2 replicates (2 sheets were tested per test condition).

Both 2 % sucrose and 2 % lutensol exhibited improved distribution and mean surface concentration for all phages. In the case of lutensol, T5 and ST3 activity was detected following air drying, a different result from the drying experiment, in which they degraded fully. As already mentioned, this is likely due to the lack of a 30 °C overnight drying step. In the case of distribution, improved coverage was observed as large continuous regions of bacteriophage activity. In the case of T4, ST3 and PLS27, activity was detected in every grid tested, whilst for T5, 75 to 80 % of grids tested contained phage. The surfactant properties of lutensol have been used to achieve improved protein distribution in past works (Repka *et al*., 2020). The similar results observed for sucrose suggest that it also acts to promote distribution. One source of error for this experiment was the fact that formulations had to be dried first in order to quantify phages on the surface, whereby bacteriophage degradation may have resulted in lower apparent distribution. In the case of the IPA formulations, for example, phages may have been as well distributed as for their lutensol and sucrose counterparts. Yet, due to the apparent degradation that occurred, they were not detected in the assay.

**Table 4.4:** Mean surface concentration values for bacteriophages T5, T5, ST3 and PLS27 in formulations of 2 % sucrose, 15 % IPA, 2 % lutensol following immobilisation onto corona discharge- treated PE. Data for the unformulated control is also provided.

| Formulation | T4 | T5 | ST3 | PLS27 |
|---|---|---|---|---|
| No Formulation | 5.71E+02 | 2.21E+01 | 2.27E+03 | 5.24E+01 |
| 2 % Sucrose | 2.03E+04 | 7.17E+00 | 8.39E+03 | 3.10E+02 |
| 15 % IPA | 1.58E+01 | 3.78E-01 | 2.40E+00 | 2.73E+00 |
| 2 % Lutensol | 5.95E+04 | 9.29E+00 | 3.06E+04 | 7.70E+03 |

By considering the coating thickness of the gravure used to apply the bacteriophage formulations onto the polyethylene surface (80 um) as well as the starting and final mean bacteriophage surface concentrations, the overall efficiency of the immobilisation process could be determined (Figure 4.7).

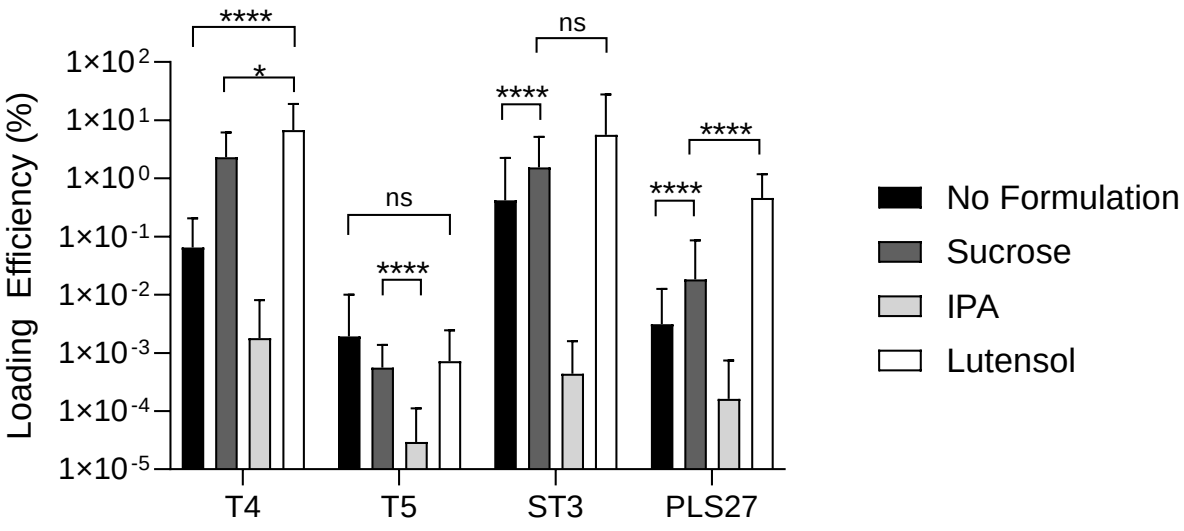


**Figure 4.7:** Loading efficiency of in percentage of bacteriophages T4, T5, ST3 and PLS27 in 2 % sucrose, 15 % IPA and 2 % lutensol following immobilisation onto PE film. Data for the unformulated controls is also provided (n = 48). Data of the 4 bacteriophage sample groups was not normally distributed as determined through a Shapiro-Wilk test of normality ($P < 0.0001$). For all statistical tests, two-tailed Mann-Whitney tests were carried out (**** = $P < 0.0001$, * =0.0378, ns = $P > 0.05$)

There were notable differences across the formulations as well as the phages in terms of loading efficiency. T5 was the worst-performing phage, where mean loading efficiency did not exceed 0.01 % for any formulation. Furthermore, unformulated T5 performed slightly better than lutensol and sucrose. This result differs from that observed in the previous chapter (Section 4.3.3), where a post-rinse binding efficiency exceeding 0.1 % was achieved for T5 on polyethylene. This suggests that other factors come into play when scaling up phage immobilisation, as was the case for this experiment. For all other phages, lutensol followed by sucrose, achieved the best results, with the highest efficiencies of just below 10 % recorded for lutensol with phages T4 and ST3. These represent desirable levels of immobilisation efficiency, especially when considering that at production levels, the capability to remain within 1 to 2 logs of the starting quantity of phages could yield significant cost benefits. It would also allow for a less arduous process, as formulations containing lower starting quantities of phage could potentially be used in the knowledge that a large proportion of them would be successfully immobilised. The fact that the immobilised formulations were not dried vigorously suggests that phage stability could be an issue once stored at elevated temperatures as part of the production cycle and/or in their final application. This was the reason for testing the combined sucrose/lutensol/lecithin formulation, in which

it was found that even following an overnight 30 °C drying cycle, distribution and mean surface concentration exceeded both lutensol and sucrose formulations that were air-dried (Figure 4.8).

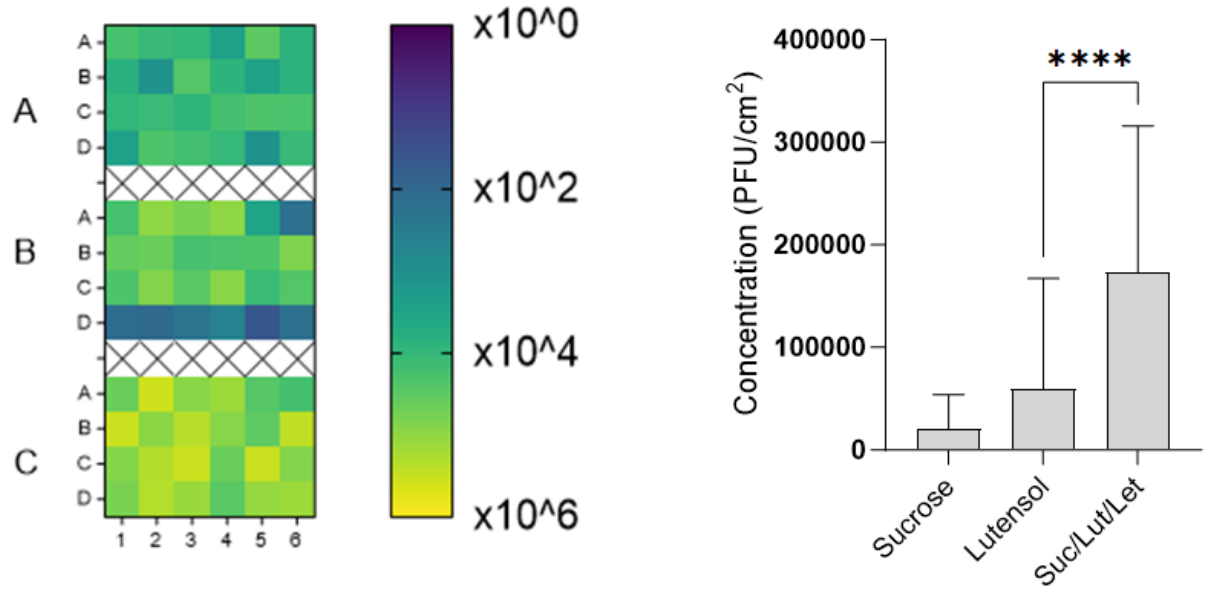


**Figure 4.8:** (Left) Heat maps showing post-immobilisation surface distribution of phage T4 in 2 % wt/vol sucrose (A), 2 % wt/vol lutensol (B) and 2 % wt/vol sucrose/2 % wt/vol lutensol/2 % wt/vol lecithin combined formulation. Results of statistical test can be found in Tables 4.5 and 4.5.

This test was only carried out for T4. Still, the results suggest that combined formulations bring about favourable results in terms of distributing as many immobilised phages as possible on a sheet surface. A significant difference between the combined formulation and lutensol was confirmed using a non-parametric Mann-Whitney test (Tables 4.5 and 4.6).

**Table 4. 5:** Table showing the results of normality testing of mean post-immobilisation concentration for lutensol and the 2% sucrose/2 % lutensol/2 % lecithin formulations.

| Test of Normality | | Sample Group | |
|---|---|---|---|
| | | Lutensol | Sucrose/Lutensol/Lecithin |
| Shapiro-Wilk test | P value | >0.0001 | >0.0001 |
| | Passed normality test (alpha=0.05)? | No | No |

**Table 4.6:** Table showing result of Mann-Whitney test comparing mean post-immobilisation concentration for lutensol and 2% sucrose/2 % lutensol/2 % lecithin formulations.

| Mann-Whitney test | Surface Concentration for Lutensol vs Sucrose/Lutensol/Lecithin Formulations |
|---|---|
| Number of pairs | 48 |
| P value | <0.0001 |
| Significantly different (P < 0.05)? | yes |

The extent to which lutensol contributes to distribution as opposed to lutensol is unclear from these results. Future work should be carried out to ascertain whether lecithin is as effective in the absence of lutensol. The fact that uniform coverage was achieved using sucrose alone for all phages apart from T5 suggests that this could be the case. Formulation components should be kept to a minimum to save costs in a scaled-up scenario.

## 4.4 CONCLUSIONS AND FURTHER WORK

Immobilised phages face considerable stresses when drying as well as post-drying during storage. The work carried out in this chapter demonstrates how formulations can be applied to tackle issues of drying and long-term stability, as well as surface distribution of immobilised phages. Lecithin emerged as a strong stabiliser during drying for all bacteriophages considered, most likely due to its ability to effectively emulsify them. Through the process of vitrification, sucrose also found to offer protection against drying to all phages, albeit to a considerably lesser extent. From the results presented here, sucrose is more effective when it comes to the long-term storage of immobilised phages once in the dried state, a likely consequence of its nature as a sugar to undergo vitrification when in a dried state, offering protection to suspended bacteriophages. The type of formulation can have a physical effect on the surface. In the case of leucine, for example, the drying it undergoes results in the formation of crystalline structures, dramatically changing the surface and physical and visual nature of the surface. The impact of formulations applied onto film surfaces should be considered depending on the final application of the phage product. There is variation across phage species in terms of both drying and post-drying stability. This suggests that the interactions between coat proteins forming bacteriophage capsids and the formulation in question influences the extent to which stabilisation occurs. Further work in this area should focus on obtaining a better understanding of the phages being considered in terms of

coat structure. There is scope to develop a model predicting the formulations best suited to stabilising specific bacteriophages, which would have applications at scale-up.

Phage distribution is also affected by formulation choice. Whilst corona discharge alone does improve most immobilisation distribution considerably, the addition of lutensol and sucrose proved to be effective at distributing phages across the surface whilst also providing protection against air drying, resulting in higher loading efficiencies. As with drying, the bacteriophage used affects the extent to which distribution and loading efficiency occurs, with T5 being singled out for its poorer performance in relation to the other phages considered.

The strategic combination of formulations facilitates the attainment of multiple benefits. This was demonstrated through a combination of lecithin and sucrose, whose respective properties allowed for the bacteriophage survival during drying as well as over long-term storage at 30 °C, whereby a mean quantity of over $10^4$ phages per unit sample was detected for a time period exceeding 200 days. Similarly, using a formulation consisting of lecithin, sucrose, and lutensol resulted in superior distribution and loading efficiency results following the gravure-mediated immobilisation on activated PE sheets. Further work should focus on the development of formulations for other substrate types with particular consideration for specific delivery strategies.

These results demonstrate the potential for immobilising phages over relatively large areas of film in a manner that is more representative of a scaled-up operation. Additionally, the formulation results show that immobilised phages can be stabilised and distributed effectively on film surfaces, allowing for future production of products that are both robust and consistent.

# Chapter 5: Immobilisation of a Bacteriophage Cocktail onto Salad Bags for Improved Shelf-Life

*The work detailed in this section was carried out in collaboration with an industrial partner. For confidentiality reasons, the name of the company in question remains undisclosed. It is referred throughout the chapter as 'Company A'.*

## 5.1 INTRODUCTION

Food spoilage represents a major challenge to the global economy, amounting to approximately 1.3 billion tonnes being destroyed (Y. Ma *et al*., 2022). It is the consequence of waste incurred across all aspects of the food supply chain, including initial production, distribution as well as retail and consumption, and aside from the considerable financial burden it represents, it also presents serious health and environmental challenges (Costello *et al*., 2016; Rudra *et al*., 2022). Bacteria are major contributors to spoilage across the food sector (Kumari *et al*., 2022). They do this through several mechanisms, including the metabolization of nutrients comprising foodstuffs followed by the release of secondary metabolites, and biofilm formation (X. Liu *et al*., 2023; Parlapani *et al*., 2017). This activity results in changes to the texture, odour, colour, and overall quality of the food, making it undesirable and potentially hazardous to consumers. Bacterial-driven spoilage affects all major processed and packaged food types, including dairy, meat and fish, as well as cut and prepared fruit and vegetables (Lorenzo *et al*., 2018). Strategies commonly employed to combat spoilage involve the reduction of bacterial contamination through the use of antibiotics, disinfectants, and feed additives (Kumar *et al*., 2020; Risikat *et al*., 2012). In some cases, bacterial load is reduced through rinsing (Gibson *et al*., 2019). A drawback of these approaches is the impact they may have on the foodstuff and the fact that they do not always specifically target the bacterial strains responsible for spoilage. Additionally, antibiotic use is a promotor of antimicrobial resistance (Kumar *et al*., 2020). A recent development is the use of bioactive food fresh-keeping films whereby bioactive substances are incorporated into the food packaging material instead of the food itself (Bhardwaj *et al*., 2022). Bacteriophage-based solutions are being increasingly considered with respect to this strategy (Wagh *et al*., 2023). The aim of the work discussed in this chapter is to increase the shelf-life of packaged salad using bags incorporating immobilised phages, drawing on the work already carried out in previous chapters.

Numerous bacterial genera contribute to food spoilage, including, but not limited to, *Pseudomonas*, *Escherichia*, *Salmonella* and *Klebsiella* (Lorenzo *et al*., 2018). Pseudomonads, in particular, are amongst the leading problem bacteria with regard to food spoilage on account of their ubiquity and adaptability (Raposo *et al*., 2016). The application of free phage to reduce food spoilage represents a

broad field of study, and several free-phage products are commercially available (Wagh *et al*., 2023). The direct application of free bacteriophages brings with it certain challenges in the context of packaged food. Introducing a liquid into a 'semi-closed' system, like a salad package, could inadvertently promote spoilage by creating a conducive environment for bacterial growth, as increased moisture often fuels such proliferation (Qiu *et al*., 2022). Moreover, integrating the application step into the production process would require precision, necessitating the addition of specific quantities of the phage cocktail (typically stored in refrigerated conditions) directly onto the salad leaves just before packaging. This extra step not only imposes substantial financial strain on production but also demands the inclusion of specialized machinery. Immobilizing bacteriophages onto the inside of the bags before the addition of the salad leaves offers a non-invasive solution within the process, eliminating the need for direct application onto the food product.

Several studies have investigated the bacteriophages efficacy in targeting food strains of interest (Wagh *et al*., 2023). Radford *et al*. (2017) showed that poly(lactic acid) films activated coated with xanthan-based bacteriophage formulations significantly reduced the growth of *Salmonella* sp. and *L. monocytogenes* survival on turkey ham slices. In a separate study, bacteriophage vB_PaeM_CEB_DP1 immobilised onto bottle caps was found to reduce the prevalence of *Pseudomonas aeruginosa* in mineral water bottles by 0.53 logs over 14 days (Novello *et al*., 2020). Alves *et al*. (2019) reported on the significant reduction of *Pseudomonas fluorescens* growth on chicken breast fillets after contact with sodium alginate-based films containing immobilised IBB-PF7A bacteriophage. Studies showing the effect of bacteriophage-incorporated packaging at the consumer level remain understudied.

The initial work presented in this chapter involves the means testing of a phage cocktail against several salad types to confirm its efficacy in extending shelf-life. This particular cocktail was originally developed by NexaBiome ltd for extending the shelf-life of spinach leaves. It comprises four bacteriophages: PMA, PFS, PLS27 and LAX. The first three phages target three species of *Pseudomonas*; *P. marginalis*, *P. fluorescens* and *P. aeruginosa*, whilst LAX is a lytic phage isolated against *Lelliotta amnigena*. All of these bacterial species have been implicated in the spoilage of packaged salad with the exception of *L. amnigena*, which is more commonly a causative agent of soft

rot in potatoes (Osei *et al*., 2022). For the initial pilot study described, the phage cocktail was applied in free form onto spinach, mixed leaf and iceberg lettuce bags bought locally from a supermarket. Following this, shelf-life was compared with various control groups to confirm the cocktail still functioned to increase shelf-life as intended. The next stage of the study involves carrying out a larger trial to test the efficacy of the immobilised cocktail on the shelf-life of spinach leaves. This required the consistent production of plastic bags incorporating the immobilised cocktail and was carried out as part of a collaboration with Company A, a plastic film producer based in the UK. The company has the suitable apparatus and expertise for plastic bag production. Like many plastic producers, Company A uses corona discharge to increase film wettability which facilitates printing and colouring. Corona discharge treatment is, therefore, integrated into its film production automation process, making the company a good candidate for testing bacteriophage immobilisation at a larger scale. Following knowledge transfer of phage immobilisation to the company and confirmation of this using T4 as a model phage, phage cocktail immobilisation and bag production was carried out at Company A's facility using its proprietary film, which is a derivative of biaxially orientated polypropylene (BOPP). This allowed for a blinded trial to then be conducted to assess the shelf-life of the newly packaged spinach leaves.

This work endeavours to achieve several key objectives. As previously highlighted, food spoilage is associated with significant financial, environmental, and healthcare implications, emphasising the need to showcase the effectiveness of alternative bacteriophage-based strategies. The novelty of this work lies in its approach to phage delivery; immobilising phages inside bags using corona discharge, and thus allowing direct interaction with target bacterial strains. This method holds promise for scaled-up phage-on-film applications, offering a streamlined integration into existing plastic production processes due to its relative ease of implementation.

## 5.2 MATERIALS AND METHODS

### 5.2.1 Materials and Equipment

Bacteriophages T4, PLS27, PMA, PFS and LAX; host cell cultures of *E. coli* 11303; *P. aeruginosa* AK44; *P. marginalis*; *P. fluorescens;* and *L. amnigena;* Lutensol T089; phosphate buffered saline; 10 mL spray canister (Zhiye, CN); sterile forceps; sticky tape; RK corona treatment system; MaxQ600 incubator (Fisher, UK); Petri dishes (Fisher, UK); nutrient broth and agar; tryptic soy broth and agar; brain heart broth and agar; vertical fill form seal machine (n/a, n/a); sterile loops (Fisher, UK); BOPP plastic films (Company A, UK).

### 5.2.3 Bacteriophage Propagation and Purification

Purified lysates of bacteriophages T4, PLS27, PMA, PFS and LAX were produced as detailed in Chapter 2 (see Section 2.2.2). In the case of PMA, PFS and LAX, respective host strains of *P. marginalis*, *P. fluorescens* and *L. amnigena* were used. Growth conditions for the three bacteria are provided below:

**Table 5.1:** Tables showing growth conditions for *P. marginalis*, *P. fluorescens* and *L. amnigena* bacterial strains.

| Strain | Growth Media | Incubation Temperature (°C) |
|---|---|---|
| *P. marginalis* | Nutrient | 30 |
| *P. fluorescens* | Nutrient | 30 |
| *L. amnigena* | Brain Heart Infusion | 30 |

### 5.2.4 Grading of Salad Bags

A salad grading scale was constructed for people volunteering to assess salad bags. Volunteers were asked to grade leaves based on colour and texture (see Table 5.2).

**Table 5.2:** The grading scale used by volunteers during the initial pilot study as well as the offsite trial.

| Rating | Texture | Colour |
|---|---|---|
| 4 (Very Good) | No wilting/curling across the leaf and no breakdown at the edges of leaf. | Consistent colour across the entire leaf. No visible browning on any part of the leaf. |
| 3 (Good) | Minor curling/wilting at edges. Small wet patches on leaves. | Minor darkening of leaves. Minor browning at leaf edges. |

| | | |
|---|---|---|
| 2 (Fair) | Noticeable wilting. Holes in leaf tissue may be present | Noticeable darkening or browning of leaves (≤ 30 %). |
| 1 (Poor) | Major wilting and breakdown of leaf tissue. Some sections of the bag will have a mushy texture. | Major darkening and/or browning of leaves (≈ 50 %). |
| 0 (Very Poor) | Total breakdown of leaf structure. Mushy texture is ubiquitous across leaves. | Most leaves (> 80 %) are completely brown or dark. |

Graders were also asked to indicate whether they would buy the salad bag or not at the time of assessment. Bags that would be bought were given a rating of 1, with 'unbuyable' bags given a rating of 0.

### 5.2.5 Bacteriophage Cocktail Pilot Study

A pilot study testing the ability of the free phage to increase the shelf life of packaged salad was carried out. Three salad types were considered for this initial study. These were iceberg lettuce, crunchy mixed leaf and baby leaf spinach. All salad bags were purchased from a local ASDA store. Only bags with the same use-by date were considered for a given salad type. To treat bags with the bacteriophage cocktail, a small incision was made at the top of each bag. Bacteriophages were applied by spraying the cocktail through the incision. A total of 10 sprays (equating to approximately 2 mL) were applied to each bag. Bags were immediately sealed with air-tight adhesive tape after bacteriophage application. In addition to bags treated with the cocktail, PBS-treated controls were also set up in the same way. An opened/closed control, in which bags were cut open and immediately sealed, as well as an unopened control, were also considered.

**Table 5.3:** Table summarising the number of replicates considered for each sample type during the free phage the pilot study. The number of replicates considered was limited by the supermarket stocks.

| Salad Type | Cocktail | PBS | Opened/Closed | Unopened |
|---|---|---|---|---|
| Iceberg Lettuce | 10 | 10 | 5 | 5 |
| Crunchy Mixed Leaf | 9 | 9 | 4 | 4 |
| Baby Leaf Spinach | 8 | 8 | 4 | 4 |

Bags were left to incubate in a dark, dry storage unit at room temperature and were periodically graded by blinded volunteers using the grading scale described in the previous section. In the case of iceberg lettuce, grading was carried out on days 0, 1, 2, 3, 4 and 7, whilst for crunchy mixed leaf and baby leaf spinach, grading was carried out on days 0, 1, 2, 3, 6, 7, 8 and 10. The deterioration of leaf quality was compared between sample groups for all leaf types.

### 5.2.6 Off-site Immobilisation and Testing of T4 Bacteriophage onto Plastic Sheets

Before attempting to immobilise the salad bacteriophage cocktail, immobilisation at the external company was means tested using their bespoke corona discharge machine (see Figure 5.1). This was an automated set-up in which a reel of plastic sheet passes through a corona discharge field before being gravure-coated in the substance of interest. The sheet is then passed through an oven zone, where it is dried before being collected.

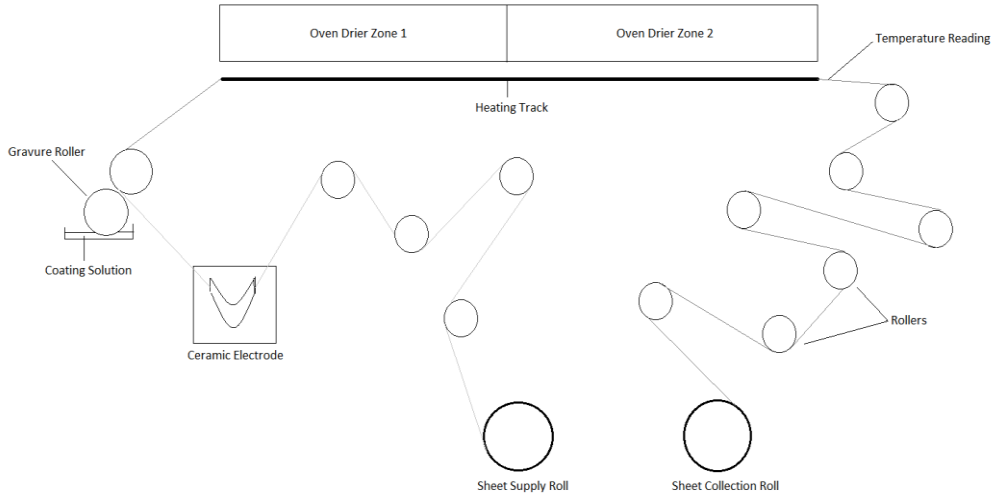


**Figure 5.1:** Schematic of RK coater used for activation of BOPP sheets at Company A's facility. A reel of polymer sheet is inserted into the sheet supply roll and then manually wound through the RK system until it is joined to the sheet collection roll. Once the machine is activated, the film moves from the supply roll to the electrode, whereby it is activated with corona discharge. Following this, the coating is applied onto the treated side of the film via gravure rollers. After passing through 2 oven zones and drying, sheets are collected in a reel wind.

T4 was considered as a model phage. A purified solution of bacteriophage T4 (> 1 L) at a concentration of 5 x $10^8$ PFU/mL was provided by NexaBiome ltd. The solution was transported under refrigerated conditions and stored at 4 °C on arrival until use. Lutensol, the company's favoured antimist agent, was added to the phage solution at a concentration of 1 % (vol/vol). 500 mL of the T4-lutensol mixture was added to the film coating system. A BOPP plastic sheet reel was treated with corona discharge at an intensity setting of 5 kJ/$m^2$ and a reel speed of 10 m/min. Bacteriophages were applied using a 120 lip gravure. A lutensol-free control was also immobilised. Samples were dried in the ovens at 75 °C and 50 °C as well and air dried at ambient temperature. After coming out of the oven zone, A4-sized pieces of film were immediately cut before being subjected to any roller pressure. Following drying, samples were sent back to NexaBiome for testing. The equivalence bacteriophage loading assay described in Chapter 2 (see Section 2.2.4) was carried out to enumerate immobilised T4 phage on 1 cm by 1 cm sheet cut-outs. Three in-house stress tests were carried out at Company A on lutensol samples dried at 50 °C. These included a reel test whereby the film underwent contact with 4 rollers before being collected in the reel. The other tests were a rubbing test where the immobilised phage surface was rubbed with 1 kg of pressure by an abrasive cloth, and a block test where the film was subjected to 175 kg/$m^2$ of pressure for 10 minutes. A4-sized sheets of stress-tested film were sent to NexaBiome for testing.

### 5.2.7 Design of Packaged Spinach Trial

Following the results of the pilot study, spinach was selected as the salad to be tested for the full trial. Three main sample groups were considered. These were bags incorporating the immobilised bacteriophage cocktail, bags immobilised with PBS instead, as well as plain plastic bags which had not. A sample list is provided below:

**Table 5.4:** Breakdown of sample types considered for the trial at the Company A facility. 20 phage cocktail and 20 PBS (control) samples were considered. The samples groups were sub-divided onto 2 groups of 10 bags. These sub-groups were graded by separate groups of volunteers.

| Sample Type | Immobilised | Salad | Number of Replicates |
|---|---|---|---|
| 1 | Phage cocktail | 10 g spinach | 20 |
| 2 | PBS (control) | 10 g spinach | 20 |

**Figure 5.2:** Image of packed salad bags. 10 cm x 20 cm bags were produced using BOPP sheets and filled with 10 g of spinach leaves obtained from a local supplier.

Following the production of the bags, these were stored at room temperature conditions and periodically assessed by blinded volunteers using the grading scale described in Section 5.2.4. Graders were split into two groups comprising four (groups A) and five (group B) people. Each group graded 10 phage cocktail-treated bags and 10 control bags. For group A, grading took place on days 1, 2, 3, 5, 6 and 7, while for group B, grading was carried out every day until day 8. Data from both groups was pooled for data analysis.

5.2.8 Immobilisation of Bacteriophage Cocktail onto Plastic Sheets and Production of Spinach Bags

The bacteriophage cocktail was combined with 1 % lutensol and immobilised onto the partner company's proprietary plastic sheets in the same way as described previously (see Section 2.2.4). Drying was carried out at 50 °C. The PBS-coated control sheets were prepared in the same way. 10 cm by 20 cm plastic bags were then produced from phage-coated sheets and PBS-coated sheets using a vertical fill form sealing machine (see Figure 5.3).

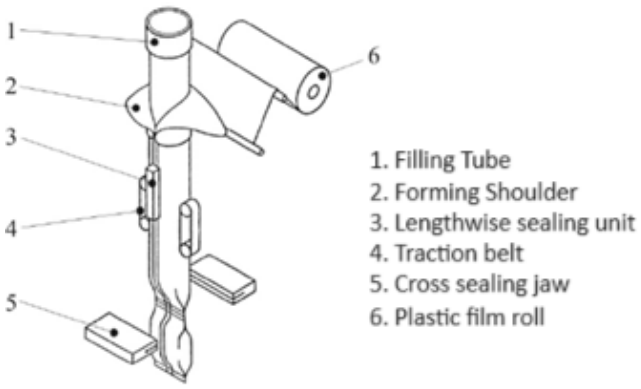


**Figure 5.3:** Schematic of vertical fill form seal machine used at Company A for sealing the bags used in the trial. Plastic roll is wrapped around the filling tube. The cross-sealing jaw then move across the underside and side where the ends of the film meet, heat sealing the film to form a plastic bag. The final bag size was 10 cm x 20 cm.

Fresh, unpackaged spinach leaves were sourced from a distributor local to the partner company. 10 g of leaves were weighed and added to each bag, which was then sealed using a vertical fill form seal machine.

### 5.2.9 Data Analysis of Trial Results

GraphPad Prism 10 was used to carry out all statistical analysis. Trial data for each bag was organised in terms of colour, texture and buyability over the test period. Each bag was considered individually, with graphs plotting mean colour, texture and buyability against time in terms of days being constructed. The resultant curves were analysed using non-linear, second-order polynomial regression analysis.

Two quality threshold levels were chosen for each characteristic. In the case of colour and texture, these were 3.5 and 3, whilst for buyability, percentage points of 80 % and 50 % were selected. Using the polynomial equations generated for each graph, the time taken to reach the defined thresholds for colour, texture and buyability were determined. Two-tailed t-tests were performed to establish the difference between the mean threshold times of phage-treated and controlled samples. In cases where data was not normally distributed, Mann-Whitney tests were carried out.

## 5.3 RESULTS AND DISCUSSION

### 5.3.1 Effect of free bacteriophage cocktail on shelf-life of bagged salad

Shelf-life results varied across the three salad types considered (Figure 5.4). In the case of iceberg lettuce, the unopened controls performed notably better than the other three sample types, with the mean value not dropping below 3 until the final test day (Day 7). The other sample types behaved similarly to one another, dropping below a mean quality value of 3 within 1 day, and steadily declining over 4 days, after which a quality rating below 2 was recorded. This suggests that in the case of iceberg lettuce, the mere opening and sealing of bags was enough to promote spoilage, with the phage cocktail unable to provide any apparent shelf-life benefits when it came to leaf quality. Iceberg lettuce has a higher water content than both spinach and mixed leaf salad, and it is likely that the opening of the bags, and the resultant introduction of ambient air, together with bag agitation, resulted in higher levels of spoilage. It is also possible that the phage cocktail was ineffective against the spoilage bacteria present in the iceberg lettuce leaves such that there was no notable difference between phage-treated samples and the opened controls.

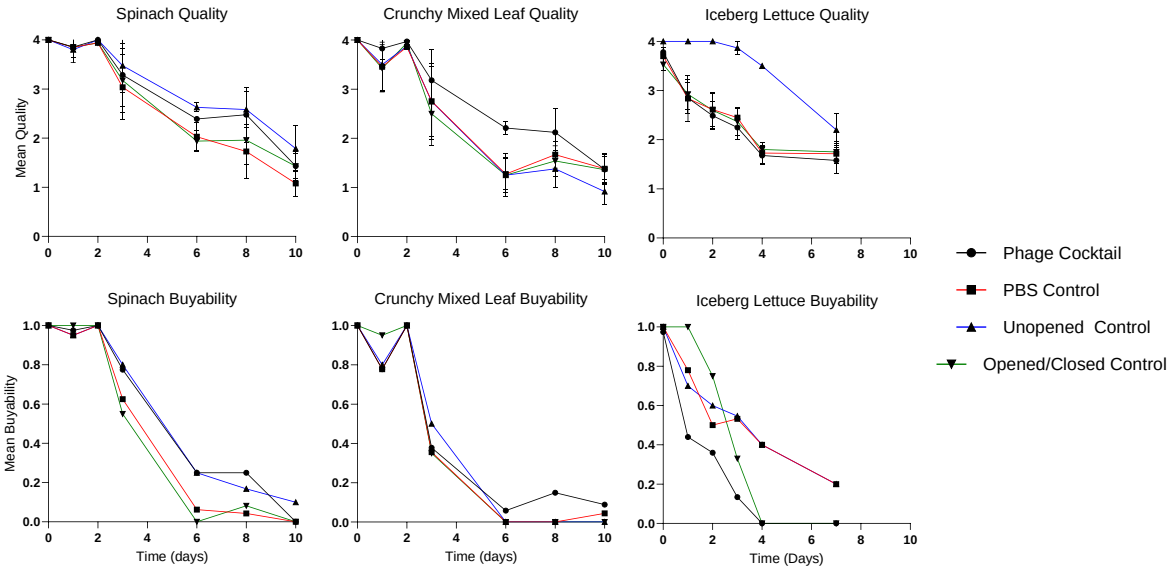


**Figure 5.4:** Graphs showing decline in quality and mean buyability over time for spinach, crunchy mixed leaf and iceberg lettuce bags treated with the phage cocktail, PBS control, opened and closed and unopened. To inoculate bags with the phages or PBS, spray cannisters were used to s[pray approximately 2 mL of liquid onto the bags before they were sealed with tape and incubated at room temperature. Refer to Table 5.3 for details concerning number of replicates for each sample group.

Spinach and mixed leaf salad differed from iceberg lettuce in that their quality ratings remained fairly stable for about two days before steady declines were observed between days 2 and 6. This was also reflected in the buyability data, where sharp declines were observed after day 2 for both salad types. There was no significant difference between the unopened control and the other sample types, suggesting that for spinach and mixed leaf salad, the opening of the bags did not result in spoilage being promoted to the same extent as for the iceberg lettuce. For both salad types, there was a slightly improved performance for phage-treated samples over PBS and opened/closed controls. This was recorded as a 0.25 – 0.5 increased quality rating for spinach and 0.5 - 1 for mixed leaf salad between days 2 and 8. This indicates that bacteria-driven spoilage occurs during this period and that the phage cocktail was partially effective in reducing spoilage. In the case of spinach leaves, this was also indicated by the buyability tests, whereby phage-treated as well as unopened bags retained a percentage buyability exceeding 80 % for a day longer than the other samples. As already mentioned, salad spoilage can be attributed to a range of bacterial genera, with these results suggest that some of the major spoilers in the spinach and salad bags considered belonged to the *Pseudomonas* and/or *Lelliotta* genera and that these were successfully targeted by the cocktail phages. The phages were applied by spraying atomised cocktail into the bags and distributing through agitation. Therefore, any bacteriophage activity that occurred would have taken place in a 'free-phage' context, with the non-immobilised phages able to disperse around the bag and infect host cells. The success of the cocktail in this context meant that a larger offsite trial testing the effect of immobilised phage on shelf-life could be pursued.

### 5.3.2 Offsite corona discharge-mediated immobilisation of T4 phage onto BOPP sheets

T4 phage was successfully immobilised onto BOPP sheets using Company A's RK coating system. This represents the first-time bacteriophages have been immobilised using corona discharge externally from to NexaBiome ltd. There was no notable difference between the pure T4 and T4 /lutensol formulations when it came to post-immobilisation concentration (Figure 5.5). The former yielded a mean surface concentration of 200 PFU/cm$^2$, with the latter having one of just under 100 PFU/cm$^2$. Despite this subtle difference, the mean values were within error of each other. This contradicts the

results from the previous chapter whereby addition of lutensol was found to improve T4 viability post drying in air by almost two orders of magnitude (see Section 4.3.5). One reason for this could be the ambient temperature conditions at Company A, which may have differed from those at NexaBiome; however, a more likely reason is the time between immobilisation and testing. Following the preparation, samples needed to be packed and sent to NexaBiome for testing. In practice, this took longer than a week. Immobilised phages stored in conditions of relatively high moisture, which would be expected following ambient drying, can be subject to increased rates of deterioration (Qiu *et al*., 2022). The partially dried surfaces, coupled with the extended time until testing, may have resulted in the lower values recorded for both pure and lutensol-based formulations. Additionally, a 1 % (v /v) lutensol formulation was favoured over the 2 % formulation to accommodate preferences at Company A (the company routinely uses 1 % lutensol coatings for its anti-mist properties).

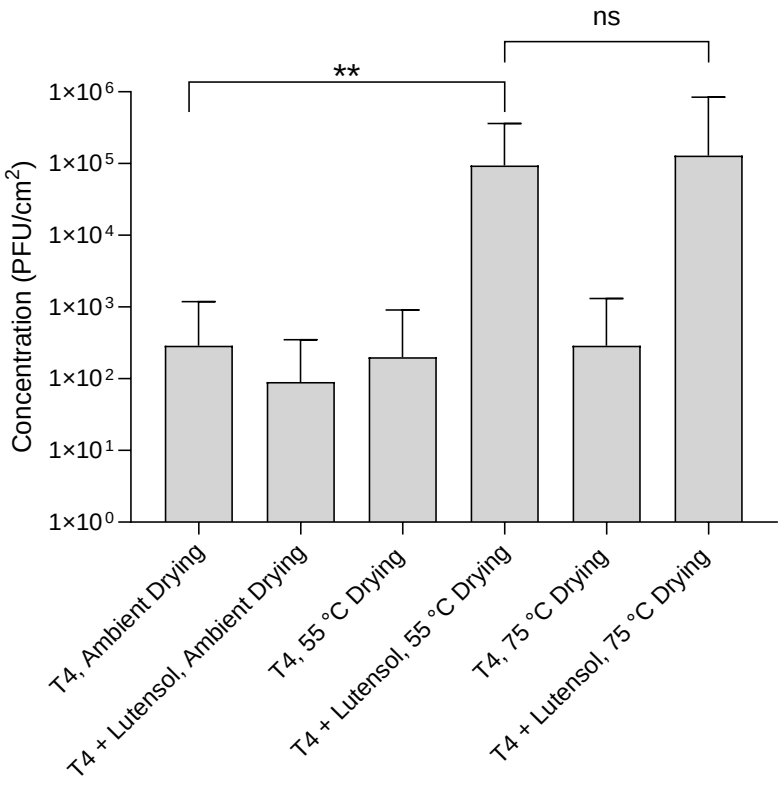


**Figure 5.5:** Histogram showing the different mean phage loading values for T4 immobilised at Company A's facility using the RK corona discharge coater. Samples considered included pure T4 and T4 + 1 % (vol/vol) lutensol immobilised onto BOPP sheets and dried in air, 55 °C and 75 °C. 48 replicates were considered for each sample. Data for all sample groups was not normally distributed, as determined by a Shapiro-Wilk test of normality ($P < 0.001$). Significant difference between ambient drying and drying in lutensol at 55 °C observed following a two-tailed Mann-Whitney test ($P (0.05) = 0.0035$). There was no significant difference between lutensol formulations dried at 55 °C and 75 °C (two-tailed Mann-Whitney test, $P = 0.2173$).

This hypothesis is further supported by the results of the oven-dried samples, where the anticipated stabilisation due to the presence of lutensol resulted in concentrations approximately 3 logs higher than for unformulated phage. Although no moisture content analysis was carried out, surfaces appeared to be completely dry after 1 minute of drying at both 55 °C and 75 °C. The survival of the unformulated phages suggests that this method of drying is gentler than overnight incubation at 30 °C as carried out in the previous chapter (see Section 4.3.3). If it were found to be as effective at drying, then the fact that it is much faster and easy to incorporate into an automated system, as seen here (see Figure 5.5), whilst allowing for a higher degree of bacteriophage survival, would make it a preferable drying method for scaled-up production of phages onto sheet surfaces.

Similar concentrations were recorded for pure T4 phage formulations that underwent oven drying, suggesting that quick exposure to temperatures exceeding 50 °C is not necessarily any harsher than ambient drying. This was particularly unexpected for the elevated temperature 75 °C. Phage degradation during drying occurs due to elevated temperatures as well as the loss of water molecules from the system (Y. Zhang *et al*., 2020). The quick removal of water over a 1-minute period may be preferable to phage stability compared to a longer-term process, as would be the case for air drying. This would correspond to findings reported elsewhere, where the presence of moisture in immobilised phage samples resulted in lower overall stability (Malik *et al*., 2017b).

Some of the physical stress tests carried out at Company A affected T4 surface concentration when compared to the unstressed controls (Figure 5.6). A slightly higher mean concentration of $2.9 \times 10^4$ PFU/cm$^2$, compared to the $1.3 \times 10^4$ PFU/cm$^2$ for the control, was recorded following the real test. Of the tests performed, this test subjected the film to the lowest amount of physical stress. This difference is within error of the control and likely represents random variation between samples.

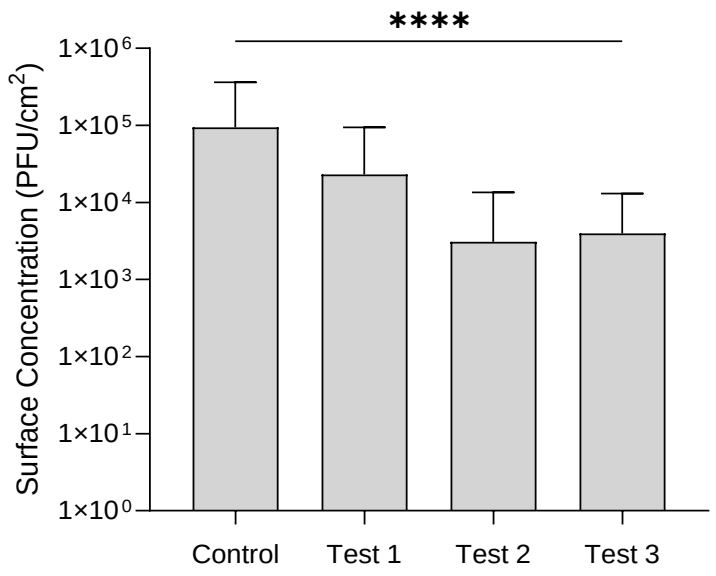


**Figure 5.6:** Histogram showing surface concentration of immobilised T4 phage following stress testing at Company A. Stress tests included a contact roller and reel test (test1), a rubbing test (test 2) and a block pressure test (Test 3). See Section 5.2.6 for test conditions. Mann-Whitney tests carried out between Control and Test 1, Test 2 and Test 3 data, with respective p-values of <0.0001 for each test.

For the rubbing and block tests, a mean surface concentration of approximately 3 x $10^3$ PFU/$cm^2$ was recorded. These tests are more physically stressful, and it is possible that phage activity was reduced slightly through the removal of layers of plastic or even lutensol from the surface. This could have occurred through layers being scraped off as well as layers sticking to the underside of the block following sustained pressure. These tests are carried at Company A to simulate stresses associated with the long-term storage of films produced on-site. Despite the significant reductions observed across the tests performed, the results demonstrate that a scaled-up product can be stored in a reel or packed under considerable mass with the physical stresses associated with such storage contributing to no more than log of phage activity. Such reduction in a final product could be mitigated by greatly increasing the initial phage loading per unit area.

5.3.3 Effect of immobilised phage cocktail on the shelf-life of bagged spinach

As with the pilot study utilizing free phage, the degradation rate of overall leaf quality reached its peak after Day 2, with a noticeable steepening of the graph's slope beyond this point (Figure 5.7). Despite this, buyability remained high for an extra day, with it beginning its decline following Day 3. This is not a major difference from the free phage pilot study, although a noteworthy observation is that in this case, salad bag buyability did not begin to decline until leaf quality dropped below a mean score of 3. The sourcing of spinach leaves for the immobilised phage trial by Company A from a local supplier, variations in the assessed bags, and subjective differences among the panels in the two trials could potentially account for this observed distinction.

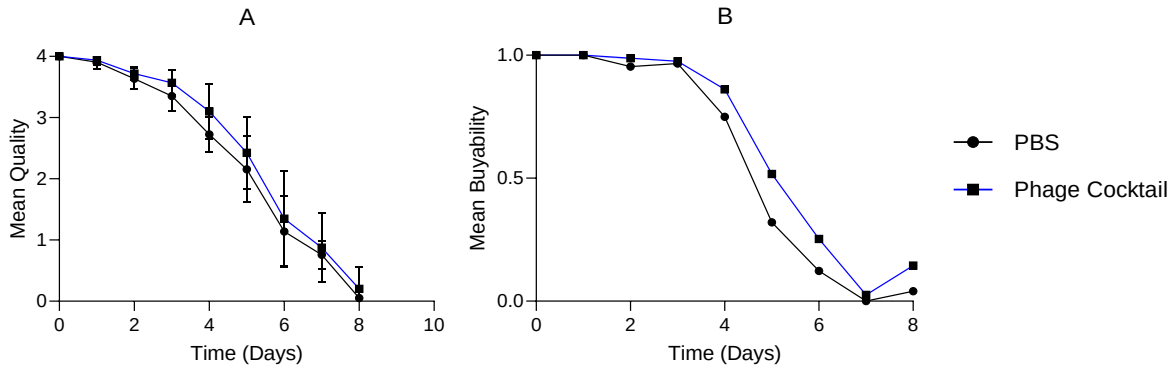


**Figure 5.7:** Graphs showing deterioration in mean quality (A) and mean buyability (B) over time for the spinach bags containing the immobilised bacteriophage cocktail as well as the PBS control (n = 20).

For both mean quality as well as mean buyability, bags containing the immobilised cocktail exhibited slightly more gradual rates of decline between Days 2 and 6, with phage-treated bags declining between 0.5 - 1 day slower than their non-phage counterparts. As with the free phage pilot study, this indicates that the cocktail may have been at least partly effective in reducing spoilage by targeting one or more key target bacteria.

**Figure 5.8:** Photo showing comparison between salad bag with immobilised phage cocktail (left) and PBS-coated control bag on day 5 of the trial. As can be seen from the photos, phage cocktail-treated bags deteriorated at a slower rate compared to the control bags.

When it came to carrying out statistical analysis of the results, the bags exhibited second-order polynomial decay with respect to both texture and colour. The non-linear second-order polynomial regressions carried out on the graphs yielded strong curves with high mean values (all above 0.85) for all data sets (Figure 5.9). These values allowed for the accurate determination of corresponding times to reach the set threshold values of 3.5 and 3.

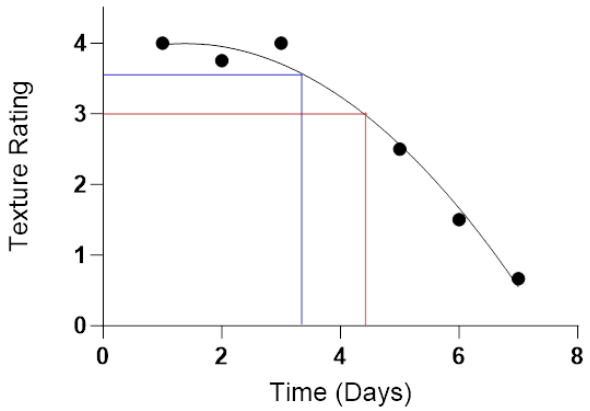


| Sample Group | Mean $R^2$ Value |
|---|---|
| Phage cocktail Colour | 0.98037 ± 0.0112 |
| Phage cocktail Texture | 0.96694 ± 0.0232 |
| Phage cocktail Buyability | 0.85616 ± 0.0852 |
| PBS control Colour | 0.95375 ± 0.0514 |
| PBS control Texture | 0.97122 ± 0.0171 |
| PBS control Buyability | 0.86715 ± 0.0483 |

**Figure 5.9:** Graph showing mean texture rating vs time for one of the phage cocktail bag samples (left) and table providing the mean $R^2$ values of the non-linear second order polynomial regressions carried for each sample group. Each sample group consisted of 20 replicates.

For both colour and texture, the phage-treated bags took a longer time than the controls to reach the defined thresholds (Figure 5.10). In the case of colour, there was a respective mean difference between thresholds 3.5 and 3 of 0.6 and 0.8 days respectively (Table 5.5). When it came to texture, there was almost a whole day difference for both thresholds to be reached (0.8 and 0.9 respectively).

**0**

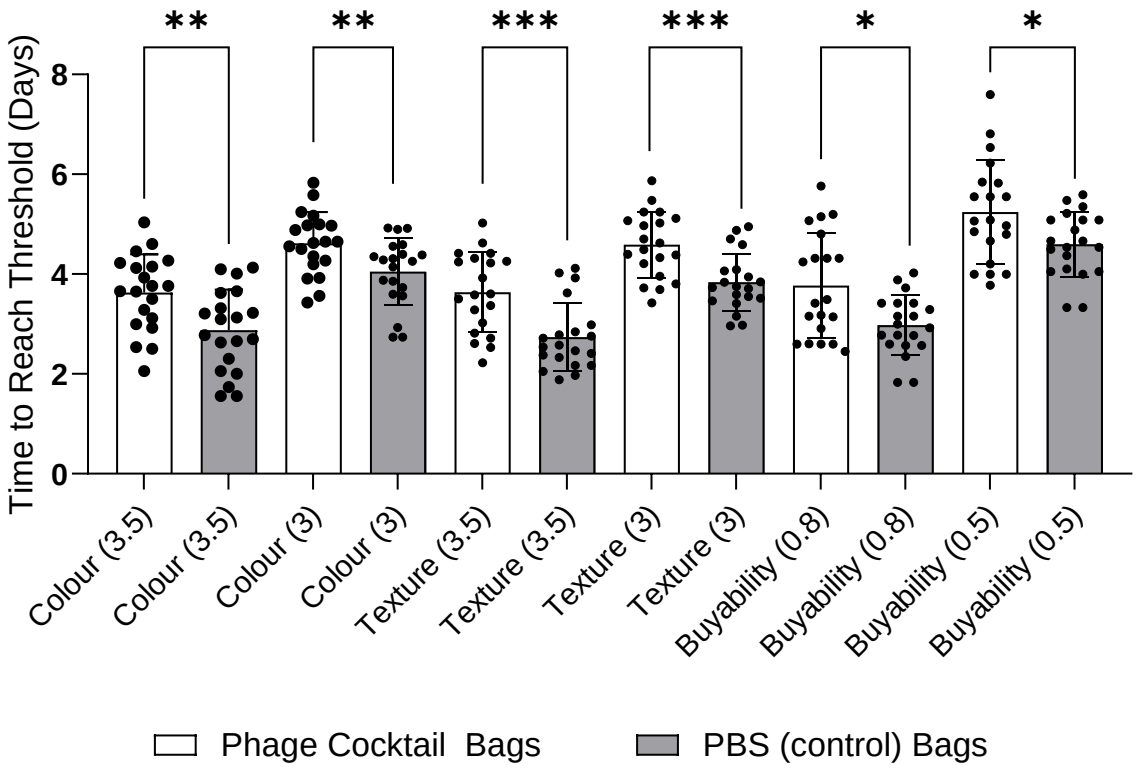


**Figure 5.10:** Histograms with scatter plots showing time taken to reach colour (left) and texture threshold levels of 3.5 and 3 for spinach bags with immobilised phage (phages) and PBS controls, as well as buyability threshold values of 0.8 and 0.5 (n = 20). For details of statistical analysis caried out, see Figure 5.11 and Table 5.6.

These differences are reflective of the pooled graph constructed for mean quality (Figure 5.7). Tests of normality carried out on each data set revealed each set to comprise normally distributed data apart from texture at a threshold of 3.5 (Figure 5.11). Following the resultant two-tailed t-tests, or Mann-Whitney test, in the case of texture at the 3.5 threshold, all differences between the phage-treated and PBS

controls were found to be significant (Table 5.6). This strongly indicates that immobilised phages comprising the cocktail used could successfully target spoilage bacteria in spinach leaves to increase shelf-life as defined by texture and colour. Thus, it can be concluded that immobilised cocktail was effective at increasing bagged spinach shelf-life by between 0.5 and 1 day.

**Table 5.5:** Table summarising mean differences between phage cocktail samples and PBS controls in terms of time taken to reach thresholds of 3.5 and 3 for texture and buyability and 0.8 and 0.5 for buyability.

| Characteristic | Threshold | Sample Group | Mean Difference (days) |
|---|---|---|---|
| Colour | 3.5 | PBS (control) | 0.8 |
| | | Phage | |
| | 3 | PBS (control) | 0.6 |
| | | Phage | |
| Texture | 3.5 | PBS (control) | 0.8 |
| | | Phage | |
| | 3 | PBS (control) | 0.9 |
| | | Phage | |
| Buyability | 0.8 | PBS (control) | 0.79 |
| | | Phage | |
| | 0.5 | PBS (control) | 0.65 |
| | | Phage | |

The mean time values for bag buyability to drop to below the threshold values of 0.8 and 0.5 were also found to be significantly higher in the case of immobilised phages compared to the PBS counterparts (Tables 5.5 and 5.6). In the case of the 80 % buyability, this equated to a mean difference of 0.79 days whilst there it took, on average 0.65 days longer for half of phage-immobilised bags to be deemed unbuyable compared to the control samples. This determination involved conducting a Mann-Whitney

test for the 0.8 threshold dataset and a two-tailed t-test for the 0.5 threshold dataset, with the tests performed based on the confirmation of non-parametric data and normality for the respective datasets. The results for buyability fall within a similar range to those of leaf quality. This further confirms those results, strengthening the conclusion already made.

In order for immobilised phages to successfully bring about a favourable effect, such as shelf-life as described here, some of the immobilised phages first need to come into contact with bacterial strains of interest. Following this, any resultant phage bursting out of bacterial cells is free and able to disperse across the bag to infect more cells. The initial targeting presents a challenge in that since the phages are immobilised, unless any target cells come into contact with them, they technically will be unable to infect a host to initiate the lytic cycle. The results shown here suggest that the phages were successful in targeting some of the strains of interest, indicating that there were sufficient numbers of host cells across the bag that could be targeted. It is also likely that not all of the phages incorporated into the bags were bound strongly or irreversibly, as was shown to be the case in previous chapters (see Section 3.3). Loosely bound phages could potentially be removed from the surface through interactions with water evolved within bags on account of respiration processes and leaf spoilage (Kapetanakou *et al*., 2019). It should be noted that only 10 g of spinach leaves were placed in each bag for this experiment. This means there was a much larger bag surface-to-leaf mass ratio, meaning that leaves were more likely to be in contact with part of the bag when compared to a conventional salad bag, which could contain up to 200 g of leaves. The bag size used for these experiments was the largest permitted by the vertical fill form bag sealer available at Company A; however, it is recommended that a future trial involves the consideration of larger salad bags to be more representative of a commercial product.

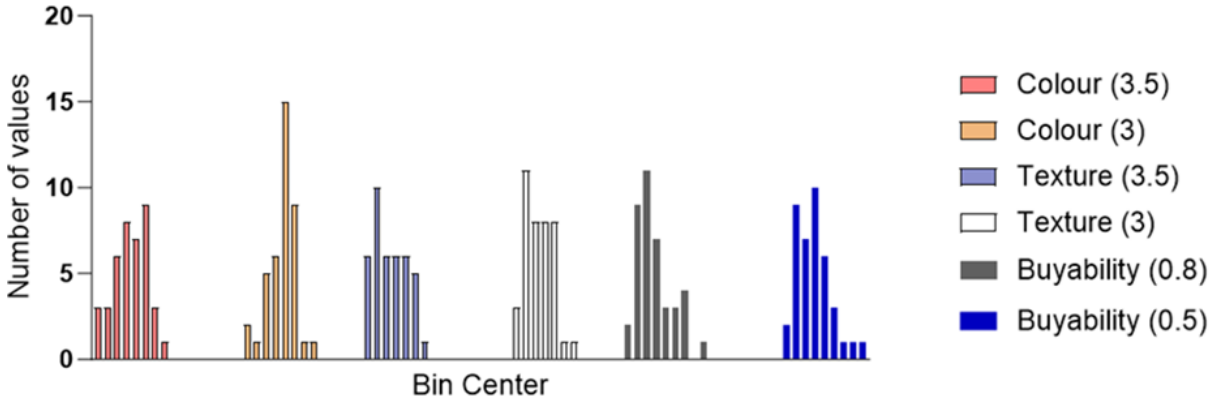


| Normality Test | Colour (3.5) | Colour (3) | Texture (3.5) | Texture (3) | Buyability (0.8) | Buyability (0.5) |
|---|---|---|---|---|---|---|
| Shapiro-Wilk | 0.6211 | 0.4342 | 0.0323 | 0.3482 | 0.0223 | 0.1942 |

**Figure 5.11:** Frequency distribution plots for pooled data sets of colour, texture and buyability at thresholds of 3 and 3.5 for colour and texture as well as 0.8 and 0.5 for buyability. Each pooled sample set comprised 40 replicates (20 phage cocktail bags as well as 20 PBS control bags). A table showing the results a Shapiro-Wilk test of normality is also presented. Results which failed normality testing are highlighted in red.

**Table 5.6:** Table showing the statistical comparisons of the mean time to reach threshold levels 3.5 and 3 for colour and texture as well as 0.8 and 0.5 for buyability. Two-tailed t-tests were carried out for normal data whilst non-parametric data sets (Texture (3.5) and Buyability (0.8)), non-parametric Mann-Whitney (MW) tests were performed.

| Parameter | Colour (3.5) | Colour (3) | Texture (3.5) | Texture (3) | Buyability (0.8) | Buyability (0.5) |
|---|---|---|---|---|---|---|
| Test Type | t-test | t-test | MW | t-test | MW | t-test |
| P value | 0.0005 | 0.0093 | 0.0005 | 0.0005 | 0.0238 | 0.0223 |
| Significantly different (P < 0.05)? | Yes | Yes | Yes | Yes | Yes | Yes |
| One or two-tailed P value? | Two-tailed | Two-tailed | Two-tailed | Two-tailed | Two-tailed | Two-tailed |
| t, df | t=3.893, df=38 | t=2.741, df=38 | N/A | t=3.823, df=38 | N/A | t=2.382, df=31.95 |

Apart from bag size, future studies should also incorporate the inclusion of more bacteriophages in the phage cocktail to maximise strain coverage. The cocktail used for this study consisted of 4 bacteriophages, which is a relatively small number considering the broad and diverse array of bacterial species associated with salad spoilage (Alegbeleye *et al*., 2022). Most phage cocktail experiments that have been referred to in this dissertation consisted of 2 to 4 phages, however, in all cases, cocktails were applied in challenge studies consisting of defined bacterial targets. For applications such as the one described in this section of work, a larger cocktail targeting a more representative sample of the most prominent spoilage strains may have resulted in improved outcomes in terms of shelf-life extension. A

more targeted approach would involve the determination of specific spoilage bacteria prevalent in the spinach leaves being considered. No microbiome study into the leaves used for both the pilot study and the offsite trial was carried out. A prior analysis of the microbiome would allow for a more extensive understanding of the bacterial strains present in the salad of interest, which could help improve targeting through the selection of lytic phages from a library or through new isolates.

No directed evolution was carried out against the strains targeted by the cocktail. This refers to the continued exposure of cocktail phages against any emergent resistant target strains, which can result as a response to continuous bacteriophage activity (Oechslin, 2018). In their study on *Pseudomonas* phage cocktails Yang *et al*., (2020) used directed evolution of bacteriophage PaoP5 to target a strain of *P. aeruginosa,* which had developed resistance. Following the addition of the evolved phage, the resultant cocktail was able to target emergent bacterial mutants, increasing its efficacy over the long-term. The principle of directed evolution could be applied to future development processes of phage cocktail for packaged food to improve outcomes. It is anticipated that should this type of technology be applied as a solution, then additional periodic biomonitoring of the foodstuff in question would be required to identify emergent strains of interest and alter the phage cocktail accordingly.

Due to time constraints, no bacteriophage quantification work was carried out for any of the phages forming part of the immobilised cocktail. An important aspect of phage treatment is the definition of optimal dosage levels. This would be of commercial importance to any scaled-up immobilisation process, as costs would be significantly reduced by using as low a concentration of phage lysate as possible when immobilising whilst still having a positive effect on shelf-life. Future work in this area should therefore focus on defining minimum quantities of bacteriophage required to increase shelf-life.

## 5.4 CONCLUSIONS AND FURTHER WORK

A crucial aspect of upscaling the application of immobilised phage is the transfer of the technology to manufacturing plants. The results presented showed that it was possible to produce bacteriophage-coated BOPP sheets using an automated system at an offsite location. Using the RK corona machine at

Company A, viable T4 bacteriophage was successfully immobilised onto BOPP films as part of a lutensol formulation and dried at temperatures of up to 75 °C, retaining a mean surface concentration of up to 1 x $10^5$ PFU/$cm^2$. Phage activity on these sheets dropped following physical stress testing, suggesting that there a proportion of the less well-bound phages can are removed during physical stress. Future work should be carried out to determine the effect of long-term reel storage on the shelf-life of immobilised phage, as this would have logistical implications in a manufacturing scenario where phage-immobilised is produced and stored for longer periods of time. Improved formulations for the shelf-life of immobilised phages would also need to be considered, building on the work carried out in the previous chapter.

The work summarised in this chapter represents the first study investigating the effect of immobilised phage food packaging on salad shelf-life. While previous studies have shown that immobilised phage in this context does act to reduce target bacteria, there has yet to be any data demonstrating the beneficial effects of this technology at a consumer level. The results presented here showed that packaging spinach leaves in bags made of BOPP incorporated with an immobilised phage cocktail targeting 4 spoilage strains resulted in between half and a full day's shelf life in terms of perceived salad leaf quality as well as buyability. This could have significant implications for both consumers and suppliers, who would stand to benefit from longer-lasting salad bags from a logistical standpoint. There is scope for further improvements to shelf-life through prior microbiome analysis of the foodstuff in question for more precise strain targeting, increasing the size of the phage cocktail and using directed evolution to mitigate the risk of any emergent resistance.

# Chapter 6: General Discussion and Future Work

The relevance of bacteriophage-based technology as a viable strategy to tackle problems arising from antibiotic-resistant bacteria is expected to increase steadily. Bacteriophages are most often strain-specific, able to self-amplify and are relatively harmless to non-prokaryotic cell types, making them an interesting alternative to more conventional strategies. The overlying aim of this thesis was to address one of the main issues facing bacteriophage application: their effective delivery. The use of phages in free form has been widely reported and their currently exist several commercial liquid-based phage products for neutralising problem strains in the agricultural sector. Despite this, free phage preparations are limited in scope due to the fact that they cannot be fixed spatially onto or within a site of interest. Furthermore, at manufacturing scale, liquid preparations are harder to transport and would require cold chain logistics in order to retain viability over the long-term. The need to overcome these challenges has resulted in increased focus on the incorporation of viable phages onto or within solid substrates. In this regard, bacteriophage immobilisation has emerged as an important process, with the unique application of corona discharge treatment as a mediator for immobilisation underpinning most of the work carried out in this collection of works.

The first challenge that was addressed involved establishing a standardised and verifiable protocol for enumerating immobilised bacteriophages. Despite prior studies on immobilised phages that have been carried out, there remains a need for a robust and relatively simple protocol tailored towards semi high-throughput capacity, as would be typically encountered in a research laboratory. A simple method was developed in Chapter 2 whereby the number of viable phages per unit quantity of substrate was determined according to the equivalent activity of free phage standards. This was verified statistically, confirming that there was no significant difference between results obtained using the ‘equivalence phage loading’ protocol described and standard plaque assays. The work summarised in this chapter underpinned all of the enumeration work performed throughout the rest of the project and, at the time of writing, is the first microbiological assay of its kind to be used for quantifying viable, immobilised phages. Further work in this area should focus on developing a quantification assay for slow growing phages, in particular, those of anaerobic bacteria, which often exhibit growth curves spanning several days.

Linker-free approaches to the immobilisation of biological entities onto substrates are desirable with respect to ease of operation and cost in a scaled-up setting. In this regard, the primary objective of Chapter 3 was to demonstrate the effectiveness of corona discharge as a mediator for bacteriophage immobilisation. As expected, the application of corona discharge onto polymer surfaces resulted in the incorporation of polar species on the surface. An increase in surface energy was observed for all 5 polymers considered and the presence of free surface radicals was also detectable on the PE and N6 surfaces tested. From the results, both of these characteristics appear to be proportional to corona discharge treatment intensity. Future work involving plasma or corona discharge-mediated immobilisation should consider the choice of polymer, as rapid rates of post-treatment hydrophobic recovery could potentially disrupt phage immobilisation and/or subsequent product efficacy. It should be noted that of the five polymers considered, only CP exhibited a notably drop in surface energy, returning to it baseline with a couple of days. The post-rinse phage loading results suggest that several factors contribute to the irreversible binding of phages, including corona treatment intensity, the choice of bacteriophage as well as the choice of substrate. For all the phages considered apart from PLS27, optimal binding occurred at the lower treatment intensities of 5.2 and 40 $kJ/m^2$, suggesting that overtreating the surface can result in lower phage retention. Despite this, the results for phages T4, T5 and ST3 strongly suggest that corona discharge improves irreversible binding by up to a factor of 10. This is likely due to a combination of free radical-mediated covalent linkage as well as non-specific binding interactions promoted by the incorporation of polar groups on the polymer surface. Further work should focus on fine-tuning corona discharge treatment intensity settings for individual phages to increase the extent of this improvement.

Apart from improving phage immobilisation onto surfaces of interest, another crucial aspect of producing bacteriophage-based products is the stability and distribution of the phages in question when in the immobilised state. The work discussed in Chapter 4 was carried out to address these issues through the preparation and testing of various formulations. There were differences between individual phages in terms of which formulations they responded best to, underlying the importance of testing specific phages in formulations of interest before embarking on the scaled-up manufacture of a product.

For example, lutensol-based formulations were effective at protecting bacteriophages T4 and PLS27 from drying stresses but had no such effect for T5 and ST3. Despite this, lecithin and sucrose emerged as two substances of interest, with their corresponding providing universal protection to all of the phages considered with the exception of 10 % wt/vol sucrose, which failed to protect T5 adequately. These substances are able to preserve phages through different mechanisms; vitrification in the case of sugars such as sucrose and emulsification in the case of lecithin. Further investigation showed that whilst lecithin offers the better protection during the drying stage, sucrose is more effective as a long-term promoter of stability, suggesting that the stresses immobilised phages are subjected to during these two periods are different. A notable finding emerged in that lecithin and sucrose could be combined in a mixed formulation to offer protective effects against drying as well as long-term storage. There is scope for increased work in this area, specifically with regard to carrying out a comprehensive review of various formulation combinations and their ability to stabilise immobilised phages. The second part of the chapter focused on bacteriophage distribution, where lutensol and sucrose were found to be particularly effective at distributing immobilised phages across polyethylene films following gravure application. As with stabilisation, combined formulations showed promise in their ability to maximise distribution. The chapter concluding with an experiment demonstrating the effectiveness of a combined sucrose/lutensol/lecithin mixture with respect to distribution and post-drying loading concentration of immobilised T4 bacteriophage. The results from this chapter show that carefully selected formulations that are relatively simple to prepare can significantly improve bacteriophage immobilisation outcomes when it comes to stability and surface distribution. This could have implications for scaled-up manufacturing processes, where product shelf-life and efficacy need to be maximised whilst keeping costs as low as possible.

While there has been a recent surge in studies on bacteriophage immobilisation, a notable gap persists in real-world trials for immobilised phage products. The final experimental chapter aimed to showcase the effectiveness of an immobilised phage cocktail in mitigating bacteria-induced spoilage in packaged salads. The significance of addressing food waste resulting from spoilage, a global economic and health burden, underscores the need for innovative solutions. Most of the experimentation was carried out in

collaboration with a plastic production company with the work representing the culmination of the previous three thesis chapters. An initial pilot study indicated the efficacy of a pre-developed free phage cocktail in extending the shelf life of two out of three salad types. While promising, the use of free phages poses challenges due to refrigeration requirements and constraints on application into salad bags. Immobilisation resolves these issues, allowing for the production of plastic sheets with incorporated bacteriophages that can be stored long-term without the need for cold chain storage. This streamlined process facilitates integration into existing plastic film manufacturing processes. Subsequent experiments in Chapter 5 demonstrated the feasibility of immobilising bacteriophages at Company A's manufacturing plant, emphasising the transferability and manufacturing potential of corona discharge-mediated bacteriophage immobilisation. In a blinded trial, salad bags containing an immobilised phage cocktail significantly increased the shelf life of packaged spinach by at least half a day. Future efforts should focus on enhancing the cocktail by incorporating additional bacteriophages and improving existing ones through successive exposure techniques to mitigate resistance emergence. This trial represented one of the first instances of immobilised phages being used to demonstrate a desirable effect at the consumer level. Whilst the result was encouraging there is a need for studies of this kind across other sectors including animal and human health to exhibit the commercial value of immobilised phage products.

To conclude, the work in this thesis shows that corona discharge can be used to irreversibly bind bacteriophages onto polymeric surfaces. Immobilised bacteriophages retain their bioactivity, providing the substrate in question with antimicrobial properties against the specific bacterial strains the phages in question target. The choice of formulation can have a profound effect on post-immobilisation stability and distribution, and it is anticipated that this will be a major area of interest moving forward. Finally, an immobilised bacteriophage cocktail formulation was found to significantly increased the shelf-life of packaged spinach leaves. This underscores the potential impact of this technology in addressing challenges related to food preservation and other bacteria-related problems.

# References


Ackermann, H.-W., Tremblay, D., & Moineau, S. (2004). Long-Term Bacteriophage Preservation. *WFCC Newsletter*, *38*, 35–40.

Ackermann, H. W. (2003). Bacteriophage observations and evolution. *Research in Microbiology*, *154*(4), 245–251. https://doi.org/10.1016/S0923-2508(03)00067-6

Ackermann, H. W. (2007). 5500 Phages examined in the electron microscope. *Archives of Virology*, *152*(2), 227–243. https://doi.org/10.1007/s00705-006-0849-1

Aksyuk, A. A., Leiman, P. G., Kurochkina, L. P., Shneider, M. M., Kostyuchenko, V. A., Mesyanzhinov, V. V., & Rossmann, M. G. (2009). The tail sheath structure of bacteriophage T4: A molecular machine for infecting bacteria. *EMBO Journal*, *28*(7), 821–829. https://doi.org/10.1038/emboj.2009.36

Al-Hindi, R. R., Teklemariam, A. D., Alharbi, M. G., Alotibi, I., Azhari, S. A., Qadri, I., Alamri, T., Harakeh, S., Applegate, B. M., & Bhunia, A. K. (2022). Bacteriophage-Based Biosensors: A Platform for Detection of Foodborne Bacterial Pathogens from Food and Environment. *Biosensors*, *12*(10), 905. https://doi.org/10.3390/bios12100905

Alegbeleye, O., Odeyemi, O. A., Strateva, M., & Stratev, D. (2022). Microbial spoilage of vegetables, fruits and cereals. *Applied Food Research*, *2*(1), 100122. https://doi.org/10.1016/j.afres.2022.100122

Alvarez-Gonzalez, E., Alfadhel, M., Mane, P., Ford, S. J., Moore, B. D., & van der Walle, C. F. (2012). Bioprocessing of bacteriophages via rapid drying onto microcrystals. *Biotechnology Progress*, *28*(2), 540–548. https://doi.org/10.1002/btpr.740

Alves, D., Marques, A., Milho, C., Costa, M. J., Pastrana, L. M., Cerqueira, M. A., & Sillankorva, S. M. (2019). Bacteriophage ϕIBB-PF7A loaded on sodium alginate-based films to prevent microbial meat spoilage. *International Journal of Food Microbiology*, *291*, 121–127. https://doi.org/10.1016/j.ijfoodmicro.2018.11.026

Anany, H., Chen, W., Pelton, R., & Griffiths, M. W. (2011). Biocontrol of Listeria monocytogenes and Escherichia coli O157:H7 in meat by using phages immobilized on modified cellulose membranes. *Applied and Environmental Microbiology*, *77*(18), 6379–6387. https://doi.org/10.1128/AEM.05493-11

Angeli, L., Imperiale, S., Ding, Y., Scampicchio, M., & Morozova, K. (2021). A novel stoichio-kinetic model for the dpph• assay: The importance of the side reaction and application to complex mixtures. *Antioxidants*, *10*(7). https://doi.org/10.3390/antiox10071019

Aronino, R., Dlugy, C., Arkhangelsky, E., Shandalov, S., Oron, G., Brenner, A., & Gitis, V. (2009). Removal of viruses from surface water and secondary effluents by sand filtration. *Water Research*, *43*(1), 87–96. https://doi.org/10.1016/j.watres.2008.10.036

Ashiani, D., Keihan, A. H., Rashidiani, J., Dashtestani, F., & Eskandari, K. (2016). Oriented T4 bacteriophage immobilization for recognition of Escherichia coli in capacitance method. *International Journal of Electrochemical Science*, *11*(12), 10087–10095. https://doi.org/10.20964/2016.12.16

Awais, R., Fukudomi, H., Miyanaga, K., Unno, H., & Tanji, Y. (2006). A recombinant bacteriophage-based assay for the discriminative detection of culturable and viable but nonculturable Escherichia coli O157:H7. *Biotechnology Progress*, *22*(3), 853–859. https://doi.org/10.1021/bp060020q

Azam, A. H., & Tanji, Y. (2019). Bacteriophage-host arm race: an update on the mechanism of phage resistance in bacteria and revenge of the phage with the perspective for phage therapy. *Applied Microbiology and Biotechnology*, *102*, 2121–2131. https://doi.org/10.1007/s00253-019-09629-x

Back, J. F., Oakenfull, D., & Smith, M. B. (1979). Increased thermal stability of proteins in the presence of sugars and polyols. *Biochemistry*, *18*(23), 5191–5196. https://doi.org/10.1021/bi00590a025

Baer, A., & Kehn-Hall, K. (2014). Viral concentration determination through plaque assays: Using traditional

and novel overlay systems. *Journal of Visualized Experiments*, *93*, 1–10. https://doi.org/10.3791/52065

Balcão, V. M., Glasser, C. A., Chaud, M. V., del Fiol, F. S., Tubino, M., & Vila, M. M. D. C. (2014). Biomimetic aqueous-core lipid nanoballoons integrating a multiple emulsion formulation: A suitable housing system for viable lytic bacteriophages. *Colloids and Surfaces B: Biointerfaces*, *123*, 478–485. https://doi.org/10.1016/j.colsurfb.2014.09.045

Bales, R. C., Li, S., Maguire, K. M., Yahya, M. T., & Gerba, C. P. (1993). MS-2 and poliovirus transport in porous media: Hydrophobic effects and chemical perturbations. *Water Resources Research*, *29*(4), 957–963. https://doi.org/10.1029/92WR02986

Bean, J. E., Alves, D. R., Laabei, M., Esteban, P. P., Thet, N. T., Enright, M. C., & Jenkins, A. T. A. (2014). Triggered Release of Bacteriophage K from Agarose/Hyaluronan Hydrogel Matrixes by *Staphylococcus aureus* Virulence Factors. *Chemistry of Materials*, *26*(24). https://doi.org/10.1021/cm503974g

Bennett, A. R., Davids, F. G. C., Vlahodimou, S., Banks, J. G., & Betts, R. P. (1997). The use of bacteriophage-based systems for the separation and concentration of Salmonella. *Journal of Applied Microbiology*, *83*(2), 259–265. https://doi.org/10.1046/j.1365-2672.1997.00257.x

Bernardy, C., & Malley, J. (2023). Virus Behavior after UV254 Treatment of Materials with Different Surface Properties. *Microorganisms*, *11*(9), 2157. https://doi.org/10.3390/microorganisms11092157

Bertani, G., & Weigle, J. J. (1953). Host controlled variation in bacterial viruses. *Journal of Bacteriology*, *65*(2), 113–121. http://www.ncbi.nlm.nih.gov/pubmed/13034700

Bertozzi Silva, J., Storms, Z., & Sauvageau, D. (2016). Host receptors for bacteriophage adsorption. In *FEMS Microbiology Letters* (Vol. 363, Issue 4). Oxford University Press. https://doi.org/10.1093/femsle/fnw002

Bhardwaj, A., Sharma, N., Sharma, V., Alam, T., & Shafia, S. (2022). Smart Food Packaging Systems. In *Smart and Sustainable Food Technologies* (pp. 235–260). Springer Nature Singapore. https://doi.org/10.1007/978-981-19-1746-2_8

Bielke, L., Higgins, S., Donoghue, A., Donoghue, D., & Hargis, B. M. (2007). Salmonella host range of bacteriophages that infect multiple genera. *Poultry Science*, *86*(12), 2536–2540. https://doi.org/10.3382/ps.2007-00250

Bilek, M. M., & McKenzie, D. R. (2010). Plasma modified surfaces for covalent immobilization of functional biomolecules in the absence of chemical linkers: Towards better biosensors and a new generation of medical implants. *Biophysical Reviews*, *2*, 55–65. https://doi.org/10.1007/s12551-010-0028-1

Bitterncourt, J. A. (2004). Fundamentals of plasma physics. In *Wiley series in plasma physics* (3rd ed.). Springer New York LLC. https://doi.org/10.1007/978-1-4757-4030-1

Bone, S., Alum, A., Markovski, J., Hristovski, K., Bar-Zeev, E., Kaufman, Y., Abbaszadegan, M., & Perreault, F. (2018). Physisorption and chemisorption of T4 bacteriophages on amino functionalized silica particles. *Journal of Colloid and Interface Science*, *532*, 69–76. https://doi.org/10.1016/j.jcis.2018.07.107

Bonilla, N., Rojas, M. I., Netto, G., Cruz, F., Hung, S., Rohwer, F., & Barr, J. J. (2016). Phage on tap – a quick and efficient protocol for the preparation of bacteriophage laboratory stocks. *PeerJ*. https://doi.org/10.7717/peerj.2261

Brown, T. L., Petrovski, S., Chan, H. T., Angove, M. J., & Tucci, J. (2018). Semi-solid and solid dosage forms for the delivery of phage therapy to epithelia. *Pharmaceuticals*, *11*(1), 1–12. https://doi.org/10.3390/ph11010026

Brown, T. L., Thomas, T., Odgers, J., Petrovski, S., Spark, M. J., & Tucci, J. (2017). Bacteriophage formulated into a range of semisolid and solid dosage forms maintain lytic capacity against isolated cutaneous and opportunistic oral bacteria. *Journal of Pharmacy and Pharmacology*, *69*(3). https://doi.org/10.1111/jphp.12673

Brum, J. R., Schenck, R. O., & Sullivan, M. B. (2013). Global morphological analysis of marine viruses shows minimal regional variation and dominance of non-tailed viruses. *ISME Journal*, *7*(9), 1738–1751. https://doi.org/10.1038/ismej.2013.67

Cademartiri, R., Anany, H., Gross, I., Bhayani, R., Griffiths, M., & Brook, M. A. (2010). Immobilization of bacteriophages on modified silica particles. *Biomaterials*, *31*(7), 1904–1910. https://doi.org/10.1016/j.biomaterials.2009.11.029

Cao, Y., Khanal, D., Kim, J., Chang, R. Y. K., Byun, A. S., Morales, S., Banaszak Holl, M. M., & Chan, H.-K. (2023). Stability of bacteriophages in organic solvents for formulations. *International Journal of Pharmaceutics*, *646*, 123505. https://doi.org/10.1016/j.ijpharm.2023.123505

Cariddi, C., Saponari, M., Boscia, D., De Stradis, A., Loconsole, G., Nigro, F., Porcelli, F., Potere, O., & Martelli, G. P. (2014). Isolation of a Xylella fastidiosa strain infecting olive and oleander in Apulia, Italy. *Journal of Plant Pathology*, *96*(2), 425–429. https://doi.org/10.4454/JPP.V96I2.024

Cassini, A., Högberg, L. D., Plachouras, D., Quattrocchi, A., Hoxha, A., Simonsen, G. S., Colomb-Cotinat, M., Kretzschmar, M. E., Devleesschauwer, B., Cecchini, M., Ouakrim, D. A., Oliveira, T. C., Struelens, M. J., Suetens, C., Monnet, D. L., Strauss, R., Mertens, K., Struyf, T., Catry, B., … Hopkins, S. (2019). Attributable deaths and disability-adjusted life-years caused by infections with antibiotic-resistant bacteria in the EU and the European Economic Area in 2015: a population-level modelling analysis. *The Lancet Infectious Diseases*, *19*(1), 56–66. https://doi.org/10.1016/S1473-3099(18)30605-4

Cerofolini, G. F., Meda, L., & Bandosz, T. J. (1998). Adsorption with soft adsorbents or adsorbates. Theory and practice. In *Adsorption and its Applications in Industry and Environmental Protection Studies in Surface Science and Catalysis* (Vol. 120, pp. 227–272). https://doi.org/10.1016/S0167-2991(99)80554-0

Chan, B. K., Abedon, S. T., & Loc-carrillo, C. (2013). Phage cocktails and the future of phage therapy. *Future Microbiology*, *8*(6), 769–783. https://doi.org/10.2217/fmb.13.47

Chang, J. S., Lawless, P. A., & Yamamoto, T. (1991). Corona Discharge Processes. *IEEE Transactions on Plasma Science*, *19*(6), 1152–1166. https://doi.org/10.1109/27.125038

Chang, R. Y. K., Chen, K., Wang, J., Wallin, M., Britton, W., Morales, S., Kutter, E., Li, J., & Chan, H.-K. (2018). Proof-of-Principle Study in a Murine Lung Infection Model of Antipseudomonal Activity of Phage PEV20 in a Dry-Powder Formulation. *Antimicrobial Agents and Chemotherapy*, *62*(2). https://doi.org/10.1128/AAC.01714-17

Chang, R. Y., Wong, J., Mathai, A., Morales, S., Kutter, E., Britton, W., Li, J., & Chan, H. K. (2017). Production of highly stable spray dried phage formulations for treatment of Pseudomonas aeruginosa lung infection. *European Journal of Pharmaceutics and Biopharmaceutics*, *121*, 1–13. https://doi.org/10.1016/j.ejpb.2017.09.002

Chen, J., & Davidson, J. H. (2003). Ozone Production in the Negative DC Corona: The Dependence of Discharge Polarity. *Plasma Chemistry and Plasma Processing*, *23*(3), 501–518. https://doi.org/10.1023/A:1023235032455

Chen, L., Lee, W., Ma, Y., Jang, S. S., Fong, K., & Wang, S. (2022). The efficacy of different sanitizers against MS2 bacteriophage introduced onto plastic or stainless steel surfaces. *Current Research in Food Science*, *5*, 175–181. https://doi.org/10.1016/j.crfs.2022.01.004

Chen, P., Konarov, A., Dong, D., Zhang, Y., & Sutaria, S. (2013). Binding Mechanism and Electrochemical Properties of M13 Phage-Sulfur Composite. *PLoS ONE*. https://doi.org/10.1371/journal.pone.0082332

Choi, I., Lee, J.-S., & Han, J. (2023). Maltodextrin-trehalose miscible system-based bacteriophage encapsulation: Studies of plasticizing effect on encapsulated phage activity and food application as an antimicrobial agent. *Food Control*, *146*, 109550. https://doi.org/10.1016/j.foodcont.2022.109550

Clokie, M. R. J., Millard, A. D., Letarov, A. V, & Heaphy, S. (2011). (2011) Phages in nature. *Bacteriophage*, *1*(1), 31–45.

Coad, B. R., Jasieniak, M., Griesser, S. S., & Griesser, H. J. (2013). Controlled covalent surface immobilisation of proteins and peptides using plasma methods. *Surface and Coatings Technology*, *233*, 169–177. https://doi.org/10.1016/j.surfcoat.2013.05.019

Collaud, M., Groening, P., Nowak, S., & Schlapbach, L. (1994). Plasma treatment of polymers: the effect of the plasma parameters on the chemical, physical, and morphological states of the polymer surface and on the metal-polymer interface. *Journal of Adhesion Science and Technology*, *8*(10), 1115–1127. https://doi.org/10.1163/156856194X00979

Comyn, J., Mascia, L., Xiao, G., & Parker, B. M. (1996). Corona-discharge treatment of polyetheretherketone (PEEK) for adhesive bonding. *International Journal of Adhesion and Adhesives*, *16*(4), 301–304. https://doi.org/10.1016/S0143-7496(96)00010-3

Costello, C., Birisci, E., & McGarvey, R. G. (2016). Food waste in campus dining operations: Inventory of pre- and post-consumer mass by food category, and estimation of embodied greenhouse gas emissions. *Renewable Agriculture and Food Systems*, *31*(3), 191–201. https://doi.org/10.1017/S1742170515000071

Courval, G. J., Gray, D., & Goring, D. A. I. (1976). Chemical modification of polyethylene surfaces in a nitrogen corona. *Journal of Polymer Sciences*, *14*(4). https://doi.org/https://doi.org/10.1002/pol.1976.130140410

De Geyter, N., Morent, R., & Leys, C. (2007). Surface characterization of plasma-modified polyethylene by contact angle experiments and ATR-FTIR spectroscopy. *Surface and Interface Analysis*, *40*(3–4). https://doi.org/10.1002/sia.2611

De Paepe, M., & Taddei, F. (2006). Viruses' life history: Towards a mechanistic basis of a trade-off between survival and reproduction among phages. *PLoS Biology*, *4*(7), 1248–1256. https://doi.org/10.1371/journal.pbio.0040193

Dini, C., & de Urraza, P. J. (2013). Effect of buffer systems and disaccharides concentration on Podoviridae coliphage stability during freeze drying and storage. *Cryobiology*, *66*(3). https://doi.org/10.1016/j.cryobiol.2013.03.007

Dixon, M. C. (2008). Quartz crystal microbalance with dissipation monitoring: Enabling real-time characterization of biological materials and their interactions. *Journal of Biomolecular Techniques*, *19*(3), 151–158.

Duckworth, D. H. (1976). "Who discovered bacteriophage?". *Bacteriological Reviews*, *40*(4), 793–802. http://www.ncbi.nlm.nih.gov/pubmed/795414%0Ahttp://www.pubmedcentral.nih.gov/articlerender.fcgi?artid=PMC413985

Dutta, D., Kumar, N., & D. P. Willcox, M. (2016). Antimicrobial activity of four cationic peptides immobilised to poly-hydroxyethylmethacrylate. *Biofouling*, *32*(4), 429–438. https://doi.org/10.1080/08927014.2015.1129533

Duyvejonck, H., Merabishvili, M., Vaneechoutte, M., de Soir, S., Wright, R., Friman, V.-P., Verbeken, G., De Vos, D., Pirnay, J.-P., Van Mechelen, E., & Vermeulen, S. J. T. (2021). Evaluation of the Stability of Bacteriophages in Different Solutions Suitable for the Production of Magistral Preparations in Belgium. *Viruses*, *13*(5), 865. https://doi.org/10.3390/v13050865

DyneTesting. (n.d.). *Dyne Testing Surface Energy Testing*. https://dynetesting.com/surface-energy-measurement/dyne-pens/#squelch-taas-tab-content-0-1

Eberly, A. R., Elvert, J. L., & Schuetz, A. N. (2022). Best Practices for the Pre Analytic Phase of Anaerobic Bacteriology. *Clinical Microbiology Newsletter*, *44*(7), 63–71. https://doi.org/10.1016/j.clinmicnews.2022.04.001

Encinas, N., Díaz-Benito, B., Abenojar, J., & Martínez, M. A. (2010). Extreme durability of wettability changes on polyolefin surfaces by atmospheric pressure plasma torch. *Surface and Coatings Technology*, *205*(2), 396–402. https://doi.org/10.1016/j.surfcoat.2010.06.069

Ershov, S., Khelifa, F., Lemaur, V., Cornil, J., Cossement, D., Habibi, Y., Dubois, P., & Snyders, R. (2014). Free Radical Generation and Concentration in a Plasma Polymer: The Effect of Aromaticity. *ACS Applied Materials & Interfaces*, *6*(15), 12395–12405. https://doi.org/10.1021/am502255p

Evoy, S., Singh, A., & Glass, N. (2010). *Bacteriophage Immobilisazation for Biosensors* (US 2010/0291541 A1). United States Patent and Trademark Office.

Farkas, K., Varsani, A., & Pang, L. (2015). Adsorption of Rotavirus, MS2 Bacteriophage and Surface-Modified Silica Nanoparticles to Hydrophobic Matter. *Food and Environmental Virology*, *7*(3), 261–268. https://doi.org/10.1007/s12560-014-9171-3

Farooq, U., Yang, Q., Ullah, M. W., & Wang, S. (2018). Bacterial biosensing: Recent advances in phage-based bioassays and biosensors. In *Biosensors and Bioelectronics*. https://doi.org/10.1016/j.bios.2018.07.058

Fauré, N. E., Halling, P. J., & Wimperis, S. (2014). A solid-state NMR study of the immobilization of α-chymotrypsin on mesoporous silica. *Journal of Physical Chemistry C*, *118*(2), 1042–1048. https://doi.org/10.1021/jp4098414

Favia, P., & D'Agostino, R. (1998). Plasma treatments and plasma deposition of polymers for biomedical applications. *Surface and Coatings Technology*, *98*(1–3), 1102–1106. https://doi.org/10.1016/S0257-8972(97)00285-5

Felix d'Herelle Reference Centre for Bacteterial Viruses. (2006, April 29). *HER 200*. Phages Catalog.

Feng, A. L., Boraey, M. A., Gwin, M. A., Finlay, P. R., Kuehl, P. J., & Vehring, R. (2011). Mechanistic models facilitate efficient development of leucine containing microparticles for pulmonary drug delivery. *International Journal of Pharmaceutics*, *409*(1–2), 156–163. https://doi.org/10.1016/j.ijpharm.2011.02.049

Fister, S., Robben, C., Witte, A. K., Schoder, D., Wagner, M., & Rossmanith, P. (2016). Influence of Environmental Factors on Phage–Bacteria Interaction and on the Efficacy and Infectivity of Phage P100. *Frontiers in Microbiology*, *7*. https://doi.org/10.3389/fmicb.2016.01152

Fortier, L.-C., & Moineau, S. (2009). *Phage Production and Maintenance of Stocks, Including Expected Stock Lifetimes* (pp. 203–219). https://doi.org/10.1007/978-1-60327-164-6_19

Frenzel, A., Kügler, J., Helmsing, S., Meier, D., Schirrmann, T., Hust, M., & Dübel, S. (2017). Designing Human Antibodies by Phage Display. *Transfusion Medicine and Hemotherapy*, *44*(5), 312–318. https://doi.org/10.1159/000479633

Furfaro, L. L., Payne, M. S., & Chang, B. J. (2018). Bacteriophage Therapy: Clinical Trials and Regulatory Hurdles. *Frontiers in Cellular and Infection Microbiology*, *8*. https://doi.org/10.3389/fcimb.2018.00376

Gao, R., Wang, Y., Tong, J., Zhou, P., & Yang, Z. (2016). Strategies for the Immobilization of Bacteriophages Applied in the Biosensors. *Proceedings - 2015 International Conference on Computational Intelligence and Communication Networks, CICN 2015*, 178–182. https://doi.org/10.1109/CICN.2015.42

Gervais, L., Gel, M., Allain, B., Tolba, M., Brovko, L., Zourob, M., Mandeville, R., Griffiths, M., & Evoy, S. (2007). Immobilization of biotinylated bacteriophages on biosensor surfaces. *Sensors and Actuators, B: Chemical*, *125*(2), 615–621. https://doi.org/10.1016/j.snb.2007.03.007

Gibson, K. E., Almeida, G., Jones, S. L., Wright, K., & Lee, J. A. (2019). Inactivation of bacteria on fresh produce by batch wash ozone sanitation. *Food Control*, *106*, 106747. https://doi.org/10.1016/j.foodcont.2019.106747

Golec, P., Dąbrowski, K., Hejnowicz, M. S., Gozdek, A., Łoś, J. M., Węgrzyn, G., Łobocka, M. B., & Łoś, M. (2011). A reliable method for storage of tailed phages. *Journal of Microbiological Methods*, *84*(3), 486–489. https://doi.org/10.1016/j.mimet.2011.01.007

Guang-Han, O., Leang-Chung, C., Vellasamy, K. M., Mariappan, V., Li-Yen, C., & Vadivelu, J. (2016). Experimental phage therapy for Burkholderia pseudomallei infection. *PLoS ONE*, *11*(7), 1–16.

https://doi.org/10.1371/journal.pone.0158213

Guerrero-Ferreira, R. C., Viollier, P. H., Ely, B., Poindexter, J. S., Georgieva, M., Jensen, G. J., & Wright, E. R. (2011). Alternative mechanism for bacteriophage adsorption to the motile bacterium Caulobacter crescentus. *Proceedings of the National Academy of Sciences*, *108*(24), 9963–9968. https://doi.org/10.1073/pnas.1012388108

Guntupalli, R., Sorokulova, I., Krumnow, A., Pustovyy, O., Olsen, E., & Vodyanoy, V. (2008). Real-time optical detection of methicillin-resistant Staphylococcus aureus using lytic phage probes. *Biosensors and Bioelectronics*, *24*(1), 151–154. https://doi.org/10.1016/j.bios.2008.03.003

Guntupalli, R., Sorokulova, I., Long, R., Olsen, E., Neely, W., & Vodyanoy, V. (2011). Phage Langmuir monolayers and Langmuir-Blodgett films. *Colloids and Surfaces B: Biointerfaces*, *82*(1), 182–189. https://doi.org/10.1016/j.colsurfb.2010.08.032

Guntupalli, R., Sorokulova, I., Olsen, E., Globa, L., Pustovyy, O., & Vodyanoy, V. (2013). Biosensor for Detection of Antibiotic Resistant Staphylococcus Bacteria. *Journal of Visualized Experiments*, *75*. https://doi.org/10.3791/50474

Haaber, J., Leisner, J. J., Cohn, M. T., Catalan-Moreno, A., Nielsen, J. B., Westh, H., Penadés, J. R., & Ingmer, H. (2016). Bacterial viruses enable their host to acquire antibiotic resistance genes from neighbouring cells. *Nature Communications*, *7*. https://doi.org/10.1038/ncomms13333

Hadley, P. (1928). The Twort-D'Herelle Phenomenon: A Critical Review and Presentation of a New Conception (Homogamic Theory) Of Bacteriophage Action. *The Journal of Infectious Diseases*, *42*(4), 263–434.

Han, J., Jin, Y., & Willson, C. S. (2006). Virus retention and transport in chemically heterogeneous porous media under saturated and unsaturated flow conditions. *Environmental Science and Technology*, *40*(5), 1547–1555. https://doi.org/10.1021/es051351m

Harada, L. K., Silva, E. C., Campos, W. F., Del Fiol, F. S., Vila, M., Dąbrowska, K., Krylov, V. N., & Balcão, V. M. (2018). Biotechnological applications of bacteriophages: State of the art. *Microbiological Research*, *212–213*, 38–58. https://doi.org/10.1016/j.micres.2018.04.007

Hershey, A. D., & Chase, M. (1952). Independent functions of viral protein and nucleic acid in growth of bacteriophage. *The Journal of General Physiology*, *36*(1), 39–56. http://www.ncbi.nlm.nih.gov/pubmed/12981234

Hiep Nguyen, H., & Kim, M. (2017). An Overview of Techniques in Enzyme Immobilization. *Appl. Sci. Converg. Technol*, *26*(6), 157–163. https://doi.org/10.5757/ASCT.2017.26.6.157

Hillborg A'b, H., & Gedde A'b', U. W. (1998). Hydrophobicity recovery of polydimethylsiloxane after exposure to corona discharges. *Polymer*, *39*(10), 1991–1998.

Hirsh, S. L., Bilek, M. M. M., Nosworthy, N. J., Kondyurin, A., Dos Remedios, C. G., & McKenzie, D. R. (2010). A Comparison of covalent immobilization and physical adsorption of a cellulase enzyme mixture. *Langmuir*, *26*(17), 14380–14388. https://doi.org/10.1021/la1019845

Hitchcock, N. M., Devequi Gomes Nunes, D., Shiach, J., Valeria Saraiva Hodel, K., Dantas Viana Barbosa, J., Alencar Pereira Rodrigues, L., Coler, B. S., Botelho Pereira Soares, M., & Badaró, R. (2023). Current Clinical Landscape and Global Potential of Bacteriophage Therapy. *Viruses*, *15*(4), 1020. https://doi.org/10.3390/v15041020

Horikawa, S., Bedi, D., Li, S., Shen, W., Huang, S., Chen, I. H., Chai, Y., Auad, M. L., Bozack, M. J., Barbaree, J. M., Petrenko, V. A., & Chin, B. A. (2011). Effects of surface functionalization on the surface phage coverage and the subsequent performance of phage-immobilized magnetoelastic biosensors. *Biosensors and Bioelectronics*, *26*(5), 2361–2367. https://doi.org/10.1016/j.bios.2010.10.012

Hosseinidoust, Z., Olsson, A. L. J., & Tufenkji, N. (2014). Going viral: Designing bioactive surfaces with bacteriophage. *Colloids and Surfaces B: Biointerfaces*, *124*, 2–16.

https://doi.org/10.1016/j.colsurfb.2014.05.036

Hosseinidoust, Z., Van De Ven, T. G. M., & Tufenkji, N. (2011). Bacterial capture efficiency and antimicrobial activity of phage-functionalized model surfaces. *Langmuir*. https://doi.org/10.1021/la200102z

Houk, K. N., Leach, A. G., Kim, S. P., & Zhang, X. (2003). Binding affinities of host-guest, protein-ligand, and protein-transition-state complexes. *Angewandye Chemie (International Ed. in English)*, *42*(40), 4872–4897.

Hristea, E. N., Caproiu, M. T., Pencu, G., Hillebrand, M., Constantinescu, T., & Balaban, A. T. (2006). Reaction of 2,2-Diphenyl-1-picrylhydrazyl with HO • , HO-, and HOO-Radicals and Anions. *Int. J. Mol. Sci*, *7*, 7. www.mdpi.org/ijms/

Huang, Q., & Zhu, Y. (2018). Gravure Printing of Water-based Silver Nanowire ink on Plastic Substrate for Flexible Electronics. *Scientific Reports*, *8*(1), 1–10. https://doi.org/10.1038/s41598-018-33494-9

Huang, S., Yang, H., Lakshmanan, R. S., Johnson, M. L., Wan, J., Chen, I. H., Wikle, H. C., Petrenko, V. A., Barbaree, J. M., & Chin, B. A. (2009). Sequential detection of Salmonella typhimurium and Bacillus anthracis spores using magnetoelastic biosensors. *Biosensors and Bioelectronics*, *24*(6), 1730–1736. https://doi.org/10.1016/j.bios.2008.09.006

Iwata, H., Kishida, A., Suzuki, M., Hata, Y., & Ikada, Y. (1988). Oxidation of polyethylene surface by corona discharge and the subsequent graft polymerization. *Journal of Polymer Science Part A: Polymer Chemistry*, *26*(12), 3309–3322. https://doi.org/10.1002/pola.1988.080261216

Izdebska, J. (2016). Corona Treatment. In J. Izdebska & S. Thomas (Eds.), *Printing on Polymers* (pp. 123–142). William Andrew Publishing.

Jabrane, T., Dubé, M., Griffiths, M., & Mangin, P. J. (2011). Towards a commercial production of phage-based bioactive paper. *J-For*, *1*(1), 6–13.

Jabrane, T., Dubé, M., & Mangin, P. J. (2009). *Bacteriophage Immobilization on Paper Surface:: Effect of Cationic Pre-coat Layer*. https://www.researchgate.net/publication/267717075

Jamal, M., Bukhari, S. M. A. U. S., Andleeb, S., Ali, M., Raza, S., Nawaz, M. A., Hussain, T., Rahman, S. u., & Shah, S. S. A. (2019). Bacteriophages: an overview of the control strategies against multiple bacterial infections in different fields. *Journal of Basic Microbiology*, *59*(2), 123–133. https://doi.org/10.1002/jobm.201800412

Janczuk, M., Richter, Ł., Hoser, G., Kawiak, J., Łoś, M., Niedziółka-Jönsson, J., Paczesny, J., & Hołyst, R. (2017). Bacteriophage-Based Bioconjugates as a Flow Cytometry Probe for Fast Bacteria Detection. *Bioconjugate Chemistry*, *28*(2), 419–425. https://doi.org/10.1021/acs.bioconjchem.6b00596

Jarrell, K. F., & Kropinski, A. M. (1981a). Isolation and characterization of a bacteriophage specific for the lipopolysaccharide of rough derivatives of Pseudomonas aeruginosa strain PAO. *Journal of Virology*, *38*(2), 529–538. https://doi.org/10.1128/jvi.38.2.529-538.1981

Jarrell, K. F., & Kropinski, A. M. B. (1981b). Isolation and Characterization of a Bacteriophage Specific for the Lipopolysaccharide of Rough Derivatives of Pseudomonas aeruginosa Strain PAO. In *JOURNAL OF VIROLOGY*.

Jin Ho Lee, & Hai Bang Lee. (2008). A wettability gradient as a tool to study protein adsorption and cell adhesion on polymer surfaces. *Journal of Biomaterials Science, Polymer Edition*, *4*(5), 467–481. https://doi.org/10.1163/156856293x00131

Jończyk-Matysiak, E., Łodej, N., Kula, D., Owczarek, B., Orwat, F., Międzybrodzki, R., Neuberg, J., Bagińska, N., Weber-Dąbrowska, B., & Górski, A. (2019). Factors determining phage stability/activity: challenges in practical phage application. *Expert Review of Anti-Infective Therapy*, *17*(8), 583–606. https://doi.org/10.1080/14787210.2019.1646126

Jończyk, E., Kłak, M., Międzybrodzki, R., & Górski, A. (2011). The influence of external factors on

bacteriophages—review. *Folia Microbiologica*, *56*(3). https://doi.org/10.1007/s12223-011-0039-8

Kalapat, N., Amornsakchai, T., & Srikhirin, T. (2013). Surface modification of biaxially oriented polypropylene (BOPP) film using acrylic acid-corona treatment: Part II. Long term aging surface properties. *Surface and Coatings Technology*, *234*, 67–75. https://doi.org/10.1016/j.surfcoat.2013.05.012

Kamali, S., Yavarmanesh, M., Habibi Najafi, M. B., & Koocheki, A. (2022). Development of whey protein concentrate/pullulan composite films containing bacteriophage A511: Functional properties and anti-Listerial effects during storage. *Food Packaging and Shelf Life*, *33*, 100902. https://doi.org/10.1016/j.fpsl.2022.100902

Kapetanakou, A. E., Taoukis, P., & Skandamis, P. N. (2019). Model development for microbial spoilage of packaged fresh–cut salad products using temperature and in-package CO2 levels as predictor variables. *LWT*, *113*, 108285. https://doi.org/10.1016/j.lwt.2019.108285

Karlsson, F., Borrebaeck, C. A. K., Nilsson, N., & Malmborg-Hager, A. C. (2003). The mechanism of bacterial infection by filamentous phages involves molecular interactions between TolA and phage protein 3 domains. *Journal of Bacteriology*, *185*(8), 2628–2634. https://doi.org/10.1128/JB.185.8.2628-2634.2003

Kedare, S. B., & Singh, R. P. (2011). Genesis and development of DPPH method of antioxidant assay. *Journal of Food Science and Technology*, *48*(4), 412–422. https://doi.org/10.1007/s13197-011-0251-1

Kiaei, D., Hoffman, A., & Horbett, T. (1993). Tight Binding of Albumin to Glow Discharge Treated Polymers. *Journal of Biomaterials Science, Polymer Edition*, *4*(3), 35–44. https://doi.org/10.1163/156856293X00401

Kim, H., Kim, M., Jee, S.-N., Heu, S., & Ryu, S. (2022). Development of a Bacteriophage Cocktail against Pectobacterium carotovorum Subsp. *carotovorum* and Its Effects on *Pectobacterium* Virulence. *Applied and Environmental Microbiology*, *88*(19). https://doi.org/10.1128/aem.00761-22

Kivelä, H. M., Kalkkinen, N., & Bamford, D. H. (2002). Bacteriophage PM2 has a protein capsid surrounding a spherical proteinaceous lipid core. *Journal of Virology*, *76*(16), 8169–8178. https://doi.org/10.1128/JVI.76.16.8169

Kłopot, A., Zakrzewska, A., Lecion, D., Majewska, J. M., Harhala, M. A., Lahutta, K., Kazmierczak, Z., Łaczmanski, Ł., Kłak, M., & Dabrowska, K. (2017). Real-Time qPCR as a method for detection of antibody-neutralized phage particles. *Frontiers in Microbiology*, *8*(2170). https://doi.org/10.3389/fmicb.2017.02170

Kondyurin, A., Lau, K., Tang, F., Akhavan, B., Chrzanowski, W., Lord, M. S., Rnjak-Kovacina, J., & Bilek, M. M. (2018). Plasma Ion Implantation of Silk Biomaterials Enabling Direct Covalent Immobilization of Bioactive Agents for Enhanced Cellular Responses. *ACS Applied Materials and Interfaces*, *10*(21), 17605–17616. https://doi.org/10.1021/acsami.8b03182

Kostyuchenko, V. A., Chipman, P. R., Leiman, P. G., Arisaka, F., Mesyanzhinov, V. V., & Rossmann, M. G. (2005). The tail structure of bacteriophage T4 and its mechanism of contraction. *Nature Structural and Molecular Biology*, *12*(9), 810–813. https://doi.org/10.1038/nsmb975

Kostyuchenko, V. A., Leiman, P. G., Chipman, P. R., Kanamaru, S., Van Raaij, M. J., Arisaka, F., Mesyanzhinov, V. V., & Rossmann, M. G. (2003). Three-dimensional structure of bacteriophage T4 baseplate. *Nature Structural Biology*, *10*(9), 688–693. https://doi.org/10.1038/nsb970

Kratz, F., Grass, S., Umanskaya, N., Scheibe, C., Müller-Renno, C., Davoudi, N., Hannig, M., & Ziegler, C. (2015). Cleaning of biomaterial surfaces: Protein removal by different solvents. *Colloids and Surfaces B: Biointerfaces*, *128*, 28–35. https://doi.org/10.1016/j.colsurfb.2015.02.016

Küchler, A., Adamcik, J., Mezzenga, R., Schlüter, A. D., & Walde, P. (2015). Enzyme immobilization on silicate glass through simple adsorption of dendronized polymer-enzyme conjugates for localized enzymatic cascade reactions. *RSC Advances*, *5*, 44530–44544. https://doi.org/10.1039/c5ra06268c

Kukkaro, P., & Bamford, D. H. (2009). Virus-host interactions in environments with a wide range of ionic

strengths. *Environmental Microbiology Reports*, *1*(1), 71–77. https://doi.org/10.1111/j.1758-2229.2008.00007.x

Kumar, S. B., Arnipalli, S. R., & Ziouzenkova, O. (2020). Antibiotics in Food Chain: The Consequences for Antibiotic Resistance. *Antibiotics*, *9*(10), 688. https://doi.org/10.3390/antibiotics9100688

Kumari, R., Jayachandran, L. E., & Kumar, S. (2022). Role of Microbes in the Food Industry. In *Role of Microbes in Industrial Products and Processes* (pp. 59–79). Wiley. https://doi.org/10.1002/9781119901198.ch3

Kutateladze, M., & Adamia, R. (2008). Phage therapy experience at the Eliava Institute. *Medecine et Maladies Infectieuses*, *38*(8), 426–430. https://doi.org/10.1016/j.medmal.2008.06.023

Kuzuya, M., Kamiyai, K., Yanagiharai, Y., & Matsuno, Y. (1993). Nature of plasma-induced free- radical formation of several fibrous polypeptides. *Plasma Sources Science and Technology*, *2*(1), 51–57. https://doi.org/10.1088/0963-0252/2/1/012

Kuzuya, M., Niwa, J., & Ito, H. (1993). Nature of Plasma-Induced Surface Radicals of Powdered Polyethylene Studied by Electron Spin Resonance. *Macromolecules*. https://doi.org/10.1021/ma00060a030

Lagier, J. C., Edouard, S., Pagnier, I., Mediannikov, O., Drancourt, M., & Raoult, D. (2015). Current and past strategies for bacterial culture in clinical microbiology. *Clinical Microbiology Reviews*, *28*(1), 208–236. https://doi.org/10.1128/CMR.00110-14

Lau, Y. T., Chin, O. H., Lee, H. C., Chiu, W. S., & Woo, H. J. (2022). Plasma surface treatment of polystyrene in a low power low frequency argon glow discharge. *Applied Surface Science*, *578*, 151963. https://doi.org/10.1016/j.apsusc.2021.151963

Lavigne, R., Briers, Y., Hertveldt, K., Robben, J., & Volckaert, G. (2004). Identification and characterization of a highly thermostable bacteriophage lysozyme. *Cellular and Molecular Life Sciences*, *61*(21), 2753–2759. https://doi.org/10.1007/s00018-004-4301-y

Lee, L. A., & Wang, Q. (2006). Adaptations of nanoscale viruses and other protein cages for medical applications. *Nanomedicine: Nanotechnology, Biology, and Medicine*, *2*(3), 137–149. https://doi.org/10.1016/j.nano.2006.07.009

Lehocký, M., Drnovská, H., Lapčíková, B., Barros-Timmons, A. M., Trindade, T., Zembala, M., & Lapčík, L. (2003). Plasma surface modification of polyethylene. *Colloids and Surfaces A: Physicochemical and Engineering Aspects*, *222*(1–3), 125–131. https://doi.org/10.1016/S0927-7757(03)00242-5

Leiman, P. G., Chipman, P. R., Kostyuchenko, V. A., Mesyanzhinov, V. V, Rossmann, M. G., & Black, L. (2004). Three-Dimensional Rearrangement of Proteins in the Tail of Bacteriophage T4. *Cell*, *118*(4), 419–429.

Leiman, P. G., & Shneider, M. M. (2012). Contractile Tail Machines of Bacteriophages. *Advances in Experimental Medicine and Biology*, *726*, 93–114. https://doi.org/10.1007/978-1-4614-0980-9_5

Leung, S. S. Y., Parumasivam, T., Gao, F. G., Carter, E. A., Carrigy, N. B., Vehring, R., Finlay, W. H., Morales, S., Britton, W. J., Kutter, E., & Chan, H.-K. (2017). Effects of storage conditions on the stability of spray dried, inhalable bacteriophage powders. *International Journal of Pharmaceutics*, *521*(1–2). https://doi.org/10.1016/j.ijpharm.2017.01.060

Leung, V., Szewczyk, A., Chau, J., Hosseinidoust, Z., Groves, L., Hawsawi, H., Anany, H., Griffiths, M. W., Ali, M. M., & Filipe, C. D. M. (2017). Long-Term Preservation of Bacteriophage Antimicrobials Using Sugar Glasses. *ACS Biomaterials Science & Engineering*, *4*(11), 3802–3808. https://doi.org/10.1021/acsbiomaterials.7b00468

Leung, V., Szewczyk, A., Chau, J., Hosseinidoust, Z., Groves, L., Hawsawi, H., Anany, H., Griffiths, M. W., Monsur Ali, M., & Filipe, C. D. M. (2018). Long-Term Preservation of Bacteriophage Antimicrobials Using Sugar Glasses. *ACS Biomaterials Science and Engineering*.

https://doi.org/10.1021/acsbiomaterials.7b00468

Lewis, C. L., Craig, C. C., & Senecal, A. G. (2014). Mass and Density Measurements of Live and Dead Gram-Negative and Gram-Positive Bacterial Populations. *Applied and Environmental Microbiology*, *80*(12), 3622–3631. https://doi.org/10.1128/AEM.00117-14

Lindner, M., Rodler, N., Jesdinszki, M., Schmid, M., & Sängerlaub, S. (2018). Surface energy of corona treated PP, PE and PET films, its alteration as function of storage time and the effect of various corona dosages on their bond strength after lamination. *Journal of Applied Polymer Science*, *135*(11), 1–9. https://doi.org/10.1002/app.45842

Litt, P. K., & Jaroni, D. (2017). Isolation and Physiomorphological Characterization of *Escherichia coli* O157:H7-Infecting Bacteriophages Recovered from Beef Cattle Operations. *International Journal of Microbiology*, *2017*. https://doi.org/10.1155/2017/7013236

Liu, J., He, B., Chen, Q., Li, J., Xiong, Q., Yue, G., Zhang, X., Yang, S., Liu, H., & Liu, Q. H. (2016). Direct synthesis of hydrogen peroxide from plasma-water interactions. *Scientific Reports*, *6*. https://doi.org/10.1038/srep38454

Liu, S., Hon, K., Bouras, G. S., Psaltis, A. J., Shearwin, K., Wormald, P.-J., & Vreugde, S. (2022). APTC-C-SA01: A Novel Bacteriophage Cocktail Targeting Staphylococcus aureus and MRSA Biofilms. *International Journal of Molecular Sciences*, *23*(11), 6116. https://doi.org/10.3390/ijms23116116

Liu, X., Yao, H., Zhao, X., & Ge, C. (2023). Biofilm Formation and Control of Foodborne Pathogenic Bacteria. *Molecules*, *28*(6), 2432. https://doi.org/10.3390/molecules28062432

Łobocka, M. B., Głowacka, A., & Golec, P. (2018). Methods for Bacteriophage Preservation. In J. Azaredo & S. Sillankorva (Eds.), *Bacteriophage Therapy* (Vol. 1693). Humana Press. https://doi.org/10.1007/978-1-4939-7395-8_17

Lorenzo, J. M., Munekata, P. E., Dominguez, R., Pateiro, M., Saraiva, J. A., & Franco, D. (2018). Main Groups of Microorganisms of Relevance for Food Safety and Stability. In *Innovative Technologies for Food Preservation* (pp. 53–107). Elsevier. https://doi.org/10.1016/B978-0-12-811031-7.00003-0

Lu, Q., Wang, H., Li, L., & Chu, P. (2010). The surface properties modification of polyethylene by enhanced glow discharge plasma immersion ion implantation. *INEC 2010 - 2010 3rd International Nanoelectronics Conference, Proceedings*, 1100–1101. https://doi.org/10.1109/INEC.2010.5425012

Lubkowski, J., Hennecke, F., Plückthun, A., & Wlodawer, A. (1999). Filamentous phage infection: Crystal structure of g3p in complex with its coreceptor, the C-terminal domain of TolA. *Structure*, *7*(6), 711–722. https://doi.org/10.1016/S0969-2126(99)80092-6

Ly-Chatain, M. H. (2014). The factors affecting effectiveness of treatment in phages therapy. *Frontiers in Microbiology*, *5*, 51. https://doi.org/10.3389/fmicb.2014.00051

Ma, C., Nikiforov, A., De Geyter, N., Morent, R., & Ostrikov, K. (Ken). (2022). Plasma for biomedical decontamination: from plasma-engineered to plasma-active antimicrobial surfaces. *Current Opinion in Chemical Engineering*, *36*, 100764. https://doi.org/10.1016/j.coche.2021.100764

Ma, Y., Yang, W., Xia, Y., Xue, W., Wu, H., Li, Z., Zhang, F., Qiu, B., & Fu, C. (2022). Properties and Applications of Intelligent Packaging Indicators for Food Spoilage. *Membranes*, *12*(5), 477. https://doi.org/10.3390/membranes12050477

Malik, D. J., Sokolov, I. J., Vinner, G. K., Mancuso, F., Cinquerrui, S., Vladisavljevic, G. T., Clokie, M. R. J., Garton, N. J., Stapley, A. G. F., & Kirpichnikova, A. (2017a). Formulation, stabilisation and encapsulation of bacteriophage for phage therapy. *Advances in Colloid and Interface Science*, *249*(March), 100–133. https://doi.org/10.1016/j.cis.2017.05.014

Malik, D. J., Sokolov, I. J., Vinner, G. K., Mancuso, F., Cinquerrui, S., Vladisavljevic, G. T., Clokie, M. R. J., Garton, N. J., Stapley, A. G. F., & Kirpichnikova, A. (2017b). Formulation, stabilisation and encapsulation

of bacteriophage for phage therapy. In *Advances in Colloid and Interface Science* (Vol. 249, pp. 100–133). Elsevier B.V. https://doi.org/10.1016/j.cis.2017.05.014

Manbua, N., Suteewong, T., & Sae-Ueng, U. (2022). Efficacy of sugar excipients on lyophilized C22 phage infectivity evaluated by atomic force microscopy. *Biological Control*, *170*, 104922. https://doi.org/10.1016/j.biocontrol.2022.104922

Mangin, P. J., Jabrane, T., Jeaidi, J., & Dubé, M. (2008). Gravure printing of enzymes and phages. In *Advances in Printing and Media Technology* (Vol. 35). https://www.researchgate.net/publication/228500923

Martin, L., Bilek, M. M., Weiss, A. S., & Kuyucak, S. (2016). Force fields for simulating the interaction of surfaces with biological molecules. *Interface Focus*, *6*(1). https://doi.org/10.1098/rsfs.2015.0045

Martin, L. J., Akhavan, B., & Bilek, M. M. M. (2018). Electric fields control the orientation of peptides irreversibly immobilized on radical-functionalized surfaces. *Nature Communications*. https://doi.org/10.1038/s41467-017-02545-6

Martínez-Negro, M., Russo, D., Prévost, S., Teixeira, J., Morsbach, S., & Landfester, K. (2022). Poly(ethylene glycol)-Based Surfactant Reduces the Conformational Change of Adsorbed Proteins on Nanoparticles. *Biomacromolecules*, *23*(10), 4282–4288. https://doi.org/10.1021/acs.biomac.2c00744

Martínez, B., García, P., & Rodríguez, A. (2019). Swapping the roles of bacteriocins and bacteriophages in food biotechnology. *Current Opinion in Biotechnology*, *56*, 1–6. https://doi.org/10.1016/j.copbio.2018.07.007

Marton, H. L., Styles, K. M., Kilbride, P., Sagona, A. P., & Gibson, M. I. (2021). Polymer-Mediated Cryopreservation of Bacteriophages. *Biomacromolecules*, *22*(12), 5281–5289. https://doi.org/10.1021/acs.biomac.1c01187

Marvin, D. A., Symmons, M. F., & Straus, S. K. (2014). Structure and assembly of filamentous bacteriophages. *Progress in Biophysics and Molecular Biology*, *114*(2), 80–122. https://doi.org/10.1016/j.pbiomolbio.2014.02.003

Maulois, M., Ribière, M., Eichwald, O., Yousfi, M., & Azaïs, B. (2016). Chemical kinetics and relaxation of non-equilibrium air plasma generated by energetic photon and electron beams. *Physics of Plasmas*, *23*(4). https://doi.org/10.1063/1.4944923

McClaren, D. (1954). ADSORPTION AND REACTIONS OF Enyzymes and Proteins ON KAOLINITE. *Journal of Physical Chemistry*, *58*(2), 129–137. https://doi.org/10.1021/j150512a008

Mckean, L. (2017). Production of Films, Containers, and Membranes. In *Permeability Properties of Plastics and Elastomers* (4th ed., pp. 41–60). Elsevier.

Mensink, M. A., Frijlink, H. W., van der Voort Maarschalk, K., & Hinrichs, W. L. J. (2017). How sugars protect proteins in the solid state and during drying (review): Mechanisms of stabilization in relation to stress conditions. *European Journal of Pharmaceutics and Biopharmaceutics*, *114*, 288–295. https://doi.org/10.1016/j.ejpb.2017.01.024

Mindich, L., & Lehman, J. (1979). Cell Wall Lysin as a Component of the Bacteriophage c6 Virion. *JOURNAL OF VIROLOGY*, *30*(2), 489–496.

Mira, P., Yeh, P., & Hall, B. G. (2022). Estimating microbial population data from optical density. *PLoS ONE*, *17*(10 October). https://doi.org/10.1371/journal.pone.0276040

Moak, M., & Molineux, I. J. (2004). Peptidoglycan hydrolytic activities associated with bacteriophage virions. *Molecular Microbiology*, *51*(4), 1169–1183. https://doi.org/10.1046/j.1365-2958.2003.03894.x

Moghimian, P., Srot, V., Pichon, B. P., Facey, S. J., & Aken, P. A. van. (2016). Stability of M13 Phage in Organic Solvents. *Journal of Biomaterials and Nanobiotechnology*, *7*(2). https://doi.org/10.4236/jbnb.2016.72009

Moghtader, F., Tomak, A., Zareie, H. M., & Piskin, E. (2018). Bacterial detection using bacteriophages and gold

nanorods by following time-dependent changes in Raman spectral signals. *Artificial Cells, Nanomedicine and Biotechnology*, *46*(2), 122–120. https://doi.org/10.1080/21691401.2018.1452251

Mohamad, N. R., Marzuki, N. H. C., Buang, N. A., Huyop, F., & Wahab, R. A. (2015). An overview of technologies for immobilization of enzymes and surface analysis techniques for immobilized enzymes. *Biotechnology and Biotechnological Equipment*, *29*(2), 205–220. https://doi.org/10.1080/13102818.2015.1008192

Molineux, I. J. (2001). No syringes please, ejection of phage T7 DNA from the virion is enzyme driven. *Molecular Microbiology*, *40*(1), 1–8. https://doi.org/10.1046/j.1365-2958.2001.02357.x

Monk, A. B., Rees, C. D., Barrow, P., Hagens, S., & Harper, D. R. (2010). Bacteriophage applications: Where are we now? *Letters in Applied Microbiology*, *51*(4), 363–369. https://doi.org/10.1111/j.1472-765X.2010.02916.x

Montag, D., Riede, I., Eschbach, M. L., Degen, M., & Henning, U. (1987). Receptor-recognizing proteins of T-even type bacteriophages. Constant and hypervariable regions and an unusual case of evolution. *Journal of Molecular Biology*, *196*(1), 165–174. https://doi.org/10.1016/0022-2836(87)90519-5

Morent, R., De Geyter, N., Leys, C., Gengembre, L., & Payen, E. (2008). Comparison between XPS- And FTIR-analysis of plasma-treated polypropylene film surfaces. *Surface and Interface Analysis*. https://doi.org/10.1002/sia.2619

Mozetič, M. (2023). Aging of Plasma-Activated Polyethylene and Hydrophobic Recovery of Polyethylene Polymers. *Polymers*, *15*(24), 4668. https://doi.org/10.3390/polym15244668

Naidoo, R., Singh, A., Arya, S. K., Beadle, B., Glass, N., Tanha, J., Szymanski, C. M., & Evoy, S. (2012). Surface-immobilization of chromatographically purified bacteriophages for the optimized capture of bacteria. *Bacteriophage*, *2*(1), 15–24. https://doi.org/10.4161/bact.19079

Natyanun, S., & Pussadee, N. (2018). Hydrophobicity Recovery of Polydimethylsiloxane Treated with Oxygen Plasma and Ion Implantation. *Journal of Physics: Conference Series*, *1144*(1). https://doi.org/10.1088/1742-6596/1144/1/012110

Nogueira, F., Karumidze, N., Kusradze, I., Goderdzishvili, M., Teixeira, P., & Gouveia, I. C. (2017). Immobilization of bacteriophage in wound-dressing nanostructure. *Nanomedicine: Nanotechnology, Biology, and Medicine*, *13*(8), 2475–2484. https://doi.org/10.1016/j.nano.2017.08.008

Novák, I., Pollák, V., & Chodák, I. (2006). Study of Surface Properties of Polyolefins Modified by Corona Discharge Plasma. *Plasma Processes and Polymers*, *3*(4–5), 355–364. https://doi.org/10.1002/ppap.200500163

Novello, J., Sillankorva, S., Pires, P., Azeredo, J., Wanke, C. H., Tondo, E. C., & Bianchi, O. (2020). Inactivation of Pseudomonas aeruginosa in mineral water by DP1 bacteriophage immobilized on ethylene-vinyl acetate copolymer used as seal caps of plastic bottles. *Journal of Applied Polymer Science*, *137*(35). https://doi.org/10.1002/app.49009

O'Hare, L. A., Leadley, S., & Parbhoo, B. (2002). Surface physicochemistry of corona-discharge-treated polypropylene film. *Surface and Interface Analysis*. https://doi.org/10.1002/sia.1217

Oechslin, F. (2018). Resistance Development to Bacteriophages Occurring during Bacteriophage Therapy. *Viruses*, *10*(7), 351. https://doi.org/10.3390/v10070351

Ogodo, A. C., Agwaranze, D. I., Daji, M., & Aso, R. E. (2022). Microbial techniques and methods: Basic techniques and microscopy. In *Analytical Techniques in Biosciences: from Basics to Applications* (pp. 201–220). Elsevier. https://doi.org/10.1016/B978-0-12-822654-4.00003-8

Ohtake, S., Kita, Y., & Arakawa, T. (2011). Interactions of formulation excipients with proteins in solution and in the dried state. In *Advanced Drug Delivery Reviews* (Vol. 63, Issue 13, pp. 1053–1073). https://doi.org/10.1016/j.addr.2011.06.011

Olia, A. S., Al-Bassam, J., Winn-Stapley, D. A., Joss, L., Casjens, S. R., & Cingolani, G. (2006). Binding-induced Stabilization and Assembly of the Phage P22 Tail Accessory Factor Gp4. *Journal of Molecular Biology*, *363*(2), 558–576. https://doi.org/10.1016/j.jmb.2006.08.014

Oliveira, J., Mahony, J., Hanemaaijer, L., Kouwen, T. R. H. M., Neve, H., MacSharry, J., & van Sinderen, D. (2017). Detecting Lactococcus lactis prophages by mitomycin C-mediated induction coupled to flow cytometry analysis. *Frontiers in Microbiology*, *8*, 1–11. https://doi.org/10.3389/fmicb.2017.01343

Olofsson, L., Ankarloo, J., Andersson, P. O., & Nicholls, I. A. (2001). Filamentous bacteriophage stability in non-aqueous media. *Chemistry & Biology*, *8*(7). https://doi.org/10.1016/S1074-5521(01)00041-2

Olsson, A. L. J., Wargenau, A., & Tufenkji, N. (2016). Optimizing Bacteriophage Surface Densities for Bacterial Capture and Sensing in Quartz Crystal Microbalance with Dissipation Monitoring. *ACS Applied Materials and Interfaces*, *8*(22), 13698–13706. https://doi.org/10.1021/acsami.6b02227

Ong, E., Gilkes, N. R., Antony, R., Warren, J., Miller, R. C., & Kilburn, D. G. (1989). Enzyme immobilization using the cellulose-binding domain of a cellulomonas fimiexoglucanase. *Bio/Technology*, *7*, 604–607. https://doi.org/10.1038/nbt0689-604

Osei, R., Yang, C., Cui, L., Ma, T., Li, Z., & Boamah, S. (2022). Isolation, identification, and pathogenicity of Lelliottia amnigena causing soft rot of potato tuber in China. *Microbial Pathogenesis*, *164*, 105441. https://doi.org/10.1016/j.micpath.2022.105441

Parfitt, T. (2005). *Georgia: an unlikely stronghold for bacteriophage therapy*. https://www.thelancet.com/action/showPdf?pii=S0140-6736%2805%2966759-1

Park, S.-J., & Jin, J.-S. (2001). Effect of Corona Discharge Treatment on the Dyeability of Low-Density Polyethylene Film. *Journal of Colloid and Interface Science*, *236*(1), 155–160. https://doi.org/10.1006/jcis.2000.7380

Park, S., & Nakai, T. (2003). Bacteriophage control of Pseudomonas plecoglossicida infection in ayu, Plectoglossis altivelis. *Diseases of Aquatic Organisms*, *53*, 33–39. https://doi.org/10.3354/dao053033

Parlapani, F. F., Mallouchos, A., Haroutounian, S. A., & Boziaris, I. S. (2017). Volatile organic compounds of microbial and non-microbial origin produced on model fish substrate un-inoculated and inoculated with gilt-head sea bream spoilage bacteria. *LWT*, *78*, 54–62. https://doi.org/10.1016/j.lwt.2016.12.020

Pavlovich, M. J., Clark, D. S., & Graves, D. B. (2014). Quantification of air plasma chemistry for surface disinfection. *Plasma Sources Science and Technology*, *23*(6). https://doi.org/10.1088/0963-0252/23/6/065036

Pearson, H. A., Sahukhal, G. S., Elasri, M. O., & Urban, M. W. (2013). Phage-bacterium war on polymeric surfaces: Can surface-anchored bacteriophages eliminate microbial infections? *Biomacromolecules*, *14*(5), 1257–1261. https://doi.org/10.1021/bm400290u

Peek, & F W. (1915). Dielectric Phenomena in High Voltage Engineering. In *McGraw-Hill Book Company* (pp. 38–78).

Pegalajar-Jurado, A., Easton, C. D., Styan, K. E., & McArthur, S. L. (2014). Antibacterial activity studies of plasma polymerised cineole films. *Journal of Materials Chemistry B*, *2*(31), 4993–5002. https://doi.org/10.1039/c4tb00633j

Peng, B., Liu, N., Lin, Y., Wang, L., Zhang, W., Niu, Z., Wang, Q., & Su, Z. (2011). Self-assembly of anisotropic tobacco mosaic virus nanoparticles on gold substrate. *Science China Chemistry*, *54*(1), 137–143. https://doi.org/10.1007/s11426-010-4177-7

Pickard, D., Toribio, A. L., Petty, N. K., Van Tonder, A., Yu, L., Goulding, D., Barrell, B., Rance, R., Harris, D., Wetter, M., Wain, J., Choudhary, J., Thomson, N., & Dougan, G. (2010). A conserved acetyl esterase domain targets diverse bacteriophages to the Vi capsular receptor of Salmonella enterica serovar typhi. *Journal of Bacteriology*, *192*(21), 5746–5754. https://doi.org/10.1128/JB.00659-10

Pignata, C., D'Angelo, D., Fea, E., & Gilli, G. (2017). A review on microbiological decontamination of fresh produce with nonthermal plasma. *Journal of Applied Microbiology*, *122*(6), 1438–1455. https://doi.org/10.1111/jam.13412

Pinto, F., Maillard, J. Y., Denyer, S. P., & McGeechan, P. (2010). Polyhexamethylene biguanide exposure leads to viral aggregation. *Journal of Applied Microbiology*, *108*(6), 1880–1888. https://doi.org/10.1111/j.1365-2672.2009.04596.x

Ploss, M., & Kuhn, A. (2010). Kinetics of filamentous phage assembly. *Physical Biology*, *7*(4). https://doi.org/10.1088/1478-3975/7/4/045002

Polymer Properties Database. (2015). *No Title*. https://polymerdatabase.com/polymer physics/sigma.html

Qiu, Y., Zhou, Y., Chang, Y., Liang, X., Zhang, H., Lin, X., Qing, K., Zhou, X., & Luo, Z. (2022). The Effects of Ventilation, Humidity, and Temperature on Bacterial Growth and Bacterial Genera Distribution. *International Journal of Environmental Research and Public Health*, *19*(22), 15345. https://doi.org/10.3390/ijerph192215345

Radford, D., Guild, B., Strange, P., Ahmed, R., Lim, L.-T., & Balamurugan, S. (2017). Characterization of antimicrobial properties of Salmonella phage Felix O1 and Listeria phage A511 embedded in xanthan coatings on Poly(lactic acid) films. *Food Microbiology*, *66*, 117–128. https://doi.org/10.1016/j.fm.2017.04.015

Ramirez, J. C. C., & Tumolva, T. P. (2018). Analysis and optimization of water-based printing ink formulations for polyethylene films. *Applied Adhesion Science*, *6*(1), 1–21. https://doi.org/10.1186/s40563-017-0102-z

Raposo, A., Pérez, E., de Faria, C. T., Ferrús, M. A., & Carrascosa, C. (2016). Food Spoilage by Pseudomonas spp.— An Overview. In *Foodborne Pathogens and Antibiotic Resistance* (pp. 41–71). Wiley. https://doi.org/10.1002/9781119139188.ch3

Raya, R. R., Oot, R. A., Moore-Maley, B., Wieland, S., Callaway, T. R., Kutter, E. M., & Brabban, A. D. (2011). Naturally resident and exogenously applied T4-like and T5-like bacteriophages can reduce Escherichia coli O157:H7 levels in sheep guts. *Bacteriophage*, *1*(1), 15–24. https://doi.org/10.4161/bact.1.1.14175

Recek, N., Jaganjac, M., Kolar, M., Milkovic, L., Mozetič, M., Stana-Kleinschek, K., & Vesel, A. (2013). Protein adsorption on various plasma-treated polyethylene terephthalate substrates. *Molecules*, *18*(10), 12441–12463. https://doi.org/10.3390/molecules181012441

Řepka, D., Kurillová, A., Murtaja, Y., & Lapčík, L. (2023). Application of Physical-Chemical Approaches for Encapsulation of Active Substances in Pharmaceutical and Food Industries. *Foods*, *12*(11), 2189. https://doi.org/10.3390/foods12112189

Repka, D., Kurillova, A., Murtaya, Y., & Lapcik, L. (2020). Preparation of Model Protein-Loaded PLGA Microparticles Using Lutensol XL 80 Emulsifier. *Pharmaceutical Frontiers*, *2*. https://doi.org/10.20900/pf20200001

Richter, Ł., Bielec, K., Leśniewski, A., Łoś, M., Paczesny, J., & Hołyst, R. (2017). Dense Layer of Bacteriophages Ordered in Alternating Electric Field and Immobilized by Surface Chemical Modification as Sensing Element for Bacteria Detection. *ACS Applied Materials and Interfaces*, *9*(23), 19622–19629. https://doi.org/10.1021/acsami.7b03497

Risikat, A., Abdulmumeen, H. A., Risikat, A. N., & Sururah, A. R. (2012). Food: Its preservatives, additives and applications. *IJCBS*, *1*, 36–47. https://doi.org/10.13140/2.1.1623.5208

Roach, D. R., & Donovan, D. M. (2015). Antimicrobial bacteriophage-derived proteins and therapeutic applications. *Bacteriophage*, *5*(3), e1062590. https://doi.org/10.1080/21597081.2015.1062590

Rodríguez-Rubio, L., Gutiérrez, D., Donovan, D. M., Martínez, B., Rodríguez, A., & García, P. (2016). Phage lytic proteins: Biotechnological applications beyond clinical antimicrobials. *Critical Reviews in Biotechnology*, *36*(3), 542–552. https://doi.org/10.3109/07388551.2014.993587

Rodríguez-Rubio, L., Martínez, B., Donovan, D. M., Rodríguez, A., & García, P. (2013). Bacteriophage virion-associated peptidoglycan hydrolases: Potential new enzybiotics. *Critical Reviews in Microbiology*, *39*(4), 427–434. https://doi.org/10.3109/1040841X.2012.723675

Rodríguez-Rubio, L., Martínez, B., Rodríguez, A., Donovan, D. M., Götz, F., & García, P. (2013). The Phage Lytic Proteins from the Staphylococcus aureus Bacteriophage vB_SauS-phiIPLA88 Display Multiple Active Catalytic Domains and Do Not Trigger Staphylococcal Resistance. *PLoS ONE*, *8*(5). https://doi.org/10.1371/journal.pone.0064671

Rosenberg, M. (2006). Microbial adhesion to hydrocarbons: Twenty-five years of doing MATH. *FEMS Microbiology Letters*, *262*(2), 129–134. https://doi.org/10.1007/s00026-006-0278-6

Rosner, D., & Clark, J. (2021). Formulations for Bacteriophage Therapy and the Potential Uses of Immobilization. *Pharmaceuticals*, *14*(4), 359. https://doi.org/10.3390/ph14040359

Rossmann, M. G., Morais, M. C., Leiman, P. G., & Zhang, W. (2005). Combining X-ray crystallography and electron microscopy. *Structure*, *13*(3), 355–362. https://doi.org/10.1016/j.str.2005.01.005

Rudra, S. G., Basu, S., & Chanda, A. (2022). Editorial: Food storage, spoilage and shelf life: Recent developments and insights. *Frontiers in Sustainable Food Systems*, *6*. https://doi.org/10.3389/fsufs.2022.953983

Salmond, G. P. C., & Fineran, P. C. (2015). A century of the phage: Past, present and future. *Nature Reviews Microbiology*, *13*(12), 777–786. https://doi.org/10.1038/nrmicro3564

Santos Gomes, B., Morgan, D. J., Langbein, W., Borri, P., & Masia, F. (2022). Biofunctionalisation of gallium arsenide with neutravidin. *Journal of Colloid and Interface Science*, *608*, 2399–2406. https://doi.org/10.1016/j.jcis.2021.10.135

Sason, E., Kolitz-Domb, M., Chill, J. H., & Margel, S. (2019). Engineering of Durable Antifog Thin Coatings on Plastic Films by UV-Curing of Proteinoid Prepolymers with PEG-Diacrylate Monomers. *ACS Omega*, *4*(5), 9352–9360. https://doi.org/10.1021/acsomega.9b00336

Sassolas, A., Blum, L. J., & Leca-Bouvier, B. D. (2012). Immobilization strategies to develop enzymatic biosensors. In *Biotechnology Advances*. https://doi.org/10.1016/j.biotechadv.2011.09.003

Sausset, R., Krupova, Z., Guédon, E., Peron, S., Grangier, A., Petit, M., De Sordi, L., & De Paepe, M. (2023). Comparison of interferometric light microscopy with nanoparticle tracking analysis for the study of extracellular vesicles and bacteriophages. *Journal of Extracellular Biology*, *2*(2). https://doi.org/10.1002/jex2.75

Schuch, R., Nelson, D., & Fischetti, V. A. (2002). A bacteriolytic agent that detects and kills Bacillus anthracis. *Nature*, *418*(6900), 884–889. https://doi.org/10.1038/nature01026 Full-text links

Serwer, P., Hayes, S. J., Lieman, K., & Griess, G. A. (2007). In situ fluorescence microscopy of bacteriophage aggregates. *Journal of Microscopy*, *228*(3), 309–321. https://doi.org/10.1111/j.1365-2818.2007.01855.x

Shin, H., Lee, J. H., Kim, H., Choi, Y., Heu, S., & Ryu, S. (2012). Receptor diversity and host interaction of bacteriophages infecting Salmonella enterica Serovar Typhimurium. *PLoS ONE*, *7*(8). https://doi.org/10.1371/journal.pone.0043392

Silhavy, T. J., Kahne, D., & Walker, S. (2010). The bacterial cell envelope. In *Cold Spring Harbor perspectives in biology* (Vol. 2, Issue 5). https://doi.org/10.1101/cshperspect.a000414

Silva, Y. J., Costa, L., Pereira, C., Cunha, Â., Calado, R., Gomes, N. C. M., & Almeida, A. (2014). Influence of environmental variables in the efficiency of phage therapy in aquaculture. *Microbial Biotechnology*, *7*(5). https://doi.org/10.1111/1751-7915.12090

Singh, A., Glass, N., Tolba, M., Brovko, L., Griffiths, M., & Evoy, S. (2009). Immobilization of bacteriophages on gold surfaces for the specific capture of pathogens. *Biosensors and Bioelectronics*, *24*(12), 3645–3651.

https://doi.org/10.1016/j.bios.2009.05.028

Sinha, S., Rajdeep, K. G., & Soumen, R. (2018). Modeling Bacteria–Phage Interactions and Its Implications for Phage Therapy. In S. Sariaslani & G. M. Gadd (Eds.), *Advances in Applied Microbiology* (pp. 103–141). https://doi.org///doi.org/10.1016/bs.aambs.2018.01.005.

Siringan, P., Connerton, P. L., Payne, R. J. H., & Connerton, I. F. (2011). Bacteriophage-Mediated Dispersal of Campylobacter jejuni Biofilms. *Applied and Environmental Microbiology*, *77*(10), 3320–3326. https://doi.org/10.1128/aem.02704-10

Smietana, M., Bock, W. J., Mikulic, P., Ng, A., Chinnappan, R., Zourob, M., Zourob, M., Mohr, S., Brown, B. J., Fielden, P. R., McDonnell, M. B., Goddard, N. J., Taylor, A. D., Yu, Q., Chen, S., Homola, J., Jiang, S., Van Dorst, B., Mehta, J., … Robbens, J. (2005). Detection of bacteria using bacteriophages as recognition elements immobilized on long-period fiber gratings. *Sens. Actuators B Chem*, *107*(1), 202–208.

Smith, G. P. (1985). Filamentous Fusion Phage: Novel Expression Vectors that Display Cloned Antigens on the. *New Series*, *228*(4705), 1315–1317.

Snoeck, N., De Mol, M. L., Van Herpe, D., Goormans, A., Maryns, I., Coussement, P., Peters, G., Beauprez, J., De Maeseneire, S. L., & Soetaert, W. (2019). Serine integrase recombinational engineering (SIRE): A versatile toolbox for genome editing. *Biotechnology and Bioengineering*, *116*(2), 364–374. https://doi.org/10.1002/bit.26854

Spyridakis, I., Tzanakakis, V. A., Pashalidis, I., Kalderis, D., & Anastopoulos, I. (2022). Polyamide nylon 6 as a potential carrier of nitrate anions in aqueous environments. *Journal of Molecular Liquids*, *352*, 118706. https://doi.org/10.1016/j.molliq.2022.118706

Stishkov, Y. K., Samusenko, A. V., & Ashikhmin, I. A. (2018). Corona discharge and electrogasdynamic flows in the air. *Uspekhi Fizicheskih Nauk*, *188*(12), 1331–1345. https://doi.org/10.3367/ufnr.2018.06.038358

Sutherland, I., Popat, R. P., Brewis, D. M., & Calder, R. (1994). Corona discharge treatment of polyolefins. *The Journal of Adhesion*, *46*(1–4), 79–88. https://doi.org/10.1080/00218469408026651

Svircev, A., Roach, D., & Castle, A. (2018). Framing the future with bacteriophages in agriculture. *Viruses*, *10*(5), 1–13. https://doi.org/10.3390/v10050218

Szentgyörgyvölgyi, R. (2016). Gravure Printing. In J. Izdebska & S. Thomas (Eds.), *Printing on Polymers Fundamentals and Applications* (pp. 199–215). William Andrew. https://doi.org/https://doi.org/10.1016/C2014-0-02411-2

Tabaniag, J. S. U., Abad, M. Q. D., Morcelos, C. J. R., Geraldino, G. V. B., Alvarado, J. L. M., & Lopez, E. C. R. (2023). Stabilization of oil/water emulsions using soybean lecithin as a biobased surfactant for enhanced oil recovery. *Journal of Engineering and Applied Science*, *70*(1), 154. https://doi.org/10.1186/s44147-023-00322-5

Tåg, C.-M., Toiviainen, M., Juuti, M., Rosenholm, J. B., Backfolk, K., & Gane, P. A. C. (2012). The Effect of Isopropyl Alcohol and Non-Ionic Surfactant Mixtures on the Wetting of Porous Coated Paper. *Transport in Porous Media*, *94*(1), 225–242. https://doi.org/10.1007/s11242-012-0001-5

Taj, M. K., Ling, J. X., Bing, L. L., Qi, Z., Taj, I., Hassani, T. M., Samreen, Z., & Yunlin, W. (2014). Effect of dilution, temperature and pH on the lysis activity of T4 phage against E. coli BL21. *Journal of Animal and Plant Sciences*, *24*(4), 1252–1255.

Takamatsu, T., Uehara, K., Sasaki, Y., Miyahara, H., Matsumura, Y., Iwasawa, A., Ito, N., Azuma, T., Kohno, M., & Okino, A. (2014). Investigation of reactive species using various gas plasmas. *RSC Advances*, *4*(75), 39901–39905. https://doi.org/10.1039/c4ra05936k

Tawil, N., Sacher, E., Mandeville, R., & Meunier, M. (2013). Strategies for the immobilization of bacteriophages on gold surfaces monitored by surface plasmon resonance and surface morphology. *Journal of Physical Chemistry C*, *117*(13), 6689–6691. https://doi.org/10.1021/jp400565m

Thissen, H. (2015). Plasma-based surface modification for the control of biointerfacial interactions. In *Biosynthetic Polymers for Medical Applications* (pp. 129–144). Elsevier Inc. https://doi.org/10.1016/B978-1-78242-105-4.00005-5

Timoshkin, I. V., MacGregor, S. J., Given, M. J., Beveridge, J. R., & Lehr, J. M. (2008). Dynamic characteristics of corona discharges in point-plane electrode topologies influenced by space charge. *Proceedings of the 2008 IEEE International Power Modulators and High Voltage Conference, PMHVC*, 495–498. https://doi.org/10.1109/IPMC.2008.4743699

Tolba, M., Minikh, O., Brovko, L. Y., Evoy, S., & Griffiths, M. W. (2010). Oriented immobilization of bacteriophages for biosensor applications. *Applied and Environmental Microbiology*, *76*(2), 528–535. https://doi.org/10.1128/AEM.02294-09

Tovkach, F., Zhuminska, G., & Khushkina, A. (2012). Long-term preservation of unstable bacteriophages of enterobacteria. *Mīkrobiologīchniĭ Zhurnal*, *74*, 60–66.

Tran, C. T. H., Craggs, M., Smith, L. M., Stanley, K., Kondyurin, A., Bilek, M. M., & McKenzie, D. R. (2016). Covalent linker-free immobilization of conjugatable oligonucleotides on polypropylene surfaces. *RSC Advances*, *6*, 83328–83336. https://doi.org/10.1039/c6ra16034d

Tran, C. T. H., Nosworthy, N., Bilek, M. M. M., & McKenzie, D. R. (2015). Covalent immobilization of enzymes and yeast: Towards a continuous simultaneous saccharification and fermentation process for cellulosic ethanol. *Biomass and Bioenergy*, *81*, 234–241. https://doi.org/10.1016/j.biombioe.2015.07.009

Turner, D., Shkoporov, A. N., Lood, C., Millard, A. D., Dutilh, B. E., Alfenas-Zerbini, P., van Zyl, L. J., Aziz, R. K., Oksanen, H. M., Poranen, M. M., Kropinski, A. M., Barylski, J., Brister, J. R., Chanisvili, N., Edwards, R. A., Enault, F., Gillis, A., Knezevic, P., Krupovic, M., … Adriaenssens, E. M. (2023). Abolishment of morphology-based taxa and change to binomial species names: 2022 taxonomy update of the ICTV bacterial viruses subcommittee. *Archives of Virology*, *168*(2), 74. https://doi.org/10.1007/s00705-022-05694-2

Tytgat, H. L. P., Schoofs, G., Driesen, M., Proost, P., Van Damme, E. J. M., Vanderleyden, J., & Lebeer, S. (2015). Endogenous biotin-binding proteins: An overlooked factor causing false positives in streptavidin-based protein detection. *Microbial Biotechnology*, *8*(1), 164–168. https://doi.org/10.1111/1751-7915.12150

Vagenende, V., Yap, M. G. S., & Trout, B. L. (2009). Mechanisms of Protein Stabilization and Prevention of Protein Aggregation by Glycerol. *Biochemistry*, *48*(46). https://doi.org/10.1021/bi900649t

Van Voorthuizen, E. M., Ashbolt, N. J., & Schäfer, A. I. (2001). Role of hydrophobic and electrostatic interactions for initial enteric virus retention by MF membranes. *Journal of Membrane Science*, *194*(1), 69–79. https://doi.org/10.1016/S0376-7388(01)00522-1

Vandenberghe, J., Thompson, F. L., Gomez-Gil, B., & Swings, J. (2003). Phenotypic diversity amongst Vibrio isolates from marine aquaculture systems. *Aquaculture*, *219*(1–4), 9–20. https://doi.org/10.1016/S0044-8486(02)00312-5

Veldhuizen, E. M. Van, & Rutgers, W. R. (2001). Corona discharges : fundamentals and diagnostics. *Frontiers in Low Temperature Plasma Diagnostics Conference; 4th, Frontiers in Low Temperature Plasma Diagnostics*, *January 2001*, 40–49.

Vonasek, E., Lu, P., Hsieh, Y. Lo, & Nitin, N. (2017). Bacteriophages immobilized on electrospun cellulose microfibers by non-specific adsorption, protein–ligand binding, and electrostatic interactions. *Cellulose*, *24*(10), 4581–4589. https://doi.org/10.1007/s10570-017-1442-3

Wagh, R. V., Priyadarshi, R., & Rhim, J.-W. (2023). Novel Bacteriophage-Based Food Packaging: An Innovative Food Safety Approach. *Coatings*, *13*(3), 609. https://doi.org/10.3390/coatings13030609

Wakelin, E. A., Kondyurin, A. V., Wise, S. G., McKenzie, D. R., Davies, M. J., & Bilek, M. M. M. (2015). Bio-activation of polyether ether ketone using plasma immersion ion implantation: A kinetic model. *Plasma Processes and Polymers*. https://doi.org/10.1002/ppap.201400149

Wang, C., Sauvageau, D., & Elias, A. (2016). Immobilization of Active Bacteriophages on Polyhydroxyalkanoate Surfaces. *ACS Applied Materials and Interfaces*, *8*(2), 1128–1138. https://doi.org/10.1021/acsami.5b08664

Wang, I.-N., Smith, D. L., & Young, R. (2000). Holins: The Protein Clocks of Bacteriophage Infections. *Annual Review of Microbiology*, *54*(1), 799–825. https://doi.org/10.1146/annurev.micro.54.1.799

Wang, J., Li, H., Li, C., Ding, Y., Wang, Y., Zhu, W., Wang, J., Shao, Y., Pan, H., & Wang, X. (2022). EIS biosensor based on a novel Myoviridae bacteriophage SEP37 for rapid and specific detection of Salmonella in food matrixes. *Food Research International*, *158*. https://doi.org/10.1016/j.foodres.2022.111479

Wang, Y., Zhao, Y., Guo, L., Han, F., & Li, X. (2022). Enhanced flotation of high density polyethylene and polyvinyl chloride mixtures based on clean corona modification. *Physics and Chemistry of the Earth, Parts A/B/C*, *128*, 103264. https://doi.org/10.1016/j.pce.2022.103264

Willmann, M., Steglich, M., Bunk, B., Peter, S., & Neher, R. A. (2017). *Rapid and Consistent Evolution of Colistin Resistance in Extensively Drug-Resistant Pseudomonas aeruginosa during Morbidostat Culture*. *61*(9), 1–16.

Wu, S., Lan, X., Zhao, W., Li, Y., Zhang, L., Wang, H., Han, M., & Tao, S. (2011). Biosensors and Bioelectronics Controlled immobilization of acetylcholinesterase on improved hydrophobic gold nanoparticle / Prussian blue modified surface for ultra-trace organophosphate pesticide detection. *Biosensors and Bioelectronics*, *27*(1), 82–87. https://doi.org/10.1016/j.bios.2011.06.020

Yahaya, E. A. (2014). Power loss due to Corona on High Voltage Transmission Lines. *IOSR Journal of Electrical and Electronics Engineering*, *8*(3), 14–19. https://doi.org/10.9790/1676-0831419

Yang, Y., Shen, W., Zhong, Q., Chen, Q., He, X., Baker, J. L., Xiong, K., Jin, X., Wang, J., Hu, F., & Le, S. (2020). Development of a Bacteriophage Cocktail to Constrain the Emergence of Phage-Resistant Pseudomonas aeruginosa. *Frontiers in Microbiology*, *11*. https://doi.org/10.3389/fmicb.2020.00327

Yang, Y., Wang, Z., Peng, X., Huang, Z., & Fang, P. (2022). Influence of Crosslinking Extent on Free Volumes of Silicone Rubber and Water Diffusion after Corona Discharge. *Materials*, *15*(19), 6833. https://doi.org/10.3390/ma15196833

Yang, Y., Wang, Z., Wang, Y., Zhang, J., Peng, X., & Fang, P. (2024). EIS study on corona discharge degradation of epoxy resin: micro-structure evaluation and water diffusion. *Journal of Materials Science: Materials in Electronics*, *35*(1). https://doi.org/10.1007/s10854-023-11755-2

Yap, M. L., & Rossmann, M. G. (2014). Structure and function of bacteriophage T4. *Future Microbiology*, *9*, 1319–1327. https://doi.org/10.2217/fmb.14.91

Yazdi, Z. R., Leaper, M. C., & Malik, D. J. (2023). The Development of Oral Solid Dosage Forms Using the Direct-Compression Tableting of Spray-Dried Bacteriophages Suitable for Targeted Delivery and Controlled Release. *Processes*, *11*(11), 3146. https://doi.org/10.3390/pr11113146

Yeo, G. C., Kondyurin, A., Kosobrodova, E., Weiss, A. S., & Bilek, M. M. M. (2017). A sterilizable, biocompatible, tropoelastin surface coating immobilized by energetic ion activation. *Journal of the Royal Society Interface*, *14*(127). https://doi.org/10.1098/rsif.2016.0837

Yoo, P. J., Nam, K. T., Qi, J., Lee, S.-K., Park, J., Belcher, A. M., & Hammond, P. T. (2006). Spontaneous assembly of viruses on multilayered polymer surfaces. *Nature Materials*, *5*(3), 234–240. https://doi.org/10.1038/nmat1596

Yu, P., Mathieu, J., Li, M., Dai, Z., & Alvarez, P. J. J. (2016). Isolation of Polyvalent Bacteriophages by Sequential Multiple-Host Approaches. *Applied and Environmental Microbiology*, *82*(3), 808–815. https://doi.org/10.1128/aem.02382-15

Zaman, S. Bin, Hussain, M. A., Nye, R., Mehta, V., Mamun, K. T., & Hossain, N. (2017). A Review on Antibiotic Resistance: Alarm Bells are Ringing. *Cureus*, *9*(6). https://doi.org/10.7759/cureus.1403

Zhang, K., Perussello, C. A., Milosavljević, V., Cullen, P. J., Sun, D.-W., & Tiwari, B. K. (2019). Diagnostics of plasma reactive species and induced chemistry of plasma treated foods. *Critical Reviews in Food Science and Nutrition*, 812–825. https://doi.org/10.1080/10408398.2018.1564731

Zhang, Y., Zhang, H., & Ghosh, D. (2020). The Stabilizing Excipients in Dry State Therapeutic Phage Formulations. In *AAPS PharmSciTech* (Vol. 21, Issue 4). Springer. https://doi.org/10.1208/s12249-020-01673-5

Zhao, J., Li, Y., Xu, L., Timira, V., Zhang, Z., Chen, G., Zhang, L., Lin, H., & Li, Z. (2022). Improved protein extraction from thermally processed shrimp (Litopenaeus vannamei) for reliable immunodetection via a synergistic effect of buffer additives. *LWT*, *154*, 112790. https://doi.org/10.1016/j.lwt.2021.112790

Zheng, H. (2023). Devitrification of lyoprotectants: A critical determinant for bacteriophages inactivation in freeze-drying and storage. *Food Research International*, *173*, 113307. https://doi.org/10.1016/j.foodres.2023.113307

Zhou, Y., Marar, A., Kner, P., & Ramasamy, R. P. (2017). Charge-Directed Immobilization of Bacteriophage on Nanostructured Electrode for Whole-Cell Electrochemical Biosensors. *Analytical Chemistry*, *89*(11), 5734–5741. https://doi.org/10.1021/acs.analchem.6b03751

Zivanovic, Y., Confalonieri, F., Ponchon, L., Lurz, R., Chami, M., Flayhan, A., Renouard, M., Huet, A., Decottignies, P., Davidson, A. R., Breyton, C., & Boulanger, P. (2014). Insights into Bacteriophage T5 Structure from Analysis of Its Morphogenesis Genes and Protein Components. *Journal of Virology*, *88*(2), 1162–1174. https://doi.org/10.1128/jvi.02262-13

Zurabov, F., Glazunov, E., Kochetova, T., Uskevich, V., & Popova, V. (2023). Bacteriophages with depolymerase activity in the control of antibiotic resistant Klebsiella pneumoniae biofilms. *Scientific Reports*, *13*(1). https://doi.org/10.1038/s41598-023-42505-3

# APPENDIX A

**Corona discharge**

Corona discharge was originally characterised as an undesired phenomenon, emitted from high conductors used for industrial applications. This was due to side effects such as power loss, radio interference and harmful ozone gas (Chang *et al*., 1991; Chen & Davidson, 2003; Yahaya, 2014). Ways of reducing or stopping corona discharge include the use of corona rings, increasing conductor area as well as increasing the distance between two electrodes. Aside from being an undesired biproduct, corona discharge has several industrial applications including the manufacture of ozone, air ionization and increasing the altering of polymeric surfaces (Chang *et al*., 1991). Despite its low power when compared with other plasma techniques, corona discharge treatment is relatively cheap to carry out and allows for larger coverage area.

**Generation of Corona Discharge Plasma**

Corona discharge arises from the ionisation of air surrounding an electrically charged electrode, termed the 'corona source'. This occurs when the electric field of a conductor exceeds its 'critical energy' ($E_{cr}$). Following this, free ions are accelerated through the nearby air, producing more ions through collisions with atoms and molecules. Corona discharge initiates when ionic saturation is reached. This is the total kinetic energy of the moving ions needed ionic saturation. In the case of coaxial electrodes, this critical point be defined using Peek's formula (Peek, 1915):

$$E_{cr} = m_v g_v r ln\left(\frac{S}{r}\right)$$

where $E_{cr}$ is the critical voltage, $m_v$ is the electrode smoothness ratio, r is the radius of the electrodes in cm, S is the interelectrode distance and $g_v$ is the visual critical electric field. gv can, itself, be expressed as:

$$g_v = g_0 \delta \left(1 + \frac{c}{\sqrt{\delta r}}\right)$$

where $\delta$ is the factor air density compared to standard temperature and pressure conditions, $g_0$ is the disruptive electric field and c is a dimensional constant. This formula can be applied to electrodes with radiuses ranging between 0.01 – 1 cm and applies to pressures of 0.1 – 10 atm. Electrode roughness contributes to the critical energy, with up to a 20 % drop in its value when rough electrodes are considered (Stishkov *et al*., 2018). Electrode configuration and shape also influences the critical voltage. Unequal electrode arrangements make for lower critical voltage values.

When ionic saturation is reached, an electron avalanche is initiated (Stishkov *et al*., 2018). This starts with the initial ionisation of an air molecule or atom in the vicinity of the corona source, which results in the generation of a primary free electron. This is accelerated across an electric field, in the direction of the anode which, depending on whether positive or negative corona is being produced, can be the 'corona source electrode', or its counterpart on the other side of the interelectrode space, termed the 'collecting electrode'. With their high charge/mass ratio, free electrons collide inelastically neutral air molecules occupying the interelectrode space, resulting in their subsequent ionization. This process continues, with newly freed electrons bombarding more neutral particles and ionizing them as they move towards the positive electrode. Depending on their charge, atomic and molecular ions will also travel towards the electrode possessing an opposing charge to their own. Ion-induced secondary ions initiate new electron avalanches to maintaining the discharge. Corona discharge appears as a purple-blue glow emerging from the corona source, with the discharge current dependent on the voltage being applied, electrode shape and configuration, gas compound, density and medium conductivity. Electron avalanches occur within the glow.

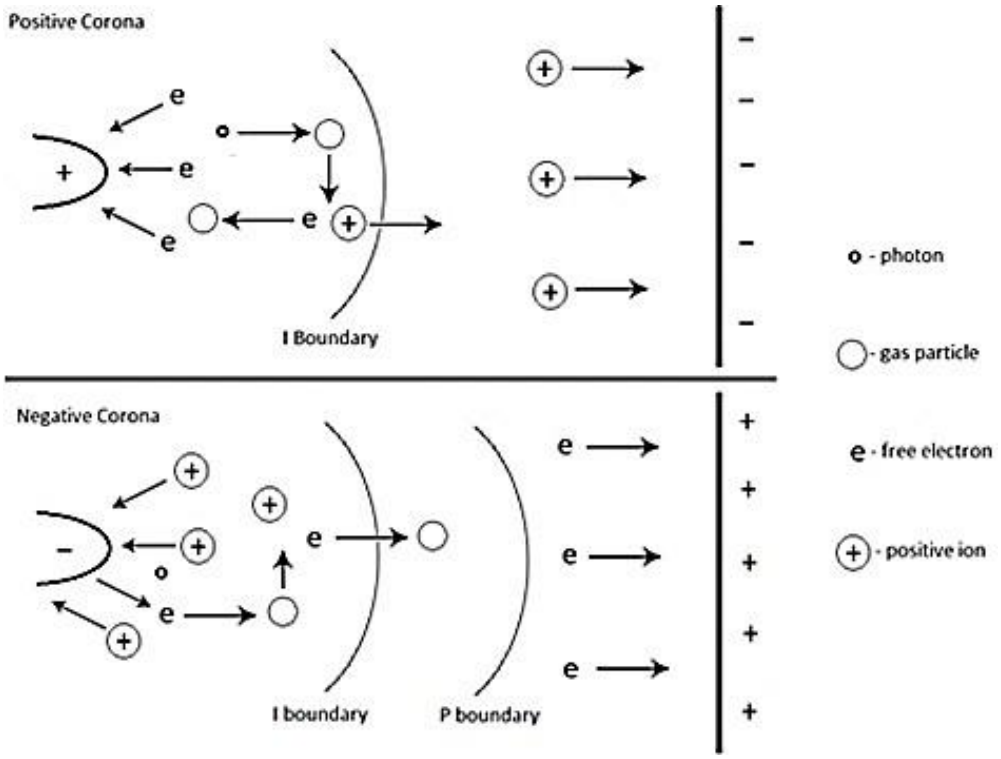


Schematic showing the formation of positive and negative corona. For both corona types, initial ionisation occurs within the ionisation boundary (I boundary). Electrons resulting from primary ionisation move inwards towards the positively charged corona source electrode with the opposite being true for negative corona. Secondary ionization in the former occurs through collisions between outgoing photons and gaseous particles. Subsequent electron collisions move inwards movement. For this reason, the I boundary and plasma boundary (P boundary overlap). In negative corona, photon release following gaseous particle relaxation results in a secondary electron being expelled from the corona source. Electron avalanches move outwards across the interelectrode space. Beyond the P boundary, the air is dominated by negatively charged species.

Corona discharge is generated using non-uniform electrodes (Stishkov *et al*., 2018; Timoshkin *et al*., 2008; Veldhuizen & Rutgers, 2001). The corona source is normally needle or wire-shaped, opposing a higher-area collecting electrode. The process can be powered either using DC or AC voltages which are either high, continuous or pulsed. The charge of the corona source electrode determines whether the corona discharge is 'positive' or 'negative'. Discharge originating from a cathode (negative electrode) is negative corona, whilst positive corona emanates from anode (positive electrode) corona sources. As a result, these corona forms arise through different mechanisms. In the case of positive corona, the electron avalanche moves towards the positively charged corona source electrode whilst positive ions move away from it. Positive ions and electrons within the plasma can recombine, resulting in the release of a photon as the atom or molecule returns to its ground state. Some of these photons radiate away from the corona source electrode and out of the corona region, where they ionise neutral gas particles. The

resultant secondary electrons move towards the anode, initiating new electron avalanches, maintaining the corona discharge. In negative corona discharge, the electron avalanche moves away from the corona source. Neutral gas particles, therefore, cannot be used to generate electron avalanches within the corona field. These are, instead, initiated from the electrode, which expels secondary electrons in response to a photon being released by gaseous particle relaxation.

Positive corona is therefore generated from gas surrounding the corona region whilst negative corona from the corona source electrode. For this reason, positive corona discharge appears smaller than negative corona, as electron avalanches move inwards instead of outward (positive corona ionization boundaries overlap with the plasma boundary). They are also characterised by uniform gradients across the corona source electrode. In the case of negative corona, gradient vary depending on the surface features of the electrode. The constant source of electrons being released from a strongly charged conductor means that many more free electrons occur in negative coronas. Despite this, the electrons in positive coronas occur in close vicinity to the source conductor, with the greater potential gradient here imparting higher energy on them. As a result, positive coronas are more suited to reactions requiring higher energy.